Characterization of the antiviral STING pathway in 'Drosophila melanogaster': signalling and NF-κB factor activation

Juliette Schneider

UNIVERSITÉ DE STRASBOURG

ÉCOLE DOCTORALE DES SCIENCES DE LA VIE ET DE LA SANTÉ

UPR9022 – Modèles Insectes d'Immunité Innée

THÈSE présentée par :

Juliette SCHNEIDER

soutenue le : **19 septembre 2022**

pour obtenir le grade de : **Docteur de l'université de Strasbourg**

Discipline/ Spécialité : Aspects moléculaires et cellulaires de la biologie

Caractérisation de la voie antivirale STING chez *Drosophila melanogaster* : signalisation et activation du facteur NF-κB

THÈSE dirigée par :

Pr. Jean-Luc IMLER	Professeur des Universités, Institut de biologie moléculaire et cellulaire, université de Strasbourg, France.

RAPPORTEURS :

Dr Nadine LAGUETTE	Directrice de recherches, Institut de génétique humaine, université de Montpellier, France
Pr. Nick GAY	Professeur des Université, Département de Biochimie, université de Cambridge, Royaume-Uni

AUTRES MEMBRES DU JURY :

Dr Frédéric GROS	Maître de conférence, Centre de recherche en biomédecine de Strasbourg, université de Strasbourg, France

---

INVITÉ :

Dr Carina de OLIVEIRA MANN	Directrice de recherches, Institut de Virologie, université technique de Munich, Allemagne

Abstract

Viral infections are a threat to all living organisms who developed diverse mechanisms to resist them. Working on the model organism *Drosophila melanogaster*, my host laboratory discovered a new antiviral pathway involving the ortholog of the well-known mammalian antiviral protein STING and two components of the antibacterial Imd pathway, the kinase IKKß and the NF-κB-like transcription factor Relish. During my thesis I attempted to answer two questions about this new pathway: (i) how is the STING pathway triggered in drosophila? and (ii) how does STING activate IKKß and Relish?

In the first part of my thesis, I participated in the work demonstrating that drosophila STING can be activated by injection of cyclic dinucleotides (CDN) into adult flies and that the product of the mammalian enzyme cGAS, 2'3'-cGAMP, is a better agonist of drosophila STING than bacterial CDNs. This suggested the existence of cGAS-like receptors in flies, which were indeed subsequently identified and that I started to functionally characterize. Injection of 2'3'-cGAMP also provided a useful assay to activate STING and screen for new components of the pathway.

In the second part of my thesis, I exploited the interactomes of STING and IKKß to identify factors that may connect the two proteins and participate in STING signaling. I identified Fadd as an interactant of both STING and IKKß and showed that induction of STING-regulated genes by 2'3'-cGAMP is impaired in Fadd mutant flies. I further showed that the caspase Dredd is also involved in the pathway and required to cleave Relish. Thus, two other components of the Imd pathway, Fadd and Dredd, are also involved in the STING pathway.

In the third part of the thesis, I report preliminary results on poorly characterized NF-κB and IκB proteins in drosophila, which were identified either as interactant of IKKß or as genes regulated by STING. These results suggest that these factors participate as positive or negative regulators in the STING pathway.

Overall, the work reported here reveals new facets of the STING antiviral pathway in drosophila. The results obtained concerning the activation of Relish may provide insights on the IFN-I-independent response activated by STING in mammals, which remains ill characterized, despite recent evidence demonstrating its importance in certain pathologies such as autoimmune diseases or cancer.

Acknowledgements

The PhD is a great adventure, full of pitfalls, but above all rewarding. These four intense years allowed me to evolve and grow, thanks to all the support and guidance I received from many people.

First, I would like to express my sincere gratitude to my PhD advisor, Jean-Luc Imler, for his trust. He gave me the opportunity to join the laboratory as a master inexperienced student and supported me throughout this journey. I have learned a lot at his side, both scientifically and personally.

I sincerely thank my thesis committee's members, Dr Nadine Laguette, Dr Carina de Oliveira Mann, Pr. Nick Gay and Dr Frédéric Gros for coming to Strasbourg to evaluate my work. I also thank the members of my thesis follow-up committee, Dr Irwin Davidson and Pr. Neal Silverman for their kind help and suggestions. These annual meetings have always been a great help to me.

I was lucky to be surrounded by excellent scientists, always ready to discuss and help. I would like to thank Joao Trindade Marques for scientific discussions on the project, Carine Meignin and Nelson Martins for their great help, especially with statistics and Akira Tajima-Goto for his constant benevolent interest in the project. I would like to express my gratitude to Hua Cai for trusting me to participate in the reviewing of his article. Moreover, I am grateful to Gabrielle Haas, the goddess of molecular biology, for her help and precious advices, and for continuing part of the work. I would like to acknowledge Emilie Lauret and Estelle Santiago who helped me a lot, for their availability and their capacity to solve impossible problems. I would also like to thank the interns for their contribution to the project: Coralie Mollard, Claire Damery, Sandra Nunez and, last but not least, Elea Becker who was also a real breath of fresh air in the office.

I also deeply thank all the past and present members of the UPR9022 for having always made the laboratory a lively and warm place. All my gratitude to the wonderful human beings that I have met and who became more than just colleagues. The past colleagues with whom everything was so simple and fun, Aurélie, Gaëtan, Léa and

Loïc. Our beloved “Mother of Students”, Nathalie, for taking care of me every day. My crazy friend who makes me laugh to tears, and who is also my official candy supplier, Audrey. My lovely friend, Lucie, which has always been there for me. Our improvised tea time were the little extra soul of the days in the lab. My dear past and present members of the “Poulette office”, Ludmila, Yasmine, Mélodie, Claire, Emilie, Evelyne and Assel. You were the sunshine of rainy days. Thank you for your constant support and help, for making me laugh so hard, for sometimes chasing away my tears and for giving rise to an interest in business, even though I am sure that not all customers are as easy to convince as you!

Special attention to the colleague who became my best friend, even if I will always stay just a colleague for her, isn’t it Claire? Joke aside, you are my person, the one to whom I could confide all my doubts and fears. You always know how to rejoice for me and pull me up, no matter what my plans are. Having you near me throughout this incredible journey was a true gift and the best thing that happened to me. I will always be there, whenever you need me. I am proud of you and I am sure that a wonderful and brilliant future awaits you, no matter what you decide.

Last but not least, I deeply thank my family without whom I could never have made it here: my sister and brother-in-law, my wonderful niece, my parents, and my oldest friends who became family, Morgane and Pauline. You have always encouraged me to follow my dreams. By repeating to me that I was capable of accomplishing anything, I finally believed it. Finally, how could I talk about family without talking about you, Matthieu? I can't express how lucky I am to have crossed your path ten years ago. You have been my strength and guide since day one. I know I could never have done any of this without your constant support. I am confident in the future because I know that I will spend it by your side.

I would like to dedicate this manuscript to my grandmother, an extremely intelligent woman who was born at a time that prevented her from following the major studies she dreamed of. I hope she is proud of me, wherever she is.

Abbreviations

AIM2: **a**bsent **i**n **m**elanoma **2**

AMP: **a**nti**m**icrobial **p**eptide

ARR: **a**nkyrin **r**each **r**egion

Att-A: **Att**acin-**A**

BSA: **b**ovin **s**erum **a**lbumin

BTZ: **B**or**te**z**o**mib

C-ter: **c**arboxy-**ter**minal

CBASS: **c**yclic oligonucleotide-**b**ased **a**nti-phage **s**ignaling **s**ystem

CD-NTase: **c**GAS/**D**ncV-like **n**ucleo**t**idyltransfer**ase**

CDN: **c**yclic **di**nucleotide

cGAMP: **c**yclic **G**MP-**AMP**

cGAS: **c**yclic **G**MP-**A**MP **s**ynthase

cGLR: **cG**AS-**l**ike **r**eceptor

CTN: **c**yclic **t**ri**n**ucleotide

CTT: **C**-**t**erminal **t**ail

DAMP: **d**amage-**a**ssociated **m**olecular **p**attern

DCV: **d**rosophila **C** **v**irus

DD: **d**eath **d**omain

DED: **d**eath **e**ffector **d**omain

Dif: **d**orsal-related **i**mmunity **f**actor

dl: **d**orsa**l**

DMSO: **di**ethyl**s**ulf**o**xyde

DNA: **d**eoxyribo**n**ucleic **a**cid

Dpt: **D**i**pt**ericin

Dredd: **D**eath **r**elated ced-3/N**edd**2-like caspase

dsRNA: **d**ouble-**s**trand **r**ibo**n**ucleic **a**cid

ER: **e**ndoplasmic **r**eticulum

Fadd: **F**as-**a**ssociated protein with **d**eath **d**omain

FADS2: **f**atty **a**cid **de**s**a**turase **2**

FLuc: **f**irefly **luc**iferase

GNBP: **G**ram-**n**egative **b**inding **p**rotein

HKE: **h**eat-**k**illed *E. coli*

HRP: **h**orse**r**adish **p**eroxidase

IFN-I: type **I** **i**nter**f**ero**n**

IKK: **I**-**k**appaB **k**inase

Imd: **im**mune **d**eficiency

IP: **i**mmuno**p**recipitation

IRF: **i**nterferon **r**egulatory **f**actor

IκB: **i**nhibitor of nuclear factor **k**appa-**B**

KD: **k**nock-**d**own

kDa: **k**ilos-**Da**ltons

KO: **k**nock-**o**ut

LB: **l**uria **b**roth

MAMP: **m**icrobe-**a**ssociated **m**olecular **p**attern

MAVS: **m**itochondrial **a**nti**v**iral **s**ignaling protein

MOI: **m**ultiplicity **o**f **i**nfection

MyD88: **my**eloid **d**ifferentiation primary-response gene **88**

N-ter: **amino-ter**minal

NAD$^+$: ß-**n**icotinamide **a**denine **d**inucleotide

NEMO: **N**F-κB **e**ssential **mo**dulator

NF-κB: **n**uclear **f**actor **k**appa-**B**

NIK: **N**F-κB-**i**nducing **k**inase
NLS: **n**uclear **l**ocalization **s**ignal
NT: **n**on-**t**reated
PARP-1: **p**oly(**A**DP **r**ibose) **p**olymerase-**1**
PBS: **p**hosphate **b**uffered **s**aline
PCR: **p**olymerase **c**hain **r**eaction
pfu: **p**ore-**f**orming **u**nit
PGN: **p**eptido**g**lyca**n**
PGRP: **p**eptido**g**lycan-**r**ecognition **p**rotein
pMT: **m**etallo**t**hionein **p**romoter
PRR: **p**attern-**r**ecognition **r**eceptor
PTM: **p**ost-**t**ranslational **m**odification
RASSF: **R**as **ass**ociation **f**amily
rcf: **r**elative **c**entrifugal **f**orce
RHD: **R**el **h**omology **d**omain
RIG-I: **r**etinoic acid-**i**nducible **g**ene **I**
RIP: **r**eceptor-**i**nteracting **p**rotein
RIPK1: **r**eceptor-**i**nteracting serine/threonine-**p**rotein **k**inase **1**
RLuc: **r**enilla **luc**iferase
RNA: **r**ibo**n**ucleic **a**cid
RNAi: **RNA i**nterference
RT-qPCR: **r**eal-**t**ime **q**uantitative **PCR**
RT: **r**oom **t**emperature
S2: **S**chneider **2**
SAVI: **S**TING-**a**ssociated **v**asculopathy with onset in **i**nfancy
SEM: **s**tandard **e**rror of the **m**ean
SN: **s**uper**n**atant
SRG: **S**TING-**r**egulated **g**ene
SRR: **s**ignal **r**esponsive **r**egion
ß-TrCP: **ß**-**t**ransducing **r**epeat-**c**ontaining **p**rotein
STING: **st**imulator of **i**nterferon **g**enes
TAD: **t**rans**a**ctivation **d**omain
TBK1: **T**ANK-**b**inding **k**inase **1**
TBS: **t**ris-**b**uffered **s**aline
TIR: **T**oll-**i**nterleukin-1 **r**eceptor
TLR: **T**oll-**l**ike **r**eceptor
TNFR: **t**umor-**n**ecrosis **f**actor **r**eceptor
TRAF: **T**NF **r**eceptor-**a**ssociated **f**actor
WT: **w**ild **t**ype
yw: **y**ellow **w**hite

Table of contents

INTRODUCTION

Preamble

All living organisms are constantly surrounded by potentially dangerous microorganisms. This continuous exposure has shaped host defense systems throughout evolution.

Immune defenses of the model organism *Drosophila melanogaster* rely only on innate immunity, as insects lack an adaptive immune system. To protect themselves from the variety of existing pathogens, drosophila have developed different defense mechanisms throughout evolution. These mechanisms can be either constitutive, as it is the case for the broadly antiviral ribonucleic acid interference (RNAi), or induced upon infection. The latter can be illustrated by the well-known Toll and immune deficiency (Imd) signaling pathways, which confer antibacterial and antifungal immunity. However, it recently became clear that inducible responses are also important to defend flies from viral infections.

Over the past 20 years, my host team has been particularly interested in these inducible antiviral defenses (Deddouche et al., 2008; Dostert et al., 2005; Kemp et al., 2013; Sabatier et al., 2003). Notably, the team identified viral suppressors of the Imd pathway in several deoxyribonucleic acid (DNA) viruses, suggesting that this pathway restricts viral infections (Lamiable et al., 2016). While further exploring a possible role of the Imd pathway in antiviral defenses, the team has discovered a novel pattern-recognition receptor (PRR) triggered pathway regulating antiviral defenses in drosophila. Indeed, shortly before my arrival in the laboratory the team described that two components of the Imd pathway, the nuclear-factor kappa-B (NF-κB) transcription factor Relish and the I-kappa-B kinase (IKK)-ß, played an important role in host-defense against the picorna-like virus drosophila C virus (DCV). These proteins are involved in an antiviral signaling pathway relying on the drosophila homolog of stimulator of interferon genes (STING). Curiously, the other components of the canonical Imd pathway did not seem to participate in this pathway (Goto et al., 2018). These results are intriguing, as Relish needs to be cleaved to translocate to the nucleus and induce gene expression and this cleavage is mediated by the caspase-8 homolog Death related ced-3/Nedd2-like caspase (Dredd) in the Imd pathway (Kim et al., 2014;

Stoven et al., 2003; Stöven et al., 2000). Moreover, the regulatory subunit of the IKK complex, IKKγ, is also essential for a good activation of Relish-target genes (Ertürk-Hasdemir et al., 2009). The fact that none of these components seemed to be involved in the STING pathway raised the question of the mechanism by which Relish controls the transcriptional response upon STING pathway activation. Another key question when I joined the laboratory was the way the STING pathway is activated upon viral infection. The goal of my PhD project was to shed light on these questions

To provide background to the general theme of my thesis, I have structured the introduction in three parts. The first part provides a review on immune responses in *Drosophila melanogaster*. The second part of the introduction covers the STING pathway and its conservation during evolution. Finally, the last part of the introduction is an overview of NF-κB pathways and their regulation in animals.

I. Immune pathways in *Drosophila melanogaster*

When an individual encounters an infectious agent, the initial layer of defense is mechanical. It relies on the physical barrier which delimits the “self” from the “non-self” environment. Most of the time, this first line of defense prevents the pathogen to enter the body and initiate the infection. If this barrier is overcome or evaded, other components of the immune system come into play in order to preserve the organism. In all multicellular organisms, we find a variety of PRR. PRRs are proteins responsible for the recognition of conserved molecules frequently found in microorganisms, called microorganisms-associated molecular patterns (MAMP). For example, flagellin, the major protein composing bacterial flagellum, is recognized by Toll-like receptor (TLR)-5 in animals (Hayashi et al., 2001). Alternatively, PRRs are able to sense damage-associated molecular patterns (DAMP) such as uric acid released by damaged cells (Shi et al., 2003). The recognition of their ligand by PRRs allows the activation of innate immunity, resulting in a non-specific and rapid response to infection. In vertebrates, this branch of the immune response allows the activation of subsequent adaptive immunity, slower to implement but specific and which gives rise to an immune memory (reviewed in Hoffmann et al., 1999).

My host laboratory studies innate immunity in the fruit fly *Drosophila melanogaster* which belongs to the order Diptera. It presents numerous advantages among which its small size, fast generation time and easy handling. Moreover, the variety of genetic tools it offers and the absence of adaptive immunity make it a very attractive model to study the innate immune response. Importantly, insects represent nearly 70% of the terrestrial fauna and are susceptible to pathogens similar to those infecting humans. The study of their immune mechanisms can thus reveal strategies that can be either conserved in or transposed to humans (reviewed in Martins et al., 2016). A notable example of this is the identification of inducible signaling pathways mediating antimicrobial peptides (AMP) expression in drosophila (reviewed in Imler, 2014). AMPs are small and cationic proteins produced by the fat body (functional equivalent of the mammalian liver) and secreted into the hemolymph (fluid analogous to vertebrates

blood). They exhibit various activities against bacteria and fungi (reviewed in Imler and Bulet, 2005). Expression of AMP genes is regulated by two distinct signaling pathways, the Toll and Imd pathways (reviewed in Hoffmann, 2003; Lemaitre and Hoffmann, 2007).

1. Anti-bacterial and anti-fungal defenses

a. Toll pathway

Interestingly, binding sites for NF-κB/Rel transcription factors were identified in promoters of AMP genes. Mutation of these sites abolished the induction of AMPs upon immune challenges (Engström et al., 1993; Kappler et al., 1993). This suggested an involvement of members of the NF-κB family in immune pathways in drosophila. At the time, only one member of the NF-κB family was identified in drosophila, dorsal (dl). dl participate in the dorso-ventral patterning of the early embryo (Nüsslein-Volhard et al., 1980). Activation of this transcription factor was shown to be similar to the induction of NF-κB during inflammatory response in mammals. Indeed, it depends on its dissociation from the protein Cactus (an inhibitory protein homologous to inhibitor of NF-κB (IκB)). This event is triggered by the binding of the cytokine-like protein called Spätzle to the transmembrane receptor Toll, resulting in activation of signaling (Weber et al., 2003; reviewed in St Johnston and Nüsslein-Volhard, 1992). The drosophila Toll receptor was then shown to be important to counter fungal and Gram-positive infections (Lemaitre et al., 1996; Rutschmann et al., 2002). Importantly, the NF-κB transcription factor responsible for AMPs expression regulation is not dorsal, but the closely related factor Dif (dorsal-related immunity factor)(Ip, 1993; Meng et al., 1999; Rutschmann et al., 2000a).

This discovery in drosophila prompted the search and subsequent identification of a family of TLRs in mammals. Whereas Toll acts as a receptor for the cytokine Spätzle in drosophila, mammalian TLRs are PRRs, which directly sense infections by recognizing a variety of MAMPs (Medzhitov et al., 1997; Poltorak et al., 1998; Rock et al., 1998). In flies, sensing of infection occurs upstream of Toll. Lys-type peptidoglycans (PGN) present in the outer membrane of Gram-positive bacteria are

sensed by PGRP (peptidoglycan-recognition protein)-SA and GNBP (gram-negative binding protein)-1 (Gobert et al., 2003; Michel et al., 2001). ß-glucans composing the cell wall of fungi are recognized by the GNBP-3 sensor (Gottar et al., 2006; Mishima et al., 2009). Alternatively, proteases secreted by entomopathogenic fungi, but also Gram-positive and -negative bacteria, induce the maturation of the zymogen Persephone into an active protease (El Chamy et al., 2008; Gottar et al., 2006; Issa et al., 2018). Ultimately, these sensing systems converge and lead to the extracellular proteolytic maturation of Spätzle (DeLotto and DeLotto, 1998; Mizuguchi et al., 1998). A dimer of active Spätzle binds to the extracytoplasmic domain of a dimer of Toll transmembrane receptors. This induces the crosslink of the two Toll ectodomains and subsequent conformational changes leading to signaling (Hu et al., 2004; Weber et al., 2003, 2005, 2007). Upon activation, the cytoplasmic adaptor myeloid differentiation primary-response gene 88 (MyD88) is recruited through interaction of its Toll/interleukin-1 receptor (TIR) domain with the TIR domain of the intracytoplasmic tail of the Toll receptor. Through its death domain (DD), MyD88 recruits the adaptor Tube, which has a bivalent DD and will, in turn, recruit the DD-containing serine-threonine kinase Pelle (Tauszig-Delamasure et al., 2002). Ultimately, the homolog of mammalian IκB, Cactus, is phosphorylated, leading to its ubiquitination and degradation. This allows the release of the NF-κB like transcription factor dorsal (in embryos) or Dif (in adults), followed by its nuclear translocation and activation of target genes, among those AMPs such as *Drosomycin* (**Figure 1A**). The drosophila Toll pathway is homologous to the mammalian signaling cascade downstream of the interleukin-1 receptor and the TLRs, pointing to a common ancestry of these different immune mechanisms (Medzhitov et al., 1998; reviewed in Hoffmann, 2003; Hoffmann et al., 1999).

b. Imd pathway

The Imd pathway was named after a mutation called *immune deficiency* that impaired the expression of some AMPs, but not *Drosomycin* which is regulated by the Toll pathway. *imd* flies showed a high susceptibility to Gram-negative bacteria but were resistant to fungi and Gram-positive bacteria. Importantly, overexpression of *imd* leads

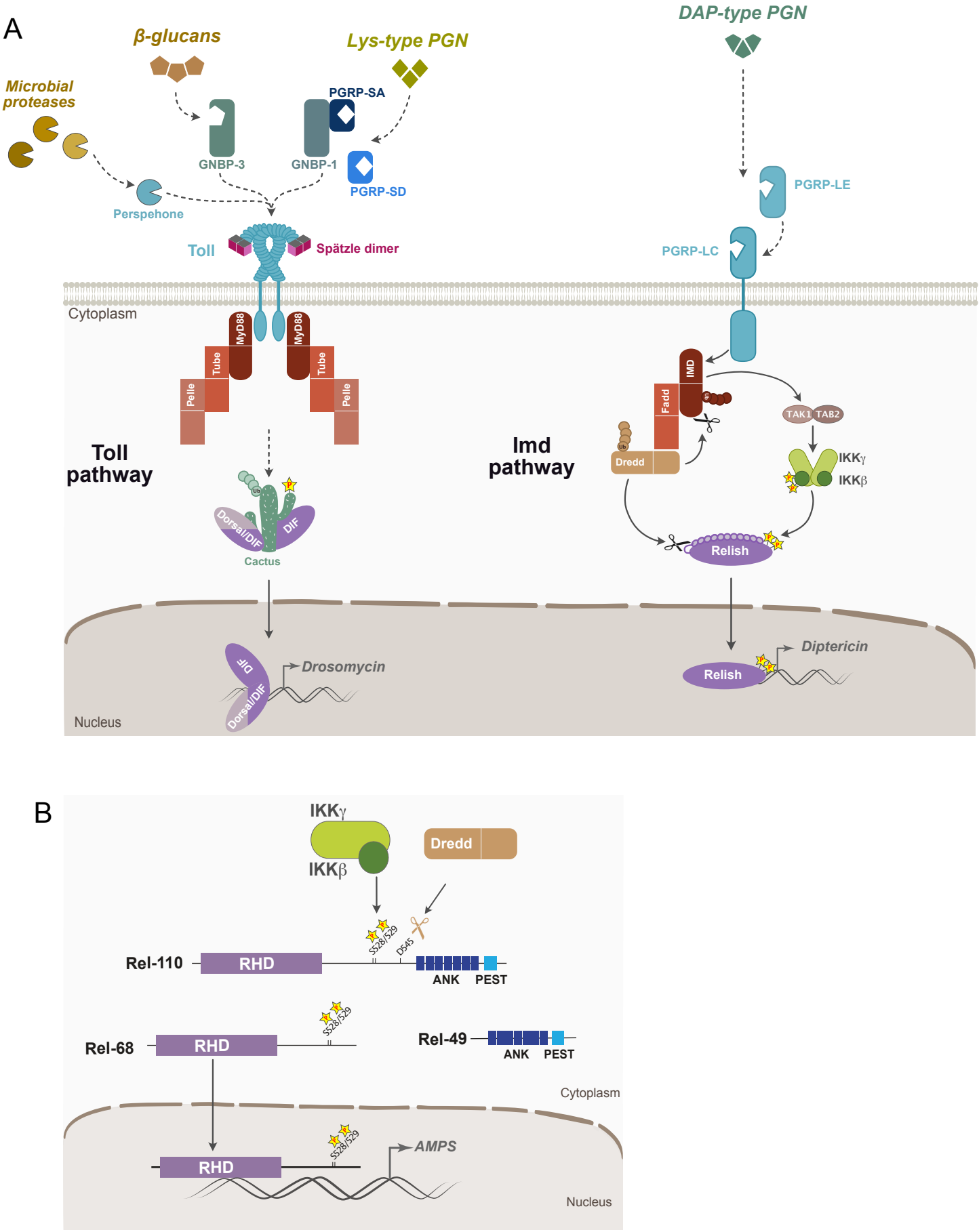

Figure 1: Toll and Imd pathways in drosophila. A) Schematic representation of Toll (left) and Imd (right) pathways. See the text for details. **B)** Schematic representation of Relish activation mechanisms downstream of Imd pathway. See the text for details. **A and B)** Ubiquitin chains are represented by circle sequences, phosphorylations are represented by yellow stars with red "P" inside.

to an increased expression of AMPs in non-infected conditions, demonstrating its central role in the systemic immune response of drosophila (Georgel et al., 2001). The protein encoded by *imd* contain a DD which present sequence similarities with the DD of mammalian receptor-interacting protein (RIP)(Georgel et al., 2001).

Diaminopimelic acid-type PGNs contained in the cell envelope of Gram-negative bacteria are recognized by the transmembrane receptor PGRP-LC or by cytoplasmic or secreted isoforms of the PGRP-LE receptor. On the one hand, the cytoplasmic form of PGRP-LE is involved in the activation of autophagy upon infection by intracellular bacteria, independently of the Imd pathway (Yano et al., 2008). On the other hand, activation of both PGRPs by ligand binding leads to the activation of the Imd pathway by the recruitment of the proximal adaptor Imd. This protein functions as a signaling hub initiating two distinct processes, ultimately responsible for the activation of the NF-κB like transcription factor Relish (Choe et al., 2002; Gottar et al., 2002; Hedengren et al., 1999; Takehana et al., 2004).

The first process starts with the recruitment of the adaptor protein Fas-associated protein with death domain (Fadd) by Imd through DD-DD interaction. Subsequently, Fadd recruits the caspase Dredd by interaction of their respective dead effector domain (DED)-domain (Leulier et al., 2000, 2002; Naitza et al., 2002). Dredd is then ubiquitinated (Meinander et al., 2012), rendering it active and allowing it to cleave Relish at a specific residue (aspartic acid in position 545, D545). This processing releases the active amino-terminal (N-ter) part (Rel68) presenting the Rel homology domain (RHD) from the inhibitory carboxy-terminal (C-ter) part (Rel49) containing ankyrin repeats and a PEST sequence (Kim et al., 2014; Stoven et al., 2003; Stöven et al., 2000). This process enables the nuclear translocation of Rel68, while Rel49 stays in the cytoplasm (**Figure 1A and B**).

Moreover, to efficiently activate the transcription of its target genes, such as the AMP coding gene *Diptericin* (Dpt), Relish needs to be phosphorylated. This second process relies on Dredd-dependent cleavage of a N-ter fragment of Imd, allowing its K63-ubiquitination (Meinander et al., 2012; Paquette et al., 2010). Imd is then able to recruit and activate the Tab2/Tak1 complex. This complex is responsible for the activation of the drosophila inhibitor of the IKK complex (IKKß-IKKγ) by phosphorylation

(Kleino et al., 2005; Lu et al., 2001; Rutschmann et al., 2000b; Silverman et al., 2000). Ultimately, the IKK complex phosphorylates two serine residues of Relish (S528 and S529), necessary for an efficient recruitment of RNA polymerase II to the promoters of Relish target genes **(Figure 1A and B**)(Ertürk-Hasdemir et al., 2009; Silverman et al., 2000). This pathway is homologous to the tumor-necrosis factor receptor (TNFR) dependent pathway in mammals (reviewed in Hoffmann, 2003).

2. Antiviral immunity

Our knowledge of the antiviral immune response in drosophila has long been limited to RNAi. However, although this response is essential to defend the organism against all types of viruses, it is now known that inducible antiviral responses exist and are also important for the survival of flies to viral infections.

The knowledge acquired and the recent advances on the antiviral immunity of drosophila were the subject of a review published in 2021 in the journal Developmental and Comparative Immunology (Schneider and Imler, 2021).

Developmental and Comparative Immunology 117 (2021) 103985

Contents lists available at ScienceDirect

Developmental and Comparative Immunology

journal homepage: www.elsevier.com/locate/devcompimm

Review

Sensing and signalling viral infection in drosophila

Juliette Schneider [a], Jean-Luc Imler [a,b,*]

[a] Université de Strasbourg, CNRS UPR9022, Institut de Biologie Moléculaire et Cellulaire, Strasbourg, France
[b] Sino-French Hoffmann Institute, School of Basic Medical Science, Guangzhou Medical University, Guangzhou 511436, China

ARTICLE INFO

Keywords:
NF-κB
STING
RNA interference
Innate immunity
Antiviral factors
Virus

ABSTRACT

The fruitfly *Drosophila melanogaster* is a valuable model to unravel mechanisms of innate immunity, in particular in the context of viral infections. RNA interference, and more specifically the small interfering RNA pathway, is a major component of antiviral immunity in drosophila. In addition, the contribution of inducible transcriptional responses to the control of viruses in drosophila and other invertebrates is increasingly recognized. In particular, the recent discovery of a STING-IKKβ-Relish signalling cassette in drosophila has confirmed that NF-κB transcription factors play an important role in the control of viral infections, in addition to bacterial and fungal infections. Here, we review recent developments in the field, which begin to shed light on the mechanisms involved in sensing of viral infections and in signalling leading to production of antiviral effectors.

1. Introduction

All living organisms face viral infections during their lifetime. To defend themselves, hosts developed various antiviral immune responses throughout evolution. In this regard, insects represent an interesting opportunity, in light of the fantastic biodiversity they represent, with over 1 million known species and an evolutionary history covering 350 million years (Misof et al., 2014). Historically, insect-virus interactions were first studied in the context of diseases affecting economically important insects, such as silkworms (Lü et al., 2018) or bees (Manley et al., 2015). Insect viruses also rapidly became of interest as biological control agents (e.g. baculoviruses (Lacey et al., 2015)). Finally, important animal and human viral diseases are transmitted by *Culex* and *Aedes* mosquitoes, e.g. West Nile, Yellow Fever, Dengue, Zika and Chikungunya (Shaw and Catteruccia, 2019). Pioneering studies in drosophila and genome sequencing have, since the early 2000s, promoted the expansion of the field of insect antiviral immunity.

Among insects, the fruit fly *Drosophila melanogaster* has a special status as an invaluable model organism, used since the beginning of the XXth century to understand the genetic basis of heredity, embryonic development as well as a range of biomedical problems, including immunity (reviewed in (Wangler et al., 2015)). Research on drosophila host defence against bacterial and fungal infections led to the identification of two evolutionarily conserved signalling pathways, Toll and Immune deficiency (IMD), regulating transcription factors of the NF-κB family to induce production of antimicrobial peptides (AMPs; reviewed in (Hoffmann et al., 1999; Hultmark, 2003; Lemaitre and Hoffmann, 2007)). Cellular responses, driven by hemocytes, also participate in the control of infections (Gold and Brückner, 2015; Lamiable et al., 2016a; Letourneau et al., 2016; Nainu et al., 2015; Weavers et al., 2016). More recently, the interest for antiviral resistance mechanisms in drosophila has grown, initially taking advantage of the pioneering work of Philippe Lhéritier and Nadine Plus who described the first drosophila viruses, Sigma virus and Drosophila C virus (DCV, Table 1 (Jousset et al., 1972; Lhéritier, 1958)). This led to the identification of the first genes encoding restriction factors (e.g. (Cao et al., 2017, 2016; Gay, 1978)), the description of induced responses (e.g. (Dostert et al., 2005; Kemp et al., 2013; Merkling et al., 2015b; Xu et al., 2012)), the discovery of the important role of RNA interference (RNAi ((Galiana-Arnoux et al., 2006; van Rij et al., 2006; Wang et al., 2006)) and the characterization of evolutionarily conserved host factors used by viruses or participating in the control of infections (e.g. (Eleftherianos et al., 2011; Majzoub et al., 2014; Panda et al., 2013)). In addition, the characterization of the drosophila virome led to the discovery of more than 20 new viruses, which represent a goldmine for future studies on virus-host interactions (Webster et al., 2015). Especially, the first natural DNA virus of *Drosophila melanogaster*, Kallithea virus (KV, Table 1), has been described and characterised (Palmer et al., 2018a).

Research carried on the genetics of drosophila antiviral immunity over the past 15 years led to the identification of many genes and pathways associated with host restriction factors, inducible responses and antiviral RNA interference (RNAi), which have been reviewed

* Corresponding author. Université de Strasbourg, CNRS UPR9022, Institut de Biologie Moléculaire et Cellulaire, Strasbourg, France.
E-mail address: jl.imler@ibmc-cnrs.unistra.fr (J.-L. Imler).

https://doi.org/10.1016/j.dci.2020.103985
Received 4 November 2020; Received in revised form 16 December 2020; Accepted 17 December 2020
Available online 23 December 2020

(Chow and Kagan, 2018; Liu et al., 2017; Mondotte and Saleh, 2018; Mussabekova et al., 2017; Palmer et al., 2018b; Segrist and Cherry, 2020; Swevers et al., 2018; Talide et al., 2020). Here, we focus on the recent advances in the field with a particular interest for the latest developments on RNA-based antiviral defences (RNAi) and on inducible responses. We also discuss remaining questions to better understand drosophila defences against viruses.

2. RNA-based antiviral immunity

RNAi, initially identified as a major antiviral pathway in plants, also plays an important role in drosophila immunity (reviewed in (Guo et al., 2019)). Small RNA silencing encompasses three different pathways in flies (Ghildiyal and Zamore, 2009), each of which participates in host-virus interaction, albeit at different levels. Two of these pathways involve small RNAs produced by Dicer (Dcr) enzymes, the 22-23 nucleotide (nt) long micro (mi) RNAs produced by Dcr-1 and the 21 nt-long small interfering (si) RNAs produced by Dcr-2. Dicers are RNaseIII enzymes that process double-stranded (ds) RNA precursors into small RNA duplexes. In the case of miRNAs, a complex composed of another RNase III enzyme, Drosha, and a dsRNA binding protein (dsRBP), Pasha, processes the primary transcripts of mi-RNA (pri--miRNA) in the nucleus. After export to the cytoplasm, the precursor of the miRNA (pre-miRNA) containing a stem loop structure, is recognized and cleaved by Dcr-1 (Ha and Kim, 2014; Lee et al., 2004). In the case of Dcr-2, the template is a long dsRNA, which can result from either convergent transcription or the presence of long inverted repeats in a transcript (endo-siRNAs), but also from internalized dsRNAs (exo--siRNAs)(Czech et al., 2008; Kawamura et al., 2008; Marques et al., 2010) or intermediates of replication typically produced during a viral infection (vsiRNAs) (Aliyari et al., 2008; Bronkhorst et al., 2012; Mueller et al., 2010; Sabin et al., 2013; Vodovar et al., 2011). These small RNAs are then loaded onto enzymes of the Argonaute (AGO) family, AGO1 for miRNAs and AGO2 for siRNAs, where one of the strands will be discarded. The remaining strand, known as the guide strand, is used to direct the AGO enzyme towards its target RNA for translation inhibition or degradation, thus achieving silencing of gene expression. The third pathway involves slightly longer small RNAs, the 24-28 nt-long PIWI-associated RNAs (piRNAs), which are produced by a Dcr-independent mechanism and associate with a different clade of AGO enzymes, known as PIWI (Saito et al., 2006; Vagin et al., 2006). The drosophila genome encodes three of these, Piwi, AGO3 and Aubergine (Senti and Brennecke, 2010; Siomi et al., 2011).

2.1. Activation of the siRNA pathway by viral and non viral RNAs

The multiple lines of evidence supporting a major role in antiviral defense for the siRNA pathway, including (i) the phenotypic characterization of flies mutant for the genes encoding the three core components of the pathway, *Dcr-2*, *r2d2* and *AGO2*; (ii) the identification of virus-derived siRNAs in infected flies; and (iii) the identification of viral suppressors in several insect viruses, have been reviewed elsewhere (Aguiar et al., 2016; Guo et al., 2019; Nayak et al., 2013; Schuster et al., 2019). The importance of the pressure put by viruses on the siRNA pathway to escape it is probably best illustrated by the viral suppressor of RNAi encoded by the Cricket Paralysis virus (CrPV, Table 1), CrPV-1A. This small viral protein targets AGO2 by two different mechanisms, directly blocking its RNA slicing activity and, at the same time, recruiting cellular proteins to assemble a virus-hijacked E3 ligase to destabilize the enzyme (Nayak et al., 2018; Watanabe et al., 2017). Intriguingly, CrPV-1A can also repress host transcription through a different domain, suggesting that this viral protein may also act as a suppressor of inducible responses (Khong et al., 2017).

Important remaining questions in the field pertain to the mechanism by which Dcr-2 recognizes viral RNA and the exact nature of the viral templates that are sensed by the enzyme. Interestingly, it was recently shown that Dcr-2 initiates cleavage of dsRNA differently depending on their extremities. Whereas the platform-PAZ domain recognizes templates with 3′OH overhang extremities, dsRNA with blunt termini engage the N-terminal helicase domain (Sinha et al., 2018). This helicase domain belongs to the superfamily (SF) 2 group of helicases, like the retinoic acid-inducible gene (RIG)-I like receptors in vertebrates, which sense viral RNAs in the cytosol and trigger interferons (IFNs) synthesis. SF2 helicases exhibit three subdomains, Hel1, Hel2i and Hel2, which change conformation upon binding viral RNA, thus triggering signaling (in the case of RIG-I like receptors (Kolakofsky et al., 2012; Kowalinski et al., 2011)) or processive cleavage of dsRNA (in the case of Dcr-2 (Sinha et al., 2018, 2015)). This suggests an ancestral function for the helicase domain of Dcr-2 in antiviral immunity, associated to a role in recognition of non-self RNA. By contrast, the platform-PAZ domain, located downstream of the N-terminal helicase domain, may mediate recognition of self RNA and participate in the cellular regulatory functions of Dcr-2 (e.g. endo-siRNA pathway). Small dsRBPs, such as Loquacious (Loqs) and R2D2, play important roles in the modulation of the different activities of Dcr-2 (Cenik et al., 2011; Hansen et al., 2019; Marques et al., 2010; Trettin et al., 2017). These dsRBPs have two or three dsRNA binding motifs, which bind either dsRNAs or, following loss of amino-acids important for nucleic acid binding, other proteins to regulate their activity. Interestingly, some of these dsRBPs interact with the helicase domain of Dcr-2 and modulate its functions (Donelick et al., 2020; Hansen et al., 2019). For example, the PD isoform of Loqs is essential for the generation of endo- and exo-siRNAs but dispensable for the production of vsiRNAs (Marques et al., 2013). This observation, confirmed by reconstitution experiments in human cells with drosophila genes (Girardi et al., 2015; Kennedy et al., 2017), reveals that cofactors of the core components Dcr-2, R2D2 and AGO2 play important roles in the siRNA pathway. Thus, Dcr-2 may be able to sense viral dsRNAs with blunt termini as non-self through its helicase domain, while requiring loqs-PD for the processing of endo siRNAs. Intriguingly, in *Aedes* mosquitoes, which are important vectors for Dengue and other viruses,

Table 1
Characteristics of the viruses mentioned in the text.

Name	Family	Genome	Identified immune suppressor		
			Name	Targeted pathway	Mechanism
Drosophila C virus (DCV)	*Dicistroviridae*	ssRNA(+)	DCV-1A	siRNA	dsRNA binding protein: long dsRNA
Cricket Paralysis virus (CrPV)	*Dicistroviridae*	ssRNA(+)	CrPV-1A	siRNA; transcription	AGO2 binding: inhibition & degradation
Sindbis virus (SINV)	*Togaviridae*	ssRNA(+)	/	/	/
Flock House virus (FHV)	*Nodaviridae*	ssRNA(+)	FHV-B2	siRNA	dsRNA binding protein: long dsRNA & siRNA duplexes
Nora virus	Unclassified	ssRNA(+)	Nora-VP1	siRNA	AGO2 binding: inhibition
Sigma virus (SV)	*Rhabdoviridae*	ssRNA(−)	/	/	/
Drosophila X virus (DXV)	*Birnaviridae*	dsRNA	DXV-VP3	siRNA	dsRNA binding protein: long dsRNA & siRNA duplexes
Kallithea virus (KV)	*Nudiviridae*	dsDNA	gp83	Toll	NF-kB transcription factors
			?	Jak-STAT?	?
Invertebrate Iridescent virus 6 (IIV-6)	*Iridoviridae*	dsDNA	IIV6-340R	siRNA	dsRNA binding protein: long dsRNA & siRNA duplexes
			?	IMD/Toll	Relish-mediated transcriptional activation/?

the *Loqs* gene has been duplicated and *Loqs2*, one of the two paralogues, is required for the antiviral siRNA pathway, but dispensable for the endo- and exo-siRNA pathways (Olmo et al., 2018). Overall, these results point to the importance of characterizing the termini of the dsRNAs processed by Dcr-2 in virus infected cells or flies to better understand its function. Identifying the exact role of Loqs and related proteins represents another frontier for the field in the coming years, all the more so because other small dsRBD proteins appear to be involved in RNAi. One of them is Blanks, a testis specific factor, which is required to export dsRNAs from the nucleus to the cytosol, where they can be processed by Dcr-2 (Nitschko et al., 2020). Interestingly, innate immunity genes are upregulated in the testis of *blanks* mutant flies, pointing to a possible connection between RNAi and other innate immunity pathways (Gerbasi et al., 2011). While Blanks does not seem to participate in antiviral immunity, another related protein, DISCO interacting protein 1 (DIP1), has been proposed to play a role in the control of viral infections although the mechanism remains unknown (Zhang et al., 2015).

Finally, antiviral RNAi in drosophila has also been reported to involve a systemic component, associated with reverse transcription of viral RNA into DNA and production of secondary siRNAs. The characterization of the specific components of systemic RNAi and the mechanisms involved represent an important challenge for the field (Goic et al., 2013; Mondotte et al., 2018; Poirier et al., 2018; Saleh et al., 2009; Tassetto et al., 2017).

2.2. Regulation of gene expression by Dcr-1 and Dcr-2 contributes to virus-host interaction in flies

Although primarily involved in the regulation of cellular gene expression, the miRNA pathway is also involved in host-virus interactions in many animals, including flies. For example, several DNA viruses produce miRNAs that modulate expression of host genes to facilitate dissemination of the virus (reviewed in (Tuddenham and Pfeffer, 2011)). The identification of an abundant miRNA, produced by KV, with up to few hundreds putative targets in the drosophila genome, paves the way to the characterization of this type of regulation in flies (Webster et al., 2015). In addition, some cellular miRNAs have been shown to modulate DCV replication by regulating proviral genes (e.g. miR-8-5p and dJun ((Monsanto-Hearne et al., 2017a)) or antiviral genes (e.g. miR956 and Ect4 ((Monsanto-Hearne et al., 2017b)).

Besides its role in RNA silencing, Dcr-2 also participates in non-canonical cytoplasmic poly-adenylation of a subset of messenger RNAs in drosophila embryos. Of note, at least two immunity related genes, Toll and R2D2, depend on Dcr-2 for their poly-adenylation (Coll et al., 2018). This study suggests that a complex composed of Dcr-2 and Wispy, a cytoplasmic poly(A) polymerase, is necessary for cytoplasmic poly-adenylation of these genes. This newly described function of Dcr-2, which affects the translation efficiency of the targeted genes, may help explain other roles of Dcr-2 that seem to be RNAi-independent. These include an involvement of Dcr-2 in resistance to various stresses, such as starvation, cold, but also oxidative or endoplasmic reticulum stresses (Lim et al., 2011). A direct post-transcriptional effect of Dcr-2, involving interaction between the helicase domain and the mRNA, may also regulate the expression of genes associated with host defense, e.g. the single von Willebrand factor-C (SVC) domain proteins like Vago in drosophila, which participate in antiviral immunity in flies, mosquitoes and bumblebees (Asad et al., 2018; Deddouche et al., 2008; Deng et al., 2020; Harsh et al., 2018; Paradkar et al., 2012; Wang et al., 2017).

2.3. The piRNA pathway and the control of foreign genetic elements

In drosophila, the piRNA pathway plays a crucial role in the protection of the germline against transposable elements (Brennecke et al., 2007; Pélisson et al., 2007; Senti and Brennecke, 2010). Ten years ago, piRNAs derived from viruses persistently infecting a drosophila cell line derived from ovaries (OSS cells) were reported, raising the possibility that the piRNA pathway participated in antiviral immunity in the germline and possibly also in somatic tissues (Wu et al., 2010). Rapidly, a role for this pathway was also proposed in *Aedes* mosquitoes, based on expansion of the Piwi family in these insects, some of which are clearly expressed in somatic tissue, and the identification of virus-derived piRNAs first in cell lines but also in mosquitoes for Chikungunya virus (reviewed in (Miesen et al., 2016)). In drosophila, subsequent *in vivo* experiments ruled out a role for the germline-specific piRNA pathway in antiviral defense, even in ovaries where the piRNA pathway is primarily active (Martins et al., 2019; Petit et al., 2016) and the biological relevance of the initial observation in the OSS cell line remains unclear. Thus, flies appear to be different from mosquitoes regarding a possible role of piRNAs in antiviral immunity. This observation highlights the need to proceed with caution when extrapolating results from drosophila to other insects, as further emphasized below.

A recent pan-arthropod metagenomic analysis revealed that somatic piRNAs targeting transposable elements are common among arthropods, unlike drosophila. The same study suggested that although some viruses may be targeted by somatic piRNAs in mosquitoes, the primary antiviral defense against viruses across arthropod relies on siRNAs, as observed in flies (Lewis et al., 2018). Of note, the importance of the siRNA pathway in antiviral defense in drosophila and in the nematode *Caenorhabditis elegans*, two popular laboratory animal models, has led to the assumption that RNAi represented the default antiviral pathway in invertebrates, before the emergence of IFNs in vertebrates (tenOever, 2016). Interestingly, this view has been challenged lately as metagenomic sequencing analysis failed to identify canonical vsiRNAs in most animals belonging to divergent phyla (Porifera, Cnidaria, Echinodermata, Mollusca and Annelida) (Waldron et al., 2018). Even in drosophila, antiviral resistance mechanisms independent of RNA silencing are emerging in some tissues, e.g. epithelia (Martins et al., 2019; Mondotte et al., 2018; Palmer et al., 2020). Therefore, the prominent role of RNAi in antiviral immunity described for arthropods and nematodes may not be representative of the majority of invertebrates (Waldron et al., 2018).

3. Inducible responses to virus infection in flies

The recent discovery of IFN-like induced responses to virus infection in oysters (Lafont et al., 2020; Martins, 2020) and the conservation of the cGAS-STING pathway in the sea anemone *Nematostella vectensis* (Kranzusch et al., 2015) suggest that ancestral metazoan antiviral immunity involved induced expression of antiviral factors. Virus infection in drosophila is associated with important modifications of the host transcriptome (e.g. Dostert et al., 2005; Kemp et al., 2013; Merkling et al., 2015b; Xu et al., 2012). Some of these modifications reflects the altered physiology of infected flies. For example, DCV infection of the smooth muscle cells surrounding the crop, a food storage organ at the entry of the midgut, results in accumulation of peritrophic matrix at the entry of the midgut and intestinal obstruction. This alters the physiology of the flies and results in strong repression of a large number of genes associated with digestion (e.g. Jonah proteases) upon DCV infection (Arnold et al., 2013; Chtarbanova et al., 2014). Viral infections are also associated with cellular and tissular stress (e.g. inhibition of cap-dependent translation by internal ribosome entry site (IRES)-containing viruses, release of cell debris upon cell lysis, accumulation of unfolded proteins). Such stress can result in gene induction, as suggested by the upregulation of heat-shock proteins upon viral infection (Merkling et al., 2015b). The first pathway reported to be associated with antiviral immunity in flies, the Janus kinase/signal transducer and activator of transcription (Jak/STAT) pathway, highlights the difficulty to dissociate stress responses from *bona fide* immune mechanisms.

3.1. The Jak/STAT pathway and antiviral defense in drosophila

The Jak/STAT signalling pathway is highly conserved in metazoan.

In mammals, there are 4 Jak kinases and 7 STAT factors that mediate signalling downstream of receptors for many cytokines, including IFNs (Aaronson and Horvath, 2002). In drosophila, the pathway is composed of a single Jak kinase, Hopscotch (Hop (Hanratty and Dearolf, 1993; Perrimon and Mahowald, 1986)) and a single STAT factor STAT92E (Hou et al., 1996; Yan et al., 1996), acting downstream of the receptor Domeless (Dome), a homologue of the gp130 subunit of the receptors for cytokines of the interleukin-6 family (Brown et al., 2001). The drosophila genome encodes three cytokine-like Unpaired (Upd) proteins, which function as activating ligands for the Dome receptor (Harrison et al., 1998; Hombría et al., 2005; Wang et al., 2014). Initially characterized in drosophila for its developmental functions, the Jak/-STAT pathway is also involved in tissue homeostasis in adult flies (reviewed in (Zeidler and Bausek, 2013)). Whereas Upd1 appears to function mainly in development, Upd2 and 3 are induced by a number of stresses, including viral infection (Kemp et al., 2013; West and Silverman, 2018; Wright et al., 2011).

Analysis of the transcriptome of DCV-infected flies revealed induction of a number of genes enriched for STAT92E binding sites in their promoter regions. Mutational analysis of the promoter of the highly induced marker gene *vir-1* confirmed that these sites were essential for gene induction (Dostert et al., 2005). Genetic analysis confirmed that *vir-1* and a number of other genes are no longer induced by DCV infection in *Hop* mutant flies. Moreover, these flies are more sensitive to DCV and CrPV infection, although no phenotype was observed for other RNA or DNA viruses (Kemp et al., 2013). These results point to a role for Jak/STAT regulated genes in antiviral response against *Dicistroviridae*, even if antiviral effectors induced by the pathway have not yet been identified (Dostert et al., 2005b; Kemp et al., 2013, Fig. 1). In another study, Merkling et *al.* reported a role for *G9a*, encoding a histone H3 lysine 9 methyltransferase, in the regulation of the Jak/STAT pathway (Merkling et al., 2015a). *G9a* mutant flies present a shortened lifespan upon infection with the RNA viruses DCV, CrPV, Flock House virus (FHV, Table 1) and Drosophila X virus (DXV, Table 1), which is not associated with increased viral load but rather with a hyperactivation of the Jak/STAT pathway. These results suggest that the epigenetic regulator G9a modulates the activation of the Jak/STAT pathway in response to infection by RNA viruses, in order to prevent deleterious effects caused by hyperactivation (Fig. 1). Of note, the authors observed induction of *vir-1* and of the stress-induced *Turandot* genes, *TotA* and *TotM* (Ekengren et al., 2001), 24h after DCV, CrPV, DXV and FHV infections. In contrast, Kemp and collaborators did not detect induction of *vir-1* upon DXV infection and only observed upregulation of *Tot* genes a few days after DCV infection, when the flies were starting to die (Kemp et al., 2013). These discrepancies may be explained by differences in the genetic background of the flies used, which could affect induction patterns

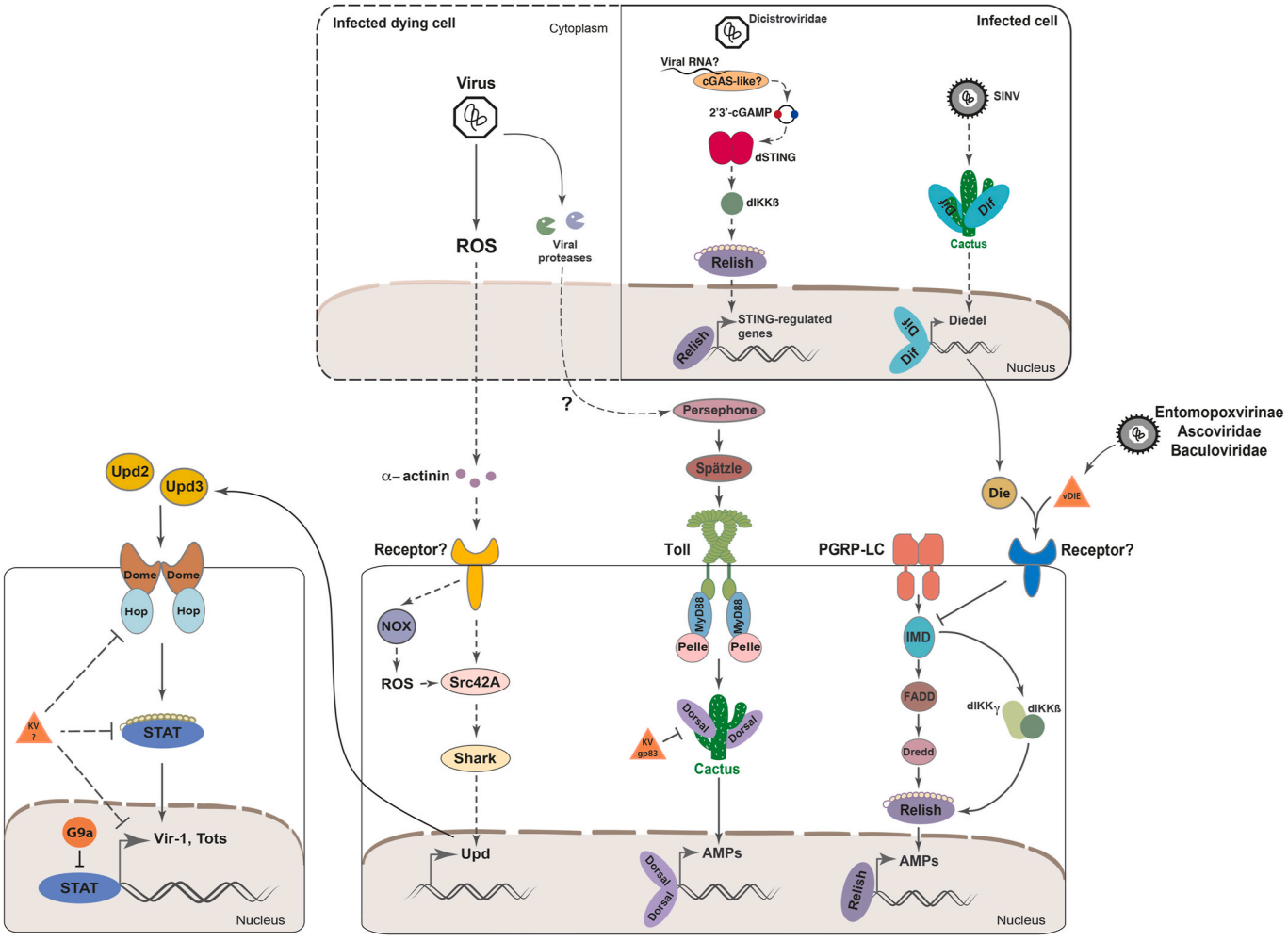

Fig. 1. Inducible antiviral responses in drosophila. The main signalling pathways associated with antiviral immunity in *D. melanogaster* are shown. Some responses are thought to be induced in infected cells, upon sensing infection (e.g. STING pathway), while others occur in response to cytokines (e.g. Diedel, Spätzle, Upd). Infected dying cells can release cellular components (e.g. α-actinin), detected as danger signals in a paracrine manner by other cells. Viral suppressors targeting these pathways are shown as orange triangles. See the text for details. (For interpretation of the references to colour in this figure legend, the reader is referred to the Web version of this article.)

of the *Turandot* and *vir-1* genes depending on the virus used for the infection, or environmental conditions of infection (e.g. dose of virus, fly media, microbiota).

The role of the Jak/STAT pathway is not limited to the response against RNA viruses, as it also controls the DNA virus Invertebrate iridescent virus (IIV)-6 (Table 1). IIV-6 infection significantly decreases the lifespan of STAT92E silenced flies (West and Silverman, 2018). Using S2 cells and flies carrying Upd hypomorphic alleles, these authors further demonstrated that IIV-6 infection induces expression of the three Upd proteins, which function redundantly to activate the Jak/STAT pathway. In these circumstances, the induction of the cytokines relies on the MAP-kinase p38b, one of the three drosophila p38 homologs. Accordingly, p38b mutant flies succumb more rapidly to IIV-6 infection than controls. West and Silverman further showed that induction of Upd expression required the NADPH oxidase NOX, suggesting that reactive oxygen species (ROS) production, resulting from the viral infection, is triggering activation of p38b. Of note, α-actinin, a component of the cortical cytoskeleton, which can be released upon tissue injury, was also shown to induce Upd3 in a NOX-dependent manner leading to the activation of the Jak/STAT pathway (Gordon et al., 2018; Srinivasan et al., 2016). Notably, signalling to Upd3 induction involved Shark and Src42A, the drosophila homologs of the mammalian Tyrosine kinases Syk and Src, respectively, which mediate induction of inflammation and adaptative immunity upon sensing actin, another cortical component of the cytoskeleton. Altogether, these data suggest that release of α-actinin upon IIV-6 triggered cell death induces production of Upd cytokines, leading to the activation of the Jak/STAT pathway (Fig. 1).

In summary, the Jak/STAT pathway seems to be induced primarily as a result of cell damage caused by viral infection, rather than by directly sensing viral molecular patterns in drosophila. In addition, this pathway appears to primarily increase resilience to infection, rather than resistance, as mutant flies exhibit increased lethality, with little or no impact on viral titres (Merkling et al., 2015a; West and Silverman, 2018). Alternatively, the viruses tested may have evolved suppressor mechanisms opposing antiviral effectors induced by the Jak/STAT pathway. In this regard, it is interesting to note that infection of S2 cells by the newly discovered DNA virus KV resulted in downregulation of a reporter gene driven by a synthetic promoter composed of 10 STAT-binding sites (Palmer et al., 2019). This suggests that KV encodes a suppressor, the characterization of which would provide strong evidence for the importance of the Jak/STAT pathway in antiviral immunity in flies.

3.2. Control of viral infections by the Toll pathway

Two distinct pathways, Toll and IMD, rely on NF-κB transcription factors to regulate expression of AMPs genes in drosophila ((Buchon et al., 2014) and references therein). Toll regulates Dorsal (Dl) and Dorsal-related immunity factor (DIF), whereas IMD controls the third member of the family in drosophila, Relish. These pathways have well established roles in the control of bacterial and fungal infections but involvement in antiviral defence has also been suggested (Fig. 1).

A comprehensive study by Teixeira and collaborators reported the involvement of the Toll pathway in the defence against a broad range of RNA viruses (DCV, CrPV, FHV, Nora virus (Table 1)(Ferreira et al., 2014)). Interestingly, the authors observed that the Toll pathway is important to survive oral infection but not systemic infection by these viruses, even though activation of the Toll pathway is detected in the fat body following both types of infection. This emphasizes the importance of the route of infection for host-pathogen interaction (Martins et al., 2013). Furthermore, the data suggest that the Toll pathway is targeting a step of the viral cycle occurring specifically in the course of oral infection and bypassed by an injection directly in the hemocoel (Ferreira et al., 2014). Of note, in addition to *spaetzle, Toll* and *pelle*, *dorsal* mutants presented an increased susceptibility to oral infection while *Dif* mutant did not. These results suggest that, while DIF mediates the Toll-dependent response triggered by bacteria and fungi infection (Rutschmann et al., 2000), Dl is responsible for antiviral defences (Ferreira et al., 2014), providing an explanation for the long-noted expression of Dl in the fat body of adult flies (Lemaitre et al., 1995).

Obbard and colleagues did not observe increased sensitivity of Toll pathway mutant flies to infection with the DNA virus KV, which may be explained by the fact that they did not use an oral infection model. However, they reported a strong suppression of Toll pathway activity in KV infected flies (Palmer et al., 2019). They further identified a previously uncharacterized KV gene, gp83, which encodes a potent suppressor of Toll signalling (Fig. 1). The mode of action of this nuclear protein, which appears to act downstream of DIF or Dl, is still mysterious. Whatever the mechanism, identification of a viral suppressor provides further evidence for a role of the Toll pathway in antiviral immunity.

Overall, these findings raise the question of the mechanism by which viral infection may activate the Toll pathway. One possibility is that tissue damage and necrosis caused by viral infection may result in activation of the Toll pathway through activation of the Persephone (psh) protease (Fig. 1 (Ming et al., 2014; Tang et al., 2008)). Another important question pertains to the induction of an antiviral versus antifungal response by the Toll pathway. While it could be argued that DIF and Dl may regulate antifungal and antiviral effector genes, respectively, it is intriguing that some reports suggest an involvement of DIF, rather than Dl, in antiviral immunity, independently of the canonical Toll pathway. Indeed, *dif*, but not *spz*, *Tl*, *tube* or *pelle,* mutant flies were reported to exhibit increased sensitivity to DXV (Zambon et al., 2005). Although the genetic background was not controlled in these early experiments, it is intriguing that induction of the cytokine Diedel (Die) following Sindbis virus (SINV, Table 1) infection depends on DIF but not MyD88, which is the adaptor of the canonical Toll pathway (Lamiable et al., 2016b, Fig. 1). Finally, a recent report points to the activation of a non-canonical pathway leading to expression of two Toll-regulated AMPs, drosomycin and attacin-A in response to DCV infection (Zhang et al., 2020). This highlights the importance of further investigations on the role of the Toll pathway in antiviral immunity and on the respective contributions of DIF and Dl in the expression of genes involved in antiviral defenses.

3.3. Relish-dependent antiviral immunity

A role of the IMD pathway in the resistance to CrPV and SINV was first reported in 2009 (Avadhanula et al., 2009; Costa et al., 2009), followed a few years later by the description of antiviral activity for two antimicrobial peptides, Diptericin-B and Attacin-C (Huang et al., 2013). It is interesting to note that, besides its role in the expression of antibacterial peptides, the IMD pathway is also implicated in the regulation of apoptosis (Georgel et al., 2001; Tavignot et al., 2017; Zhai et al., 2018). Indeed, programmed cell death represents an efficient antiviral defense, interrupting viral replication (Liu et al., 2013). Efficient phagocytosis of apoptotic cells further prevents dissemination of viruses (Lamiable et al., 2016a; Nainu et al., 2015). In drosophila, apoptosis is largely controlled at the level of the inhibitory protein DIAP1, which prevents activation of caspases. The IMD pathway may regulate apoptosis in the context of viral infection by triggering DIAP1 protein degradation via DIAP2-mediated polyubiquitination (Herman-Bachinsky et al., 2007). However, the situation is likely to be more complex as IMD signalling antagonizes apoptosis in some tissues during development by upregulating *DIAP1* gene transcription (Tavignot et al., 2017). Of note, DCV was shown to suppress the N-end rule pathway, one of the mechanisms causing DIAP1 degradation. This enables the virus to block or slow down programmed cell death resulting in enhanced replication (Wang et al., 2017).

Characterization of the virus-induced gene *Die* confirmed a role of the IMD pathway in antiviral immunity (Lamiable et al., 2016b). Indeed, *Die* mutant flies were more sensitive to infection with SINV than controls

and early lethality was not accompanied by increased viral titer but rather correlated with strong upregulation of IMD target genes. Flies double mutant for *Die* and *IMD* or *ikkγ* resisted like wild-type flies to SINV infection, confirming that it was the overactivation of the IMD pathway, rather than the lack of Die *per se*, that caused the demise of the flies. *Die* encodes a small circulating protein that probably functions as an immunomodulatory cytokine downregulating the IMD pathway by an unknown mechanism (Lamiable et al., 2016b). Intriguingly, this cytokine also appears to inhibit apoptosis in developmental contexts (Mlih et al., 2018). *Die*-related genes can be found in the genomes of DNA viruses belonging to at least three families (Ascoviridae, Entomopoxviridae, Baculoviridae, Fig. 1), and at least one of them can rescue the phenotype of *Die*-mutant flies (Lamiable et al., 2016b). This result indicates that insect viruses have, on several occasions, hijacked a suppressor gene of the IMD pathway, suggesting that activation of this pathway during infection exerts a pressure on viruses. Interestingly, IIV-6 does not encode a Die homologue but expresses another as yet poorly characterized suppressor of IMD signalling, acting in the nucleus at the level of Relish-mediated transcriptional activation (West et al., 2019).

Together with previous results reporting inhibition of NF-κB signalling by vankyrin proteins encoded by polydnaviruses (Gueguen et al., 2013), these recent findings prompted a careful examination of the role of the IMD pathway in the control of viral infection in the S2 cell line. This revealed that silencing of IKKβ and Relish resulted in significantly increased replication of DCV. Unexpectedly, silencing of the other genes of the IMD pathway did not affect viral load, with the exception of IKKγ/NEMO, the regulatory subunit of the IKK complex, for which viral replication was decreased (Goto et al., 2018). This suggested that downstream components of the pathway could be activated independently of IMD in response to a viral infection. One of the genes induced by DCV infection in an IKKβ and Relish-dependent manner is the homologue of the gene STING (stimulator of interferon genes). In mammals, STING is a key component of the cytosolic DNA sensing system, activating IFN genes in response to a second messenger, the cyclic dinucleotide (CDN) 2′3′-cyclic GMP-AMP (2′3′-cGAMP). This CDN contains one 2′,5′ phosphodiester bond joining G to A and one canonical 3′,5′-phosphodiester bond joining A to G. It is produced by the enzyme cyclic GMP-AMP synthase (cGAS), which becomes activated upon binding DNA or DNA/RNA duplexes in the cytosol (reviewed in (Ablasser and Chen, 2019)). Of note, STING can also be activated by CDNs of bacterial origin, which contain two canonical 3′,5′ phosphodiester-linkages (3′3′-cGAMP, c-di-GMP, c-di-AMP (Margolis et al., 2017)). In drosophila cells, ectopic expression of dSTING can prevent replication of DCV in an IKKβ- and Relish-dependent manner, suggesting that dSTING acts upstream of these two proteins in a new pathway activated by viral infections (Goto et al., 2018). Interestingly, similar results were reported in *Bombyx mori*, where a homologue of STING activates Relish and antiviral immunity in response to infection by nucleopolyhedrovirus (NPV (Hua et al., 2018)). Altogether, these results suggest that an ancestral function of the evolutionarily ancient molecule STING is the regulation of NF-κB-dependent transcription of antiviral genes, predating the appearance of IFNs (Fig. 1). Of note, activation of Relish by the IMD pathway in response to bacterial infections requires both its phosphorylation by IKKβ and its cleavage by the caspase DREDD in a process that involves the IKKγ/NEMO protein (reviewed in (Buchon et al., 2014)). By contrast, activation of Relish by dSTING does not appear to require DREDD and is opposed by IKKγ/NEMO (Goto et al., 2018).

It is noteworthy that an IMD-independent function of Relish has previously been described in salivary gland degradation during metamorphosis (Nandy et al., 2018). Thus, besides the IMD pathway, Relish can be regulated by non-classical pathways and activate transcriptional outputs distinct from the IMD pathway, probably in association with specific transcription cofactors (Zhai et al., 2018). Interestingly, Relish regulates expression of the gene *Atg1* in salivary glands to trigger autophagy-dependent cell death. This may provide a connection with the role of dSTING in antiviral immunity. Indeed, in mammals, besides expression of IFNs, STING also regulates autophagy, which is thought to represent an ancestral antiviral function (Gui et al., 2019; Margolis et al., 2017). Similarly, dSTING was reported to induce autophagy in the drosophila brain to control ZIKA virus replication (Liu et al., 2018).

A major question at this point pertains to the activation of Relish in virus-infected flies. In the absence of bacterial infection, the IMD pathway may be activated by a response to necrotic cells possibly driven by dysbiosis (Kosakamoto et al., 2020) or by deregulation of the expression of the receptors PGRP-LC or -LF (Nandy et al., 2018; Tavignot et al., 2017). The involvement of dSTING in the regulation of Relish activity in the context of viral infections now raises the question of the mechanisms by which it gets activated. The drosophila genome encodes one obvious cGAS homologue, CG7194, which does not seem to participate in antimicrobial defenses (Martin et al., 2018; Wu et al., 2014). This led Goodman and colleagues to propose that in drosophila, dSTING is activated by bacterial CDNs, rather than the host-produced second messenger 2′3′-cGAMP. However, we recently observed that 2′3′-cGAMP is a more potent activator of STING-regulated genes in drosophila than 3′3′-linked bacterial CDNs (Cai et al., 2020). This suggests that a cGAS-like enzyme might exist in drosophila, as already reported in the sea anemone *Nematostella vectensis* (Kranzusch et al., 2015) and as proposed in the Lepidopteran insect *B. mori* (Hua et al., 2018).

4. Concluding remarks

Recent work in the field of drosophila antiviral immunity, while improving our understanding on the contribution of small regulatory RNAs, have provided increasing evidence that induced immune responses, and in particular NF-κB pathways, also play an important role. Interestingly, inducible antiviral immune responses appear to play an important role in other invertebrates as well (e.g. (Lafont et al., 2017)). While initial studies suggested that invertebrates primarily relied on ancestral RNAi response to control viruses, which was replaced by IFN-regulated inducible responses in vertebrates, a more complex picture is now emerging. In particular, it is now clear that inducible antiviral immune responses predate the appearance of IFNs in vertebrates, and that some antiviral genes (e.g. cGAS, viperin, STING) were inherited from procaryotes (Bernheim et al., 2020; Cohen et al., 2019; Morehouse et al., 2020; Sen and Peters, 2007). Of note, important differences among insects are also becoming apparent (e.g. presence of virus-derived piRNAs in mosquitoes but not in drosophila; absence of the STING gene in mosquitoes). These differences are not surprising in light of the strong pressures exerted on host genomes by rapidly mutating viruses. Documenting these differences and their analysis can reveal important information on the mechanisms at play in the arms race between viruses and the immune system of their hosts (Daugherty and Malik, 2012). In summary, while *D. melanogaster* will continue to be an invaluable tool in future work to decipher the complex host-virus interactions (e.g. molecular mechanisms of pathogenesis (Chow et al., 2017)), caution should be exerted before extrapolating findings in this model to other insects, all the more so to invertebrates in general.

The basic mechanisms involved in the restriction of viruses by the siRNA pathway in drosophila have now been well characterized, although key questions remain. Among them, the question of the sensing of viral RNAs is central, as it is now clear that there is more to it than the double strandedness of replication intermediates, for example. Future work will need to determine if the discrimination between viral and self RNAs involves the quantity of template for Dcr-2, differences at the extremities of the RNAs or their subcellular localization, all of which contribute to the activation of nucleic acid sensing pattern recognition receptors (PRRs) in mammalian cells (Roers et al., 2016). Clarification of the role of dsRBPs cofactors represents another priority for the field, together with the elucidation of the mechanism by which an intrinsically cell autonomous process (Roignant et al., 2003) can generate a systemic

response in the context of viral infections (Saleh et al., 2009; Tassetto et al., 2017).

Regarding the emerging role of induced responses, the key question for future work relates to the identification of the receptors sensing viral infections, in particular whether these responses involve *bona fide* PRRs, and in this case what types of molecular patterns are recognized. The field will also greatly benefit from the investigation of the modes of action of viral suppressors of inducible responses, which could reveal new regulatory facets of inducible immunity pathways. The interplay of the IMD- and dSTING-dependent Relish functions in response to bacterial and viral infections, respectively, also deserves attention, as highlighted by the contribution of the microbiota to antiviral immunity (Sansone et al., 2015; Teixeira et al., 2008; Xu et al., 2013). Last but not least, a major unsolved question is the function of the many induced genes, which contribute to the control of viral infections. Indeed, the functional characterization of new antiviral factors could reveal original targets for the design of therapy against families of viruses infecting both insects and mammals, such as picorna-like viruses, alphaviruses, rhabdoviruses or poxviruses (Shi et al., 2016).

Acknowledgements

We thank our colleagues Joao T. Marques and Nelson Martins for critical reading of the manuscript and helpful suggestions. Work in our laboratory is supported by CNRS, the Investissements d'avenir program (Labex NetRNA: ANR-10-LABX-0036; Equipex I2MC: ANR-11-EQPX-0022) and ANR (ANR-17-CE15-0014). JS is supported by a fellowship from the Ministère de l'Enseignement supérieur, de la Recherche et de l'Innovation and JLI acknowledges financial support from the Institut Universitaire de France.

References

Aaronson, D.S., Horvath, C.M., 2002. A road map for those who don't know JAK-STAT. Science 296, 1653–1655. https://doi.org/10.1126/science.1071545.

Ablasser, A., Chen, Z.J., 2019. cGAS in action: expanding roles in immunity and inflammation. Science 363. https://doi.org/10.1126/science.aat8657.

Aguiar, E.R.G.R., Olmo, R.P., Marques, J.T., 2016. Virus-derived small RNAs: molecular footprints of host-pathogen interactions, 7. Wiley Interdiscip Rev RNA, pp. 824–837. https://doi.org/10.1002/wrna.1361.

Aliyari, R., Wu, Q., Li, H.-W., Wang, X.-H., Li, F., Green, L.D., Han, C.S., Li, W.-X., Ding, S.-W., 2008. Mechanism of induction and suppression of antiviral immunity directed by virus-derived small RNAs in Drosophila. Cell Host Microbe 4, 387–397. https://doi.org/10.1016/j.chom.2008.09.001.

Arnold, P.A., Johnson, K.N., White, C.R., 2013. Physiological and metabolic consequences of viral infection in Drosophila melanogaster. J. Exp. Biol. 216, 3350–3357. https://doi.org/10.1242/jeb.088138.

Asad, S., Parry, R., Asgari, S., 2018. Upregulation of Aedes aegypti Vago1 by Wolbachia and its effect on dengue virus replication. Insect Biochem. Mol. Biol. 92, 45–52. https://doi.org/10.1016/j.ibmb.2017.11.008.

Avadhanula, V., Weasner, B.P., Hardy, G.G., Kumar, J.P., Hardy, R.W., 2009. A novel system for the launch of alphavirus RNA synthesis reveals a role for the Imd pathway in arthropod antiviral response. PLoS Pathog. 5, e1000582 https://doi.org/10.1371/journal.ppat.1000582.

Bernheim, A., Millman, A., Ofir, G., Meitav, G., Avraham, C., Shomar, H., Rosenberg, M. M., Tal, N., Melamed, S., Amitai, G., Sorek, R., 2020. Prokaryotic viperins produce diverse antiviral molecules. Nature. https://doi.org/10.1038/s41586-020-2762-2.

Brennecke, J., Aravin, A.A., Stark, A., Dus, M., Kellis, M., Sachidanandam, R., Hannon, G. J., 2007. Discrete small RNA-generating loci as master regulators of transposon activity in Drosophila. Cell 128, 1089–1103. https://doi.org/10.1016/j.cell.2007.01.043.

Bronkhorst, A.W., van Cleef, K.W.R., Vodovar, N., Ince, I.A., Blanc, H., Vlak, J.M., Saleh, M.-C., van Rij, R.P., 2012. The DNA virus Invertebrate iridescent virus 6 is a target of the Drosophila RNAi machinery. Proc. Natl. Acad. Sci. U.S.A. 109, E3604–E3613. https://doi.org/10.1073/pnas.1207213109.

Brown, S., Hu, N., Hombría, J.C., 2001. Identification of the first invertebrate interleukin JAK/STAT receptor, the Drosophila gene domeless. Curr. Biol. 11, 1700–1705. https://doi.org/10.1016/s0960-9822(01)00524-3.

Buchon, N., Silverman, N., Cherry, S., 2014. Immunity in Drosophila melanogaster–from microbial recognition to whole-organism physiology. Nat. Rev. Immunol. 14, 796–810. https://doi.org/10.1038/nri3763.

Cai, H., Holleufer, A., Simonsen, B., Schneider, J., Lemoine, A., Gad, H.H., Huang, Jingxian, Huang, Jieqing, Chen, D., Peng, T., Marques, J.T., Hartmann, R., Martins, N.E., Imler, J.-L., 2020. 2'3'-cGAMP triggers a STING- and NF-κB-dependent broad antiviral response in Drosophila. Sci. Signal. 13 https://doi.org/10.1126/scisignal.abc4537.

Cao, C., Cogni, R., Barbier, V., Jiggins, F.M., 2017. Complex coding and regulatory polymorphisms in a restriction factor determine the susceptibility of Drosophila to viral infection. Genetics 206, 2159–2173. https://doi.org/10.1534/genetics.117.201970.

Cao, C., Magwire, M.M., Bayer, F., Jiggins, F.M., 2016. A polymorphism in the processing body component Ge-1 controls resistance to a naturally occurring rhabdovirus in Drosophila. PLoS Pathog. 12, e1005387 https://doi.org/10.1371/journal.ppat.1005387.

Cenik, E.S., Fukunaga, R., Lu, G., Dutcher, R., Wang, Y., Tanaka Hall, T.M., Zamore, P.D., 2011. Phosphate and R2D2 restrict the substrate specificity of dicer-2, an ATP-driven ribonuclease. Mol. Cell 42, 172–184. https://doi.org/10.1016/j.molcel.2011.03.002.

Chow, J., Kagan, J.C., 2018. Chapter three - the fly way of antiviral resistance and disease tolerance. In: Alt, F. (Ed.), Advances in Immunology. Academic Press, pp. 59–93. https://doi.org/10.1016/bs.ai.2018.08.002.

Chow, J., Márka, Z., Bartos, I., Márka, S., Kagan, J.C., 2017. Environmental stress causes lethal neuro-trauma during asymptomatic viral infections. Cell Host Microbe 22, 48–60. https://doi.org/10.1016/j.chom.2017.06.010 e5.

Chtarbanova, S., Lamiable, O., Lee, K.-Z., Galiana, D., Troxler, L., Meignin, C., Hetru, C., Hoffmann, J.A., Daeffler, L., Imler, J.-L., 2014. Drosophila C virus systemic infection leads to intestinal obstruction. J. Virol. 88, 14057–14069. https://doi.org/10.1128/JVI.02320-14.

Cohen, D., Melamed, S., Millman, A., Shulman, G., Oppenheimer-Shaanan, Y., Kacen, A., Doron, S., Amitai, G., Sorek, R., 2019. Cyclic GMP-AMP signalling protects bacteria against viral infection. Nature 574, 691–695. https://doi.org/10.1038/s41586-019-1605-5.

Coll, O., Guitart, T., Villalba, A., Papin, C., Simonelig, M., Gebauer, F., 2018. Dicer-2 promotes mRNA activation through cytoplasmic polyadenylation. RNA 24, 529–539. https://doi.org/10.1261/rna.065417.117.

Costa, A., Jan, E., Sarnow, P., Schneider, D., 2009. The Imd pathway is involved in antiviral immune responses in Drosophila. PLoS ONE 4, e7436. https://doi.org/10.1371/journal.pone.0007436.

Czech, B., Malone, C.D., Zhou, R., Stark, A., Schlingeheyde, C., Dus, M., Perrimon, N., Kellis, M., Wohlschlegel, J.A., Sachidanandam, R., Hannon, G.J., Brennecke, J., 2008. An endogenous small interfering RNA pathway in Drosophila. Nature 453, 798–802. https://doi.org/10.1038/nature07007.

Daugherty, M.D., Malik, H.S., 2012. Rules of engagement: molecular insights from host-virus arms races. Annu. Rev. Genet. 46, 677–700. https://doi.org/10.1146/annurev-genet-110711-155522.

Deddouche, S., Matt, N., Budd, A., Mueller, S., Kemp, C., Galiana-Arnoux, D., Dostert, C., Antoniewski, C., Hoffmann, J.A., Imler, J.-L., 2008. The DExD/H-box helicase Dicer-2 mediates the induction of antiviral activity in drosophila. Nat. Immunol. 9, 1425–1432. https://doi.org/10.1038/ni.1664.

Deng, P., Khan, A., Jacobson, D., Sambrani, N., McGurk, L., Li, X., Jayasree, A., Hejatko, J., Shohat-Ophir, G., O'Connell, M.A., Li, J.B., Keegan, L.P., 2020. Adar RNA editing-dependent and -independent effects are required for brain and innate immune functions in Drosophila. Nat. Commun. 11, 1580. https://doi.org/10.1038/s41467-020-15435-1.

Donelick, H.M., Talide, L., Bellet, M., Aruscavage, J., Lauret, E., Aguiar, E., Marques, J.T., Meignin, C., Bass, B.L., 2020. In Vitro Studies Provide Insight into Effects of Dicer-2 Helicase Mutations in Drosophila melanogaster. RNA. https://doi.org/10.1261/rna.077289.120.

Dostert, C., Jouanguy, E., Irving, P., Troxler, L., Galiana-Arnoux, D., Hetru, C., Hoffmann, J.A., Imler, J.-L., 2005a. The Jak-STAT signaling pathway is required but not sufficient for the antiviral response of drosophila. Nat. Immunol. 6, 946–953. https://doi.org/10.1038/ni1237.

Dostert, C., Jouanguy, E., Irving, P., Troxler, L., Galiana-Arnoux, D., Hetru, C., Hoffmann, J.A., Imler, J.-L., 2005b. The Jak-STAT signaling pathway is required but not sufficient for the antiviral response of drosophila. Nat. Immunol. 6, 946–953. https://doi.org/10.1038/ni1237.

Ekengren, S., Tryselius, Y., Dushay, M.S., Liu, G., Steiner, H., Hultmark, D., 2001. A humoral stress response in Drosophila. Curr. Biol. 11, 714–718. https://doi.org/10.1016/s0960-9822(01)00203-2.

Eleftherianos, I., Won, S., Chtarbanova, S., Squiban, B., Ocorr, K., Bodmer, R., Beutler, B., Hoffmann, J.A., Imler, J.-L., 2011. ATP-sensitive potassium channel (K(ATP))-dependent regulation of cardiotropic viral infections. Proc. Natl. Acad. Sci. U.S.A. 108, 12024–12029. https://doi.org/10.1073/pnas.1108926108.

Ferreira, Á.G., Naylor, H., Esteves, S.S., Pais, I.S., Martins, N.E., Teixeira, L., 2014. The Toll-dorsal pathway is required for resistance to viral oral infection in Drosophila. PLoS Pathog. 10, e1004507 https://doi.org/10.1371/journal.ppat.1004507.

Galiana-Arnoux, D., Dostert, C., Schneemann, A., Hoffmann, J.A., Imler, J.-L., 2006. Essential function in vivo for Dicer-2 in host defense against RNA viruses in drosophila. Nat. Immunol. 7, 590–597. https://doi.org/10.1038/ni1335.

Gay, P., 1978. [Drosophila genes which intervene in multiplication of sigma virus (author's transl)]. Mol. Gen. Genet. 159, 269–283. https://doi.org/10.1007/BF00268263.

Georgel, P., Naitza, S., Kappler, C., Ferrandon, D., Zachary, D., Swimmer, C., Kopczynski, C., Duyk, G., Reichhart, J.M., Hoffmann, J.A., 2001. Drosophila immune deficiency (IMD) is a death domain protein that activates antibacterial defense and can promote apoptosis. Dev. Cell 1, 503–514. https://doi.org/10.1016/s1534-5807(01)00059-4.

Gerbasi, V.R., Preall, J.B., Golden, D.E., Powell, D.W., Cummins, T.D., Sontheimer, E.J., 2011. Blanks, a nuclear siRNA/dsRNA-binding complex component, is required for Drosophila spermiogenesis. Proc. Natl. Acad. Sci. U. S. A. 108, 3204–3209. https://doi.org/10.1073/pnas.1009781108.

Ghildiyal, M., Zamore, P.D., 2009. Small silencing RNAs: an expanding universe. Nat. Rev. Genet. 10, 94–108. https://doi.org/10.1038/nrg2504.
Girardi, E., Lefèvre, M., Chane-Woon-Ming, B., Paro, S., Claydon, B., Imler, J.-L., Meignin, C., Pfeffer, S., 2015. Cross-species comparative analysis of Dicer proteins during Sindbis virus infection. Sci. Rep. 5, 10693. https://doi.org/10.1038/srep10693.
Goic, B., Vodovar, N., Mondotte, J.A., Monot, C., Frangeul, L., Blanc, H., Gausson, V., Vera-Otarola, J., Cristofari, G., Saleh, M.-C., 2013. RNA-mediated interference and reverse transcription control the persistence of RNA viruses in the insect model Drosophila. Nat. Immunol. 14, 396–403. https://doi.org/10.1038/ni.2542.
Gold, K.S., Brückner, K., 2015. Macrophages and cellular immunity in Drosophila melanogaster. Semin. Immunol. 27, 357–368. https://doi.org/10.1016/j.smim.2016.03.010.
Gordon, O., Henry, C.M., Srinivasan, N., Ahrens, S., Franz, A., Deddouche, S., Chakravarty, P., Phillips, D., George, R., Kjaer, S., Frith, D., Snijders, A.P., Valente, R.S., Simoes da Silva, C.J., Teixeira, L., Thompson, B., Dionne, M.S., Wood, W., Reis E Sousa, C., 2018. α-actinin accounts for the bioactivity of actin preparations in inducing STAT target genes in Drosophila melanogaster. Elife 7. https://doi.org/10.7554/eLife.38636.
Goto, A., Okado, K., Martins, N., Cai, H., Barbier, V., Lamiable, O., Troxler, L., Santiago, E., Kuhn, L., Paik, D., Silverman, N., Holleufer, A., Hartmann, R., Liu, J., Peng, T., Hoffmann, J.A., Meignin, C., Daeffler, L., Imler, J.-L., 2018. The kinase IKKβ regulates a STING- and NF-κB-Dependent antiviral response pathway in Drosophila. Immunity 49, 225–234. https://doi.org/10.1016/j.immuni.2018.07.013 e4.
Gueguen, G., Kalamarz, M.E., Ramroop, J., Uribe, J., Govind, S., 2013. Polydnaviral ankyrin proteins aid parasitic wasp survival by coordinate and selective inhibition of hematopoietic and immune NF-kappa B signaling in insect hosts. PLoS Pathog. 9, e1003580 https://doi.org/10.1371/journal.ppat.1003580.
Gui, X., Yang, H., Li, T., Tan, X., Shi, P., Li, M., Du, F., Chen, Z.J., 2019. Autophagy induction via STING trafficking is a primordial function of the cGAS pathway. Nature 567, 262–266. https://doi.org/10.1038/s41586-019-1006-9.
Guo, Z., Li, Y., Ding, S.-W., 2019. Small RNA-based antimicrobial immunity. Nat. Rev. Immunol. 19, 31–44. https://doi.org/10.1038/s41577-018-0071-x.
Ha, M., Kim, V.N., 2014. Regulation of microRNA biogenesis. Nat. Rev. Mol. Cell Biol. 15, 509–524. https://doi.org/10.1038/nrm3838.
Hanratty, W.P., Dearolf, C.R., 1993. The Drosophila Tumorous-lethal hematopoietic oncogene is a dominant mutation in the hopscotch locus. Mol. Gen. Genet. 238, 33–37. https://doi.org/10.1007/BF00279527.
Hansen, S.R., Aderounmu, A.M., Donelick, H.M., Bass, B.L., 2019. Dicer's helicase domain: a meeting place for regulatory proteins. Cold Spring Harbor Symp. Quant. Biol. 84, 185–193. https://doi.org/10.1101/sqb.2019.84.039750.
Harrison, D.A., McCoon, P.E., Binari, R., Gilman, M., Perrimon, N., 1998. Drosophila unpaired encodes a secreted protein that activates the JAK signaling pathway. Genes Dev. 12, 3252–3263. https://doi.org/10.1101/gad.12.20.3252.
Harsh, S., Ozakman, Y., Kitchen, S.M., Paquin-Proulx, D., Nixon, D.F., Eleftherianos, I., 2018. Dicer-2 regulates resistance and maintains homeostasis against Zika virus infection in Drosophila. J. Immunol. 201, 3058–3072. https://doi.org/10.4049/jimmunol.1800597.
Herman-Bachinsky, Y., Ryoo, H.-D., Ciechanover, A., Gonen, H., 2007. Regulation of the Drosophila ubiquitin ligase DIAP1 is mediated via several distinct ubiquitin system pathways. Cell Death Differ. 14, 861–871. https://doi.org/10.1038/sj.cdd.4402079.
Hoffmann, J.A., Kafatos, F.C., Janeway, C.A., Ezekowitz, R.A., 1999. Phylogenetic perspectives in innate immunity. Science 284, 1313–1318.
Hombría, J.C.-G., Brown, S., Häder, S., Zeidler, M.P., 2005. Characterisation of Upd2, a Drosophila JAK/STAT pathway ligand. Dev. Biol. 288, 420–433. https://doi.org/10.1016/j.ydbio.2005.09.040.
Hou, X.S., Melnick, M.B., Perrimon, N., 1996. Marelle acts downstream of the Drosophila HOP/JAK kinase and encodes a protein similar to the mammalian STATs. Cell 84, 411–419. https://doi.org/10.1016/s0092-8674(00)81286-6.
Hua, X., Li, B., Song, L., Hu, C., Li, X., Wang, D., Xiong, Y., Zhao, P., He, H., Xia, Q., Wang, F., 2018. Stimulator of interferon genes (STING) provides insect antiviral immunity by promoting Dredd caspase-mediated NF-κB activation. J. Biol. Chem. 293, 11878–11890. https://doi.org/10.1074/jbc.RA117.000194.
Huang, Z., Kingsolver, M.B., Avadhanula, V., Hardy, R.W., 2013. An antiviral role for antimicrobial peptides during the arthropod response to alphavirus replication. J. Virol. 87, 4272–4280. https://doi.org/10.1128/JVI.03360-12.
Hultmark, D., 2003. Drosophila immunity: paths and patterns. Curr. Opin. Immunol. 15, 12–19. https://doi.org/10.1016/S0952-7915(02)00005-5.
Jousset, F.X., Plus, N., Croizier, G., Thomas, M., 1972. [Existence in Drosophila of 2 groups of picornavirus with different biological and serological properties]. C. R. Hebd. Seances Acad. Sci. Ser. D Sci. Nat. 275, 3043–3046.
Kawamura, Y., Saito, K., Kin, T., Ono, Y., Asai, K., Sunohara, T., Okada, T.N., Siomi, M. C., Siomi, H., 2008. Drosophila endogenous small RNAs bind to Argonaute 2 in somatic cells. Nature 453, 793–797. https://doi.org/10.1038/nature06938.
Kemp, C., Mueller, S., Goto, A., Barbier, V., Paro, S., Bonnay, F., Dostert, C., Troxler, L., Hetru, C., Meignin, C., Pfeffer, S., Hoffmann, J.A., Imler, J.-L., 2013. Broad RNA interference-mediated antiviral immunity and virus-specific inducible responses in Drosophila. J. Immunol. 190, 650–658. https://doi.org/10.4049/jimmunol.1102486.
Kennedy, E.M., Kornepati, A.V.R., Bogerd, H.P., Cullen, B.R., 2017. Partial reconstitution of the RNAi response in human cells using Drosophila gene products. RNA 23, 153–160. https://doi.org/10.1261/rna.059345.116.
Khong, A., Kerr, C.H., Yeung, C.H.L., Keatings, K., Nayak, A., Allan, D.W., Jan, E., 2017. Disruption of stress granule formation by the multifunctional Cricket Paralysis virus 1A protein. J. Virol. 91 https://doi.org/10.1128/JVI.01779-16.
Kolakofsky, D., Kowalinski, E., Cusack, S., 2012. A structure-based model of RIG-I activation. RNA 18, 2118–2127. https://doi.org/10.1261/rna.035949.112.
Kosakamoto, H., Yamauchi, T., Akuzawa-Tokita, Y., Nishimura, K., Soga, T., Murakami, T., Mori, H., Yamamoto, K., Miyazaki, R., Koto, A., Miura, M., Obata, F., 2020. Local necrotic cells trigger systemic immune activation via gut microbiome dysbiosis in Drosophila. Cell Rep. 32, 107938. https://doi.org/10.1016/j.celrep.2020.107938.
Kowalinski, E., Lunardi, T., McCarthy, A.A., Louber, J., Brunel, J., Grigorov, B., Gerlier, D., Cusack, S., 2011. Structural basis for the activation of innate immune pattern-recognition receptor RIG-I by viral RNA. Cell 147, 423–435. https://doi.org/10.1016/j.cell.2011.09.039.
Kranzusch, P.J., Wilson, S.C., Lee, A.S.Y., Berger, J.M., Doudna, J.A., Vance, R.E., 2015. Ancient origin of cGAS-STING reveals mechanism of universal 2',3' cGAMP signaling. Mol. Cell. 59, 891–903. https://doi.org/10.1016/j.molcel.2015.07.022.
Lacey, L.A., Grzywacz, D., Shapiro-Ilan, D.I., Frutos, R., Brownbridge, M., Goettel, M.S., 2015. Insect pathogens as biological control agents: back to the future. J. Invertebr. Pathol. 132, 1–41. https://doi.org/10.1016/j.jip.2015.07.009.
Lafont, M., Petton, B., Vergnes, A., Pauletto, M., Segarra, A., Gourbal, B., Montagnani, C., 2017. Long-lasting antiviral innate immune priming in the Lophotrochozoan Pacific oyster, Crassostrea gigas. Sci. Rep. 7, 13143. https://doi.org/10.1038/s41598-017-13564-0.
Lafont, M., Vergnes, A., Vidal-Dupiol, J., de Lorgeril, J., Gueguen, Y., Haffner, P., Petton, B., Chaparro, C., Barrachina, C., Destoumieux-Garzon, D., Mitta, G., Gourbal, B., Montagnani, C., 2020. A sustained immune response supports long-term antiviral immune priming in the pacific oyster, Crassostrea gigas. mBio 11. https://doi.org/10.1128/mBio.02777-19.
Lamiable, O., Arnold, J., de Faria, I.J., da, S., Olmo, R.P., Bergami, F., Meignin, C., Hoffmann, J.A., Marques, J.T., Imler, J.-L., 2016a. Analysis of the contribution of hemocytes and autophagy to Drosophila antiviral immunity. J. Virol. 90, 5415–5426. https://doi.org/10.1128/JVI.00238-16.
Lamiable, O., Kellenberger, C., Kemp, C., Troxler, L., Pelte, N., Boutros, M., Marques, J. T., Daeffler, L., Hoffmann, J.A., Roussel, A., Imler, J.-L., 2016b. Cytokine Diedel and a viral homologue suppress the IMD pathway in Drosophila. Proc. Natl. Acad. Sci. U. S.A. 113, 698–703. https://doi.org/10.1073/pnas.1516122113.
Lee, Y.S., Nakahara, K., Pham, J.W., Kim, K., He, Z., Sontheimer, E.J., Carthew, R.W., 2004. Distinct roles for Drosophila Dicer-1 and Dicer-2 in the siRNA/miRNA silencing pathways. Cell 117, 69–81.
Lemaitre, B., Hoffmann, J., 2007. The host defense of Drosophila melanogaster. Annu. Rev. Immunol. 25, 697–743. https://doi.org/10.1146/annurev.immunol.25.022106.141615.
Lemaitre, B., Meister, M., Govind, S., Georgel, P., Steward, R., Reichhart, J.M., Hoffmann, J.A., 1995. Functional analysis and regulation of nuclear import of dorsal during the immune response in Drosophila. EMBO J. 14, 536–545.
Letourneau, M., Lapraz, F., Sharma, A., Vanzo, N., Waltzer, L., Crozatier, M., 2016. Drosophila hematopoiesis under normal conditions and in response to immune stress. FEBS Lett. 590, 4034–4051. https://doi.org/10.1002/1873-3468.12327.
Lewis, S.H., Quarles, K.A., Yang, Y., Tanguy, M., Frézal, L., Smith, S.A., Sharma, P.P., Cordaux, R., Gilbert, C., Giraud, I., Collins, D.H., Zamore, P.D., Miska, E.A., Sarkies, P., Jiggins, F.M., 2018. Pan-arthropod analysis reveals somatic piRNAs as an ancestral defence against transposable elements. Nat Ecol Evol 2, 174–181. https://doi.org/10.1038/s41559-017-0403-4.
Lhéritier, P., 1958. The hereditary virus of Drosophila. Adv. Virus Res. 5, 195–245. https://doi.org/10.1016/S0065-3527(08)60674-0.
Lim, D.-H., Oh, C.-T., Lee, L., Hong, J.-S., Noh, S.-H., Hwang, S., Kim, S., Han, S.-J., Lee, Y.S., 2011. The endogenous siRNA pathway in *Drosophila* impacts stress resistance and lifespan by regulating metabolic homeostasis. FEBS (Fed. Eur. Biochem. Soc.) Lett. 585, 3079–3085. https://doi.org/10.1016/j.febslet.2011.08.034.
Liu, B., Behura, S.K., Clem, R.J., Schneemann, A., Becnel, J., Severson, D.W., Zhou, L., 2013. P53-mediated rapid induction of apoptosis conveys resistance to viral infection in Drosophila melanogaster. PLoS Pathog. 9, e1003137 https://doi.org/10.1371/journal.ppat.1003137.
Liu, X., Hodgson, J.J., Buchon, N., 2017. Drosophila as a model for homeostatic, antibacterial, and antiviral mechanisms in the gut. PLoS Pathog. 13, e1006277 https://doi.org/10.1371/journal.ppat.1006277.
Liu, Y., Gordesky-Gold, B., Leney-Greene, M., Weinbren, N.L., Tudor, M., Cherry, S., 2018. Inflammation-induced, STING-dependent autophagy restricts Zika virus infection in the Drosophila brain. Cell Host Microbe 24, 57–68. https://doi.org/10.1016/j.chom.2018.05.022 e3.
Lü, P., Pan, Y., Yang, Y., Zhu, F., Li, C., Guo, Z., Yao, Q., Chen, K., 2018. Discovery of anti-viral molecules and their vital functions in Bombyx mori. J. Invertebr. Pathol. 154, 12–18. https://doi.org/10.1016/j.jip.2018.02.012.
Majzoub, K., Hafirassou, M.L., Meignin, C., Goto, A., Marzi, S., Fedorova, A., Verdier, Y., Vinh, J., Hoffmann, J.A., Martin, F., Baumert, T.F., Schuster, C., Imler, J.-L., 2014. RACK1 controls IRES-mediated translation of viruses. Cell 159, 1086–1095. https://doi.org/10.1016/j.cell.2014.10.041.
Manley, R., Boots, M., Wilfert, L., 2015. Emerging viral disease risk to pollinating insects: ecological, evolutionary and anthropogenic factors. J. Appl. Ecol. 52, 331–340. https://doi.org/10.1111/1365-2664.12385.
Margolis, S.R., Wilson, S.C., Vance, R.E., 2017. Evolutionary origins of cGAS-STING signaling. Trends Immunol. 38, 733–743. https://doi.org/10.1016/j.it.2017.03.004.
Marques, J.T., Kim, K., Wu, P.-H., Alleyne, T.M., Jafari, N., Carthew, R.W., 2010. Loqs and R2D2 act sequentially in the siRNA pathway in Drosophila. Nat. Struct. Mol. Biol. 17, 24–30. https://doi.org/10.1038/nsmb.1735.
Marques, J.T., Wang, J.-P., Wang, X., de Oliveira, K.P.V., Gao, C., Aguiar, E.R.G.R., Jafari, N., Carthew, R.W., 2013. Functional specialization of the small interfering

RNA pathway in response to virus infection. PLoS Pathog. 9, e1003579 https://doi.org/10.1371/journal.ppat.1003579.
Martin, M., Hiroyasu, A., Guzman, R.M., Roberts, S.A., Goodman, A.G., 2018. Analysis of Drosophila STING reveals an evolutionarily conserved antimicrobial function. Cell Rep. 23, 3537–3550. https://doi.org/10.1016/j.celrep.2018.05.029 e6.
Martins, N., Lemoine, A., Santiago, E., Paro, S., Imler, J.-L., Meignin, C., 2019. A transgenic Flock House virus replicon reveals an RNAi independent antiviral mechanism acting in Drosophila follicular somatic cells. G3 (Bethesda) 9, 403–412. https://doi.org/10.1534/g3.118.200872.
Martins, N.E., 2020. Towards a mechanism for poly(I·C) antiviral priming in oysters. mBio 11. https://doi.org/10.1128/mBio.00407-20.
Martins, N.E., Faria, V.G., Teixeira, L., Magalhães, S., Sucena, É., 2013. Host adaptation is contingent upon the infection route taken by pathogens. PLoS Pathog. 9, e1003601 https://doi.org/10.1371/journal.ppat.1003601.
Merkling, S.H., Bronkhorst, A.W., Kramer, J.M., Overheul, G.J., Schenck, A., Van Rij, R. P., 2015a. The epigenetic regulator G9a mediates tolerance to RNA virus infection in Drosophila. PLoS Pathog. 11, e1004692 https://doi.org/10.1371/journal.ppat.1004692.
Merkling, S.H., Overheul, G.J., van Mierlo, J.T., Arends, D., Gilissen, C., van Rij, R.P., 2015b. The heat shock response restricts virus infection in Drosophila. Sci. Rep. 5, 12758. https://doi.org/10.1038/srep12758.
Miesen, P., Joosten, J., van Rij, R.P., 2016. PIWIs go viral: arbovirus-derived piRNAs in vector mosquitoes. PLoS Pathog. 12, e1006017 https://doi.org/10.1371/journal.ppat.1006017.
Ming, M., Obata, F., Kuranaga, E., Miura, M., 2014. Persephone/Spätzle pathogen sensors mediate the activation of Toll receptor signaling in response to endogenous danger signals in apoptosis-deficient Drosophila. J. Biol. Chem. 289, 7558–7568. https://doi.org/10.1074/jbc.M113.543884.
Misof, B., Liu, S., Meusemann, K., Peters, R.S., Donath, A., Mayer, C., Frandsen, P.B., Ware, J., Flouri, T., Beutel, R.G., Niehuis, O., Petersen, M., Izquierdo-Carrasco, F., Wappler, T., Rust, J., Aberer, A.J., Aspöck, U., Aspöck, H., Bartel, D., Blanke, A., Berger, S., Böhm, A., Buckley, T.R., Calcott, B., Chen, J., Friedrich, F., Fukui, M., Fujita, M., Greve, C., Grobe, P., Gu, S., Huang, Y., Jermiin, L.S., Kawahara, A.Y., Krogmann, L., Kubiak, M., Lanfear, R., Letsch, H., Li, Yiyuan, Li, Z., Li, J., Lu, H., Machida, R., Mashimo, Y., Kapli, P., McKenna, D.D., Meng, G., Nakagaki, Y., Navarrete-Heredia, J.L., Ott, M., Ou, Y., Pass, G., Podsiadlowski, L., Pohl, H., von Reumont, B.M., Schütte, K., Sekiya, K., Shimizu, S., Slipinski, A., Stamatakis, A., Song, W., Su, X., Szucsich, N.U., Tan, M., Tan, X., Tang, M., Tang, J., Timelthaler, G., Tomizuka, S., Trautwein, M., Tong, X., Uchifune, T., Walzl, M.G., Wiegmann, B.M., Wilbrandt, J., Wipfler, B., Wong, T.K.F., Wu, Q., Wu, G., Xie, Y., Yang, S., Yang, Q., Yeates, D.K., Yoshizawa, K., Zhang, Q., Zhang, R., Zhang, W., Zhang, Yunhui, Zhao, J., Zhou, C., Zhou, L., Ziesmann, T., Zou, S., Li, Yingrui, Xu, X., Zhang, Yong, Yang, H., Wang, Jian, Wang, Jun, Kjer, K.M., Zhou, X., 2014. Phylogenomics resolves the timing and pattern of insect evolution. Science 346, 763–767. https://doi.org/10.1126/science.1257570.
Mlih, M., Khericha, M., Birdwell, C., West, A.P., Karpac, J., 2018. A virus-acquired host cytokine controls systemic aging by antagonizing apoptosis. PLoS Biol. 16, e2005796 https://doi.org/10.1371/journal.pbio.2005796.
Mondotte, J.A., Gausson, V., Frangeul, L., Blanc, H., Lambrechts, L., Saleh, M.-C., 2018. Immune priming and clearance of orally acquired RNA viruses in Drosophila. Nat. Microbiol. 3, 1394–1403. https://doi.org/10.1038/s41564-018-0265-9.
Mondotte, J.A., Saleh, M.-C., 2018. Antiviral immune response and the route of infection in Drosophila melanogaster. Adv. Virus Res. 100, 247–278. https://doi.org/10.1016/bs.aivir.2017.10.006.
Monsanto-Hearne, V., Asad, S., Asgari, S., Johnson, K.N., 2017a. Drosophila microRNA modulates viral replication by targeting a homologue of mammalian cJun. J. Gen. Virol. 98, 1904–1912. https://doi.org/10.1099/jgv.0.000831.
Monsanto-Hearne, V., Tham, A.L.Y., Wong, Z.S., Asgari, S., Johnson, K.N., 2017b. Drosophila miR-956 suppression modulates Ectoderm-expressed 4 and inhibits viral replication. Virology 502, 20–27. https://doi.org/10.1016/j.virol.2016.12.009.
Morehouse, B.R., Govande, A.A., Millman, A., Keszei, A.F.A., Lowey, B., Ofir, G., Shao, S., Sorek, R., Kranzusch, P.J., 2020. STING cyclic dinucleotide sensing originated in bacteria. Nature 586, 429–433. https://doi.org/10.1038/s41586-020-2719-5.
Mueller, S., Gausson, V., Vodovar, N., Deddouche, S., Troxler, L., Perot, J., Pfeffer, S., Hoffmann, J.A., Saleh, M.-C., Imler, J.-L., 2010. RNAi-mediated immunity provides strong protection against the negative-strand RNA vesicular stomatitis virus in Drosophila. Proc. Natl. Acad. Sci. U.S.A. 107, 19390–19395. https://doi.org/10.1073/pnas.1014378107.
Mussabekova, A., Daeffler, L., Imler, J.-L., 2017. Innate and intrinsic antiviral immunity in Drosophila. Cell. Mol. Life Sci. 74, 2039–2054. https://doi.org/10.1007/s00018-017-2453-9.
Nainu, F., Tanaka, Y., Shiratsuchi, A., Nakanishi, Y., 2015. Protection of insects against viral infection by apoptosis-dependent phagocytosis. J. Immunol. 195, 5696–5706. https://doi.org/10.4049/jimmunol.1500613.
Nandy, A., Lin, L., Velentzas, P.D., Wu, L.P., Baehrecke, E.H., Silverman, N., 2018. The NF-κB factor relish regulates Atg1 expression and controls autophagy. Cell Rep. 25, 2110–2120. https://doi.org/10.1016/j.celrep.2018.10.076 e3.
Nayak, A., Kim, D.Y., Trnka, M.J., Kerr, C.H., Lidsky, P.V., Stanley, D.J., Rivera, B.M., Li, K.H., Burlingame, A.L., Jan, E., Frydman, J., Gross, J.D., Andino, R., 2018. A viral protein restricts Drosophila RNAi immunity by regulating Argonaute activity and stability. Cell Host Microbe 24, 542–557. https://doi.org/10.1016/j.chom.2018.09.006 e9.
Nayak, A., Tassetto, M., Kunitomi, M., Andino, R., 2013. RNA interference-mediated intrinsic antiviral immunity in invertebrates. Curr. Top. Microbiol. Immunol. 371, 183–200. https://doi.org/10.1007/978-3-642-37765-5_7.
Nitschko, V., Kunzelmann, S., Fröhlich, T., Arnold, G.J., Förstemann, K., 2020. Trafficking of siRNA precursors by the dsRBD protein Blanks in Drosophila. Nucleic Acids Res. 48, 3906–3921. https://doi.org/10.1093/nar/gkaa072.
Olmo, R.P., Ferreira, A.G.A., Izidoro-Toledo, T.C., Aguiar, E.R.G.R., de Faria, I.J.S., de Souza, K.P.R., Osório, K.P., Kuhn, L., Hammann, P., de Andrade, E.G., Todjro, Y.M., Rocha, M.N., Leite, T.H.J.F., Amadou, S.C.G., Armache, J.N., Paro, S., de Oliveira, C. D., Carvalho, F.D., Moreira, L.A., Marois, E., Imler, J.-L., Marques, J.T., 2018. Control of dengue virus in the midgut of Aedes aegypti by ectopic expression of the dsRNA-binding protein Loqs2. Nat. Microbiol. 3, 1385–1393. https://doi.org/10.1038/s41564-018-0268-6.
Palmer, W.H., Dittmar, M., Gordesky-Gold, B., Hofmann, J., Cherry, S., 2020. Drosophila melanogaster as a model for arbovirus infection of adult salivary glands. Virology 543, 1–6. https://doi.org/10.1016/j.virol.2020.01.010.
Palmer, W.H., Joosten, J., Overheul, G.J., Jansen, P.W., Vermeulen, M., Obbard, D.J., Van Rij, R.P., 2019. Induction and suppression of NF-κB signalling by a DNA virus of Drosophila. J. Virol. 93 https://doi.org/10.1128/JVI.01443-18.
Palmer, W.H., Medd, N.C., Beard, P.M., Obbard, D.J., 2018a. Isolation of a natural DNA virus of Drosophila melanogaster, and characterisation of host resistance and immune responses. PLoS Pathog. 14, e1007050 https://doi.org/10.1371/journal.ppat.1007050.
Palmer, W.H., Varghese, F.S., van Rij, R.P., 2018b. Natural variation in resistance to virus infection in Dipteran insects. Viruses 10. https://doi.org/10.3390/v10030118.
Panda, D., Rose, P.P., Hanna, S.L., Gold, B., Hopkins, K.C., Lyde, R.B., Marks, M.S., Cherry, S., 2013. Genome-wide RNAi screen identifies SEC61A and VCP as conserved regulators of Sindbis virus entry. Cell Rep. 5, 1737–1748. https://doi.org/10.1016/j.celrep.2013.11.028.
Paradkar, P.N., Trinidad, L., Voysey, R., Jean-Bernard Duchemin, Walker, P.J., 2012. Secreted Vago restricts West Nile virus infection in Culex mosquito cells by activating the Jak-STAT pathway. Proc. Natl. Acad. Sci. U.S.A. 109, 18915–18920. https://doi.org/10.1073/pnas.1205231109.
Pélisson, A., Sarot, E., Payen-Groschêne, G., Bucheton, A., 2007. A novel repeat-associated small interfering RNA-mediated silencing pathway downregulates complementary sense gypsy transcripts in somatic cells of the Drosophila ovary. J. Virol. 81, 1951–1960. https://doi.org/10.1128/JVI.01980-06.
Perrimon, N., Mahowald, A.P., 1986. l(1)hopscotch, A larval-pupal zygotic lethal with a specific maternal effect on segmentation in Drosophila. Dev. Biol. 118, 28–41. https://doi.org/10.1016/0012-1606(86)90070-9.
Petit, M., Mongelli, V., Frangeul, L., Blanc, H., Jiggins, F., Saleh, M.-C., 2016. piRNA pathway is not required for antiviral defense in Drosophila melanogaster. Proc. Natl. Acad. Sci. U.S.A. 113, E4218–E4227. https://doi.org/10.1073/pnas.1607952113.
Poirier, E.Z., Goic, B., Tomé-Poderti, L., Frangeul, L., Boussier, J., Gausson, V., Blanc, H., Vallet, T., Loyd, H., Levi, L.I., Lanciano, S., Baron, C., Merkling, S.H., Lambrechts, L., Mirouze, M., Carpenter, S., Vignuzzi, M., Saleh, M.-C., 2018. Dicer-2-Dependent generation of viral DNA from defective genomes of RNA viruses modulates antiviral immunity in insects. Cell Host Microbe 23, 353–365. https://doi.org/10.1016/j.chom.2018.02.001 e8.
Roers, A., Hiller, B., Hornung, V., 2016. Recognition of endogenous nucleic acids by the innate immune system. Immunity 44, 739–754. https://doi.org/10.1016/j.immuni.2016.04.002.
Roignant, J.-Y., Carré, C., Mugat, B., Szymczak, D., Lepesant, J.-A., Antoniewski, C., 2003. Absence of transitive and systemic pathways allows cell-specific and isoform-specific RNAi in Drosophila. RNA 9, 299–308.
Rutschmann, S., Jung, A.C., Hetru, C., Reichhart, J.M., Hoffmann, J.A., Ferrandon, D., 2000. The Rel protein DIF mediates the antifungal but not the antibacterial host defense in Drosophila. Immunity 12, 569–580.
Sabin, L.R., Zheng, Q., Thekkat, P., Yang, J., Hannon, G.J., Gregory, B.D., Tudor, M., Cherry, S., 2013. Dicer-2 processes diverse viral RNA species. PLoS ONE 8, e55458. https://doi.org/10.1371/journal.pone.0055458.
Saito, K., Nishida, K.M., Mori, T., Kawamura, Y., Miyoshi, K., Nagami, T., Siomi, H., Siomi, M.C., 2006. Specific association of Piwi with rasiRNAs derived from retrotransposon and heterochromatic regions in the Drosophila genome. Genes Dev. 20, 2214–2222. https://doi.org/10.1101/gad.1454806.
Saleh, M.-C., Tassetto, M., van Rij, R.P., Goic, B., Gausson, V., Berry, B., Jacquier, C., Antoniewski, C., Andino, R., 2009. Antiviral immunity in Drosophila requires systemic RNA interference spread. Nature 458, 346–350. https://doi.org/10.1038/nature07712.
Sansone, C.L., Cohen, J., Yasunaga, A., Xu, J., Osborn, G., Subramanian, H., Gold, B., Buchon, N., Cherry, S., 2015. Microbiota-dependent priming of antiviral intestinal immunity in Drosophila. Cell Host Microbe 18, 571–581. https://doi.org/10.1016/j.chom.2015.10.010.
Schuster, S., Miesen, P., van Rij, R.P., 2019. Antiviral RNAi in Insects and Mammals: Parallels and Differences. https://doi.org/10.3390/v11050448. Viruses 11.
Segrist, E., Cherry, S., 2020. Using diverse model systems to define intestinal epithelial defenses to enteric viral infections. Cell Host Microbe 27, 329–344. https://doi.org/10.1016/j.chom.2020.02.003.
Sen, G.C., Peters, G.A., 2007. Viral stress-inducible genes. Adv. Virus Res. 70, 233–263. https://doi.org/10.1016/S0065-3527(07)70006-4.
Senti, K.-A., Brennecke, J., 2010. The piRNA pathway: a fly's perspective on the guardian of the genome. Trends Genet. 26, 499–509. https://doi.org/10.1016/j.tig.2010.08.007.
Shaw, W.R., Catteruccia, F., 2019. Vector biology meets disease control: using basic research to fight vector-borne diseases. Nat. Microbiol. 4, 20–34. https://doi.org/10.1038/s41564-018-0214-7.
Shi, M., Lin, X.-D., Tian, J.-H., Chen, L.-J., Chen, X., Li, C.-X., Qin, X.-C., Li, J., Cao, J.-P., Eden, J.-S., Buchmann, J., Wang, W., Xu, J., Holmes, E.C., Zhang, Y.-Z., 2016.

Redefining the invertebrate RNA virosphere. Nature 540, 539–543. https://doi.org/10.1038/nature20167.
Sinha, N.K., Iwasa, J., Shen, P.S., Bass, B.L., 2018. Dicer uses distinct modules for recognizing dsRNA termini. Science 359, 329–334. https://doi.org/10.1126/science.aaq0921.
Sinha, N.K., Trettin, K.D., Aruscavage, P.J., Bass, B.L., 2015. Drosophila dicer-2 cleavage is mediated by helicase- and dsRNA termini-dependent states that are modulated by loquacious-PD. Mol. Cell 58, 406–417. https://doi.org/10.1016/j.molcel.2015.03.012.
Siomi, M.C., Sato, K., Pezic, D., Aravin, A.A., 2011. PIWI-interacting small RNAs: the vanguard of genome defence. Nat. Rev. Mol. Cell Biol. 12, 246–258. https://doi.org/10.1038/nrm3089.
Srinivasan, N., Gordon, O., Ahrens, S., Franz, A., Deddouche, S., Chakravarty, P., Phillips, D., Yunus, A.A., Rosen, M.K., Valente, R.S., Teixeira, L., Thompson, B., Dionne, M.S., Wood, W., Reis e Sousa, C., 2016. Actin is an evolutionarily-conserved damage-associated molecular pattern that signals tissue injury in Drosophila melanogaster. Elife 5. https://doi.org/10.7554/eLife.19662.
Swevers, L., Liu, J., Smagghe, G., 2018. Defense mechanisms against viral infection in Drosophila: RNAi and non-RNAi. Viruses 10. https://doi.org/10.3390/v10050230.
Talide, L., Imler, J.-L., Meignin, C., 2020. Sensing viral infections in insects: a dearth of pathway receptors. Curr. Issues Mol. Biol. 34, 31–60. https://doi.org/10.21775/cimb.034.031.
Tang, H., Kambris, Z., Lemaitre, B., Hashimoto, C., 2008. A serpin that regulates immune melanization in the respiratory system of Drosophila. Dev. Cell 15, 617–626. https://doi.org/10.1016/j.devcel.2008.08.017.
Tassetto, M., Kunitomi, M., Andino, R., 2017. Circulating immune cells mediate a systemic RNAi-based adaptive antiviral response in Drosophila. Cell 169, 314–325. https://doi.org/10.1016/j.cell.2017.03.033 e13.
Tavignot, R., Chaduli, D., Djitte, F., Charroux, B., Royet, J., 2017. Inhibition of a NF-κB/Diap1 pathway by PGRP-LF is required for proper apoptosis during Drosophila development. PLoS Genet. 13, e1006569 https://doi.org/10.1371/journal.pgen.1006569.
Teixeira, L., Ferreira, A., Ashburner, M., 2008. The bacterial symbiont Wolbachia induces resistance to RNA viral infections in Drosophila melanogaster. PLoS Biol. 6, e2. https://doi.org/10.1371/journal.pbio.1000002.
tenOever, B.R., 2016. The evolution of antiviral defense systems. Cell Host Microbe 19, 142–149. https://doi.org/10.1016/j.chom.2016.01.006.
Trettin, K.D., Sinha, N.K., Eckert, D.M., Apple, S.E., Bass, B.L., 2017. Loquacious-PD facilitates Drosophila Dicer-2 cleavage through interactions with the helicase domain and dsRNA. Proc. Natl. Acad. Sci. U.S.A. 114, E7939–E7948. https://doi.org/10.1073/pnas.1707063114.
Tuddenham, L., Pfeffer, S., 2011. Roles and regulation of microRNAs in cytomegalovirus infection. Biochim. Biophys. Acta 613–622. https://doi.org/10.1016/j.bbagrm.2011.04.002.
Vagin, V.V., Sigova, A., Li, C., Seitz, H., Gvozdev, V., Zamore, P.D., 2006. A distinct small RNA pathway silences selfish genetic elements in the germline. Science 313, 320–324. https://doi.org/10.1126/science.1129333.
van Rij, R.P., Saleh, M.-C., Berry, B., Foo, C., Houk, A., Antoniewski, C., Andino, R., 2006. The RNA silencing endonuclease Argonaute 2 mediates specific antiviral immunity in Drosophila melanogaster. Genes Dev. 20, 2985–2995. https://doi.org/10.1101/gad.1482006.
Vodovar, N., Goic, B., Blanc, H., Saleh, M.-C., 2011. In silico reconstruction of viral genomes from small RNAs improves virus-derived small interfering RNA profiling. J. Virol. 85, 11016–11021. https://doi.org/10.1128/JVI.05647-11.
Waldron, F.M., Stone, G.N., Obbard, D.J., 2018. Metagenomic sequencing suggests a diversity of RNA interference-like responses to viruses across multicellular eukaryotes. PLoS Genet. 14, e1007533 https://doi.org/10.1371/journal.pgen.1007533.
Wang, H., Smagghe, G., Meeus, I., 2017a. The role of a single gene encoding the Single von Willebrand factor C-domain protein (SVC) in bumblebee immunity extends beyond antiviral defense. Insect Biochem. Mol. Biol. 91, 10–20. https://doi.org/10.1016/j.ibmb.2017.10.002.
Wang, L., Sexton, T.R., Venard, C., Giedt, M., Guo, Q., Chen, Q., Harrison, D.A., 2014. Pleiotropy of the Drosophila JAK pathway cytokine Unpaired 3 in development and aging. Dev. Biol. 395, 218–231. https://doi.org/10.1016/j.ydbio.2014.09.015.
Wang, X.-H., Aliyari, R., Li, W.-X., Li, H.-W., Kim, K., Carthew, R., Atkinson, P., Ding, S.-W., 2006. RNA interference directs innate immunity against viruses in adult Drosophila. Science 312, 452–454. https://doi.org/10.1126/science.1125694.
Wang, Z., Xia, X., Yang, X., Zhang, X., Liu, Yongxiang, Wu, D., Fang, Y., Liu, Yujie, Xu, J., Qiu, Y., Zhou, X., 2017b. A picorna-like virus suppresses the N-end rule pathway to inhibit apoptosis. Elife 6. https://doi.org/10.7554/eLife.30590.
Wangler, M.F., Yamamoto, S., Bellen, H.J., 2015. Fruit flies in biomedical research. Genetics 199, 639–653. https://doi.org/10.1534/genetics.114.171785.
Watanabe, M., Iwakawa, H.-O., Tadakuma, H., Tomari, Y., 2017. Biochemical and single-molecule analyses of the RNA silencing suppressing activity of CrPV-1A. Nucleic Acids Res. 45, 10837–10844. https://doi.org/10.1093/nar/gkx748.
Weavers, H., Evans, I.R., Martin, P., Wood, W., 2016. Corpse engulfment generates a molecular memory that primes the macrophage inflammatory response. Cell 165, 1658–1671. https://doi.org/10.1016/j.cell.2016.04.049.
Webster, C.L., Waldron, F.M., Robertson, S., Crowson, D., Ferrari, G., Quintana, J.F., Brouqui, J.-M., Bayne, E.H., Longdon, B., Buck, A.H., Lazzaro, B.P., Akorli, J., Haddrill, P.R., Obbard, D.J., 2015. The discovery, distribution, and evolution of viruses associated with Drosophila melanogaster. PLoS Biol. 13, e1002210 https://doi.org/10.1371/journal.pbio.1002210.
West, C., Rus, F., Chen, Y., Kleino, A., Gangloff, M., Gammon, D.B., Silverman, N., 2019. IIV-6 inhibits NF-κB responses in Drosophila. Viruses 11, 409. https://doi.org/10.3390/v11050409.
West, C., Silverman, N., 2018. p38b and JAK-STAT signaling protect against Invertebrate iridescent virus 6 infection in Drosophila. PLoS Pathog. 14, e1007020 https://doi.org/10.1371/journal.ppat.1007020.
Wright, V.M., Vogt, K.L., Smythe, E., Zeidler, M.P., 2011. Differential activities of the Drosophila JAK/STAT pathway ligands Upd, Upd2 and Upd3. Cell. Signal. 23, 920–927. https://doi.org/10.1016/j.cellsig.2011.01.020.
Wu, Q., Luo, Y., Lu, R., Lau, N., Lai, E.C., Li, W.-X., Ding, S.-W., 2010. Virus discovery by deep sequencing and assembly of virus-derived small silencing RNAs. Proc. Natl. Acad. Sci. U.S.A. 107, 1606–1611. https://doi.org/10.1073/pnas.0911353107.
Wu, X., Wu, F.-H., Wang, X., Wang, L., Siedow, J.N., Zhang, W., Pei, Z.-M., 2014. Molecular evolutionary and structural analysis of the cytosolic DNA sensor cGAS and STING. Nucleic Acids Res. 42, 8243–8257. https://doi.org/10.1093/nar/gku569.
Xu, J., Grant, G., Sabin, L.R., Gordesky-Gold, B., Yasunaga, A., Tudor, M., Cherry, S., 2012. Transcriptional pausing controls a rapid antiviral innate immune response in Drosophila. Cell Host Microbe 12, 531–543. https://doi.org/10.1016/j.chom.2012.08.011.
Xu, J., Hopkins, K., Sabin, L., Yasunaga, A., Subramanian, H., Lamborn, I., Gordesky-Gold, B., Cherry, S., 2013. ERK signaling couples nutrient status to antiviral defense in the insect gut. Proc. Natl. Acad. Sci. U. S. A. 110, 15025–15030. https://doi.org/10.1073/pnas.1303193110.
Yan, R., Small, S., Desplan, C., Dearolf, C.R., Darnell, J.E., 1996. Identification of a Stat gene that functions in Drosophila development. Cell 84, 421–430. https://doi.org/10.1016/s0092-8674(00)81287-8.
Zambon, R.A., Nandakumar, M., Vakharia, V.N., Wu, L.P., 2005. The Toll pathway is important for an antiviral response in Drosophila. Proc. Natl. Acad. Sci. Unit. States Am. 102, 7257–7262. https://doi.org/10.1073/pnas.0409181102.
Zeidler, M.P., Bausek, N., 2013. The Drosophila JAK-STAT pathway. JAK-STAT 2, e25353. https://doi.org/10.4161/jkst.25353.
Zhai, Z., Boquete, J.-P., Lemaitre, B., 2018. Cell-specific imd-NF-κb responses enable simultaneous antibacterial immunity and intestinal epithelial cell shedding upon bacterial infection. Immunity 48, 897–910. https://doi.org/10.1016/j.immuni.2018.04.010 e7.
Zhang, L., Xu, W., Gao, X., Li, W., Qi, S., Guo, D., Ajayi, O.E., Ding, S.-W., Wu, Q., 2020. lncRNA sensing of a viral suppressor of RNAi activates non-canonical innate immune signaling in Drosophila. Cell Host Microbe 27, 115–128. https://doi.org/10.1016/j.chom.2019.12.006 e8.
Zhang, Q., Zhang, L., Gao, X., Qi, S., Chang, Z., Wu, Q., 2015. DIP1 plays an antiviral role against DCV infection in Drosophila melanogaster. Biochem. Biophys. Res. Commun. 460, 222–226. https://doi.org/10.1016/j.bbrc.2015.03.013.

II. STING pathway throughout evolution

1. STING pathway in mammals

a. Overview of STING signaling

Viral infections are a threat to all living organisms. These intracellular obligate pathogens offer very few MAMPs for their detection by the innate immune system. Activation of the antiviral response largely relies on sensing viral nucleic acids. In vertebrates, for example, several PRRs are involved in this recognition. Concerning RNA sensing in endosomes, TLR-3 specifically recognizes double stranded (ds)-RNAs and TLR7 is responsible for sensing single stranded (ss)-RNAs. In the cytoplasm, uncapped- or ds-RNAs are recognized by retinoic acid-inducible gene (RIG-I)-like receptors. Pathogen DNA with unmethylated CpG is recognized by TLR9 in endosomes. In the cytosolic compartment the formation of the inflammasome is induced when dsDNA is sampled by AIM2 (absent in melanoma 2)(Yoneyama and Fujita, 2010). Moreover, a type-I interferon (IFN-I) and inflammatory response, detailed hereafter, is also induced upon dsDNA sensing in the cytoplasm.

In 2008, STING was identified as an endoplasmic reticulum (ER) resident protein which regulates the expression of IFN-I. This molecule was shown to be able to activate the transcription factors NF-κB and interferon regulatory factor (IRF)-3, inducing IFN-I-dependent antiviral and inflammatory responses (Ishikawa and Barber, 2008; Zhong et al., 2008). Rapidly, Barber and colleagues pursued the description of this protein and showed that STING is responsible for the induction of IFN-I by intracellular DNA derived from pathogens such as DNA viruses (Ishikawa et al., 2009). A few years later, it was demonstrated that STING is activated by direct binding of cyclic di-nucleotides (CDN). These second messengers can be either from bacterial origins (c-di-AMP, c-di-GMP, 3'3'-cGMP-AMP (cGAMP))(Burdette et al., 2011; Woodward et al., 2010) or produced by the enzyme cyclic GMP-AMP synthase (cGAS)

after it binds to long dsDNA present in the cytoplasm. cGAS is producing a unique CDN by linking ATP to GTP by a canonical 3'5'-linkage and an atypical 2'5'-phosphodiester linkage resulting in 2'3'-cGAMP (Ablasser et al., 2013; Diner et al., 2013; Sun et al., 2013).

One molecule of 2'3'-cGAMP binds to a dimer of STING in the ER, resulting in STING conformational change and trafficking. STING translocates to the membrane of the Golgi apparatus, in the perinuclear region of the cell (Ishikawa et al., 2009; Saitoh et al., 2009). Here, it recruits TANK-binding kinase 1 (TBK1) through its C-terminal tail (CTT). TBK1 phosphorylates STING, inducing the recruitment of IRF3 transcription factor to the STING-TBK1 complex. IRF3 is then phosphorylated by TBK1, leading to its nuclear translocation and subsequent induction of the genes encoding IFN-I (Ishikawa et al., 2009; Tanaka and Chen, 2012). In addition, the STING-TBK1 axis also activates the NF-κB transcription factor through a poorly characterized mechanism. It has been proposed that TNF receptor-associated factor (TRAF)-6, IKKγ, IKKß, IKKα and TBK1 participate in NF-κB activation(Abe and Barber, 2014; Fang et al., 2017; Fitzgerald et al., 2003). Overall, the transcriptional response induced by STING activation is important to resist DNA viruses and retroviruses infection, but has also antibacterial effects (**Figure 2**)(reviewed in Ahn and Barber, 2019).

b. STING pathway regulation and associated pathologies

The cGAS-STING axis results in the induction of IFN-I and pro-inflammatory cytokines, which are necessary to solve infections. However, this response can also be harmful for the host if not correctly regulated. Therefore, several regulatory mechanisms are responsible for keeping the STING pathway under control and preserve the immunological balance. An efficient means to prevent deleterious effect is to avoid the activation of the STING pathway by self dsDNAs. Indeed, cGAS is activated by long dsDNAs in a sequence-independent fashion and, thus, can bind pathogenic but also host DNAs (Li et al., 2013). In order to prevent cGAS from encountering self dsDNAs, the first layer of defense relies on compartmentalization. Indeed, in healthy cells dsDNA is sequestered in the nucleus or in mitochondria.

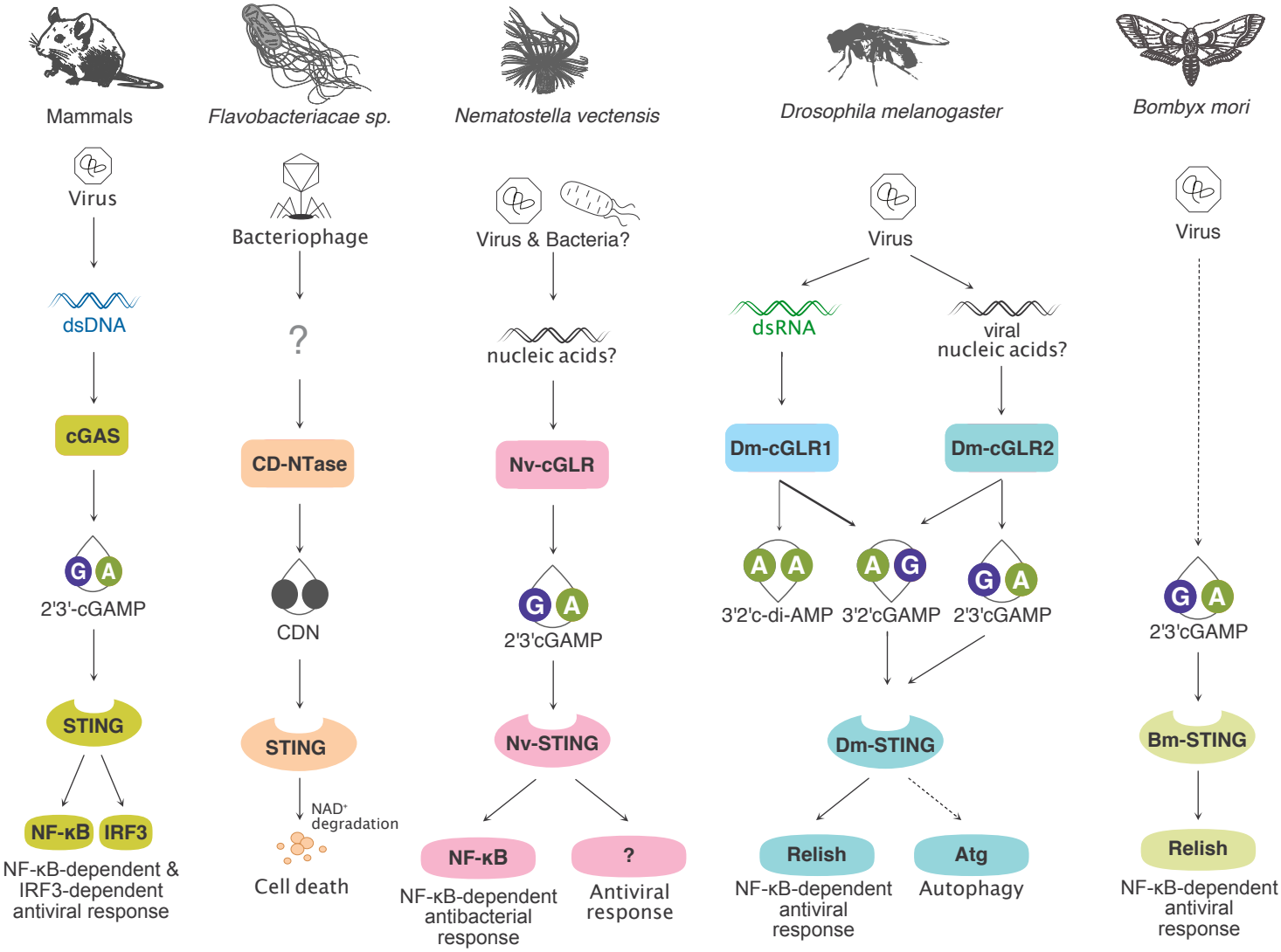

Figure 2: Schematic representation of cGAS-STING axis in different organisms. See the text for details. Nv: *Nematostella vectensis*, Dm: *Drosophila melanogaster*, Bm: *Bombyx mori*

Although cGAS is present in the nucleus, it is kept inactive by tethering to the chromatin, preventing its activation upon recognition of self-DNA (Boyer et al., 2020; Kujirai et al., 2020; Michalski et al., 2020; Orzalli et al., 2015; Zhao et al., 2020). When self-dsDNA leaks from the nucleus or mitochondria, DNase enzymes are responsible to degrade it. If this is not sufficient, a wide range of other mechanisms exists to regulate the STING pathway by modifying the stability, activity or trafficking of STING and cGAS via either post-translational/-transcriptional modifications or interactions with other proteins (reviewed in Chen et al., 2016; Li et al., 2017; Motwani et al., 2019). Additionally, other regulating mechanisms of STING signaling exists, for example through metabolism. Laguette and colleagues recently described a reciprocal negative regulatory loop between STING and the enzyme fatty acid desaturase 2 (FADS2). This regulatory mechanism allow the maintenance of metabolic homeostasis by STING on the one hand and the regulation of the STING-dependent inflammatory response by metabolism on the other (Vila et al., 2022).

Misregulation of the cGAS-cGAMP-STING axis is responsible for autoimmune and autoinflammatory diseases. In particular, inappropriate stimulation of type I IFN response is responsible for type I interferonopathies. The Aicardi-Gouttiere syndrome (AGS) is one such disease, characterized by high levels of circulating IFN-I causing central nervous system and skin inflammation. AGS can be caused by mutations in nucleases involved in cellular nucleic acids digestion. As an example single mutation of the gene encoding the 3'-DNA exonuclease TREX1 is sufficient to cause AGS. Of note, null-mutant mice for the murine homolog of TREX1 are developing the same pathological IFN-I accumulation profile. This dysregulation is completely rescued when either *Cgas* or *Sting* is deleted (Gray et al., 2015), demonstrating the involvement of this pathway in the pathology. Another type of type I interferonopathie called STING-associated vasculopathy with onset in infancy (SAVI) is caused by STING autosomal dominant gain-of-function mutations. These mutations generate spontaneous dimerization and activation of STING in the absence of ligand, leading to systemic inflammation (Liu et al., 2014). Interestingly, studies conducted in SAVI mice models showed that this pathology can develops independently of IRF3 activation and IFN-I production (Luksch et al., 2019; Warner et al., 2017).

In addition, self-DNA recognition itself can be pathogenic, causing inflammation in various tissues which can contribute to tumorigenesis. Interestingly, pro-tumoral effects of the STING-cGAS axis are, at least partially, IFN-I-independent. This was demonstrated in a study of Yan and collaborators who developed a mice model in which the STING-mediated IFN signaling is abolished while the rest of the response is intact. This model allows them to demonstrate that STING activities in T cells are mostly IFN-independent. Moreover, they showed that, in T cells, STING activation leads to cell death in an IFN-independent manner (Wu et al., 2020). Importantly, some tumors release cGAMP in the extracellular medium, which can be taken up by T cells surrounding the tumor. cGAMP then activate STING, resulting in T cells death, which is an efficient tumor immune evasion mechanism.

The two last examples highlight the necessity to understand IFN-independent functions of the STING pathway, which have been largely neglected until now. Several distinct IFN-independent mechanisms activated downstream of the STING pathway have been described. For example, STING pathway activation exerts antiproliferative activity on T cells and induces their death, as previously mentioned (Cerboni et al., 2017; Wu et al., 2019). Interestingly, the STING-cGAS-TBK1 axis also presents IFN-independent antitumoral effects (Yum et al., 2021). This pathway was also demonstrated to induce translation inhibition in response to infection by RNA viruses (Franz et al., 2018) and to activate autophagy (Gui et al., 2019; Moretti et al., 2017; Watson et al., 2015). It has been shown that mice deficient for STING-dependent activation of IRF3 are still protected against herpes simplex virus 1 (Wu et al., 2020; Yamashiro et al., 2020; Yum et al., 2021). This demonstrates that interferon-independent mechanisms are also involved in antiviral defenses. Last but not least, the STING pathway regulates NF-κB in an IRF3-independent but poorly characterized manner. The transcriptional response induced by NF-κB leads to inflammation. Interestingly, a study comparing the signaling function of the CTT of STING from 20 vertebrates revealed that STING from zebrafish and salmon were preferentially inducing NF-κB-dependent rather than IRF3-dependent transcriptional response when expressed in human cells. This result demonstrates that the activation of IRF3 is not the major transcriptional output in all vertebrate species (de Oliveira Mann et al., 2019). These observations along with the important conservation of *sting* throughout evolution

raise the question of the ancestral function of STING. This question is reinforced by the fact that appearance of STING in animals predates that of IRFs, a vertebrate innovation (Gui et al., 2019; Kranzusch et al., 2015; Margolis et al., 2017).

2. Insights on the ancestral function of the cGAS-STING axis

The question of the ancestral function of the cGAS-STING pathway can be solved by understanding its function in other organisms, evolutionarily distant from vertebrates. In this purpose, studying the important diversity of cGAS-STING pathways in nature and their outputs is essential.

a. CD-NTases enzymes and STING proteins in bacteria

It is now clear that cGAS-STING signaling takes its roots in prokaryotes. Bacteria produce CDNs to control a variety of cellular processes such as growth, chemotaxis or virulence. Bacterial enzymes producing these CDNs have been classified in three structural families. Two of them comprises only prokaryotic proteins while the third one, the cGAS/DncV-like nucleotidyltransferase (CD-NTase) family, encompasses both prokaryotic and eukaryotic proteins, including mammalian cGAS (Kranzusch, 2019; Whiteley et al., 2019). Interestingly, CDNs and cyclic trinucleotides (CTN) produced by CD-NTases in bacteria are involved in defense against bacteriophages. Indeed, introduction of the operon containing the gene coding for the CD-NTase *DncV* from *Vibrio cholerae* into a strain of *Escherichia coli* lacking this system results in the resistance of the bacteria to phages belonging to a variety of families (Cohen et al., 2019). Moreover, another gene of the same operon encodes a phospholipase able to degrade bacterial membrane, resulting in cell death, an efficient anti-phage mechanism as it prevents the spread of the infection. Importantly, this enzyme can be activated by bacterial lysates containing 3’3’-cGAMP (Severin et al., 2018). Altogether, these results demonstrate that a cyclic oligonucleotide-based anti-phage signaling system (CBASS) is responsible for anti-phage defense in bacteria. This suggests that the antiviral functions of cGAS originate in prokaryotes (Cohen et al., 2019).

Bioinformatical search identified more than 2000 distinct CDNs- and CTNs-regulated effectors in bacteria. Among those, some encode proteins with homology to STING. In addition to sharing the same overall architecture than metazoan STING, they also bind c-di-GMP (Burroughs and Aravind, 2020; Lowey et al., 2020; Morehouse et al., 2020). A bacterial STING homolog, belonging to *Flavobacteriacae sp.*, has been shown to degrade ß-nicotinamide adenine dinucleotide (NAD^+), which leads to bacterial death, thus limiting viral spread (Morehouse et al., 2020). Altogether, these discoveries showed that both CD-NTase enzymes producing CDN and STING-like molecules sensing these second messengers already functions in prokaryotic cells (**Figure 2**). Importantly, these results also proved the ancient origin of the antiviral function of the CD-NTase-STING axis.

b. STING pathways in other organisms

STING orthologs were identified in most animals genomes (with some exceptions, *e.g.*, nematodes, mosquitoes) and even in choanoflagellates, the closest living unicellular relative of animals (Margolis et al., 2017; Wu et al., 2014). Interestingly, STING orthologues identified in very different animals (belonging to Annelida, Mollusca and Cnidaria) are able to bind CDNs. However, their STING proteins do not present a CTT (vertebrate's innovation), which is important for TBK1 recruitment in mammals.

The work of Vance and collaborators demonstrates that a cGAS-like enzyme exists in the sea anemone *Nematostella vectensis*. This organism shared its last common ancestor with humans about 600 million years ago but its cGAS-like enzyme is also able to produce 2'3'-cGAMP (Gui et al., 2019; Kranzusch et al., 2015). In addition, a recent follow-up study showed that 2'3'-cGAMP induces a transcriptional response leading to induction of antibacterial and antiviral genes in *N. vectensis*. The authors also discovered that the induced antibacterial response depends on NF-κB (**Figure 2**)(Margolis et al., 2021). These findings raise the question of the function of cGAS-STING axis in invertebrates where STING's CTT and IRF3 are absent. Unravelling this could also help the comprehension of the cGAS-STING-NF-κB signaling in mammals.

To explore the cGAS-STING pathway in invertebrates and get insights on its ancestral function a possibility is to use the model organism *Drosophila melanogaster* which present an ortholog of STING (CG1667). A study conducted by Goodman and collaborators showed an impaired activation of the Imd pathway-regulated AMPs upon infection with the Gram-positive bacteria *Listeria monocytogenes* in STING mutant flies. These flies were also more sensitive to the infection by *L. monocytogenes*. Additionally, their results suggest that STING is binding to CDNs with a preference for c-di-GMP. When transfected in drosophila Schneider 2 (S2) cells, c-di-GMP was found to activate AMPs expression in an Imd- and Relish-dependent manner. The authors concluded that the ancestral function of STING was antibacterial defenses (Martin et al., 2018).

On the other hand, an antiviral function of STING in drosophila was highlighted by two different studies, although through distinct mechanisms. The work of Cherry and collaborators suggests that STING is protecting drosophila against Zika virus infection. They proposed that STING is induced in a NF-κB dependent manner and induces autophagy in flies brain to control the viral infection (Liu et al., 2018). Of note, mosquitoes, the natural vectors transmitting Zika virus to humans, do not possess a STING homolog. Moreover, in mammalian cells, autophagy has been shown to be proviral in the case of Zika virus infection, rather than antiviral (Abernathy et al., 2019).

Another STING-dependent antiviral mechanism was discovered by my host laboratory. This discovery follows-up the identification of an immunomodulatory cytokine responsible for Imd pathway downregulation, which was independently hijacked by several DNA viruses belonging to different families (Lamiable et al., 2016). The existence of viral suppressors for the Imd pathway suggested that it exerts a pressure on viruses. This prompted the team to investigate the involvement of the Imd pathway in drosophila's antiviral defenses. Silencing the proteins involved in the Imd pathway by RNAi in S2 cells, they identified that the kinase IKKß and the NF-κB transcription factor Relish, but not the Imd pathway as a whole, are necessary to defend S2 cells against DCV infection. Importantly, they confirmed *in vivo* the importance of these two proteins in antiviral defenses against picorna-like viruses. Genome-wide transcriptome analysis revealed that STING is induced in a Relish- and IKKß-dependent manner upon picorna-like virus infection. Epistasis analysis allowed

to establish that a STING-IKKß-Relish signaling axis exists in drosophila and regulates the expression of a set of genes different from Imd-dependent genes, although overlapping (**Figure 2**)(Goto et al., 2018).

More recently, we pursued the characterization of the STING pathway in drosophila by demonstrating that it is activated by CDNs in flies, as it is in mammals. We tested the four CDNs known at that time (c-di-GMP, c-di-AMP, 3'3'-cGAMP and 2'3'-cGAMP). Among the tested CDNs, the most potent for STING pathway activation was 2'3'-cGAMP (Cai et al., 2020; Martin et al., 2018). This suggests the presence of a cGAS-like receptor (cGLR) in drosophila. We discovered that co-injection of 2'3'-cGAMP along with the virus protects flies from infection. Of note, this CDN-induced protection does not depend on the canonical autophagy pathway. This result is in opposition with previously mentioned conclusions of the study led by Cherry and collaborators (Liu et al., 2018). We also found that STING mutant flies were still able to produce normal amounts of NF-κB-dependent AMPs upon infection with the bacteria *Listeria monocytogenes*. This is in agreement with the data previously described by the team, showing that STING is dispensable for defense against *E. coli* and *Micrococcus luteus* (Goto et al., 2018), but in opposition with the work of Goodman and colleagues previously discussed (Martin et al., 2018). Another striking difference between our work and theirs is the complete absence of STING-regulated genes (SRG) induction and anti-DCV protection upon c-di-GMP injection in our hands. On the contrary, they found this CDN to be the one preferentially binding to STING and inducing an antimicrobial transcriptional response (Martin et al., 2018). The reason for these discrepancies is currently unknown.

In agreement with our results, a study conducted in another insect, the silkworm *Bombyx mori*, identified an antiviral STING-NF-κB axis. This pathway induces a transcriptional response which protects the organism against nucleopolyhedrovirus, a virus belonging to *Baculoviridae* family. Interestingly, they discovered that cGAMP was produced in *Bombyx mori* cells upon viral infection, suggesting the presence of a cGLR enzyme in this insect too (**Figure 2**)(Hua et al., 2018). In line with the results obtained both in flies and *Bombyx mori*, two distinct cGLRs were recently identified in drosophila (**Figure 2**)(discussed in Chapter 1, Holleufer et al., 2021; Slavik et al., 2021).

Altogether, these results point to an ancient antiviral function of the STING-NF-κB axis, which is very conserved throughout evolution. The antiviral response induced by this pathway seems to rely principally on broad transcriptional changes, leading to induction of antiviral effectors. Of note, a minor role of STING-induced non-canonical autophagy could not be excluded so far. The understanding of the STING pathway in invertebrates is growing rapidly and should certainly help to decipher the poorly characterized STING-NF-κB axis in mammals

III. NF-κB pathways and their regulation

1. Overview of NF-κB

NF-κB proteins are a family of structurally related inducible transcription factors found in eukaryotes. They are essential for normal cellular and organismal function due to their involvement in diverse important processes such as immune responses, development, cellular growth and apoptosis. These proteins and their functions are evolutionarily conserved in organisms as different as mammals, insects, cnidarians, porifera and even in the unicellular organism *Capsaspora owczarzak*. However, NF-κB proteins are noticeably absent in some model organisms such as yeast and was probably lost throughout evolution in the nematode *Caenorhabditis elegans* (reviewed in Williams and Gilmore, 2020).

The proteins of the NF-κB family share a highly conserved DNA binding and dimerization domain at their N-ter, the RHD (Ghosh et al., 1990; Kieran et al., 1990). NF-κB transcription factors are split into two distinct subfamilies: the NF-κB proteins and the Rel proteins.

The Rel subfamily members present a transactivation domain (TAD) at their C-ter extremity. This subfamily encompasses p65 (also called RelA), RelB and c-Rel in mammals and dorsal and Dif transcription factors in *Drosophila melanogaster* (**Figure 3A**). The drosophila Rel proteins dorsal and Dif are regulated by the Toll pathway (see introduction part I). Genes encoding them are located close to each other on the second chromosome and probably arose from a recent duplication (Meng et al., 1999). The major transactivator in Toll-dependent antibacterial and antifungal defenses in adult flies is Dif while dorsal is mostly involved in early development (reviewed in Minakhina and Steward, 2006). dorsal can substitute for Dif in immune defenses in larvae (Rutschmann et al., 2000a). Of note, Teixeira and collaborators also described

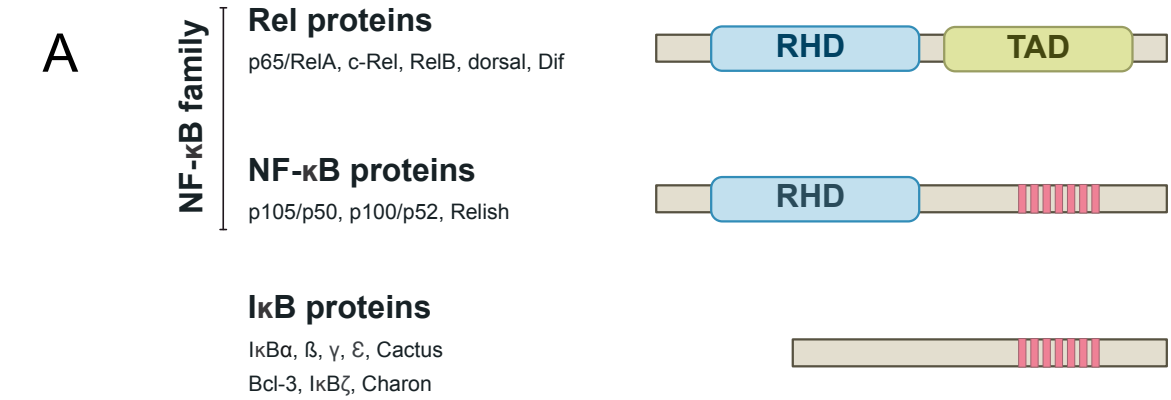

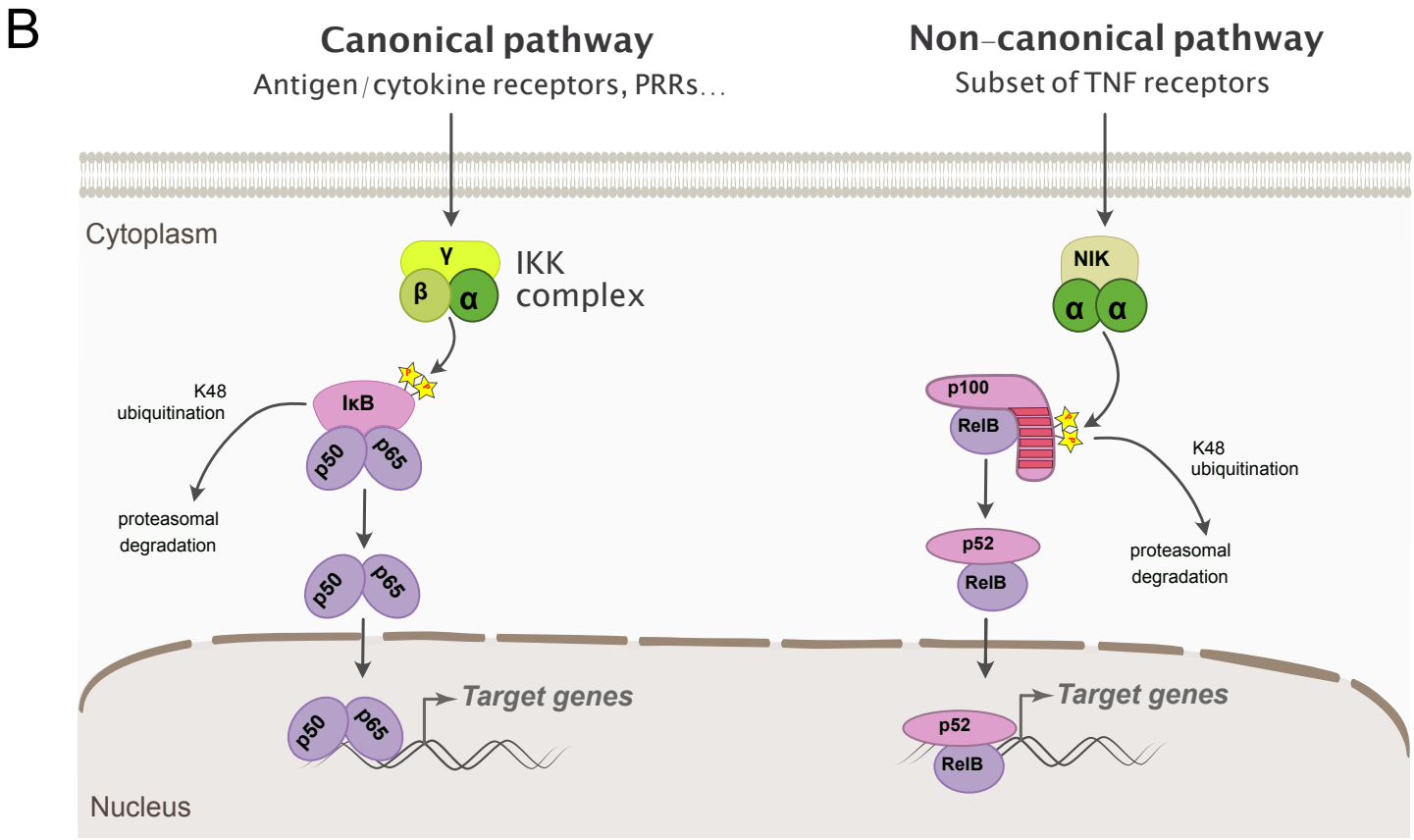

Figure 3: NF-κB proteins. A) Generalized structures of NF-κB and IκB proteins. Distinctions between Rel (top) and NF-κB (middle) subfamilies. Proteins of this family all share a conserved Rel homology domain (RHD) composed of a DNA-binding domain and a dimerization domain. C-ter half of Rel proteins present a transactivation domain (TAD). C-ter half of NF-κB proteins present ankyrin repeats inhibitory domains (red bars). The general structure of proteins belonging to the IκB family is represented (bottom). IκBs carry between five and seven ankyrin repeats in their C-ter part. **B)** Canonical (left) and non-canonical (right) NF-κB signaling pathways. See the text for details.

the involvement of dorsal in defenses against oral infection by a range of viruses (Ferreira et al., 2014).

The NF-κB subfamily members present a long C-ter domain with ankyrin repeats, which acts to inhibit the protein in cis. This subfamily contains p105/p50 and p100/p52 in mammals and Relish (Rel110/Rel68) in flies (**Figure 3A**). In order to become active, p105, p100 and Rel110 precursors need to be cleaved into p50, p52 and Rel68, respectively. Interestingly, mammalian p105 and p100 processing relies on partial degradation by the proteasome while the drosophila protein Relish is processed by endoproteolytic cleavage by the caspase-8 homolog Dredd. However, even cleaved, these NF-κB proteins are not able to activate transcription, as they do not have TADs. To overcome this, they can dimerize with TAD-containing Rel proteins. Indeed, NF-κB transcription factors always function as dimers, binding to 9-10 base pairs DNA sequences called κB sites present in promoters or enhancer of target genes (reviewed in Oeckinghaus and Ghosh, 2009).

The transcriptional response induced by NF-κB dimers is regulated by their interaction with proteins belonging to the IκB family. IκB are characterized by five to seven ankyrin repeat motifs, mediating their interaction with RHD of NF-κB dimers (**Figure 3A**). This interaction generally hide their nuclear localization signal (NLS) and interfere with the DNA binding domain present in the RHD (Malek et al., 2001). This inhibitory mechanism allows a rapid activation of the pathway after stimulation, as NF-κB dimers are already present as latent complex bound to IκB in the cytoplasm (reviewed in Hoffmann et al., 2006; Oeckinghaus and Ghosh, 2009).

2. Canonical *versus* non-canonical NF-κB pathways in mammals

A great diversity of stimuli lead to the activation of two distinct NF-κB-dependent signaling pathways in mammalian cells: the canonical and non-canonical NF-κB pathways (reviewed in Mitchell et al., 2016).

a. The canonical NF-κB pathway

The canonical pathway is triggered by various signals, including those mediated by immune receptors such as antigen receptors, cytokine receptors or PRRs for example. These stimuli result in the phosphorylation of an IKK complex. This complex is composed of two catalytic subunits, IKKα and IKKß and a regulatory subunit, IKKγ (also called NEMO, NF-κB essential modulator) which serves as a scaffold to direct the kinase activity to IκB (Schröfelbauer et al., 2012). Once activated, this kinase complex binds and phosphorylates NF-κB-linked IκB at specific serine residues present in the N-ter of the protein, within the signal responsive region. This results in subsequent K48-linked ubiquitination of the IκB protein followed by its proteasome-mediated degradation. Freed from its inhibitor, NF-κB dimer is able to translocate into the nucleus. There, it will bind to DNA at κB sites present in its target genes and trigger transcription initiation. This pathway involves the most abundant NF-κB dimers, predominantly p50/p65 and p50/c-Rel heterodimers (**Figure 3B**).

b. The non-canonical NF-κB pathway

By contrast, the NF-κB non-canonical pathway responds to the activation of specific members of tumor-necrosis factor receptor (TNFR) family (reviewed in Sun, 2011). This pathway specifically regulates the inducible processing of p100. By contrast with the canonical pathway, the non-canonical pathway does not depends on IKKγ/NEMO or IKKß but involves IKKα and the NF-κB-inducing kinase (NIK)(Senftleben et al., 2001; Xiao et al., 2001). In normal conditions, NIK is rapidly degraded in an ubiquitin-dependent manner involving TRAF3 (Liao et al., 2004). Upon activation of the pathway, TRAF3 is degraded, limiting NIK degradation. NIK is then able to phosphorylate IKKα (Liang et al., 2006). Additionally, NIK serves as a scaffold between IKKα and p100 (Ling et al., 1998; reviewed in Sun, 2011), allowing the kinase to phosphorylate p100 on two specific serine residues localized in its C-ter part (Liang et al., 2006). This phosphorylation allows the recruitment of the ß-transducing repeat-containing protein (ß-TrCP) ubiquitin ligase, which triggers p100 K48-polyubiquitination. p100 is then partially degraded by the proteasome, leading to the generation of p52. This enables

the nuclear translocation of NF-κB dimers containing p52 (mostly p52/p52 or p52/RelB)(**Figure 3B**). These dimers are mostly responsible for the regulation of immune processes such as survival and maturation of B-cells and development of lymphoid organs (reviewed in Sun, 2017).

3. NF-κB pathways regulation

The inflammatory response induced by NF-κB pathways activation is necessary to protect the host from infection and prevent pathogen spread. However, it needs to be finely tuned to prevent the development of inflammatory conditions, autoimmune diseases or cancers. To prevent the onset of these pathologies while allowing an effective response against infections, NF-κB pathways are regulated by different mechanisms.

a. IκB protein family

The first important control of the NF-κB response relies on IκB proteins. IκBs are a family of proteins possessing multiple ankyrin repeats, a common motif of helix-turn-helix conformation involved in protein-protein interactions (Li et al., 2006). In the case of IκB proteins, these ankyrin repeats allow interaction with the RHD of NF-κB proteins. Importantly, members of the IκB family have different affinities for the variety of NF-κB dimers existing in the cell. The classical role of IκB proteins is to sequester NF-κB dimers in the cytoplasm, preventing their nuclear translocation and subsequent binding to κB sites in promoters or enhancers of their target genes.

The classical IκB proteins are IκBα, IκBß and IκBε in mammals and Cactus in *Drosophila melanogaster*. IκBα is the prototypical member of this family. It binds preferentially to the most abundant NF-κB dimer, p65/p50. IκBα is rapidly K48-ubiquitinated and degraded by the proteasome machinery upon activation of the NF-κB pathway. In addition to segregating NF-κB dimers in the cytoplasm, classical IκB are also involved in the control of the duration of the NF-κB response. Indeed, NF-κB

drives IκB expression, generating a negative feedback loop to prevent a deleterious sustained inflammation. Thus, the duration of the NF-κB response relies on the kinetics of IκB induction (Hoffmann et al., 2002).

In addition to these canonical IκBs, p100 and p105 NF-κB precursors are also acting as IκBs. The RelB-containing NF-κB dimers specifically binds to p100 and none of the others NF-κB monomers. This interaction has been suggested to be important for the stabilization of NF-κB dimers containing RelB (Solan et al., 2002). Thus, p100 is essential for the regulation of RelB but could also inhibit p65-containing dimers downstream of IKKα. p105 undergoes a constitutive partial processing by the proteasome machinery, which stops at the glycine-rich region, resulting in the liberation of p50 (Lin and Ghosh, 1996; Orian et al., 1999). However, when p105 rapidly binds to other NF-κB monomers after its synthesis, it is not processed. In this case, p105 can also act as a typical IκB proteins (Rice et al., 1992).

Finally, Bcl-3 and IκBζ are atypical IκB proteins, regulating NF-κB by distinct and not completely understood mechanisms. Bcl-3 is the only TAD-containing IκB protein described. It is localized in the nucleus, where it binds to p50- and p52- containing dimers and can both inhibits or activate NF-κB-dependent transcriptional response depending on the context (Franzoso et al., 1993; Fujita et al., 1993; Nolan et al., 1993). On the one hand, this non-canonical IκB protein was shown to stabilize transcriptionally inactive p50 homodimers at κB sites, preventing the binding of TAD containing dimers and subsequent activation of target genes (Carmody et al., 2007). On the other hand, Bcl-3 has been shown to mediate the removal of p50 homodimers from κB sites, allowing transcriptionally active NF-κB dimers to regulate target genes expression (Franzoso et al., 1993; Hatada et al., 1992). When bound to p52 homodimers, Bcl-3 confers transcriptional potential, maybe through its TAD (Bours et al., 1993). Bcl-3 activity is at least partly regulated by post-translational modifications (PTM), such as phosphorylation and ubiquitination (Bours et al., 1993; Bundy and McKeithan, 1997).

IκBζ was identified through its sequence homology to Bcl-3. By contrast with Bcl-3, IκBζ regulation mostly depends on its expression level. IκBζ expression is induced

in response to the induction of MyD88-dependent NF-κB signaling pathways (Haruta et al., 2001; Kitamura et al., 2000; Yamazaki et al., 2001). Once induced, IκBζ has functions similar to Bcl-3. It binds preferentially to p50 homodimers at κB sites and also present transactivation capacities, even if it does not present a well-defined TAD. Conversely, IκBζ may bind to p65-containing dimers and negatively regulates them (Motoyama et al., 2005; Yamamoto et al., 2004). Thus, Bcl-3 and IκBζ , two atypical IκB proteins are able to positively regulate transcription, unlike the canonical inhibitory role of proteins belonging to this family.

In drosophila, the well characterized IκB protein Cactus acts as a typical IκB. Additionally, a new IκB protein, Charon (also called Pickle), has been identified more recently. Charon carries seven ankyrin repeats, localized in its C-terminal part (Ankyrin reach region, ARR). Two independent studies have shown that the ankyrin domain of Charon allows its interaction with the RHD of Relish (Ji et al., 2016; Morris et al., 2016). However, these two studies described opposing roles for Charon in the Imd pathway. On the one hand, Charon is presented as a selective negative regulator of the pathway, able to bind and repress specifically Rel-68 homodimers. This is proposed to contribute to immune tolerance towards the gut microbiota, possibly by recruiting the histone deacetylase dHDAC1 (Morris et al., 2016). On the other hand, Charon is described as a positive regulator of the pathway, since it would allow the transcription of AMP genes (including *Dpt* and *Drs*) by delivering Rel-68 to poly(ADP ribose) polymerase-1 (PARP-1) occupied promoters (Ji et al., 2016). The role of Charon in regulation of NF-κB pathways in drosophila is still mysterious and we started to analyze its possible involvement in the Relish-dependent STING signaling pathway (see chapter 3).

b. Combinatorial diversity of NF-κB dimers

Regulation of NF-κB pathways is also involved in controlling the transcriptional response induced depending on the activating signal. The combinatorial diversity of NF-κB dimers has been shown to be key to this regulation. Indeed, different dimers are able to regulate distinct, although overlapping, sets of genes. This relies at least on three underlying reasons: 1) different NF-κB dimers have different binding affinities for distinct κB sites; 2) each dimer can interact with different proteins at target

promoters; 3) physiological conditions modulate the gene activation profile differently depending on dimer composition.

In mammals, the five NF-κB monomers are able to form fifteen different dimers, among which twelve can bind to κB sites. Nine out of these twelve dimers contain at least one monomer with a TAD (RelA, cRel or RelB). Opposingly, p50:p50, p52:p52 and p50:p52 dimers do not present transactivating capacities on their own. They are usually inhibiting the transcriptional response by competing for κB sites with TAD-containing NF-κB dimers. However, these dimers can acquire transactivating properties by interacting with proteins such as the atypical IκBs. Even if these twelve dimers exist, they are present in different quantities in cells for different reasons. First of all, NF-κB proteins are thought to have different dimerization affinities (Tsui et al., 2015). These differences in interaction affinities gives rise to competition between monomers to form specific dimers (Basak et al., 2008; Tsui et al., 2015). Second, genes coding for NF-κB monomers are differentially expressed. For example, RelA is broadly expressed while cRel or RelB are expressed only in specific cell types. Finally, dimers can be stabilized by interacting with chaperones proteins. For example, it was described that IκBß increased the binding affinity of RelA homodimers (Tsui et al., 2015).

In drosophila, Ip and colleagues showed that the three NF-κB proteins dorsal, Dif and Relish are able to form each possible dimer combination in a transgenic assay. However, these dimers are formed with various degrees of efficiency. Notably, authors confirmed the existence of Dif:Relish heterodimers *in vivo* in larval extracts. These results raise the question of the impact of such heterodimers on transcriptional responses (Tanji et al., 2010).

c. Crosstalk between NF-κB-dependent transcriptional pathways

Considering that most components are shared between the canonical and non-canonical pathways, it is not surprising that crosstalk happens between both. This crosstalk has been proposed to participate in the fine-tuned regulation of the response. p100 represents a signaling node between these two pathways. Indeed, its expression

depends on the canonical pathway (Basak et al., 2008) but its processing into active p52 depends on the atypical NF-κB pathway. This processing can result either in p52 production or in p100 complete degradation. In the latter case, the inhibited NF-κB dimer is released, allowing canonical NF-κB activation (Almaden et al., 2014). Additionally, the gene coding for RelB also depends on the canonical pathway for its regulation. Therefore, the activation of the RelB:p52 dimer through non-canonical NF-κB signaling depends on the canonical pathway (Basak et al., 2008; Bren et al., 2001). Finally, NF-κB proteins endure numerous PTMs, essential for their activity. However, mechanisms leading to these PTMs are often unknown. One hypothesis is that NF-κB signaling crosstalks with other pathways and integrates distinct signals.

In drosophila, evidence for crosstalk between NF-κB-dependent pathways exists. The Dif:Relish heterodimer mentioned above could mediate a crosstalk between Imd and Toll pathway in drosophila. This is in line with the fact that most AMPs are regulated by both Toll and Imd pathway, albeit at different levels. For example, Attacin-A (Att-A) is known to be an Imd-dependent AMP but has been shown to also depends on Toll pathway (De Gregorio et al., 2002; Lemaitre et al., 1996; Rutschmann et al., 2002; Tanji et al., 2007). Interestingly, the STING pathway shared common components with the Imd pathway. In particular, both pathways controls the activation of the same NF-κB protein Relish even if they regulate distinct, although overlapping, transcriptional responses (Cai et al., 2020; Goto et al., 2018). Understanding the mechanism at play in the divergent outputs of Relish activation could help to understand the STING-dependent activation of NF-κB in mammals.

RESULTS

Preamble

As mentioned in the general preamble of the thesis, at the beginning of my PhD we knew that:

i) an inducible antiviral pathway involving STING exists in *Drosophila melanogaster*
ii) STING acts upstream of two components of the Imd pathway, the caspase-8 homolog Dredd and the kinase IKKß
iii) the STING pathway is important for defenses against picorna-like viruses
iv) the STING-IKKß-Relish axis regulates the transcription of a set of genes different from the ones regulated downstream of the Imd pathway.

These discoveries raised two major questions: 1) what is triggering the STING pathway? and 2) how is Relish activated downstream of STING?

The first chapter of the results section presents my contribution to answering the first question. In the two following chapters I present the results I obtained to answer the second question. The data reported in chapter 2 provide evidence that two other components of the Imd pathway, Fadd and Dredd, also participate in the STING pathway in drosophila. In chapter 3, I provide preliminary data pointing to the possible involvement of poorly characterized isoforms of NF-κB and IκB in the drosophila STING pathway.

Chapter 1: Activation by cyclic-dinucleotides and characterization of cGAS-like receptors

1. Preamble

I get involved in this project at the time of the 2020 article reviewing, as part of a team effort to complete the manuscript. The discovery that 2'3'-cGAMP was a potent activator of the STING pathway in drosophila was greatly valuable and I used this easy and highly efficient way to induce the pathway in my own project (see chapter 2 and 3). In the aftermath, the two cGLRs were identified and I kept contributing by performing experiments to anticipate potential reviewer requests.

2. The antiviral STING pathway is activated by 2'3'-cGAMP in *Drosophila melanogaster*

In mammals, STING is activated by CDNs of bacterial origins (cyclic di-AMPs, cyclic di-GMP, 3'3'-cyclic GMP-AMP)(Margolis et al., 2017) or produced by the enzyme cGAS (2'3'-cGAMP), a receptor for cytosolic DNA (reviewed in Ablasser and Chen, 2019). In drosophila, the STING pathway has been shown to be antiviral and to involve the IKKß kinase and the NF-kB like transcription factor Relish (Goto et al., 2018). However, the way the pathway is activated remained unknown at the time and initial studies reported that recombinant STING proteins from insects do not appear to bind CDNs (Kranzusch et al., 2015). This is why we decided to test the activation of the STING pathway by different CDNs *in vivo*. We have shown that in drosophila, as in mammals, the STING pathway is activated by CDNs, especially 2'3'-cGAMP, in a Relish- and STING-dependent manner. We also demonstrated that injection of 2'3'-cGAMP in flies protects them against infection with various DNA and RNA viruses.

In this study, I worked in association with Dr Hua Cai on the revision of the manuscript. Experiments performed allowed me to confirm that 2'3'-cGAMP, 3'3'-cGAMP and cyclic di-AMP have a dose-dependent effect on the expression of SRG1 (CG13641), with 2'3'-cGAMP being the most potent agonist (**Figure S3 of the paper**). I also demonstrated that the antiviral effect of 2'3'-cGAMP was STING- and Relish-dependent not only for protection against DCV but also cricket paralysis virus and vesicular stomatitis virus infections (**Figure 4 D-F of the paper**). Finally, I showed that the response to 2'3'-cGAMP was rescued in *STING*^{Rescue} flies (**Figure S1 C-E of the paper**). This work was published in 2020 in the journal Science Signaling (Cai et al., 2020).

IMMUNOLOGY

2′3′-cGAMP triggers a STING- and NF-κB–dependent broad antiviral response in *Drosophila*

Hua Cai[1,2], Andreas Holleufer[3], Bine Simonsen[3], Juliette Schneider[2], Aurélie Lemoine[2], Hans Henrik Gad[3], Jingxian Huang[1], Jieqing Huang[1], Di Chen[1], Tao Peng[1], João T. Marques[4,5], Rune Hartmann[3]*, Nelson E. Martins[2]*, Jean-Luc Imler[1,2]

We previously reported that an ortholog of STING regulates infection by picorna-like viruses in *Drosophila*. In mammals, STING is activated by the cyclic dinucleotide 2′3′-cGAMP produced by cGAS, which acts as a receptor for cytosolic DNA. Here, we showed that injection of flies with 2′3′-cGAMP induced the expression of dSTING-regulated genes. Coinjection of 2′3′-cGAMP with a panel of RNA or DNA viruses resulted in substantially reduced viral replication. This 2′3′-cGAMP–mediated protection was still observed in flies with mutations in *Atg7* and *AGO2*, genes that encode key components of the autophagy and small interfering RNA pathways, respectively. By contrast, this protection was abrogated in flies with mutations in the gene encoding the NF-κB transcription factor Relish. Transcriptomic analysis of 2′3′-cGAMP–injected flies revealed a complex response pattern in which genes were rapidly induced, induced after a delay, or induced in a sustained manner. Our results reveal that dSTING regulates an NF-κB–dependent antiviral program that predates the emergence of interferons in vertebrates.

INTRODUCTION

Like all animals, insects are plagued by viral infections, which they oppose through their innate immune system. Induced transcription of antiviral genes upon the sensing of infection is a common antiviral response conserved across kingdoms. In insects, inducible responses contribute to defense against viruses, together with RNA interference (RNAi) and constitutively expressed restriction factors [reviewed in (*1*)]. Apart from RNAi, these mechanisms are still poorly characterized and appear to be largely virus specific (*2*–*4*). Combining genetics and transcriptomic analysis, we previously showed that the evolutionarily conserved factor dSTING [*Drosophila* stimulator of interferon (IFN) genes], together with the kinase IKKβ (IκB kinase β) and the NF-κB (nuclear factor κB) transcription factor Relish, participates in a pathway controlling infection by the picorna-like viruses *Drosophila* C virus (DCV) and cricket paralysis virus (CrPV) in the model organism *Drosophila melanogaster* (*5*).

In mammals, STING is a central component of the mammalian cytosolic DNA sensing pathway, where it acts downstream of the receptor cyclic GMP-AMP (guanosine 5′-monophosphate–adenosine 5′-monophosphate) synthase (cGAS) (*6*). Upon binding to DNA, cGAS synthesizes 2′3′-cGAMP, a cyclic dinucleotide (CDN) secondary messenger that binds to and activates STING (*7*–*14*). Bacteria also synthesize CDNs such as c-di-AMP, c-di-GMP, and 3′3′-cGAMP, which can be sensed by STING [reviewed in (*15*)]. Upon activation, STING recruits through its C-terminal tail region the kinase TANK-binding kinase 1 (TBK1), which phosphorylates and activates the transcription factor IFN regulatory factor (IRF) 3 to trigger the IFN production (*16*–*18*). STING can also activate NF-κB and autophagy in mammalian cells independently of its C-terminal tail (*19*–*21*).

The identification of STING in animals lacking IFNs, such as insects, raises the question of the ancestral function of this molecule. Invertebrate STING lacks the C-terminal tail extension, which is essential for the activation of IRF transcription factors and induction of IFNs (*22*). In contrast, the ability of STING to regulate transcription factors of the NF-κB family (*5*, *23*, *24*) or autophagy (*25*) seems to be conserved throughout metazoa. These responses are triggered in a C-terminal tail-independent manner in mammals (*19*–*21*). Apart from the missing C-terminal tail, the global overall structure of STING is well conserved between vertebrates and invertebrates. Accordingly, in vitro studies with STING recombinant proteins from the sea anemone *Nematostella vectensis* (Cnidaria), the oyster *Crassostrea gigas* (mollusks), and the worm *Capitella teleta* (annelids) revealed that they all bind CDNs (*26*). However, binding of CDNs is not observed with recombinant STING produced from several insect species, including *Drosophila* (*26*).

The mechanism by which STING exerts its antiviral effect in insects, which could provide important clues on its ancestral function, is still unclear. Here, we identified 2′3′-cGAMP as a potent agonist of dSTING in vivo and show that it triggered a strong Relish-dependent transcriptional response that conferred protection against a broad range of RNA and DNA viruses.

RESULTS

A subset of CDNs trigger the expression of STING-dependent virus-regulated genes

To characterize in vivo the dSTING pathway, we used $dSTING^{Rxn}$ (RXN) loss-of-function mutant flies (fig. S1A). Expression of *dSTING* was reduced by 9- to 27-fold in the mutant, as previously described, but was restored to wild-type (WT) levels when a genomic rescue was introduced in the flies (fig. S1B). Basal levels or Drosophila C virus (DCV)–dependent induction of three previously described IKKβ- and dSTING-dependent genes [CG13641, CG42825, and CG33926; hereafter referred to as sting-regulated gene 1 (*srg1*), *srg2*, and *srg3*, respectively] was significantly reduced in RXN mutant flies compared with $dSTING^{Control}$ (WT) or $dSTING^{Rescue}$ flies (fig. S1, C to E). By contrast, induction of the gene *Hsp26* (*27*) by DCV (fig. S1F)

[1]Sino-French Hoffmann Institute, State Key Laboratory of Respiratory Disease, School of Basic Medical Science, Guangzhou Medical University, Guangzhou 511436, China. [2]Université de Strasbourg, CNRS UPR 9022, 67084 Strasbourg, France. [3]Department of Molecular Biology and Genetics, Aarhus University, 8000 Aarhus C, Denmark. [4]Université de Strasbourg, CNRS UPR 9022, INSERM U1257, 67084 Strasbourg, France. [5]Department of Biochemistry and Immunology, Instituto de Ciências Biológicas, Universidade Federal de Minas Gerais, Belo Horizonte, Minas Gerais CEP 31270901, Brazil.
*Corresponding author. Email: rh@mbg.au.dk (R.H.); nmartins@ibmc-cnrs.unistra.fr (N.E.M.)

or of NF-κB–dependent antimicrobial peptide genes by *Listeria monocytogenes* (fig. S2, A to E) was not affected in the RXN mutant. We noted that *dSTING* expression was still induced by DCV infection in RXN mutant flies, reaching levels close to uninfected WT 3 days post infection (dpi; fig. S1B). We hypothesize that a residual level of dSTING protein in the mutant accounts for some remaining activity of the pathway, because neither the promoter nor the open reading frame of the short form of dSTING is affected by the RXN deletion (fig. S1A).

We next analyzed whether the dSTING pathway could be activated by the naturally occurring CDNs that are agonists of STING in other organisms. Injection of c-di-AMP, 3′3′-cGAMP, and 2′3′-cGAMP into WT flies led to a dose-dependent increase in the expression of *dSTING* and *srg1–3* at 6 and 24 hours post injection (hpi) (Fig. 1, A to H, and fig. S3). Only c-di-GMP did not trigger a response in these experiments (Fig. 1, A to H, and figs. S3 and S4, A and B). These effects were recapitulated in *Drosophila* S2 cells (fig. S5, A and B). The induction of *srg1–3* by CDNs was reduced in RXN mutant flies at 6 hpi or abolished at 24 hpi (Fig. 1, B to D and F to H). For *dSTING* itself, the pattern of induction was similar in RXN and WT flies, although the level of expression was consistently substantially reduced in mutant flies (Fig. 1, A and E). Induction of *dSTING* and *srg1* was abolished in *dSTING* null mutant flies generated independently using CRISPR ($dSTING^{L76GfsTer11}$) (fig. S6, A and B). Last, induction of *dSTING* and *srg1–3* after 2′3′-cGAMP injection was restored in $dSTING^{Rescue}$ flies (fig. S6, C to G).

Induction of *srg1* and *srg2* by 2′3′-cGAMP was rapid, peaking at 3 or 6 hpi and decreasing afterward (Fig. 1, I and J). Inducible expression of *srg3* remained high at 24 hpi (Fig. 1K). Induction of *dSTING* and *srg1–3* by 2′3′-cGAMP was reduced or abolished in *Relish* null mutant flies (Fig. 1, L to O), although the basal level of *dSTING* was not altered (Fig. 1L). Overall, these data reveal that a subset of naturally occurring CDNs can trigger gene expression in *Drosophila*, in a manner dependent on dSTING and Relish.

2′3′-cGAMP affects the transcriptome of whole flies

Next, we performed a genome-wide transcriptomic analysis to identify 2′3′-cGAMP–regulated genes in whole flies. We identified 427 stimulated and 545 repressed genes, displaying at least 1.5-fold change in animals injected with 2′3′-cGAMP compared to tris buffer (Fig. 2A), with 269, 88, and 115 transcripts stimulated and 311, 53, and 63 transcripts repressed at the 6-, 12-, and 24-hour time points, respectively (fig. S7, A and B). In contrast, only four stimulated and one repressed transcripts were observed when c-di-GMP was injected into WT flies (data file S1). Clustering analysis revealed three broad categories of stimulated and repressed genes based on whether they were induced or repressed early, in a sustained manner, or in a delayed fashion (Fig. 2B and data file S2). Among the stimulated genes, *srg1* was induced rapidly, whereas *srg3* was induced after a delay, confirming our initial observation. Rapidly induced genes included those encoding antimicrobial peptides, cytokines such as *spaetzle* and *upd3*, transcription factors (for example, *Rel*, *kay*, *Ets21C*, and *FoxK*), and other signaling molecules (*Takl1*, *pirk*, *Charon*, and *dSTING*) (Fig. 2C). A canonical component of the small interfering RNA (siRNA) pathway, *AGO2*, was rapidly induced by 2′3′-cGAMP, together with *pst* and *ref(2)P*, which encode restriction factors against picorna-like viruses (*28*, *29*) and rhabdoviruses, respectively (*30*). Genes induced after a delay were mainly uncharacterized but included the JAK (Janus kinase)–STAT (signal transducer and activator of transcription)–regulated gene *vir-1* and the antiviral gene *Nazo* (Fig. 2C) (*5*, *31*). Gene ontology analysis revealed that the rapidly induced genes and those induced in a sustained manner were significantly enriched for genes involved in immunity (Fig. 2D), an enrichment not detected in the genes induced at later time points. By contrast, the 2′3′-cGAMP repressed genes were associated with mitochondria or belonged to several metabolic pathways, including carbohydrate, lipid, and protein metabolism (Fig. 2D), suggesting an effect of CDN injection on metabolism, possibly reflecting cellular reprograming.

We performed in silico analysis of predicted binding sites for transcription factors in the stimulated genes (data file S3). We found that 75% of the stimulated genes (321) contained binding sites for members of the NF-κB family. Although 84% of rapidly induced genes and 80% of the genes induced in a sustained manner contained NF-κB binding sites, only 57% (63) of the genes induced later contained such binding sites, suggesting a distinct secondary response at 24 hours post cGAMP injection (data file S4). We further analyzed a subset of genes and confirmed that they were induced by 2′3′-cGAMP but not c-di-GMP and that this induction depended on the NF-κB transcription factor Relish (fig. S8, A to H).

We found enrichment for binding sites for other transcription factors that were stimulated by 2′3′-cGAMP or for transcription factors regulated by induced cytokines (such as upd3) (Fig. 2E). Among these, STAT appears to play an important role in all temporal expression profiles, with binding sites in 22, 42, and 8% of the genes in the early, sustained, and late categories, respectively. Others, such as Ets21c, E2F1, and AP1, may participate in the early phase of the response to 2′3′-cGAMP, given their enrichment only in the rapidly stimulated genes or those stimulated in a sustained manner (Fig. 2E).

Injection of 2′3′-cGAMP protects flies against viral infections

We next addressed the functional consequences of activation of the dSTING pathway by CDN injection. Coinjection of 2′3′-cGAMP with DCV or the related CrPV resulted in a significant decrease in viral RNA accumulation in WT flies (Fig. 3, A and B). This protective effect of 2′3′-cGAMP was not observed in RXN mutant flies but was restored in $dSTING^{Rescue}$ flies (fig. S9), indicating that it depended on dSTING. Accordingly, 2′3′-cGAMP improved the survival of DCV-infected WT flies, but not that of RXN mutants (Fig. 3C). Coinjection of 2′3′-cGAMP but not of c-di-GMP also resulted in reduced accumulation of viral RNA for three other viruses, namely, the positive-strand RNA virus flock house virus (FHV), the negative-strand RNA virus vesicular stomatitis virus (VSV), and the double-strand DNA virus Kallithea virus (KV) (Fig. 3, D to F). Collectively, these results indicate that 2′3′-cGAMP triggers protection against a broad range of viruses.

The antiviral role of 2′3′-cGAMP requires the NF-κB transcription factor Relish and is independent of the siRNA response and autophagy

To identify the mechanism by which 2′3′-cGAMP exerts antiviral activity, we first analyzed the effect of CDNs on DCV and VSV infection in *AGO2* null mutant flies. We observed a reduced accumulation of viral RNAs when 2′3′-cGAMP was coinjected with the viruses in both the mutant and control flies, revealing that the antiviral function of the CDN did not depend on this key component of the antiviral siRNA pathway (Fig. 4, A and B). Similarly, 2′3′-cGAMP

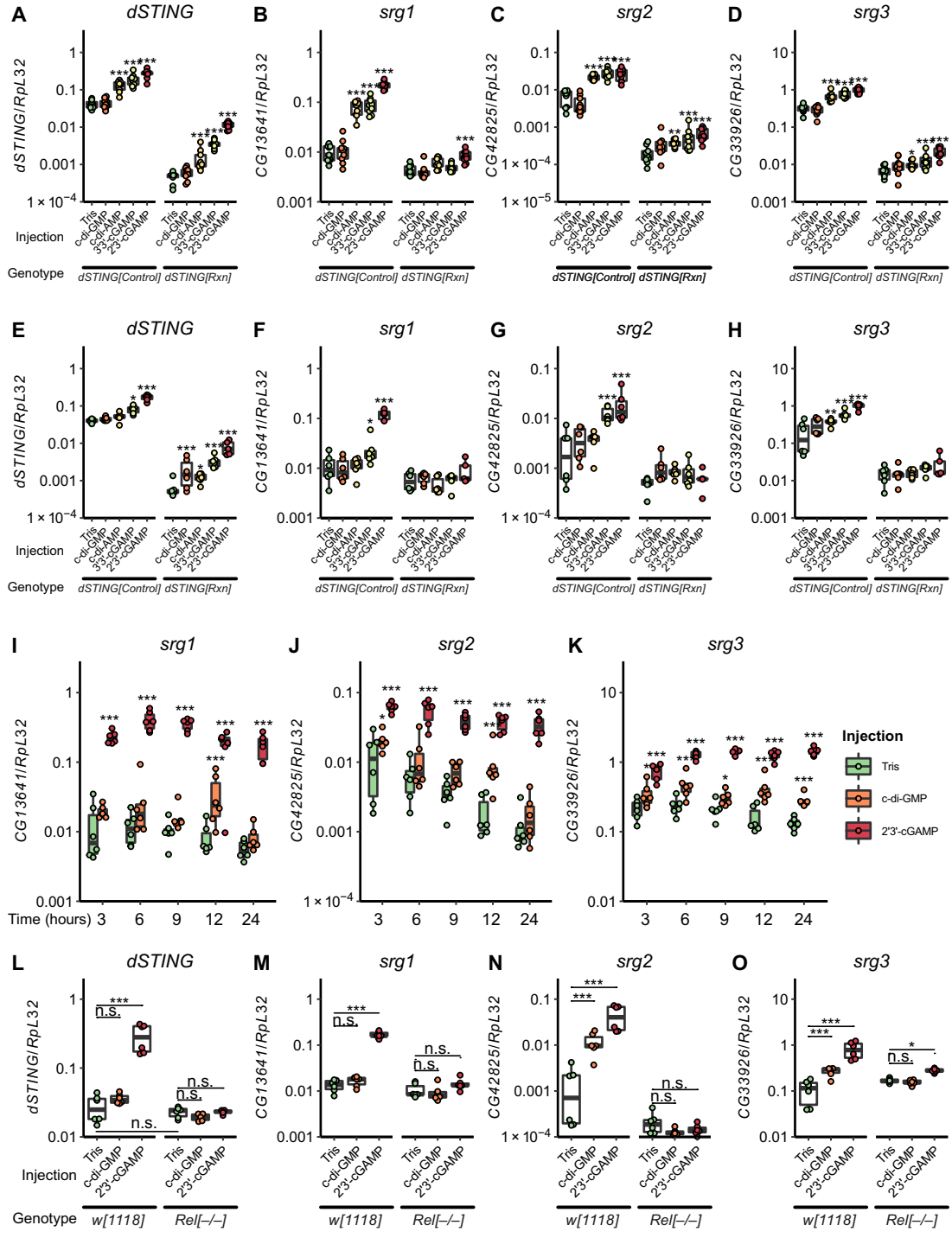

Fig. 1. 2′3′-cGAMP injection induces a dynamic dSTING-Relish–dependent transcriptional response in *D. melanogaster*. (**A** to **H**) Relative gene expression of the indicated dSTING-regulated genes at 6 (A to D) and 24 hours (E to H) after injection of tris and different CDNs in $dSTING^{Control}$ or $dSTING^{Rxn}$ mutant flies. For *dSTING* and *srg1–3* In $dSTING^{Control}$ flies, $|t| \geq 4.807$, $P < 0.001$ for tris injections compared to c-di-AMP, c-di-AMP, 3′3′-cGAMP, or 2′3′-cGAMP injections; $|t| \leq 0.184$, $P \geq 0.184$ for tris compared to c-di-GMP injection. For *srg1–3* in $dSTING^{Rxn}$ mutants, $|t| \leq 3.290$, $P \geq 0.200$ for tris injections compared to CDN injections at 24 hours. For *dSTING* in $dSTING^{Rxn}$ mutants, $|t| \geq 2.963$, $P \leq 0.017$ for tris injections compared to CDN injections, excluding c-di-GMP, $|t| \geq 19.043$, $P < 0.001$ for all pairwise comparisons control flies. (**I** to **K**) Expression of *srg1–3* at different times postinjection with tris, cyclic-di-GMP, or 2′3′-cGAMP. (**L** to **O**) Expression of *dSTING* and *srg1–3* 6 hpi with tris, c-di-GMP or 2′3′-cGAMP in control (w^{1118}) and w^{1118};Rel^{E20} ($Rel^{-/-}$) mutant flies. For *dSTING* expression after tris injection, $|t| = 0.659$, $P = 0.515$ between the control and $Rel^{-/-}$ flies. For *dSTING* and *srg1–3* expression after 2′3′-cGAMP injection, $|t| \geq 5.480$, $P \leq 0.001$ between the control and Relish mutant flies. In (A) to (K), data are from two independent experiments, and each point represents a pool of six flies. Expression is shown relative to the housekeeping gene *RpL32* and is normalized by experiment. Boxplots represent the median (horizontal line) and first/third quartiles, with whiskers extending to points within 1.5 times the interquartile range. *$P \leq 0.05$; **$P \leq 0.01$; ***$P \leq 0.001$; and n.s., $P > 0.05$. For (A) to (K), comparisons are shown relative to tris injection in a given genotype or time point.

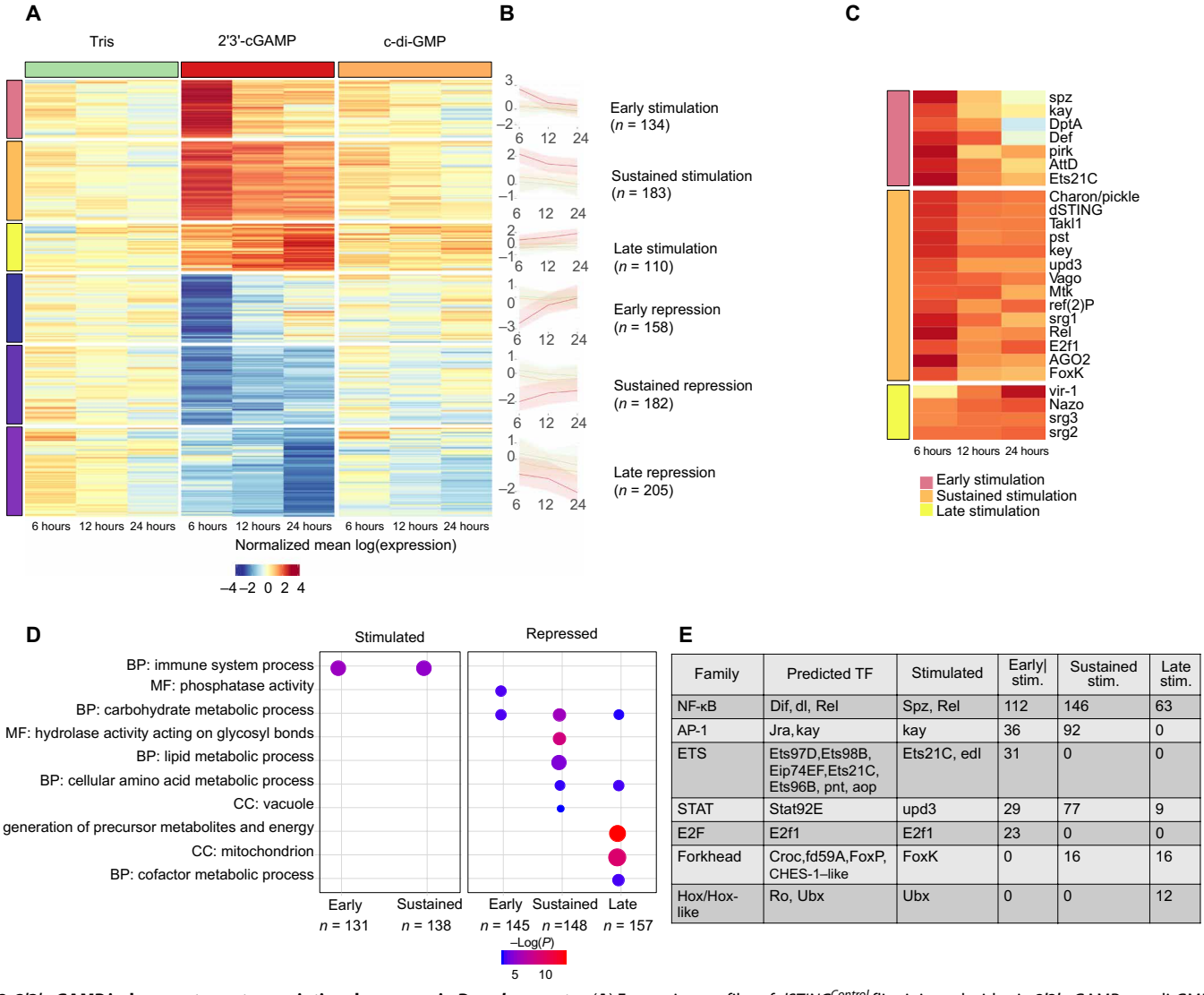

E

Family	Predicted TF	Stimulated	Early stim.	Sustained stim.	Late stim.
NF-κB	Dif, dl, Rel	Spz, Rel	112	146	63
AP-1	Jra, kay	kay	36	92	0
ETS	Ets97D,Ets98B, Eip74EF,Ets21C, Ets96B, pnt, aop	Ets21C, edl	31	0	0
STAT	Stat92E	upd3	29	77	9
E2F	E2f1	E2f1	23	0	0
Forkhead	Croc,fd59A,FoxP, CHES-1–like	FoxK	0	16	16
Hox/Hox-like	Ro, Ubx	Ubx	0	0	12

Fig. 2. 2′3′-cGAMP induces a strong transcriptional response in *D. melanogaster*. (**A**) Expression profiles of *dSTING*^{Control} flies injected with tris, 2′3′-cGAMP or c-di-GMP (6, 12, and 24 hpi). All differentially expressed genes (DEGs) between 2′,3′-cGAMP– and tris-injected flies for at least one time point or on average across all time points are shown. Values are normalized to the mean log (expression) of tris-injected flies across the three time points. Expression profiles of stimulated and repressed genes in 2′3′-cGAMP–injected flies were clustered by partition around medoids. Data are from three independent experiments. (**B**) Normalized mean gene expression by experimental condition in each temporal expression profiles and across the different time points. (**C**) Expression of the indicated representative genes. (**D**) Gene ontology enrichment analysis of the DEGs across the different temporal expression profiles. BP, biological process; MF, molecular function; and CC, cellular compartment. Size and color of circles indicate, respectively, the number of DEG and –log(*P* value) for the enrichment of each category. (**E**) Numbers of DEGs potentially regulated by stimulated transcription factors and cytokines. For a given family, RcisTarget-predicted transcription factors (Predicted TF) are listed.

substantially reduced viral RNA accumulation in *Atg7* null mutant flies, ruling out an involvement of the canonical autophagy pathway (Fig. 4C). By contrast, the protective effect of 2′3′-cGAMP against DCV, CrPV, and VSV was completely abolished in *Relish* mutant flies (Fig. 4, D and F). Together, these results reveal that 2′3′-cGAMP triggers a dSTING–NF-κB–dependent antiviral transcriptional response that is independent of or autophagy.

DISCUSSION

CDNs activate antiviral immunity in *Drosophila*

Our results revealed that three of the four naturally occurring CDNs that activate mammalian STING can also trigger the dSTING signaling pathway in flies. They raise the question of the mechanism by which 2′3′-cGAMP activates dSTING. Kranzusch *et al.* (*26*) did not detect binding of 2′3′-cGAMP to purified recombinant dSTING, suggesting that the purified protein was not folding correctly. The cryo–electron microscopy structure of full-length chicken STING revealed substantial interaction of the ligand binding domain with areas of the transmembrane domains at the N terminus of the protein (*32*). We believe that such interaction may be critical for either ligand binding or stability (or both) of the cytosolic domain of dSTING, a hypothesis supported by the sequence divergence between the transmembrane domains of STING in mammals and *Drosophila*.

Our work complements the molecular study of Kranzusch and colleagues (*26*), who reported binding of CDNs to STING from

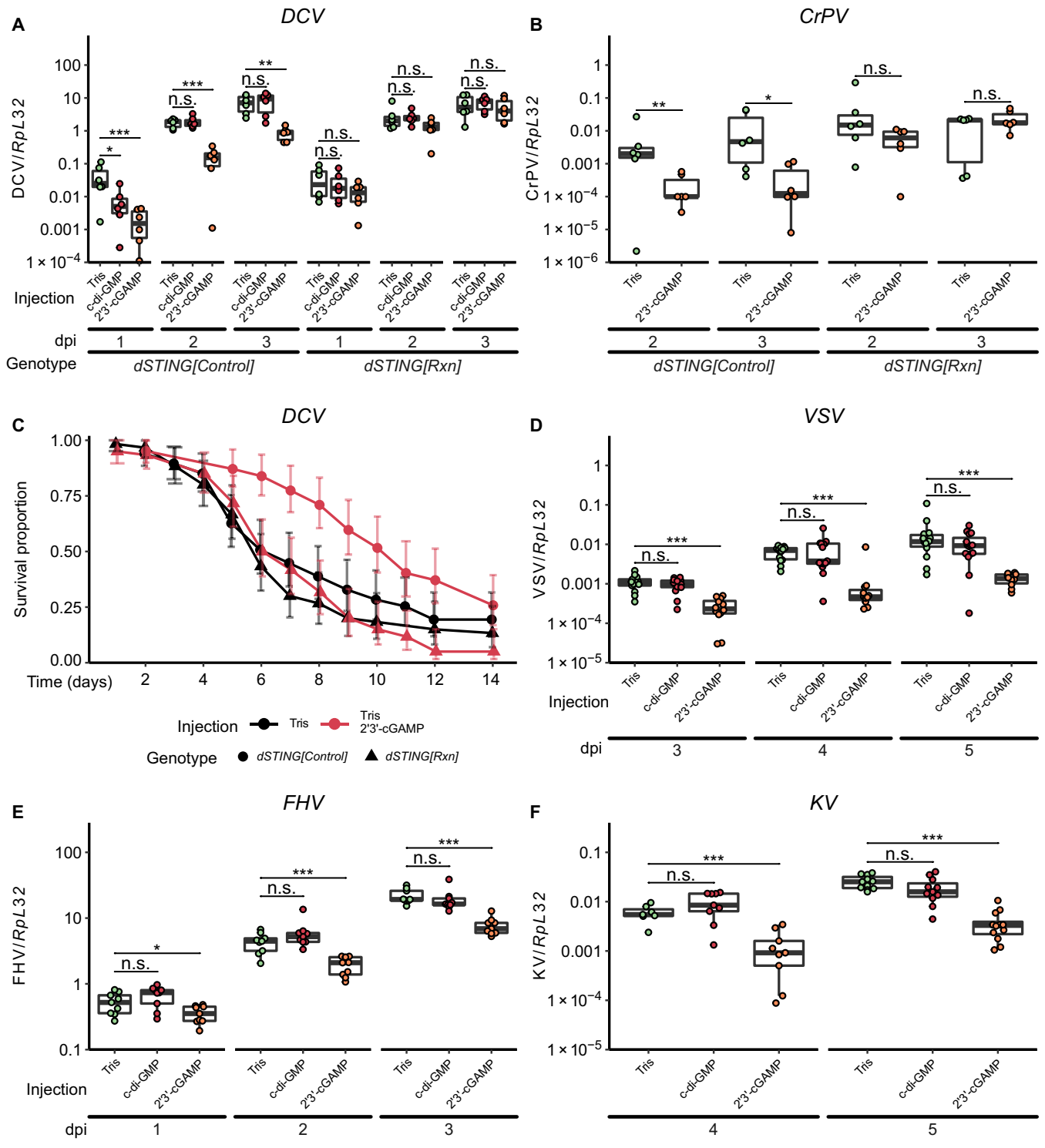

Fig. 3. 2′3′-cGAMP injection induces a broad, dSTING-dependent antiviral protection in *D. melanogaster*. (**A** and **B**) Relative DCV (A) or CrPV (B) RNA loads of $dSTING^{Control}$ and $dSTING^{Rxn}$ mutant flies coinjected with virus and tris, 2′3′-cGAMP, or c-di-GMP at different days post injection (dpi). In $dSTING^{Control}$ flies, $|t| \geq 2.712$, $P \leq 0.020$ for tris compared to 2′3′-cGAMP and $|t| \leq 0.112$, $P \geq 0.985$ for tris compared to c-di-GMP. For $dSTING^{Rxn}$ flies, $|t| \leq 1.547$, $P \geq 0.222$. (**C**) Survival after DCV infection and co-injection with tris or 2′3′-cGAMP. $z = 2.404$, $P = 0.032$ and $z = -0.433$, $P = 0.665$ for $dSTING^{Control}$ and $dSTING^{Rxn}$ flies, respectively, for the pairwise comparisons between tris and 2′3′-cGAMP after a Cox proportional hazards model. (**D** to **F**) Relative viral loads at different time points of control flies after coinjection of tris, 2′3′-cGAMP, or c-di-GMP with the viruses VSV (D), FHV (E), or KV (F). $|t| \geq 2.276$, $P \leq 0.049$ and $|t| \leq 1.769$, $P \geq 0.148$ for tris compared to 2′3′-cGAMP or c-di-GMP at the indicated dpi. Data are from two (A and B) or three (C to F) independent experiments. For (A), (B), and (D) to (F), each point represents a pool of six flies. Expression is shown relative to the housekeeping gene *RpL32* and is normalized by experiment. Boxplots represent the median (horizontal line) and first/third quartiles, with whiskers extending to points within 1.5 times the interquartile range. $^{*}P \leq 0.05$, $^{**}P \leq 0.01$, and $^{***}P \leq 0.001$.

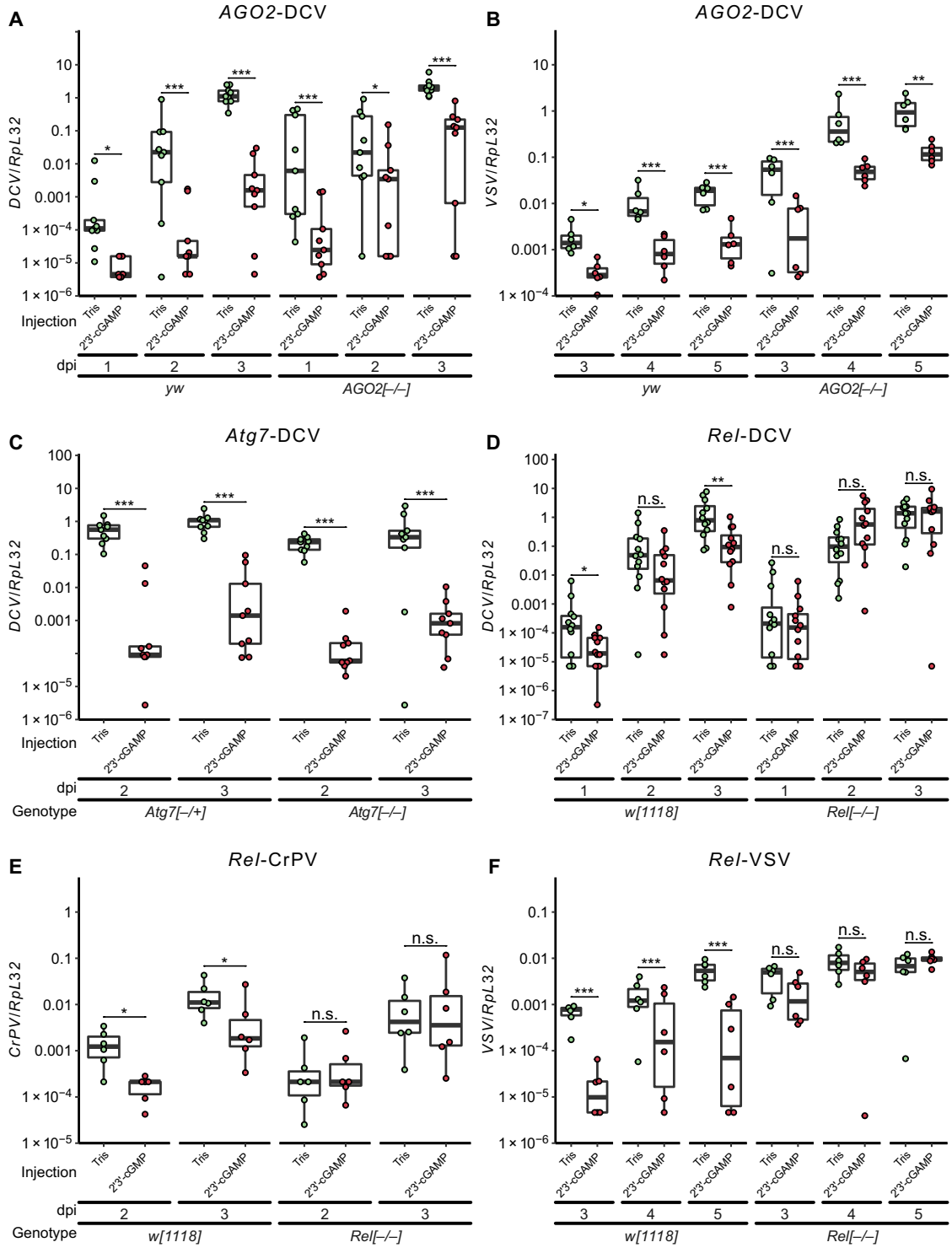

Fig. 4. 2′3′-cGAMP–induced antiviral protection depends on Relish but not Atg7 or AGO2. (**A** to **F**) Viral RNA loads at different time points after coinjection of tris or 2′3′-cGAMP with DCV or VSV in flies with mutations in the siRNA-processing pathway [*yw;Ago2*^{414} - *Ago2*$^{-/-}$ (A and B)], autophagy [*Atg7*$^{d14/d77}$ - *Atg7*$^{-/-}$ (C)], Relish [*w*^{1118};*Rel*^{E20} - *Rel*$^{-/-}$ (D to F)], or in control flies of the same genetic background (*yw*, *Atg7*^{d14}/*CG5335*^{d30} - *Atg7*$^{-/+}$, or *w*^{1118}, respectively). For viral RNA load in RNAi or autophagy-impaired flies, $|t| \geq 2.30$, $P \leq 0.024$ across all time points for tris compared to 2′3′-cGAMP. For viral RNA load in controls for RNAi or autophagy-impaired flies, $|t| \geq 2.53$, $P \leq 0.013$ across all time points for tris compared to 2′3′-cGAMP. Viral RNA load in Relish mutants, $|t| \leq 1.220$, $P \geq 0.225$ across all time points for tris compared to 2′3′-cGAMP. Data are from two (A to C) or four (D) independent experiments, and each point represents a pool of six flies. Expression is shown relative to the housekeeping gene *RpL32* and is normalized by experiment. Triangles indicate points where viral RNA could not be detected; threshold cycle (Cq) values for these points were replaced by the maximum Cq for a virus-infected sample + 1. Boxplots represent the median (horizontal line) and first/third quartiles, with whiskers extending to points within 1.5 times the interquartile range. *$P \leq 0.05$, **$P \leq 0.01$, and ***$P \leq 0.001$.

the sea anemone *N. vectensis*, and supports the hypothesis that the ancestral function of STING in metazoans was to sense CDNs. Bacteria produce various CDNs and cyclic trinucleotides, some of which could activate dSTING (*23*, *33*). Martin *et al.* (*23*) reported that c-di-GMP activates a dSTING-dependent response to *L. monocytogenes* infection. However, we did not observe an effect of c-di-GMP upon injection into flies or a contribution of dSTING to induction of antimicrobial peptides after infection by *L. monocytogenes* (fig. S2, A to E). Further experiments comparing mutant alleles and taking other parameters (such as microbiota) into consideration are required to clarify the differences between the two studies.

Bacterial CDNs have two canonical 3′,5′-phosphodiester linkages, whereas mammalian and *Nematostella* cGAS produce chemically distinct CDNs containing one 2′,5′ phosphodiester bond joining G to A and one canonical 3′,5′ phosphodiester bond joining A to G (*21*, *26*). Although we detected activity of 3′3′-CDNs, namely, of 3′3′-cGAMP and of c-di-AMP, the strongest agonist was 2′3′-cGAMP, suggesting that an enzyme producing this CDN exists in insects. Wang and colleagues (*24*) reported the inducible production of cGAMP in the cytosol of *Bombyx mori* cells infected with nucleopolyhedrovirus (NPV). Thus, the production of CDNs in the response to virus infection appears to be ancient, possibly inherited in early eukaryotes from prokaryotes (*22*, *34*). A major goal for future studies will be the identification and characterization of the cGAS enzyme in *Drosophila*.

Activation of NF-κB is an ancestral function of the dSTING pathway

One major difference between STING in mammals and invertebrates, including *Nematostella* and *Drosophila*, is the lack of the C-terminal tail that mediates interaction with and activation of the kinase TBK1 and the transcription factor IRF3 (*22*). This has led to the hypothesis that invertebrate STING regulates autophagy rather than a transcriptional response. STING activates autophagy through a mechanism that is independent of TBK1 activation and IFN induction in mammals. Furthermore, *Nematostella* STING also induces autophagy when it is ectopically expressed in human cells (*21*). In *Drosophila*, autophagy participates in the control of some viruses, although the effect is modest compared with RNAi (*35*, *36*). dSTING-dependent autophagy has been proposed to restrict Zika virus infection in the brain, although autophagy constituents are required for the replication of Zika and other flaviviruses in mammalian cells (*25*, *37*). Our results with *ATG7* mutant flies indicate that 2′3′-cGAMP can control viral infection independently from the canonical autophagy pathway but requires both dSTING and Relish. However, we cannot rule out a virus-specific role (such as for Zika virus) and the involvement of an unconventional autophagy pathway. LC3 lipidation in response to cGAMP stimulation in human cells does not depend on the unc-51 like kinases (ULK) or Beclin 1, two essential components of the classical autophagy pathway (*21*). In this regard, we note that one of the genes stimulated by cGAMP is *ref(2)P*, the ortholog of the autophagy receptor p62 and a restriction factor for Sigma virus (*30*). Although we cannot completely rule out a contribution of autophagy, our results point to the central role played by the NF-κB transcription factor Relish in the antiviral response triggered by 2′3′-cGAMP. Further analysis will be required to precisely define the contribution of Relish in this response. The dSTING-dependent transcriptional response to cGAMP injection is complex, involving stimulation and repression of gene expression occurring in different waves, with early and late responses. However, the presence of consensus binding sites for NF-κB in the *cis*-regulatory regions of ~75% of the stimulated genes, regardless of their kinetics of induction, confirms a major contribution of Relish. In addition, we identified 13 other transcription factors and two cytokines (*upd3* and *spz*) in the early and sustained stimulated genes. Among the stimulated transcription factors, *kay* (the *Drosophila* ortholog of c-*Fos*), *Ets21C*, and *FoxK* were previously implicated in immune, inflammatory, or stress responses in *Drosophila* (*38*–*40*). The *cis*-regulatory regions of the differentially expressed genes were enriched for binding sites for the mentioned transcription factors and STAT92E, the sole *Drosophila* STAT ortholog (Fig. 3D). These different transcriptional regulators may coordinate the kinetics of the response and induction of different sets of genes in the context of bacteria and virus infection.

A broad antiviral-induced response in *Drosophila*

We observed that 2′3′-cGAMP exerted antiviral activity against a broad range of viruses with DNA or RNA genomes. Our findings contrast with previous studies that reported virus-specific–induced responses (*2*, *41*–*45*), leading to the idea that RNAi is the only pathway acting on the broad range of viruses infecting invertebrates, which are devoid of IFNs. In this regard, we showed that the antiviral effect of 2′3′-cGAMP does not require AGO2, a key component of the antiviral RNAi pathway in flies, although this gene is stimulated by the CDN. Thus, in addition to RNAi, an induced antiviral response involving dSTING contributes to host defense against a range of viruses in *Drosophila*. Furthermore, the induction of AGO2 by CDNs suggests cross-talk between the two pathways such that activation of dSTING may potentiate the siRNA response. Although our data are consistent with 2′3′-cGAMP triggering dSTING-dependent antiviral immunity, it is less clear that viral infection in flies can induce CDN production and STING-dependent responses. In particular, we did not observe increased DCV replication in *dSTING* and *Relish* mutant flies, in contrast to what we previously reported (*5*). The reason for this discrepancy is not clear at present but may involve changes in the microbiota of the flies. We note that several of the dSTING- and IKKβ-dependent genes that we identified can be regulated by the microbiota (*46*). Our previous results pointed to a specific contribution of the dSTING-IKKβ-Relish pathway in resistance to DCV and CrPV and a substantial but smaller effect for VSV (*5*). This apparent discrepancy could be explained by differences between viruses in the induction of the pathway based on their tissue tropisms, the type of virus-associated molecular pattern produced, or the existence of escape strategies, all of which may be bypassed by systemic injection of 2′3′-cGAMP.

Previous studies reported strong transcriptional responses to virus infection not only in insects (*2*, *27*, *31*, *43*, *47*, *48*) but also in *Caenorhabditis elegans* (*49*), oysters (*50*), and shrimps (*51*). Analysis of the transcriptional response to viral infections in vivo is complicated by the fact that (i) cell infections are unsynchronized; (ii) host cells are modified through hijacking of cellular functions by viruses; and (iii) many viruses trigger cell lysis and tissue damage, making it complicated to discern the immune response from the nonspecific response to stress. Consequently, transcriptomic analysis of virus-infected flies provides only an imprecise image of the induced antiviral response (*2*, *27*, *31*, *43*, *44*, *48*). Identification of an agonist of dSTING bypasses the need for the use of viruses and provides a clearer picture of the modifications of the *Drosophila* transcriptome associated with induction of antiviral immunity. In particular, our data suggest

that 2′3′-cGAMP triggers the expression of cytokines (such as Spaetzle and upd3) that amplify the response and trigger expression of antiviral effectors (such as Nazo and vir-1). The tools are now at hand to characterize the induced mechanisms controlling viruses in insects, which may reveal previously unidentified targets for antiviral therapy.

MATERIALS AND METHODS

Drosophila strains

Fly stocks were raised on standard cornmeal agar medium at 25°C. All fly lines used in this study were *Wolbachia* free. w^{1118}, $dSTING^{Control}$, $dSTING^{Rxn}$, *yellow* (*y*) *white* (*w*) *DD1, yw;AGO2*^{414}, $Atg7^{d14}$/*Cyo-GFP*, $Atg7^{d77}$/*Cyo-GFP*, and $CG5335^{d30}$/*Cyo-GFP* stocks have been described previously (*35*). $Relish^{E20}$ flies isogenized to the DrosDel w^{1118} isogenic background were a gift from L. Teixeira (Instituto Gulbenkian de Ciência) (*45*).

$dSTING^{L76GfsTer11}$ mutants were generated by CRISPR-Cas–mediated mutagenesis in a *yw* mutant background. Briefly, single guide RNA encoding pUAS-attB plasmids were injected into embryos of y^1 *M{vas-int.Dm}ZH-2A w*; M{3xP3-RFP.attP}ZH-86Fb* (BDSC#24749) flies. Transgenics were then crossed with y^1 w^{1118}*; attP2{nos-Cas9}/TM6C, Sb Tb [y+]* (NIG)flies. Individual males from the F1 were then crossed with *yw; Bc,Gla/CyO* flies to establish stocks from the *CyO* progeny. This progeny was then scored for mutations by Sanger sequencing (Eurofins Genomics), using the sequencing primers described in table S1. Crossing schemes and detailed injection protocols are available upon request.

The genomic rescue of WT dSTING was established by PhiC31-mediated transgenesis. The fosmid FlyFos015653 (*52*) was injected into the y^1 w^{1118}; *PBac{y[+]-attP-9A}VK00027* (BDSC#9744) line and introgressed into a $dSTING^{Rxn}$ mutant background by standard genetic crossing techniques. Transgenesis and initial recombinant fly selection was done by the company BestGene.

Virus infection

Viral stocks were prepared in 10 mM tris-HCl, pH 7.5. Infections were performed with 3- to 5-day-old adult flies by intrathoracic injection (Nanoject II apparatus, Drummond Scientific) with 4.6 nl of DCV solution [500 plaque-forming units (PFU) per fly]. Injection of the same volume of 10 mM tris-HCl, pH 7.5, was used as a negative control.

Bacterial infections

L. monocytogenes (strain 10403S) cultures were grown in brain heart infusion (BHI) medium at 28°C. Infections were performed with 3- to 5-day-old adult flies by intrathoracic injection (Nanoject II apparatus) with 9.2 nl of *L. monocytogenes* solution in phosphate-buffered saline (PBS) [optical density (OD_{600}) = 0.001]. The dose used was determined by titration, comparing the WT strain to its listeriolysin O deletion mutant (*L. monocytogenes* Δ*hly*; a gift of P. Cossart) to ensure that the response to cytosolic *L. monocytogenes* was monitored (*53*). Injection of the same volume of PBS was used as a negative control. Injected flies were kept at 28°C and collected in pools of six individuals (three males + three females) at the indicated time points for RNA extraction and real-time quantitative polymerase chain reaction (RT-qPCR).

CDN injection with or without viruses

The CDNs (InvivoGen) were dissolved in 10 mM tris, pH 7.5, to a concentration of 0.9 mg/ml, and their integrity was monitored by chromatography, as described (*54*). Three- to 5-day-old adult flies were CDN stimulated. For CDN injection, each fly was injected with 69 nl of CDN solution or 10 mM tris, pH 7.5 (negative control), by intrathoracic injection using a Nanoject II apparatus. For CDNs and virus coinjection, 30 μl of CDNs (0.9 mg/ml) was mixed with 2 μl of virus (DCV, 5 PFU/4.6 nl; CRPV, 5 PFU/4.6 nl; VSV, 5000 PFU/4.6 nl; FHV, 500 PFU/4.6 nl; and KV). Each fly was injected with 69 nl of CDNs or 10 mM tris, pH 7.5, plus virus mixture by intrathoracic injection using a Nanoject II apparatus (Drummond Scientific), and injected flies were collected in pools of six individuals (three males + three females) at indicated time points and homogenized for RNA extraction and RT-qPCR.

CDN transfection of *Drosophila* S2 cells

Drosophila Schneider 2 (S2) cells were seeded in 12-well plates (2×10^6 cells per well) in Schneider's insect medium (Sigma-Aldrich) supplemented with 10% fetal bovine serum (FBS) (Sigma-Aldrich), penicillin (100 U/ml; Sigma-Aldrich), and streptomycin (100 μg/ml; Sigma-Aldrich). Three hours later, the cells were transfected with 10 μg of CDN per well using 2 μl of Lipofectamine 2000 (Thermo Fisher Scientific) according to the manufacturer's protocol. Unsupplemented Schneider's insect medium was used to generate the transfection complexes. After 6 or 24 hours of transfection, cells were harvested for RNA extraction and qRT-PCR.

RNA extraction and qRT-PCR of *D. melanogaster* tissues

Total RNA from collected flies was extracted using a TRIzol Reagent RT bromoanisole solution (Molecular Research Center, Inc.) according to the manufacturer's instructions. One microgram of the total RNA was reverse transcribed using an iScript genomic DNA clear cDNA synthesis kit (Bio-Rad) according to the manufacturer's instructions. The deoxyribonuclease (DNase) and RNA reaction mixture was incubated for 5 min at 25°C to remove genomic DNA. The reaction was stopped by heating at 75°C for 5 min. Reverse transcription mix was added to the DNase-treated RNA template, and cDNA was synthesized in the following PCR program: 25°C for 5 min, 46°C for 20 min, and 95°C for 1 min. cDNA was used for qRT-PCR, using iQ Custom SYBR Green Supermix Kit (Bio-Rad) according to the manufacturer's instructions and the following qPCR program: (i) 98°C for 15 s, (ii) 95°C for 2 s, (iii) 60°C for 30 s, (iv) plate read, and (v) repeat step 2 34X on a CFX384 Touch RT-PCR platform (Bio-Rad). Primers used for qRT-PCR are listed in table S1. Normalization was performed relative to the housekeeping gene *RpL32*.

RNA extraction and qRT-PCR of *Drosophila* S2 cells

Total RNA was extracted using the EZNA Total RNA Kit I (Omega Bio-tek) following the manufacturer's protocol. cDNA was generated with random hexamer primers and the RevertAid RT Reverse Transcription Kit (Thermo Fisher Scientific) using 1 μg of the total RNA as template, following the manufacturer's protocol. cDNA was diluted five times and used as templates for qRT-PCR on a LightCycler 480 Instrument II (Roche) using LightCycler 480 SYBR Green I Master reaction mix (Roche) according to the manufacturer's instructions and the following qPCR program: (i) 95°C for 5 min, (ii) 95°C for 10 s, (iii) 55°C for 10 s, (iv) 72°C for 10 s, (v) plate read, and (vi) repeat step 2 44X. Primers used for qRT-PCR are listed in table S1. Normalization was performed relative to the housekeeping gene *RpL32*.

RNA sequencing of *D. melanogaster* injected with CDNs

Male flies of $dSTING^{Control}$ were injected with 69 nl per fly of either 10 mM tris (pH 7.5), c-di-GMP (1 mg/ml), or 2′3′-cGAMP (1 mg/ml)

by intrathoracic injection (Nanoject II apparatus) in three independent experiments. Injected flies were collected in pools of six individuals at 6, 12, and 24 hpi. Total RNA was isolated from injected flies using TRIzol Reagent (Invitrogen) according to the manufacturer's protocol. RNA quantity and purity were assessed using a DW-K5500 spectrophotometer (Drawell) and Agilent 2200 TapeStation (Agilent). Ribosomal RNA (rRNA) was removed using Epicentre Ribo-Zero rRNA Removal Kit (Illumina), and RNA was converted to cDNA. Prepared cDNA was used for Illumina sequencing library preparation using NEBNext Ultra Directional RNA Library Prep Kit for Illumina (NEB), following the manufacturer's instructions. Briefly, DNA fragments were end repaired to generate blunt ends with 5′-phosphate and 3′ hydroxyl groups before adapter ligation, PCR amplification, and cleanup. Average fragment length was 300 base pairs (bp). Purity of the libraries was evaluated using an Agilent 2200 TapeStation. Libraries were used for cluster generation in situ on an HiSeq paired-end flow cell using the Rapid mode cluster generation system, followed by massively parallel sequencing (2 × 150 bp) on an HiSeq X Ten. Library construction, high-throughput sequencing, adapter removal, and initial quality control and trimming were done by the company RiboBio.

Transcriptome analysis

After quality trimming and adapter removal using Trimmomatic, reads were mapped using STAR v2.5.3 (*55*) to the *Drosophila* genome and annotation (ENSEMBL BDGP6.22). Reads mapping to the sense strand of the transcripts were counted with featureCounts v1.6.2 (*56*), using the *Drosophila* annotation files, allowing mapping to multiple genes. Differential gene expression of transcripts present in ≥20% of the libraries with at least five reads across all libraries was done using the deseq function of the "DESeq2" (v1.20) package (*57*). Variance was estimated using the local fitting method. Read counts and normalized read counts are shown in the Gene Expression Omnibus dataset GSE140955. Transcripts with $\log_2$ difference in expression ≥1.5 and Benjamini and Hochberg–corrected $P < 0.05$ were considered differentially expressed.

Clustering of temporal expression profiles

All differentially expressed genes between the tris- and 2′3′-cGAMP–injected WT flies at any time point or on average across all time points were clustered in the temporal expression categories by partitioning around medoids (PAM) clustering using the pam function in the "cluster" (v2.1.0) package. The optimal number of clusters for either stimulated or repressed genes was determined using the gap statistic method, as implemented in the fviz_nbclust function of the "factoextra" (v1.0.5) package, using default parameters (100 bootstrapped replications, 10 maximum allowed clusters). Gene expression clusters were visualized using the heatmap function of the "ComplexHeatmap" (v2.0.0) package and ggplot of the "ggplot2" (v3.2.1) package.

Ontology analysis

Differentially expressed genes between the tris- and 2′3′-cGAMP–injected WT flies in each temporal expression category were tested for enrichment relative to all genes that met the expression cutoff in any gene ontology type (Molecular Function, Cellular Compartment, and Biological Process), using the "Generic GO subset" of gene ontology terms (downloaded from http://current.geneontology.org/ontology/subsets/index.html on 10 October 2019). Gene ontology enrichment analysis was done using the enricher function of "clusterProfiler" package (v3.1.12), using default parameters (Benjamini and Hochberg–corrected *P* value cutoff of 0.05).

Transcription factor enrichment analysis

Enrichment of transcription factor binding sites in the regulatory regions of the differentially expressed genes was done using the cisTarget function of the "RcisTarget" package (v1.4.0) (*58*). The database "dm6-5 kb-upstream-full-tx-11species.mc8nr" database was used, which includes the rankings for conserved transcription factor binding sites in the noncoding regions 5 kb upstream of the transcription start site and in introns of all annotated genes in the *D. melanogaster* genome (r6.02). Gene symbols were updated to the r6.04 annotation when necessary. Transcription factor family assignment was done according to FlyBase (FB2019_05).

Statistical analysis

For quantification of the viral RNA loads and target gene expression, log-transformed ratios were compared using linear regression models using the lm function of base R. Survival curves were analyzed by Cox regression using the coxph function in the "survival" (v2.44-1.1) package. Depending on the experiment, independent variables included genotype, virus injection, CDN injection, time post injection, and all interactions between these variables. Experiment was included as an independent variable in all tests, and the values for each point were normalized by adding/subtracting the mean difference between its respective experiment to the grand mean of all log ratios.

Multiple comparisons between the groups of interest were done using the emmeans function of the "emmeans" (v1.4.1) package, using Dunnett's (to compare control to treatment) or Holm's *P* value correction. Data were analyzed using R (v3.4.2), and ggplot was used for plotting.

SUPPLEMENTARY MATERIALS

stke.sciencemag.org/cgi/content/full/13/660/eabc4537/DC1

Fig. S1. DCV infection induces a dSTING-dependent transcriptional response in *D. melanogaster*.
Fig. S2. Antimicrobial peptide gene induction is not affected in *dSTING* mutant flies after *L. monocytogenes* challenge.
Fig. S3. The CDNs 2′3′-cGAMP, 3′3′-cGAMP, and c-di-AMP have a dose-dependent effect on the expression of a *dSTING*-regulated gene.
Fig. S4. c-di-GMP injection does not induce antimicrobial peptide expression.
Fig. S5. The CDNs 2′3′-cGAMP and 3′3′-cGAMP induce dSTING-dependent genes in a cellular model.
Fig. S6. Induction of gene expression after 2′3′-cGAMP injection depends on dSTING.
Fig. S7. Differentially expressed transcripts between the tris- and 2′3′-cGAMP–injected flies at different time points.
Fig. S8. 2′3′-cGAMP–induced gene expression is *Relish* dependent.
Fig. S9. A *dSTING* rescue transgene restores 2′3′-cGAMP–induced antiviral protection.
Table S1. List of oligonucleotide primers used in this study.
Data file S1. Differentially expressed genes between the tris- and c-di-GMP–injected $dSTING^{Control}$ flies at 6, 12, and 24 hpi.
Data file S2. Differentially expressed genes between the tris- and 2′3′-cGAMP–injected $dSTING^{Control}$ flies at 6, 12, and 24 hpi.
Data file S3. Differentially expressed transcription factors or cytokines between tris- and 2′3′-cGAMP–injected $dSTING^{Control}$ flies at 6, 12, and 24 hpi.
Data file S4. Presence of binding sites for stimulated transcription factors in differentially expressed genes.
Reference (*59*)

View/request a protocol for this paper from *Bio-protocol*.

REFERENCES AND NOTES

1. A. Mussabekova, L. Daeffler, J.-L. Imler, Innate and intrinsic antiviral immunity in Drosophila. *Cellular Mol. Life Sci.* **74**, 2039–2054 (2017).

2. C. Kemp, S. Mueller, A. Goto, V. Barbier, S. Paro, F. Bonnay, C. Dostert, L. Troxler, C. Hetru, C. Meignin, S. Pfeffer, J. A. Hoffmann, J.-L. Imler, Broad RNA interference–mediated antiviral immunity and virus-specific inducible responses in *Drosophila*. *J. Immunol.* **190**, 650–658 (2013).
3. C. Cao, R. Cogni, V. Barbier, F. M. Jiggins, Complex coding and regulatory polymorphisms in a restriction factor determine the susceptibility of *Drosophila* to viral infection. *Genetics* **206**, 2159–2173 (2017).
4. C. Cao, M. M. Magwire, F. Bayer, F. M. Jiggins, A polymorphism in the processing body component Ge-1 controls resistance to a naturally occurring rhabdovirus in *Drosophila*. *PLOS Pathog.* **12**, e1005387 (2016).
5. A. Goto, K. Okado, N. Martins, H. Cai, V. Barbier, O. Lamiable, L. Troxler, E. Santiago, L. Kuhn, D. Paik, N. Silverman, A. Holleufer, R. Hartmann, J. Liu, T. Peng, J. A. Hoffmann, C. Meignin, L. Daeffler, J.-L. Imler, The kinase IKKβ regulates a STING- and NF-κB-dependent antiviral response pathway in *Drosophila*. *Immunity* **49**, 225–234.e4 (2018).
6. L. Sun, J. Wu, F. Du, X. Chen, Z. J. Chen, Cyclic GMP-AMP synthase is a cytosolic DNA sensor that activates the type I interferon pathway. *Science* **339**, 786–791 (2013).
7. J. X. Wu, L. Sun, X. Chen, F. Du, H. Shi, C. Chen, Z. J. Chen, Cyclic GMP-AMP is an endogenous second messenger in innate immune signaling by cytosolic DNA. *Science* **339**, 826–830 (2013).
8. D. Gao, J. Wu, Y. -T. Wu, F. du, C. Aroh, N. Yan, L. Sun, Z. J. Chen, Cyclic GMP-AMP synthase is an innate immune sensor of HIV and other retroviruses. *Science* **341**, 903–906 (2013).
9. A. Ablasser, M. Goldeck, T. Cavlar, T. Deimling, G. Witte, I. Röhl, K.-P. Hopfner, J. Ludwig, V. Hornung, cGAS produces a 2′-5′-linked cyclic dinucleotide second messenger that activates STING. *Nature* **498**, 380–384 (2013).
10. E. J. Diner, D. L. Burdette, S. C. Wilson, K. M. Monroe, C. A. Kellenberger, M. Hyodo, Y. Hayakawa, M. C. Hammond, R. E. Vance, The innate immune DNA sensor cGAS produces a noncanonical cyclic dinucleotide that activates human STING. *Cell Rep.* **3**, 1355–1361 (2013).
11. X. Zhang, H. Shi, J. Wu, X. Zhang, L. Sun, C. Chen, Z. J. Chen, Cyclic GMP-AMP containing mixed phosphodiester linkages is an endogenous high-affinity ligand for STING. *Mol. Cell* **51**, 226–235 (2013).
12. F. Civril, T. Deimling, C. C. de Oliveira Mann, A. Ablasser, M. Moldt, G. Witte, V. Hornung, K.-P. Hopfner, Structural mechanism of cytosolic DNA sensing by cGAS. *Nature* **498**, 332–337 (2013).
13. P. J. Kranzusch, A. S.-Y. Lee, J. M. Berger, J. A. Doudna, Structure of human cGAS reveals a conserved family of second-messenger enzymes in innate immunity. *Cell Rep.* **3**, 1362–1368 (2013).
14. P. Gao, M. Ascano, Y. Wu, W. Barchet, B. L. Gaffney, T. Zillinger, A. A. Serganov, Y. Liu, R. A. Jones, G. Hartmann, T. Tuschl, D. J. Patel, Cyclic [G(2′,5′)pA(3′,5′)p] is the metazoan second messenger produced by DNA-activated cyclic GMP-AMP synthase. *Cell* **153**, 1094–1107 (2013).
15. P. J. Kranzusch, cGAS and CD-NTase enzymes: Structure, mechanism, and evolution. *Curr. Opin. Struct. Biol.* **59**, 178–187 (2019).
16. M. Motwani, S. Pesiridis, K. A. Fitzgerald, DNA sensing by the cGAS–STING pathway in health and disease. *Nat. Rev. Genet.* **20**, 657–674 (2019).
17. C. Zhang, G. Shang, X. Gui, X. Zhang, X.-C. Bai, Z. J. Chen, Structural basis of STING binding with and phosphorylation by TBK1. *Nature* **567**, 394–398 (2019).
18. S. Liu, X. Cai, J. Wu, Q. Cong, X. Chen, T. Li, F. Du, J. Ren, Y.-T. Wu, N. V. Grishin, Z. J. Chen, Phosphorylation of innate immune adaptor proteins MAVS, STING, and TRIF induces IRF3 activation. *Science* **347**, aaa2630 (2015).
19. S. Cerboni, N. Jeremiah, M. Gentili, U. Gehrmann, C. Conrad, M.-C. Stolzenberg, C. Picard, B. Neven, A. Fischer, S. Amigorena, F. Rieux-Laucat, N. Manel, Intrinsic antiproliferative activity of the innate sensor STING in T lymphocytes. *J. Exp. Med.* **214**, 1769–1785 (2017).
20. C. C. de Oliveira Mann, M. H. Orzalli, D. S. King, J. C. Kagan, A. S. Y. Lee, P. J. Kranzusch, Modular architecture of the STING C-terminal tail allows interferon and NF-κB signaling adaptation. *Cell Rep.* **27**, 1165–1175.e5 (2019).
21. X. Gui, H. Yang, T. Li, X. Tan, P. Shi, M. Li, F. du, Z. J. Chen, Autophagy induction via STING trafficking is a primordial function of the cGAS pathway. *Nature* **567**, 262–266 (2019).
22. S. R. Margolis, S. C. Wilson, R. E. Vance, Evolutionary origins of cGAS-STING signaling. *Trends Immunol.* **38**, 733–743 (2017).
23. M. Martin, A. Hiroyasu, R. M. Guzman, S. A. Roberts, A. G. Goodman, Analysis of *Drosophila* STING reveals an evolutionarily conserved antimicrobial function. *Cell Rep.* **23**, 3537–3550.e6 (2018).
24. X. Hua, B. Li, L. Song, C. Hu, X. Li, D. Wang, Y. Xiong, P. Zhao, H. He, Q. Xia, F. Wang, Stimulator of interferon genes (STING) provides insect antiviral immunity by promoting Dredd caspase–mediated NF-κB activation. *J. Biol. Chem.* **293**, 11878–11890 (2018).
25. Y. Liu, B. Gordesky-Gold, M. Leney-Greene, N. L. Weinbren, M. Tudor, S. Cherry, Inflammation-induced, STING-dependent autophagy restricts Zika virus infection in the *Drosophila* brain. *Cell Host Microbe* **24**, 57–68.e3 (2018).
26. P. J. Kranzusch, S. C. Wilson, A. S. Y. Lee, J. M. Berger, J. A. Doudna, R. E. Vance, Ancient origin of cGAS-STING reveals mechanism of universal 2′,3′ cGAMP signaling. *Mol. Cell* **59**, 891–903 (2015).
27. S. H. Merkling, G. J. Overheul, J. T. van Mierlo, D. Arends, C. Gilissen, R. P. van Rij, The heat shock response restricts virus infection in *Drosophila*. *Sci. Rep.* **5**, 12758 (2015).
28. N. E. Martins, V. G. Faria, V. Nolte, C. Schlötterer, L. Teixeira, É. Sucena, S. Magalhães, Host adaptation to viruses relies on few genes with different cross-resistance properties. *Proc. Natl. Acad. Sci. U.S.A.* **111**, 5938–5943 (2014).
29. M. M. Magwire, D. K. Fabian, H. Schweyen, C. Cao, B. Longdon, F. Bayer, F. M. Jiggins, Genome-wide association studies reveal a simple genetic basis of resistance to naturally coevolving viruses in *Drosophila melanogaster*. *PLOS Genet.* **8**, e1003057 (2012).
30. J. Bangham, K.-W. Kim, C. L. Webster, F. M. Jiggins, Genetic variation affecting host–parasite interactions: Different genes affect different aspects of sigma virus replication and transmission in *Drosophila melanogaster*. *Genetics* **178**, 2191–2199 (2008).
31. C. Dostert, E. Jouanguy, P. Irving, L. Troxler, D. Galiana-Arnoux, C. Hetru, J. A. Hoffmann, J.-L. Imler, The Jak-STAT signaling pathway is required but not sufficient for the antiviral response of drosophila. *Nat. Immunol.* **6**, 946–953 (2005).
32. G. Shang, C. Zhang, Z. J. Chen, X.-C. Bai, X. Zhang, Cryo-EM structures of STING reveal its mechanism of activation by cyclic GMP–AMP. *Nature* **567**, 389–393 (2019).
33. A. T. Whiteley, J. B. Eaglesham, C. C. de Oliveira Mann, B. R. Morehouse, B. Lowey, E. A. Nieminen, O. Danilchanka, D. S. King, A. S. Y. Lee, J. J. Mekalanos, P. J. Kranzusch, Bacterial cGAS-like enzymes synthesize diverse nucleotide signals. *Nature* **567**, 194–199 (2019).
34. D. Cohen, S. Melamed, A. Millman, G. Shulman, Y. Oppenheimer-Shaanan, A. Kacen, S. Doron, G. Amitai, R. Sorek, Cyclic GMP-AMP signalling protects bacteria against viral infection. *Nature* **574**, 691–695 (2019).
35. O. Lamiable, J. Arnold, I. J. d. S. de Faria, R. P. Olmo, F. Bergami, C. Meignin, J. A. Hoffmann, J. T. Marques, J. L. Imler, Analysis of the contribution of hemocytes and autophagy to *Drosophila* antiviral immunity. *J. Virol.* **90**, 5415–5426 (2016).
36. S. Shelly, N. Lukinova, S. Bambina, A. Berman, S. Cherry, Autophagy is an essential component of *Drosophila* immunity against vesicular stomatitis virus. *Immunity* **30**, 588–598 (2009).
37. E. Abernathy, R. Mateo, K. Majzoub, N. van Buuren, S. W. Bird, J. E. Carette, K. Kirkegaard, Differential and convergent utilization of autophagy components by positive-strand RNA viruses. *PLoS Biol.* **17**, e2006926 (2019).
38. H. Myllymäki, S. Valanne, M. Rämet, The *Drosophila* imd signaling pathway. *J. Immunol.* **192**, 3455–3462 (2014).
39. J. Mundorf, C. D. Donohoe, C. D. McClure, T. D. Southall, M. Uhlirova, Ets21c governs tissue renewal, stress tolerance, and aging in the *Drosophila* intestine. *Cell Rep.* **27**, 3019–3033.e5 (2019).
40. D. Panda, B. Gold, M. A. Tartell, K. Rausch, S. Casas-Tinto, S. Cherry, The transcription factor FoxK participates with Nup98 to regulate antiviral gene expression. *MBio* **6**, e02509-14 (2015).
41. C. West, F. Rus, Y. Chen, A. Kleino, M. Gangloff, D. B. Gammon, N. Silverman, IIV-6 Inhibits NF-κB Responses in *Drosophila*. *Viruses* **11**, 409 (2019).
42. D. Panda, P. Pascual-Garcia, M. Dunagin, M. Tudor, K. C. Hopkins, J. Xu, B. Gold, A. Raj, M. Capelson, S. Cherry, Nup98 promotes antiviral gene expression to restrict RNA viral infection in *Drosophila*. *Proc. Natl. Acad. Sci. U.S.A.* **111**, E3890–E3899 (2014).
43. W. H. Palmer, N. C. Medd, P. M. Beard, D. J. Obbard, Isolation of a natural DNA virus of *Drosophila melanogaster*, and characterisation of host resistance and immune responses. *PLOS Pathog.* **14**, e1007050 (2018).
44. O. Lamiable, C. Kellenberger, C. Kemp, L. Troxler, N. Pelte, M. Boutros, J. T. Marques, L. Daeffler, J. A. Hoffmann, A. Roussel, J.-L. Imler, Cytokine Diedel and a viral homologue suppress the IMD pathway in *Drosophila*. *Proc. Natl. Acad. Sci. U.S.A.* **113**, 698–703 (2016).
45. A. G. Ferreira, H. Naylor, S. S. Esteves, I. S. Pais, N. E. Martins, L. Teixeira, The Toll-dorsal pathway is required for resistance to viral oral infection in *Drosophila*. *PLOS Pathog.* **10**, e1004507 (2014).
46. N. A. Broderick, N. Buchon, B. Lemaitre, Microbiota-induced changes in *Drosophila melanogaster* host gene expression and gut morphology. *MBio* **5**, e01117-14 (2014).
47. J. Carpenter, S. Hutter, J. F. Baines, J. Roller, S. S. Saminadin-Peter, J. Parsch, F. M. Jiggins, The transcriptional response of *Drosophila melanogaster* to infection with the sigma virus (Rhabdoviridae). *PLOS ONE* **4**, e6838 (2009).
48. C. West, N. Silverman, p38b and JAK-STAT signaling protect against Invertebrate iridescent virus 6 infection in *Drosophila*. *PLOS Pathog.* **14**, e1007020 (2018).
49. M. Tanguy, L. Véron, P. Stempor, J. Ahringer, P. Sarkies, E. A. Miska, An alternative STAT signaling pathway acts in viral immunity in *Caenorhabditis elegans*. *MBio* **8**, e00924-17 (2017).
50. M. Lafont, B. Petton, A. Vergnes, M. Pauletto, A. Segarra, B. Gourbal, C. Montagnani, Long-lasting antiviral innate immune priming in the Lophotrochozoan Pacific oyster, *Crassostrea gigas*. *Sci. Rep.* **7**, 13143 (2017).
51. J. Robalino, T. Bartlett, E. Shepard, S. Prior, G. Jaramillo, E. Scura, R. W. Chapman, P. S. Gross, C. L. Browdy, G. W. Warr, Double-stranded RNA induces sequence-specific antiviral silencing in addition to nonspecific immunity in a marine shrimp: Convergence of RNA interference and innate immunity in the invertebrate antiviral response? *J. Virol.* **79**, 13561–13571 (2005).

52. M. Sarov, C. Barz, H. Jambor, M. Y. Hein, C. Schmied, D. Suchold, B. Stender, S. Janosch, V. V. KJ, R. T. Krishnan, A. Krishnamoorthy, I. R. S. Ferreira, R. K. Ejsmont, K. Finkl, S. Hasse, P. Kämpfer, N. Plewka, E. Vinis, S. Schloissnig, E. Knust, V. Hartenstein, M. Mann, M. Ramaswami, K. VijayRaghavan, P. Tomancak, F. Schnorrer, A genome-wide resource for the analysis of protein localisation in *Drosophila*. *eLife* **5**, e12068 (2016).
53. T. Yano, S. Mita, H. Ohmori, Y. Oshima, Y. Fujimoto, R. Ueda, H. Takada, W. E. Goldman, K. Fukase, N. Silverman, T. Yoshimori, S. Kurata, Autophagic control of listeria through intracellular innate immune recognition in drosophila. *Nat. Immunol.* **9**, 908–916 (2008).
54. A. Holleufer, R. Hartmann, A highly sensitive anion exchange chromatography method for measuring cGAS activity in vitro. *Bio-protocol* **8**, e3055 (2018).
55. A. Dobin, C. A. Davis, F. Schlesinger, J. Drenkow, C. Zaleski, S. Jha, P. Batut, M. Chaisson, T. R. Gingeras, STAR: Ultrafast universal RNA-seq aligner. *Bioinformatics* **29**, 15–21 (2013).
56. Y. Liao, G. K. Smyth, W. Shi, featureCounts: An efficient general purpose program for assigning sequence reads to genomic features. *Bioinformatics* **30**, 923–930 (2014).
57. M. I. Love, W. Huber, S. Anders, Moderated estimation of fold change and dispersion for RNA-seq data with DESeq2. *Genome Biol.* **15**, 550 (2014).
58. H. Imrichova, G. Hulselmans, Z. K. Atak, D. Potier, S. Aerts, i-cisTarget 2015 update: Generalized cis-regulatory enrichment analysis in human, mouse and fly. *Nucleic Acids Res.* **43**, W57–W64 (2015).
59. M. Lestradet, K.-Z. Lee, D. Ferrandon, *Drosophila* as a model for intestinal infections. *Methods Mol. Biol.* **1197**, 11–40 (2014).

Acknowledgments: We thank D. J. Obbard (University of Edinburgh) for providing the Kallithea virus and L. Teixeira (Instituto Gulbenkian de Ciência) for providing the isogenized *Relish* mutant flies and w^{1118} genetic background control. **Funding:** This work was supported by the ERA-NET Infect-ERA program (ANR-14-IFEC-0005), the Agence Nationale de la Recherche (ANR-17-CE15-0014), the Investissement d'Avenir Programs (ANR-10-LABX-0036 and ANR-11-EQPX-0022), the Chinese National Overseas Expertise Introduction Center for Discipline Innovation [Project "111" (D18010)], the CNRS, and the INSERM. Further support was provided to J.-L.I. by the Institut Universitaire de France, to R.H. by the Novo Nordisk foundation grant NNF17OC0028184, and to D.C. by the Natural Science Foundation of Guangdong Province (grant 2016A030310278) and the Science and Technology Planning Project of Guangzhou (grant 201707010030). **Author contributions:** H.C., A.H., B.S., J.S., A.L., Jingxian Huang, and Jieqing Huang performed the experiments. N.E.M. performed the bioinformatics analysis. D.C., H.H.G., and T.P. provided the critical materials. H.C., A.H., J.T.M., R.H., N.E.M., and J.-L.I. designed the experiments and analyzed the data. H.C., R.H., N.E.M., and J.-L.I. wrote the manuscript. **Competing interests:** The authors declare that they have no competing interests. **Data and materials availability:** RNA-seq data for CDN-injected flies have been submitted to the GEO database (Gene Expression Omnibus: www.ncbi.nlm.nih.gov/geo/) with the accession number GSE140955. All other data needed to evaluate the conclusions in the paper are present in the paper or the Supplementary Materials.

Submitted 24 April 2020
Accepted 5 November 2020
Published 1 December 2020
10.1126/scisignal.abc4537

Citation: H. Cai, A. Holleufer, B. Simonsen, J. Schneider, A. Lemoine, H. H. Gad, J. Huang, J. Huang, D. Chen, T. Peng, J. T. Marques, R. Hartmann, N. E. Martins, J.-L. Imler, 2′3′-cGAMP triggers a STING- and NF-κB–dependent broad antiviral response in *Drosophila*. *Sci. Signal.* **13**, eabc4537 (2020).

Science Signaling
AAAS

stke.sciencemag.org/cgi/content/full/13/660/eabc4537/DC1

Supplementary Materials for

2′3′-cGAMP triggers a STING- and NF-κB–dependent broad antiviral response in *Drosophila*

Hua Cai, Andreas Holleufer, Bine Simonsen, Juliette Schneider, Aurélie Lemoine, Hans Henrik Gad, Jingxian Huang, Jieqing Huang, Di Chen, Tao Peng, João T. Marques, Rune Hartmann*, Nelson E. Martins*, Jean-Luc Imler

*Corresponding author. Email: rh@mbg.au.dk (R.H.); nmartins@ibmc-cnrs.unistra.fr (N.E.M.)

Published 1 December 2020, *Sci. Signal.* **13**, eabc4537 (2020)
DOI: 10.1126/scisignal.abc4537

The PDF file includes:

Other Supplementary Material for this manuscript includes the following:

(available at stke.sciencemag.org/cgi/content/full/13/660/eabc4537/DC1)

Data file S1 (Microsoft Excel format). Differentially expressed genes between the tris- and c-di-GMP–injected *dSTING*^{Control} flies at 6, 12, and 24 hpi.
Data file S2 (Microsoft Excel format). Differentially expressed genes between the tris- and 2′3′-cGAMP–injected *dSTING*^{Control} flies at 6, 12, and 24 hpi.
Data file S3 (Microsoft Excel format). Differentially expressed transcription factors or cytokines between tris- and 2′3′-cGAMP–injected *dSTING*^{Control} flies at 6, 12, and 24 hpi.
Data file S4 (Microsoft Excel format). Presence of binding sites for stimulated transcription factors in differentially expressed genes.

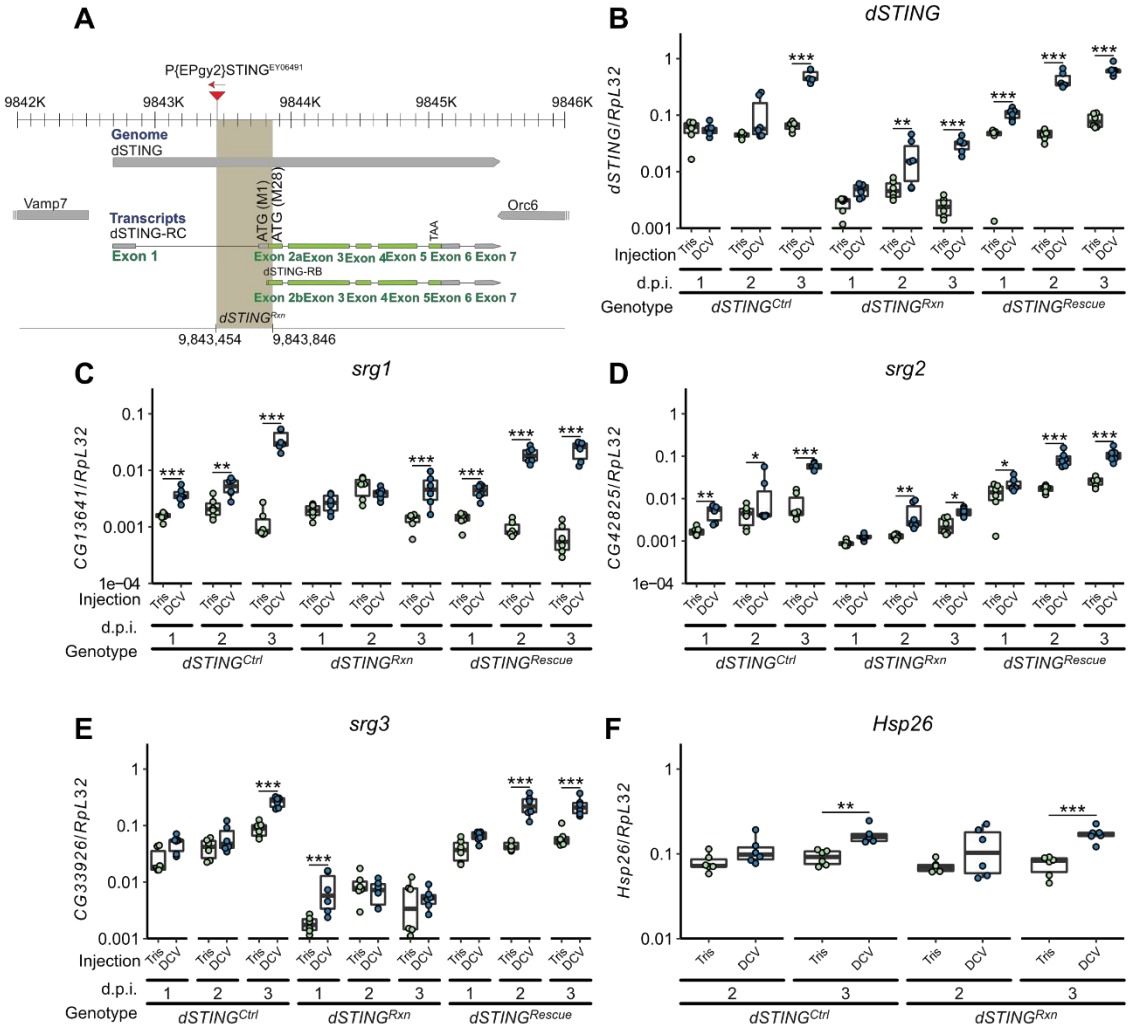

Fig. S1. DCV infection induces a dSTING-dependent transcriptional response in *D. melanogaster.*

(**A**) *dSTING*^{Rxn} mutant flies were generated by imprecise excision of the P-element P{EPgy2}Sting^{EY06491}. The boundaries of the deletion (yellow shading), which removes the 3' end of the first intron and the 5' extremity of exons 2a and 2b of the two reported transcripts (RB and RC), are indicated at the bottom. Precise excision of the transposon generated control flies (*dSTING*^{Control}) in the same genetic background. (**B-E**) Relative gene expression at different days post-injection (d.p.i.) of tris or DCV for *dSTING* (**B**) and *srg1-3* (**C-E**) in *dSTING*^{Control}, *dSTING*^{Rxn} mutant flies and *dSTING*^{Rxn} mutant flies containing a

genomic *dSTING* rescue transgene (*dSTING*^{Rescue}). Expression of *dSTING*, $t \geq -7.189$, $P \leq 0.001$ in all pairwise comparisons between control and *dSTING*^{Rxn} flies at the different timepoints; $|t| \leq 2.044$, $P \geq 0.142$ in all pairwise comparisons between control and *dSTING*^{Rescue} flies at the different timepoints. Expression of *dSTING* after DCV infection in *dSTING*^{Rxn} mutant flies, $|t| \geq 3.632$, $P \leq 0.001$ for all pairwise comparisons between tris and DCV injected *dSTING*^{Rxn}; $|t| = 2.466$, $P = 0.065$ for DCV injected *dSTING*^{Rxn} flies compared to tris injected control flies. Expression of *srg1* or *srg2* at three dpi in *dSTING*^{Rxn} mutants, $t = 0.6252$, $P = 0.002$. Expression of *srg3*, $|t| \leq 1.268$, $P \geq 0.446$ for tris compared to DCV infected *dSTING*^{Rxn} mutants 2- and 3- dpi; $|t| \geq 5.568$, $P < 0.001$. Expresssion of *dSTING*, *srg1*, or *srg2* in response to DCV infection in control or *dSTING*^{Rescue} flies at two or three dpi, $|t| \geq 2.520$, $P \leq 0.037$. Expresssion of *srg3* in response to DCV infection in control flies at 2 dpi, $t = 1.393$, $P = 0.373$. (**F**) Expression of *Hsp26*, a dSTING-independent virus-induced gene, after DCV infection in control and *dSTING*^{Rxn} flies, $|t| \leq 0.842$, $P \geq 0.405$ for tris and DCV injected flies at 2 or 3 d.p.i. In (B) to (F), data are from two independent experiments and each point represents a pool of 6 flies. Expression is shown relative to the housekeeping gene *RpL32* and is normalized by experiment. Boxplots represent the median (horizontal line) and 1st/3rd quartiles, with whiskers extending to points within 1.5 times the interquartile range. * - $P \leq 0.05$, ** - $P \leq 0.01$, *** - $P \leq 0.001$.

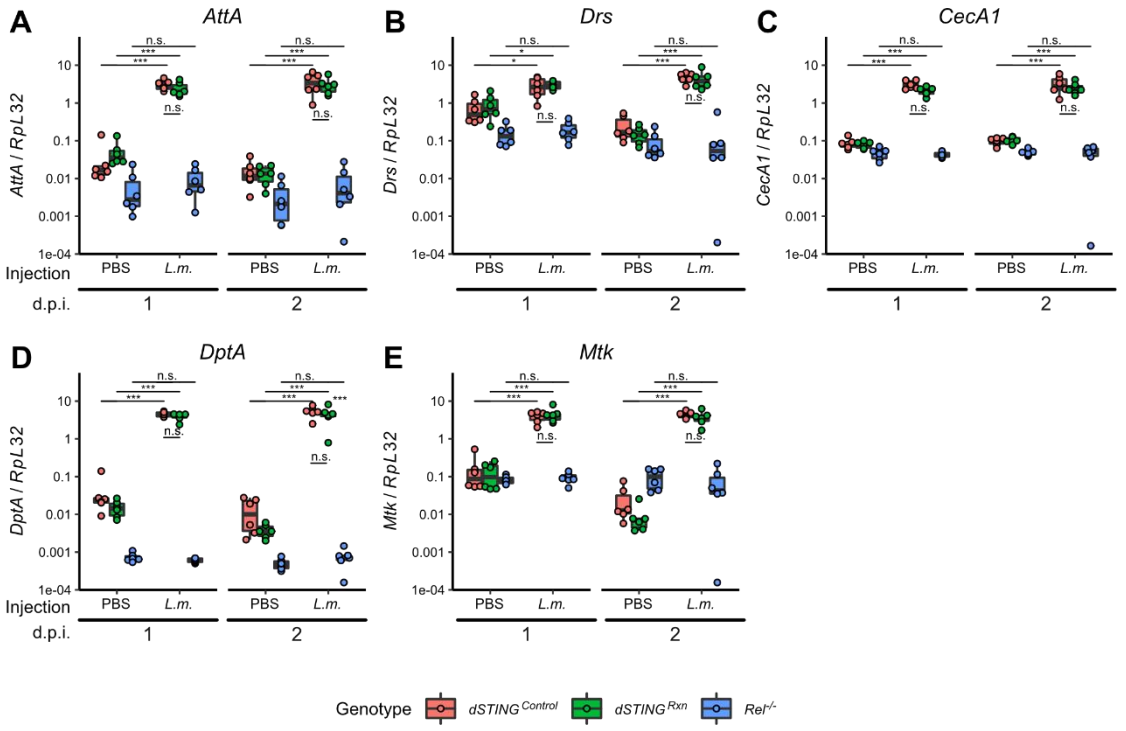

Fig. S2. Antimicrobial peptide gene induction is not affected in *dSTING* mutant flies after *L. monocytogenes* challenge.

(**A-E**) Relative expression of the indicated antimicrobial peptide (AMP) genes one and two days post-injection (d.p.i.) with buffer (PBS) or the gram-negative bacteria *Listeria monocytogenes* (*L.m.*) in control ($dSTING^{Control}$), dSTING ($dSTING^{Rxn}$) or Relish ($Rel^{-/-}$) mutant flies. *L. monocytogenes* compared to PBS injection, $|t| \geq 2.503$, $P \leq 0.047$ in control or dSTING mutants and $|t| \leq 2.241$, $P \geq 0.076$ in $Rel^{-/-}$ mutants. Control compared to *dSTING* mutants, $|t| \leq 1.911$, $P \geq 0.153$ for all comparisons except for *DptA* 1 d.p.i. after PBS injection $|t| = 2.689$, $P = 0.037$. In (A) to (E), data are from two independent experiments and each point represents a pool of 6 flies. Expression is shown relative to the housekeeping gene *RpL32* and is normalized by experiment. Boxplots represent the median (horizontal line) and 1st/3rd quartiles, with whiskers

extending to points within 1.5 times the interquartile range. * - $P \leq 0.05$, ** - $P \leq 0.01$, *** - $P \leq 0.001$, n.s. – $P > 0.05$.

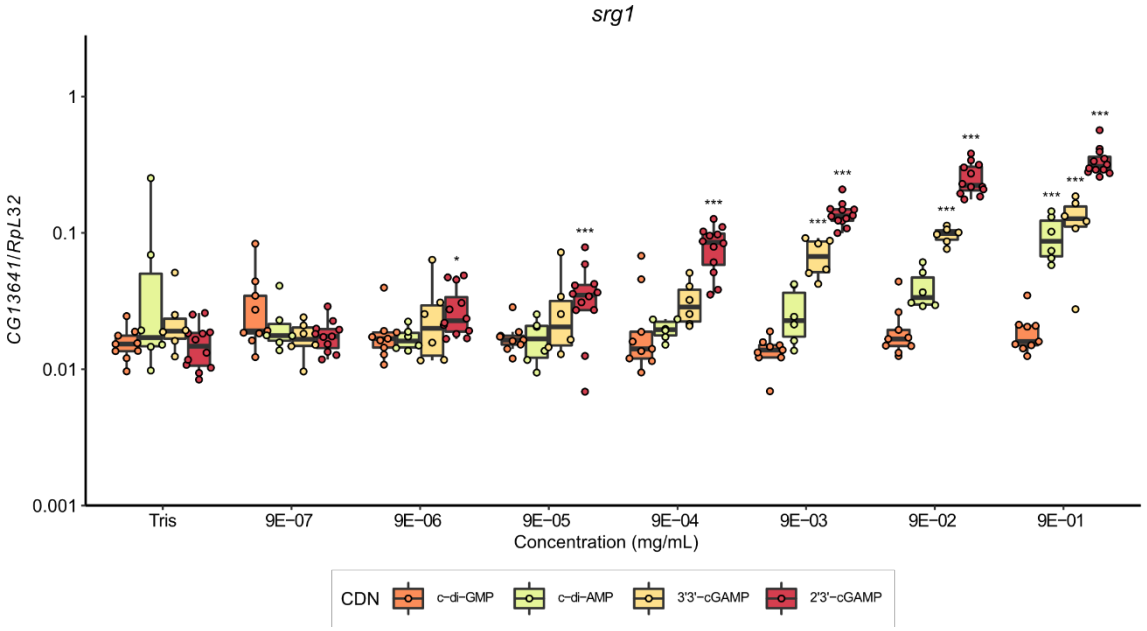

Fig. S3. The CDNs 2′3′-cGAMP, 3′3′-cGAMP, and c-di-AMP have a dose-dependent effect on the expression of a *dSTING*-regulated gene.

Relative expression of *srg1* six hours post-injection of buffer (tris) and the CDNs c-di-GMP, c-di-AMP, 3'3'-cGAMP and 2'3'-cGAMP in the indicated concentrations in control flies. Expression of *srg1* after tris injection compared to injection with $9x10^{-6}$ mg/mL of 2'3'-cGAMP, $|t| \geq 3.177$, $P \leq 0.011$; $9x10^{-3}$ mg/mL of 3'3'-cGAMP, $|t| \geq 4.358$, $P < 0.001$; 0.9 of c-di-AMP mg/mL, $|t| \geq 4.281$, $P < 0.001$; c-di-GMP at any concentration, $|t| \leq 2.476$, $P \geq 0.078$. Data are from four (2'3'-cGAMP), three (c-di-GMP) or two independent experiments (3'3'-cGAMP and c-di-AMP). Each point represents a pool of 6 flies. Expression is shown relative to the housekeeping gene *RpL32* and is normalized by experiment. Boxplots represent the median (horizontal line) and 1st/3rd quartiles, with whiskers extending to points within 1.5 times the interquartile range. * - $P \leq 0.05$, ** - $P \leq 0.01$, *** - $P \leq 0.001$. Comparisons are shown relative to the matched tris injection for a given CDN.

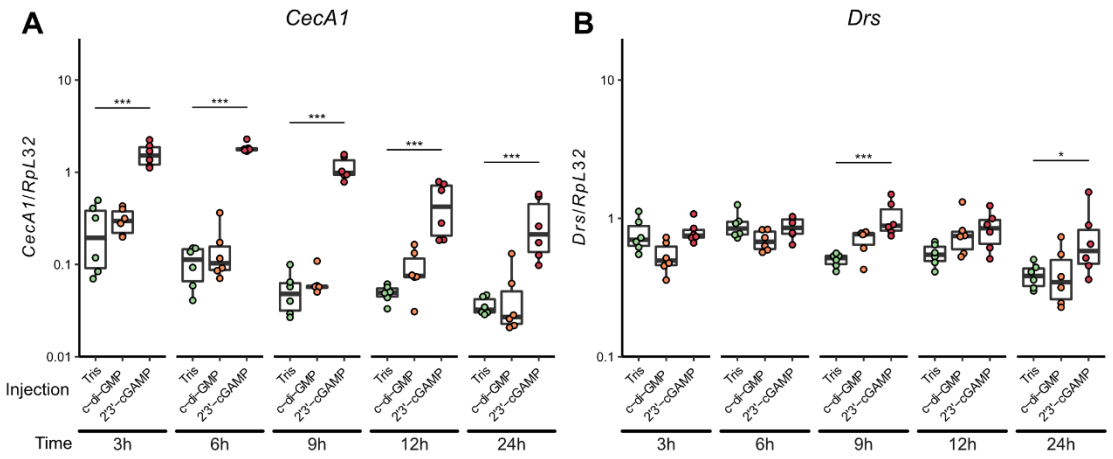

Fig. S4. c-di-GMP injection does not induce antimicrobial peptide expression.

(**A-B**) Relative expression of the indicated antimicrobial peptides in control flies across time (h). *CecA1* expression after six or three hours post-injection with 2'3'-cGAMP, $|t| \geq 6.152$, $P < 0.001$; after injection with c-di-GMP, $|t| \leq 2.506$, $P \geq 0.072$ compared with tris injection. In (A) and (B), data are from two independent experiments and each point represents a pool of 6 flies. Expression is shown relative to the housekeeping gene *RpL32* and is normalized by experiment. Boxplots represent the median (horizontal line) and 1st/3rd quartiles, with whiskers extending to points within 1.5 times the interquartile range. * - $P \leq 0.05$, ** - $P \leq 0.01$, *** - $P \leq 0.001$.

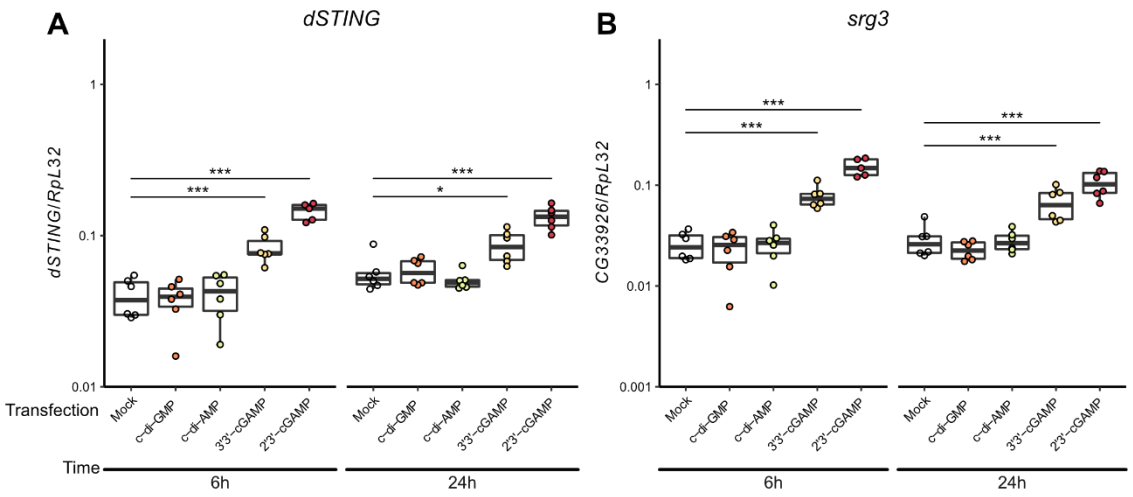

Fig. S5. The CDNs 2′3′-cGAMP and 3′3′-cGAMP induce dSTING-dependent genes in a cellular model.

Relative expression of *dSTING* (**A**) and *srg3* (**B**) six and 24 hours post-transfection with Effectene transfection reagent (Mock) and the CDNs c-di-GMP, c-di-AMP, 3'3'-cGAMP and 2'3'-cGAMP in *Drosophila* S2 cells. Expression of *dSTING* and *srg3*, $|t| \geq 2.702$, $P < 0.034$ for Mock compared to 2'3'-cGAMP or 3'3'-cGAMP transfection. Expression of *dSTING* and *srg3*, $|t| \leq 1.022$, $P \geq 0.673$ for Mock compared to c-di-AMP or c-di-GMP transfection. In (A) and (B), data are from two independent experiments and each point represents an independent pool of cells. Expression is shown relative to the housekeeping gene *RpL32*. Boxplots represent the median (horizontal line) and 1st/3rd quartiles, with whiskers extending to points within 1.5 times the interquartile range. * - $P \leq 0.05$, ** - $P \leq 0.01$, *** - $P \leq 0.001$.

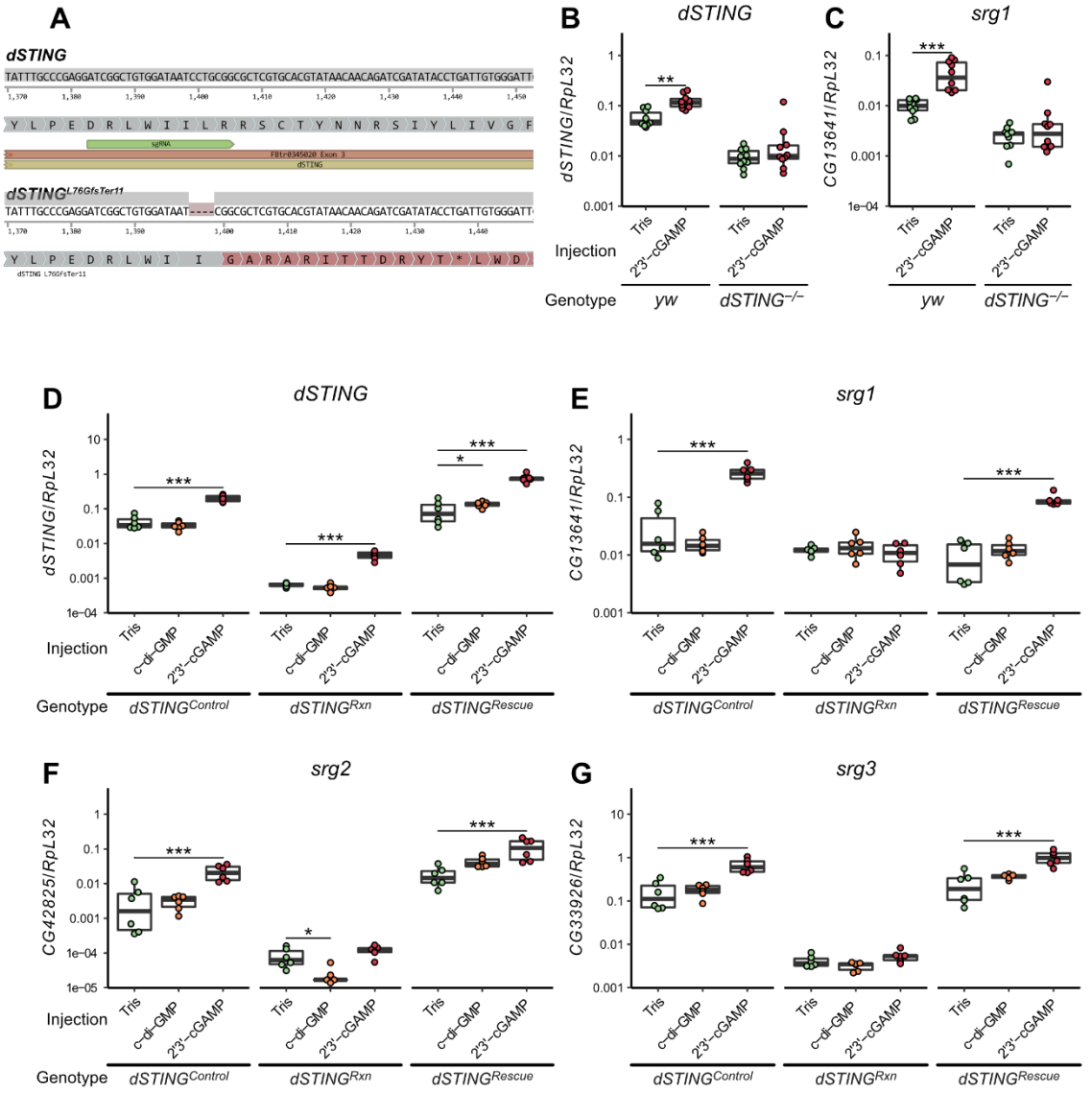

Fig. S6. Induction of gene expression after 2′3′-cGAMP injection depends on dSTING.

(**A**) Sequence of wild-type *dSTING* (top) and *dSTING*^{L76GfsTer11} (bottom) in the vicinity of the sgRNA targeted region (sg). Open reading frame translations are shown below the sequences. Coordinates are in nucleotides, relative to the gene start. (**B,C**) Relative expression of the indicated dSTING-regulated genes at 6h after injection of buffer (tris) or 2’3’-cGAMP in control (*yw*) or *yw;dSTING*^{L76GfsTer11} (*dSTING*$^{-/-}$) mutant flies. (**D-G**) Relative expression of the indicated dSTING-regulated genes at 6h after injection of buffer (tris) or 2’3’-cGAMP in control (*dSTING*^{Control}), *dSTING* mutants (*dSTING*^{Rxn}) and *dSTING*

mutants complemented by a genomic rescue of *dSTING* (FlyFos015653;$dSTING^{Rescue}$). Expression of *dSTING* and *srg1* in *yw* flies, $|t| \geq 3.009$, $P \leq 0.01$ for tris compared to 2'3'-cGAMP. Expression of *dSTING* and *srg1* in $dSTING^{-/-}$ mutants, $|t| \leq 1.561$, $P \geq 0.128$ for tris compared to 2'3'-cGAMP. Expression of *srg1-3* in control or $dSTING^{Rescue}$ flies, $|t| \geq 4.359$, $P < 0.001$ for tris compared to 2'3'-cGAMP; in $dSTING^{Rxn}$ flies, $|t| \leq 1.102$, $P \geq 0.718$ for tris compared to 2'3'-cGAMP. Expression of *dSTING* in all genotypes, $|t| \geq 7.925$, $P < 0.001$ for tris compared to 2'3'-cGAMP. Data are from three (a-b) or two (c-f) independent experiments, and each point represents a pool of 6 flies. Expression levels are shown relative to the housekeeping gene *RpL32* and are normalized by experiment. Boxplots represent the median (horizontal line) and 1st/3rd quartiles, with whiskers extending to points within 1.5 times the interquartile range. * - $P \leq 0.05$, ** - $P \leq 0.01$, *** - $P \leq 0.001$.

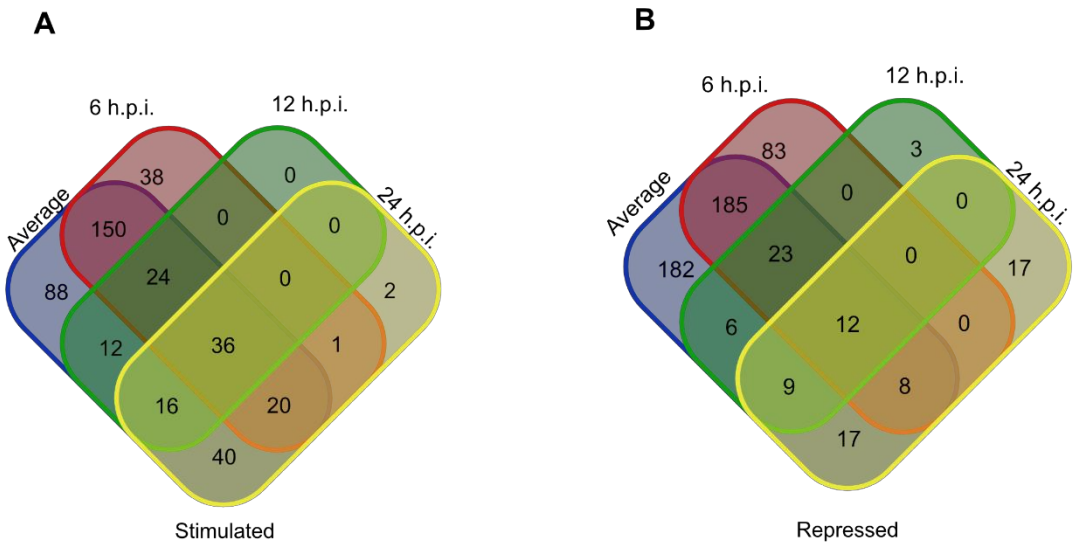

Fig. S7. Differentially expressed transcripts between the tris- and 2′3′-cGAMP–injected flies at different time points.

Venn diagram of the (**A**) stimulated and (**B**) repressed genes between 2’3’-cGAMP and tris injected *dSTING*^{Control} flies at the different timepoints (6, 12 and 24h) after injection or on average across all timepoints.

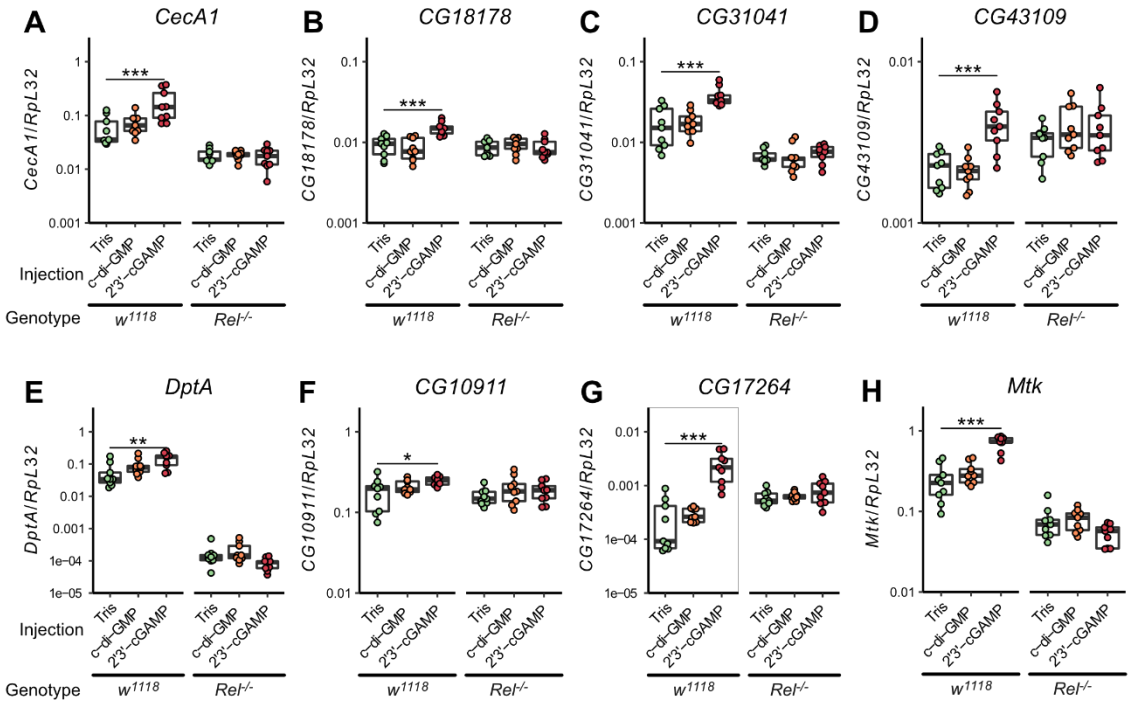

Fig. S8. 2′3′-cGAMP–induced gene expression is *Relish* dependent.

Relative expression of the indicated genes six hours post-injection of buffer (tris), c-di-GMP or 2'3'-cGAMP in control (w^{1118}) or *Relish* ($Rel^{-/-}$) mutant flies. Genes classified as early (**A-E**) or sustained (**F-H**) induced by 2'3'-cGAMP injection according to the RNAseq analysis in control flies, $|t| \geq 2.781$, $P \leq 0.031$, tris compared to 2'3'-cGAMP. Same genes in $Rel^{-/-}$ mutants, $|t| \leq 1.932$, $P \geq 0.178$, tris compared to 2'3'-cGAMP. Same genes after c-di-GMP injection, $|t| \leq 2.180$, $P \geq 0.102$. In (A) to (H), data are from three independent independent experiments and each point represents a pool of 6 flies. Expression is shown relative to the housekeeping gene *RpL32* and is normalized by experiment. Boxplots represent the median (horizontal line) and 1st/3rd quartiles, with whiskers extending to points within 1.5 times the interquartile range. * - $P \leq 0.05$, ** - $P \leq 0.01$, *** - $P \leq 0.001$.

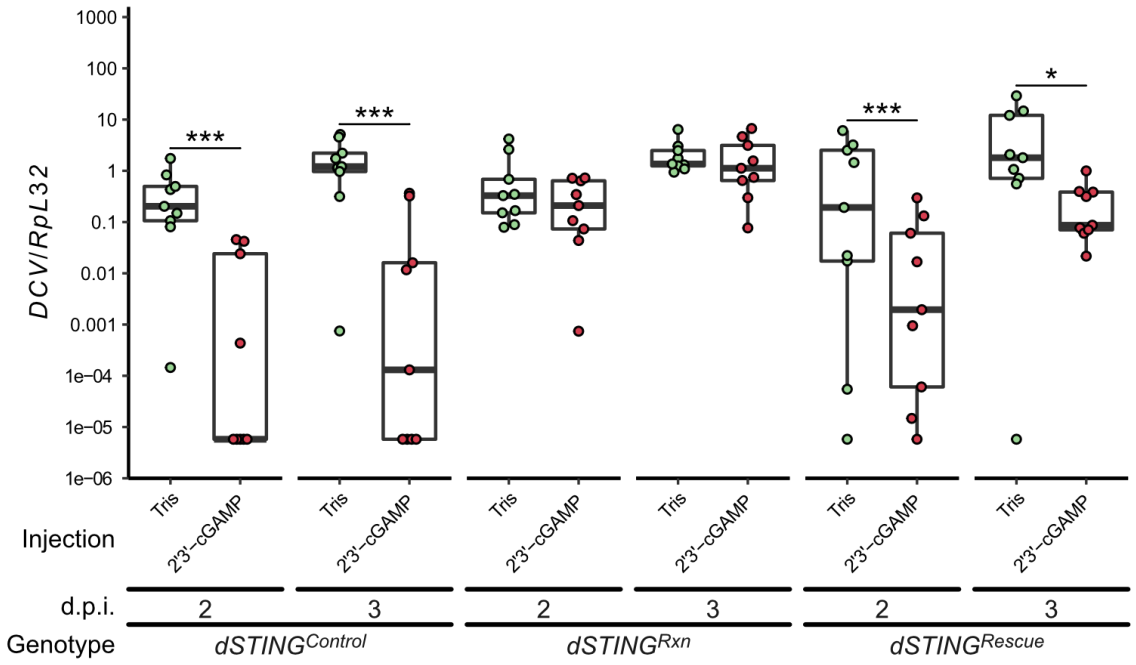

Fig. S9. A *dSTING* rescue transgene restores 2′3′-cGAMP–induced antiviral protection.

Relative load of DCV RNA at 2 and 3 days after co-injection (d.p.i.) with buffer (tris), c-di-GMP or 2'3'-cGAMP in control ($dSTING^{Control}$), *dSTING* mutants ($dSTING^{Rxn}$) and *dSTING* mutants complemented by a genomic rescue of dSTING (FlyFos015653;$dSTING^{Rescue}$). DCV RNA loads after co-injection with 2'3'-cGAMP: $|t| \geq 2.724$, $P \leq 0.019$ in control or $dSTING^{Rescue}$ flies, $|t| \leq 0.693$, $P \geq 0.976$ in $dSTING^{Rxn}$ flies, tris compared to 2'3'-cGAMP injections. Data are from three independent experiments, and each point represents a pool of 6 flies. Expression is shown relative to the housekeeping gene *RpL32* and is normalized by experiment. Boxplots represent the median (horizontal line) and 1st/3rd quartiles, with whiskers extending to points within 1.5 times the interquartile range. * - $P \leq 0.05$, ** - $P \leq 0.01$, *** - $P \leq 0.001$.

Table S1. List of oligonucleotide primers used in this study.

Target	FlyBase ID	Forward Primer	Reverse Primer	Reference
qRT-PCR				
RpL32	FBgn0002626	GCCGCTTCAAGGGACAGTATCT	AAACGCGGTTCTGCATGAG	[4]
AttA	FBgn0012042	GGCCCATGCCAATTTATTC	AGCAAAGACCTTGGCATCC	[4]
CecA1	FBgn0000276	ACGCGTTGGTCAGCACACT	ACATTGGCGGCTTGTTGAG	[4]
CG13641	FBgn0039239	GTGTCCATTATCCGCACAAG	ACTGGGGTATCTGACGGATG	[4]
dSTING	FBgn0033453	CCGGTGTCTATCGTCCTTTC	CGCTTTAGTTCCTGCATCTG	[4]
CG42825	FBgn0262007	GCGTTTTGGCCCTTATTATG	CTTTTGTAGCCGACGCAGTG	[4]
CG33926	FBgn0053926	GCGACCGTCATTGGATTGG	TGATGGTCCCGTTGATAGCC	[4]
Hsp26	FBgn0001225	CTACAAGGTTCCCGATGGC	GAATACTGACGGTGAGCACG	This work
DCV		TCATCGGTATGCACATTGCT	CGCATAACCATGCTCTTCTG	[4]
CrPV		GCTGAAACGTTCAACGCATA	CCACTTGCTCCATTTGGTTT	[4]
FHV		TTTAGAGCACATGCGTCCAG	CGCTCACTTTCTTCGGGTTA	[4]
KV		CATCAATATCGCGCCATGCC	GACCGAGTTAGCGTCAATGC	[4]
VSV		CATGATCCTGCTCTTCGTCA	TGCAAGCCCGGTATCTTATC	[4]
Drs	FBgn0283461	CGTGAGAACCTTTTCCAATATGATG	TCCCAGGACCACCAGCAT	[60]
DptA	FBgn0004240	GCTGCGCAATCGCTTCTACT	TGGTGGAGTGGGCTTCATG	[60]
Mtk	FBgn0014865	CGTCACCAGGGACCCATTT	CCGGTCTTGGTTGGTTAGGA	[60]
CG18178	FBgn0036035	CGAAGACGAAGATTCCGATGG	TTGGGCTGCGGTTTGATTGTA	This work; https://www.flyrnai.org/flyprimerbank
CG31041	FBgn0051041	ACGTCGAATGCGTGGACTAC	CCGTCGTAATTGTCCTTGCAC	This work; https://www.flyrnai.org/flyprimerbank
CG43109	FBgn0262569	CTCATCCAAGGGCGTTCTGT	TCCCAGGGTGATGATCCCTT	This work; https://www.flyrnai.org/flyprimerbank
CG10911	FBgn0034295	TCCGCCCCTGCAACTTAGTA	TCAAGGGTATGTCCACCATCG	This work; https://www.flyrnai.org/flyprimerbank
CG17264	FBgn0031490	CGTTGCAGGAAATCTCTGATCG	GGGAACAGGGAACAGATGGATAA	This work; https://www.flyrnai.org/flyprimerbank
Sequencing				
dSTING	FBgn0033453	CACCTCTATTCGCATTGTAGC	AGCCGTGAAAGTAGTTGGAG	This work

Data file S1. Differentially expressed genes between the tris- and c-di-GMP–injected *dSTING*^{Control} flies at 6, 12, and 24 hpi.

Columns show the Ensembl gene ID (gene_id) and symbol (gene_symbol), mean normalized counts after tris (TRIS_) or c-di-GMP injection (c-di-GMP_) at the different timepoints (_06,_12 or _24), together with estimated $\log_2$(fold-change) (lfc_) and Benjamini-Hochberg corrected P-values for the comparison between c-di-GMP and tris injected flies at each individual timepoint and on average across all timepoints (_AVG).

Data file S2. Differentially expressed genes between the tris- and 2′3′-cGAMP–injected *dSTING*^{Control} flies at 6, 12, and 24 hpi.

Columns show the Ensembl gene ID (gene_id) and symbol (gene_symbol), temporal expression category (category) mean normalized counts after tris (TRIS_) or 2’3’-cGAMP injection (cGAMP_) at the different timepoints (_06,_12 or _24), together with estimated $\log_2$(fold-change) (lfc_) and Benjamini-Hochberg corrected P-values for the comparison between c-di-GMP and tris injected flies at each individual timepoint and on average across all timepoints (_AVG).

Data file S3. Differentially expressed transcription factors or cytokines between tris- and 2′3′-cGAMP–injected *dSTING*^{Control} flies at 6, 12, and 24 hpi.

Columns headings are as in Data File S2, and include the transcription factor family/sub-family (Family).

Data file S4. Presence of binding sites for stimulated transcription factors in differentially expressed genes.

Differentially expressed genes between tris and 2'3'-cGAMP injected *dSTING*^{Control} flies with regulatory sequences enriched for the differentially expressed transcription factors, or for transcription factors of the same family/sub-family. Columns headings are as in Data File S3, and include the high confidence transcription factor calls predicted by Rcistarget.

3. Characterization of two cGAS-like receptors in *Drosophila melanogaster*

The efficient activation of the STING pathway by the second messenger 2'3'-cGAMP in drosophila suggests the presence of a cGAS-like enzyme in this organism. The closest drosophila cGAS homolog is CG7194 but flies deficient for this gene seem to have a normal antiviral and antibacterial immune response. Moreover, overexpression of CG7194 does not activate a STING-reporter gene (Holleufer et al., 2021; Martin et al., 2018). In collaboration with the group of Rune Hartmann (Aarhus, Denmark) we identified two cGLRs in *Drosophila melanogaster* (Holleufer et al., 2021). In parallel, Philippe Kranzusch and collaborators described a large family of cGLRs in drosophilids and characterized one of them, cGLR1 (Slavik et al., 2021). Interestingly, cGLR1 (CG12970) and cGLR2 (CG30424) appear to be activated by different molecules and produce different CDNs. Indeed, cGLR1 is activated by dsRNAs while the ligand of cGLR2 is still unidentified. Upon activation, cGLR1 produces a minor amount of c-di-AMP and mostly a novel CDN, 3'2'-cGAMP, which is a better agonist of drosophila STING than 2'3'-cGAMP. cGLR2 produces similar amount of both 2'3'- and 3'2'-cGAMP (Holleufer et al., 2021; Slavik et al., 2021).

a. cGLR2 protein: isoforms and stability

Expression of the *cglr2* gene is predicted to give rise to five different splicing isoforms, cGLR2-PF, -PC, -PD, -PE and -PB (www.flybase.org/reports/FBgn0050424) (**Figure 4**). Of note, the initial predicted full-length protein was the PD isoform. However, the annotated start methionine of this isoform is in the middle of the predicted active site and would disrupt the folding of a CDN synthase domain. An upstream in-frame methionine was identified and would allow the production of a correctly folded protein. This isoform was annotated as the PF isoform and the PD isoform may not exist naturally (Holleufer et al., 2021). The cGLR2-PE, -PB and -PC are shorter isoforms arising from alternative splicing. In addition, cGLR2-PB and -PE are also shorter splice isoforms but they present one or two small sequences absent from other

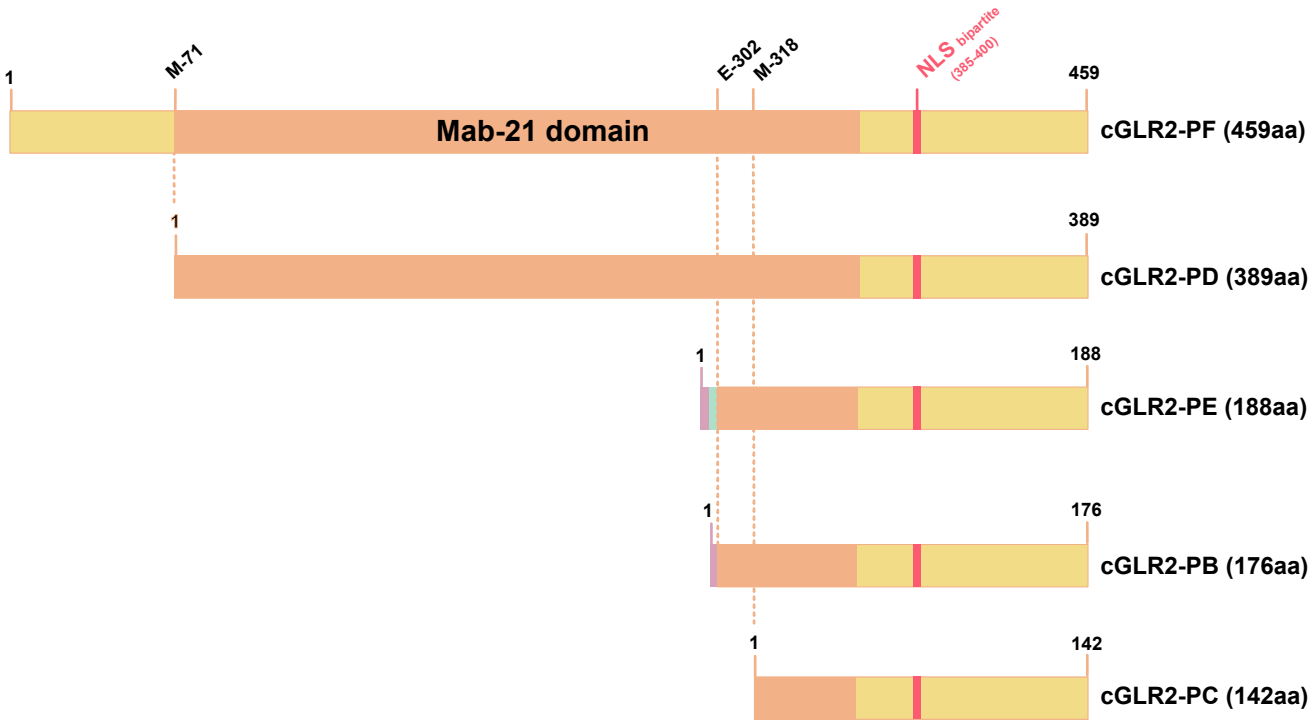

Figure 4: cGLR2 isoforms. Schematic representation of cGLR2 different splice isoforms. The Mab-21 domain is showed in orange. The bipartite NLS is indicated in red. Sequence specific to splice isoforms PE and PB is represented in pink and sequence specific to isoform PE in blue.

isoforms, respectively. Interestingly, we identified a predicted bipartite NLS in the C-ter part, common to every isoform.

We had difficulties to detect the cGLR2-PF protein in S2 cells using both Western blot and immunolocalization assays. In Western blot experiments, we always detected a protein at a size of approximately 25 kilo-Daltons (kDa) while the predicted size is 53,9 kDa. This smallest protein is probably a cleavage product (**Figure 5A**). These difficulties to detect cGLR2-PF protein suggested that it may be unstable and regulated at the post-translational level. We wondered if degradation by the proteasome was involved in cGLR2 instability. In order to test this hypothesis, we started by constructing clones encoding codon optimized versions of cGLR2 isoforms (**Figure 5B**). This allowed a more efficient translation, facilitating cGLR2-PF detection (**Figure 5A**).

These clones were used to transfect S2 cells which were then treated with the proteasome inhibitor Bortezomib (reviewed in Cvek and Dvorak, 2011). I observed that proteasome inhibition worked, as there is an accumulation of K48-ubiquitinated proteins in Bortezomib-treated conditions. I also noticed that all codon optimized cGLR2 isoforms were stabilized upon proteasome inhibition (**Figure 6**). This result suggests that degradation by the proteasome is involved in cGLR2 receptor regulation.

b. Intracellular localization of cGLR1 and cGLR2

In order to assess the subcellular localization of both receptors, I transfected cells with cGLR1 or cGLR2-PF tagged in C-ter with a V5 tag. Then, I performed immunolocalization experiments followed by observation using a confocal microscope. I observed a diffuse cytosolic localization for cGLR1, consistent with a role in sensing the presence of replicating viral RNA in this compartment. By contrast, cGLR2-PF was detected in the nucleus. Nuclear localization was no longer observed when the predicted NLS of cGLR2 is mutated, confirming that the site is functional. The cGLR2-PF NLS mutant protein localized at the plasma membrane (**Figure 7A**).

We then quantified the localization of the different codon optimized cGLR2 isoforms by immunofluorescence. cGLR2-PF^{opti}, -PE^{opti}, -PB^{opti} and -PC^{opti} isoforms localized mainly in the nucleus, as expected given the fact they all possess the NLS. However,

A

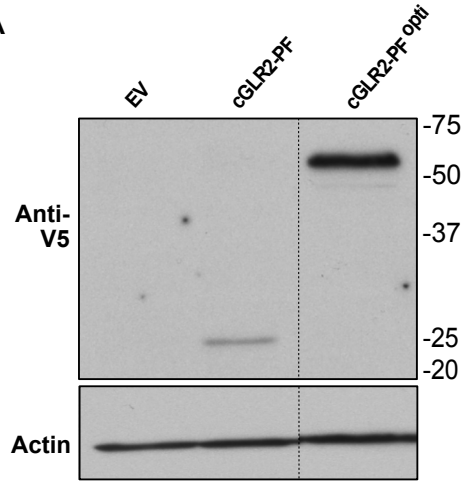

B

cGLR2-PF^{opti}
cGLR2-PF

```
1    ATGAAGGAGTCTCGAAACCTCGAGAATTTTGTTGAGAAAAAACTGTACGAATGCAAGAAAAAGTATGTTGACATTCCCAAGGACGAGGGACAACGCTATGGCAAGCACTA 110
     ||||||||||||| |||| || || || |||||| || |||||| || || |||||||| || |||||||||||||||||| |||||||||||||||||| |||||| ||||||||
1    ATGAAGGAGTCTAGAAATCTTGAAAACTTTGTGGAAAAAAAGCTCTATGAATGCAAAAAGAAGTATGTTGACATTCCAAAGGACGAGGGACAACGATATGGTAAGCACTA 110

111  CGAGGCACTGACGTCCAAGATTTTCGAGATACTGCGAAAGGAAAATCCTGAGCTGGACATAATCATCGCGGAGTTTAGCCTGGAGGGTTCGGTG--GGCGATATGCTGAA 218
      || |||||||| || || || || || ||||||| |||||||| ||||| |||||||||||| || || || ||||| ||  |||| ||  | |||  || ||||||| | ||
111  TGAAGCACTGACATCTAAAATCTTTGAAATACTGAGAAAGGAGAATCCAGAGCTGGACATCATTATTGCTGAGTTCAGTTTGGAAGG--CAGTGTCGGGGATATGTTAAA 218

219  AATCGCAAAGCCGAACGAATTCGATCTGGTCTTTAAGCTCAAGTTCCCCTATTACAAGTCGATTGCGGTGACACGTGATCCCAAGATTCCGGGCAATGTTCTTTTAGACA 328
      ||||| ||||| |||||||||||| |||| |||||| | || || || || |||||     || || ||||| || |||||| || |||||||||||| || ||  | || |
219  GATCGCGAAGCCCAACGAATTCGATTTGGTATTTAAGTTAAAATTTCCGTACTACAAAAGCATCGCCGTGACGCGAGATCCGAAAATTCCGGGCAACGTACTACTCGATA 328

329  TGACCCGAGTTCTGGAATTGCTTAAAGATGACCCTAGAGAGGATTTCCAGCGAATCCGCGAACTGATACAGGGTCGTTTGGTTGATGCCCAGAACTTCTTTGTGGTCGAC 438
     |||| || ||  | ||  | ||||| ||||| ||  | |||||||||||| |||| || |||||||| ||||||||  | || |||||| || |||||| || || || |||
329  TGACGCGCGTGTTAGAGCTCCTTAAGGATGATCCCCGCGAGGATTTCCAGAGAATTCGGGAACTGATTCAGGGTCGACTCGTGGATGCGCAAAACTTTTTCGTCGTGGAC 438

438  -CGCTTGAGGAGTTGGCTGCAATCCCTGTTCTCG-CAGGCGCTAAATCGCATCTCCTATCGGGTAGAACTAGTGGCCGGAGTCGTGAGTCACCTCAAGTATCGCACCTGC 546
       ||||  |   |||||| ||   | |||| | | |||||| || ||  | || || |||||| || || || || |||||| || |||   || |||||| ||| | ||||||
439  AGGCTT-CGTTCTTGGCTTCAGAGCTTGTT-TAGCCAGGCACTCAACAGGATATCATATCGCGTGGAGCTGGTTGCCGGCGTAGTGTCCCATCTCAAATATAGAACCTGT 546

547  GGACCCGCCCATACCATTTACGTCTACGGTGACTACGAGTACAGTGTGGATTATGTGCCGGCCATCTGTCTAGCCGCTGAGCAGAATGTTCTACCAACCAAACAGCTGGA 656
     || || |||||| || || |||||| |||||||| || |||||||  ||| || || || || || || ||||||| | || || || |||||| ||  | || || || ||  ||||
547  GGGCCGGCCCACACTATCTACGTGTACGGTGATTATGAGTACTCTGTCGACTACGTACCTGCAATCTGTTTGGCGGCCGAACAGAACGTCTTGCCCACGAAGCAATTGGA 656

657  GTGCTTCAAGCGTGCCAACACTAGTTACTGGGAGGCAATTCCAAAGCCCCTTAAACCATTGACAGAGACGAGCATGATAAGCTTCCGGAGCTCTTTCTACGCCGTAGAAA 766
     |||||| || || |||||||||  |||||||||||| ||||| ||||| || ||||||  | || || || |||||||||   ||| ||   ||| || |||||||||||| |
657  GTGCTTTAAACGCGCCAACACTTCTTACTGGGAGGCGATTCCCAAGCCTCTGAAACCCCTAACTGAAACCAGCATGATCTCCTTTCGTTCCTCGTTTTACGCCGTAGAGA 766

767  AAATCCTCCTACAGGATGTGCACGAGAACTGTAGGAATGCTA-TACGTTTCATGAAGAAATTTAGAGATGTAAAGACCAATCTGGGCAACTGC--AAGTCATACTACATC 873
     ||||  | || |||||||||||||||||| ||  ||||||| | || |||| ||||| |||||| | ||||| |||||||||  |||||||| |||  ||||  || |||||
767  AAATATTGCTGCAGGATGTGCACGAGAATTGCCGGAATGCAATTAGGTTT-ATGAAAAAATTTCGCGATGTGAAGACCAACTTGGGCAATTGCAAAAGT--TATTACATT 873

874  AAGACTCTGTTTCTGTGGAAGATTATACAAGAGCCCGAATCCTATTGGCTGAATC------CATTGAGCTTTATCCTGGCCGACATGTTCGACGATTTGGCTGAAAACTT 977
     || ||| | |||||  ||||| |||||||| || || || |||||  |||||||||       |||| |  |||    | ||||| |||||||||| ||||| || |||||
874  AAAACTTTATTTCTTTGGAAAATTATACAGGAACCAGAGTCCTACTGGCTGAATCCGCTCTCATTCA--TTT----TAGCCGATATGTTCGACGACTTGGCGGAGAACTT 977

978  GAGGCGGGGCGTCATCACGTTTTTCTGGGATCCGGAGCTTAACATGATCGACGCGCTCACCCGGGATCAAGTGTGGGAGATGTACTTATGCGTGCAGCGCATTCCTCGCG 1087
      |||||||| || || || ||||| ||||| || ||||| |||||||||||||||  | |||||||||||||| ||||| |||||| | ||||||||  | |||||  | |
978  AAGGCGGGGAGTTATTACCTTTTTTTGGGACCCCGAGCTGAACATGATCGACGCATTGACCCGGGATCAAGTTTGGGAAATGTACCTGTGCGTGCAAAGGATTCCAAGAG 1087

1088 ACTTGCGTGGGGCAGAGATCTCAAGAAACAAGTGGTCGTTCTTT-GTGCTGCGCGAGTTCTCCCACAAGAAGGAGCGGAATGTGAATCTCAAGTGTTCGAGC---CGCCG 1193
     || || | || |||||||||     | || || |||  ||| ||| || || || || |||   ||||| |||||  | ||||| ||||| |||||     |||     | ||
1088 ACCTGAGGGGCGCAGAGATCAGCCGGAATAAATGG-AGTTTTTTCGTACTTCGGGAATTCAGTCACAAAAAGGAAAGAAATGTAAATCTAAAGTG---CAGCTCTAGGCG 1193

1194 GAAGCGCAACGTCATTAAGGGCCTCAAAACAACGTCCATCTGCAAACTTAGGAACGCCCGAACTAACGGAACATGGACCGCTGGTCTATGGACGCGTCCGGGCCATGCCT 1303
      || || || || |||||||| || || || || || || |||||| || || || || |||||||||||| || ||||| ||||| || ||||| || || |||||||| |
1194 AAAACGAAATGTTATTAAGGGACTGAAGACCACTTCAATTTGCAAGCTAAGAAATGCTCGAACTAACGGTACGTGGACTGCTGGACTTTGGACTCGACCCGGCCATGCGT 1303

1304 ATCGCGGACCAAGCGAAAC--TGTCAGTACCTGGGACACAGTGAAGGATGCAGCCTGGTCCGAAGGCATTGTGGAGTGA 1380
     |  | || |||   |||||  ||||   || |||||||||||| ||||| ||||| ||||| ||||| |||||||||| |
1304 ACAGAGGCCCATCGGAAACGGTGTC--GACTTGGGACACAGTAAAGGACGCAGCGTGGTCAGAAGGGATTGTGGAGTAA 1380
```

Figure 5: Codon optimized version of cGLR2-PF isoform. A) Western blot analysis of the expression of the natural cGLR2-PF isoform and the codon optimized version of cGLR2-PF isoform. S2 cells are transfected with plasmids encoding either of the two versions of cGLR2-PF under the control of the actin promoter tagged with a V5 tag in C-ter, or with pAc-V5-HisA empty vector (EV, left) as a control. Proteins are extracted 48h after transfection and Western blot analysis is performed using anti-V5 (top) and anti-actin (bottom) antibodies. Representative results from N=3 independent experiments. **B)** Alignement of cGLR2-PF^{opti} (red) and cGLR2-PF (green) coding sequences. Alignement was realized using SnapGene.

whereas cGLR2-PF^{opti} isoform is homogeneously distributed in the nucleus, the smaller isoforms cGLR2-PE^{opti}, -PB^{opti} and -PC^{opti} formed nuclear aggregates in a significant proportion of the cells. Surprisingly, despite its NLS, cGLR2-PD^{opti} is mostly found in the cytoplasm (**Figure 7B**). These data suggest differences between cGLR1 and cGLR2 and between cGLR2 different isoforms. Further investigations will be needed to clarify the relevance of these observations.

4. Conclusions and discussion

Data presented in this chapter concern the discovery that drosophila STING pathway is activated by CDNs, as it is the case in mammals (Cai et al., 2020). These results led to the discovery of two distinct cGLRs (Holleufer et al., 2021; Slavik et al., 2021). We are now trying to figure out what are the specificities of these two receptors. Western blot and immunolocalization experiments demonstrated that cGLR2 proteins are unstable and we showed that this instability is at least partly dependent on the proteasome degradation machinery. To understand if this stabilization is important for cGLR2 function and if it occurs naturally, it would be interesting to study cGLR2 stability *in vivo*, especially knowing that the signal responsible for cGLR2 activation is still unknown. One hypothesis is that cGLR2 is constitutively active or activated by a self-signal, which will lead to its stabilization and subsequent production of CDNs.

Our results also show that cGLR1 and cGLR2 present different subcellular localizations. cGLR2 isoforms are mainly found in the nucleus, with the exception of cGLR2-PD isoform, which is mostly cytoplasmic despite the presence of an NLS. Of note, we suspect that this isoform is artificial and does not exist naturally. Interestingly, preliminary results showed that cGLR2-PF is still able to activate a STING-reporter in S2 cells when its NLS is mutated, suggesting that its function is at least partially independent of its nuclear localization (data not shown). It would be interesting to repeat this experiment with the other cGLR2 isoforms to figure out if they all participate in the STING pathway activation and if this is dependent or not of their cellular localization.

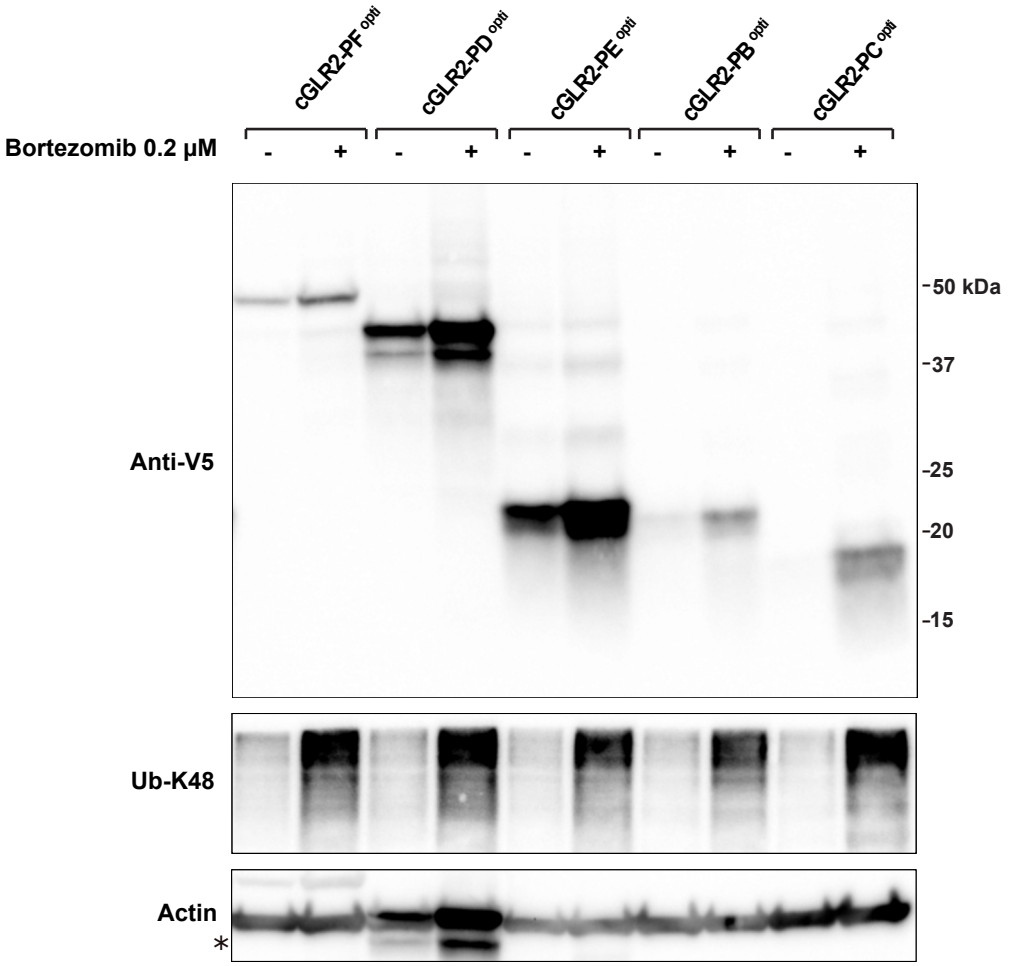

Figure 6: cGLR2 isoforms are stabilized upon proteasome inhibition. Western blot analysis of the stabilization upon Bortezomib treatment of the codon optimized versions of cGLR2 isoforms. S2 cells are transfected with plasmids encoding the optimized versions of cGLR2 under the control of the actin promoter. 48 hours later, cells are treated (+) or not (-) with 0,2 µM of the proteasome inhibitor Bortezomib for 4 hours. Proteins are extracted and Western blot analysis is performed using anti-V5 (top), anti-Ub-K48 (middle) and anti-actin (bottom) antibodies. Representative results from N=3 independent experiments. Aspecific bands are marked with a star (*).

Additionally, unraveling if cGLR2 antiviral effect depends on its nuclear localization could participate in the understanding of its function in drosophila immunity. We can imagine that infection could displace cGLR2 from the nucleus to the cytoplasm, where it can sense viral infections. Preliminary immunolocalization experiments performed in S2 cells did not show any change in cGLR2 localization upon infection with DCV, cricket paralysis virus or flock house virus (data not shown). However, cGLR2 translocation could be specific to certain cell types or tissues, such as the fat body, which is important in the immune response of drosophila or the gut, which is usually the entry door for viruses. Further experiments are required to answer these questions.

Interestingly, it has been shown that the mammalian cGAS is also predominantly localized in the nucleus, where it binds to chromatin. This binding prevents cGAS from recognizing host DNA and subsequently activating the STING pathway (Boyer et al., 2020; Kujirai et al., 2020; Michalski et al., 2020; Orzalli et al., 2015; Zhao et al., 2020). Nuclear cGAS has been proposed to have canonical function, acting as a nuclear DNA virus sensor with the help of cofactors (Lahaye et al., 2018; Orzalli et al., 2015) and also STING-independent non-canonical roles (reviewed in de Oliveira Mann and Hopfner, 2021), but globally its nuclear functions are still poorly understood. Deciphering the nuclear functions of cGLR2 could provide insights into those of cGAS.

A

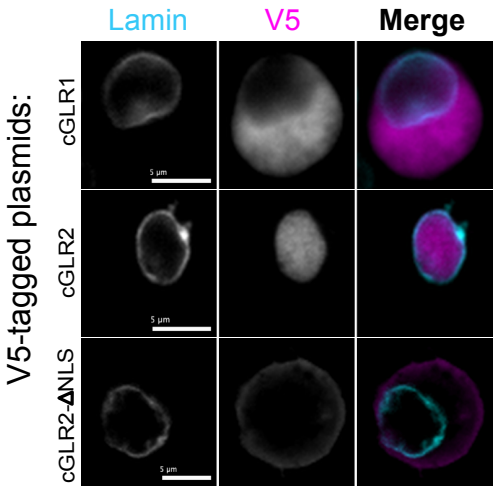

B

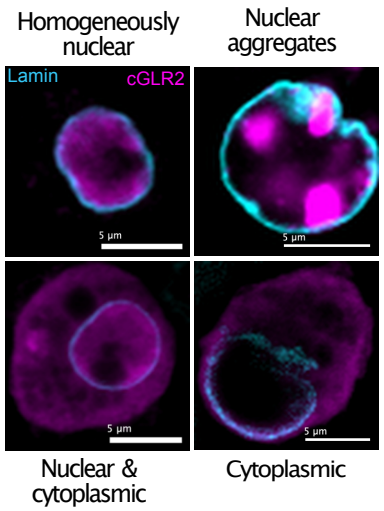

C

cGLR2-PF opti-V5	Number of cells	Percentage
Homogeneously nuclear	163	96,45
Nuclear aggregates	2	1,18
Cytoplasmic	0	0,00
Nuclear & cytoplasmic	4	2,37
TOTAL	169	100

cGLR2-PD opti-V5	Number of cells	Percentage
Homogeneously nuclear	6	4,80
Nuclear aggregates	0	0,00
Cytoplasmic	71	56,80
Nuclear & cytoplasmic	48	38,40
TOTAL	125	100

cGLR2-PE opti-V5	Number of cells	Percentage
Homogeneously nuclear	73	42,69
Nuclear aggregates	89	52,05
Cytoplasmic	1	0,58
Nuclear & cytoplasmic	8	4,68
TOTAL	171	100

cGLR2-PB opti-V5	Number of cells	Percentage
Homogeneously nuclear	130	78,79
Nuclear aggregates	35	21,21
Cytoplasmic	0	0,00
Nuclear & cytoplasmic	0	0,00
TOTAL	165	100

cGLR2-PC opti-V5	Number of cells	Percentage
Homogeneously nuclear	93	56,36
Nuclear aggregates	72	43,64
Cytoplasmic	0	0,00
Nuclear & cytoplasmic	0	0,00
TOTAL	165	100

Figure 7: Subcellular localisation of cGLRs A) S2 cells are transfected with pAc-cGLR1-V5, pAc-cGLR2-V5 or pAc-cGLR2-ΔNLS-V5 for 48 hours. Pictures representative of subcellular localization of different proteins are presented. Representative results from N=3 independent experiments. **B) and C)** S2 cells were transfected with codon optimized versions of cGLR2-PF, -PD, -PE, -PB or -PC isoforms tagged with a V5-tag in C-ter under the control of the Actin-5C promoter. Representative images of the categories of subcellular localization observed for transfected cells **(B)** and their quantification **(C)** are shown. **A, B and C)** Immunostainings are realized with a mix of the primary antibodies rabbit-anti-V5 and mouse-anti-lamin. Secondary antibodies used were anti-Mouse-Alexa594 and anti-Rabbit-Alexa488. The lamin is showed in Cyan and V5-tagged proteins in magenta. MO x630, the scale bar corresponds to 5 µm.

Chapter 2: Fadd and Dredd connects STING to NF-κB signaling in *Drosophila melanogaster*

1. The adaptor Fadd interacts with STING and IKKß

In order to identify partners of IKKß in S2 cells, Akira Goto and colleagues constructed stable cell lines expressing on the one side the bacterial biotin ligase BirA and on the other side IKKß tagged with a biotinylation target sequence (AVI tag). Three independent cell lines expressing different levels of IKKß were selected for further analysis. After immunoprecipitation (IP), using streptavidin coated beads, samples were sent to Dr. Joelle Vinh's lab (ESPCI, Paris) for mass-spectrometry analysis. 84 proteins were significantly enriched in the IKKß immunoprecipitation. The regulatory component of the IKK complex NEMO/IKKγ and Relish were among the top interactants detected, as expected. The list of interactants also included STING, although direct interaction between STING and IKKß had not been detected in previous studies (**Figure 8**)(Goto et al., 2018). In parallel, Goto et al. immunoprecipitated STING from stable cell lines expressing a tagged version of the protein and Joelle Vinh and collaborators determined its interactome. 353 proteins were found to co-immunoprecipitate with STING. Interestingly, Fadd was among the 10 proteins found to interact with both IKKß and STING (data not shown)

To confirm these results, we performed co-IP experiments in S2 cells transiently expressing tagged versions of the proteins. Pull-down of Fadd-V5 co-immunoprecipitated HA-IKKß and HA-STING (**Figure 9A**). Conversely, pull-down of STING-V5 or IKKß-V5 co-immunoprecipitated HA-Fadd (**Figure 9B**). These results indicate that Fadd can interact with both STING and IKKß and could play the role of an adaptor protein in the STING pathway.

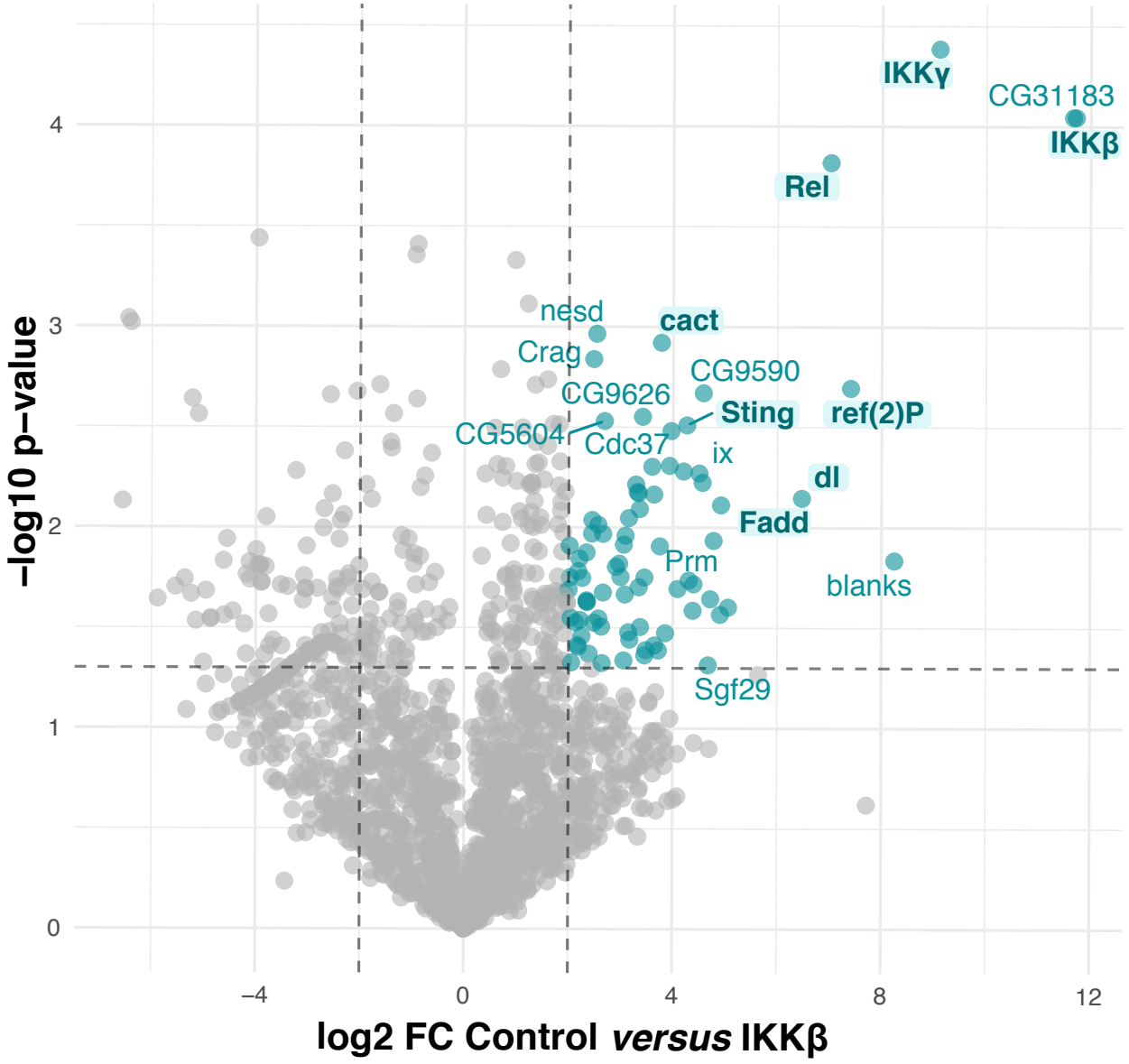

Figure 8: IKKß interacting proteins in S2 cells. The IKKß protein was tagged at the C-terminal extremity with a 15 amino-acid biotinylation target sequence and stably transfected in S2 cells expressing the bacterial biotin ligase BirA. Three independent cell lines were selected according to the IKKß expression level. The S2 cells expressing only BirA were used as negative control. Cell lysates were affinity purified in a single step on Streptavidin beads, digested with trypsin, and analyzed by nanoLC MS/MS on a FT ICR mass spectrometer. IKKß interactants were selected with a Log2 Fold change > 2 and Welch's test *p-value* < 0.05.

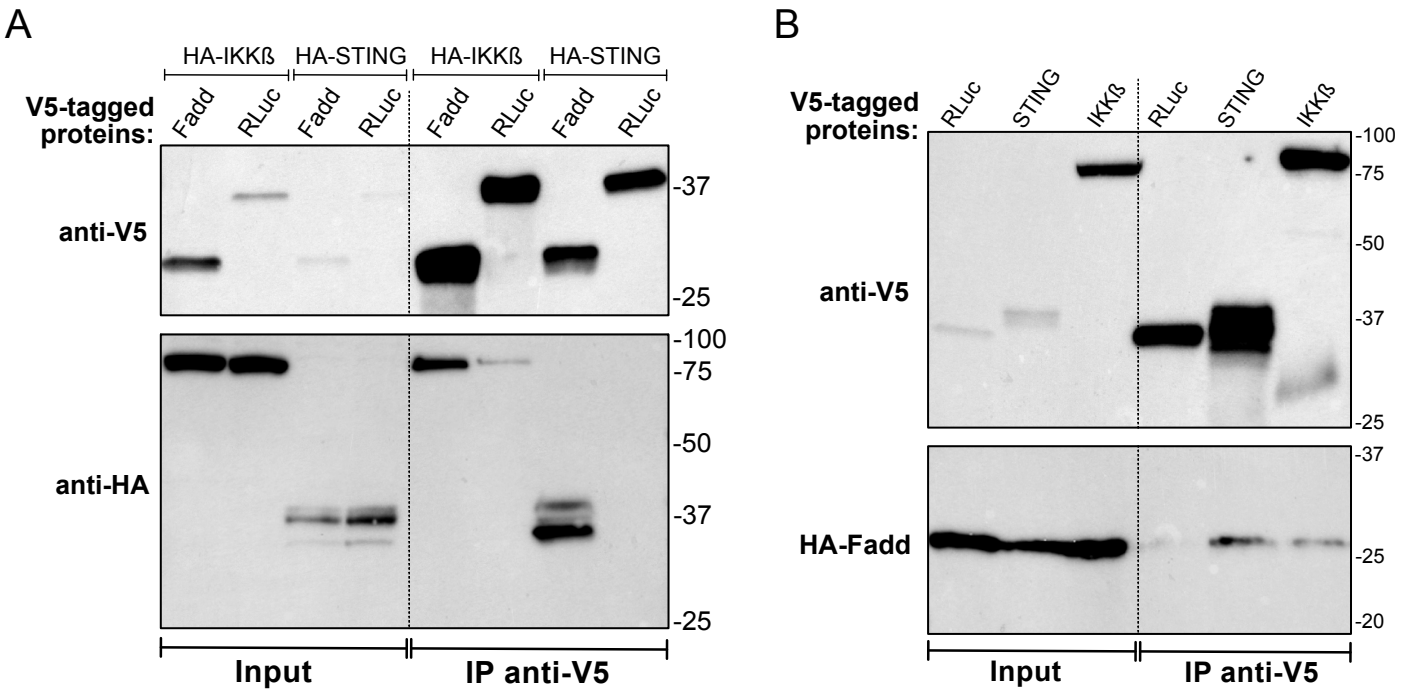

Figure 9: Fadd interacts with IKKß and STING. A) and B) Co-IP studies of **A)** Fadd-V5 or Renilla-Luciferase (RLuc)-V5 with HA-IKKß or HA-STING **B)** RLuc-V5, STING-V5 or IKKß-V5 with HA-Fadd. S2 cells are transfected with previously mentioned pAc clones and proteins extracted 48h post-transfection. IPs are performed with anti-V5 agarose beads. 30% of Input (left) and 30% of IP (right) are loaded on gels for Western blot analysis with anti-V5 antibodies (top). 20% of Input (left) and 50% of IP (right) are loaded on gels for Western blot analysis with anti-HA antibodies (bottom). Representative results from N=2 independent experiments.

2. Role of Fadd in STING signaling

To address a possible role of Fadd in STING signaling in drosophila, we used the f02804 null mutant allele of *Fadd* [52]. These flies were isogenized by eight successive backcrosses with *w1118* flies, which were used as controls for experiments described hereafter. As expected, induction of the Imd pathway regulated gene *diptericin-A* by bacterial infection is strongly reduced in *Fadd* mutant flies compared to control (**Figure 10A**). We injected 2'3'-cGAMP in these flies and monitored expression of the STING regulated genes *srg1* and *srg3* 24 hours later. We observed a drastically reduced induction of either genes in the *Fadd* mutant flies compared to controls, suggesting that Fadd is required for STING signaling in drosophila (**Figure 11A**). Accordingly, induction of *srg1* and *srg3* two- and three-days post DCV infection was reduced in Fadd mutant flies, although not completely abolished (**Figure 11B**). We previously reported that co-injection of 2'3'-cGAMP with DCV results in reduced viral RNA levels one-, two- and three-days post-infection [118,165]. We observed a reduced DCV RNA levels at day two and a downward trend at day three in $w1118^{iso}$ flies co-injected with DCV and 2'3'-cGAMP. This trend was not observed in the $Fadd^{f028204}$ mutant flies (**Figure 11C**). We note that the amount of viral RNA in *Fadd* mutant flies did not increase compared to *w1118* control flies. Finally, we monitored the survival of control and *Fadd* mutant flies following DCV infection in the absence or presence of 2'3'-cGAMP. *Fadd* mutant flies succumb to DCV infection like control flies. Surprisingly, the protection conferred by 2'3'-cGAMP injection was not abolished or decreased in *Fadd* mutant flies (**Figure 11D**). Additional experiments, using the more potent agonist 3'2'-cGAMP [118] or other viruses are required to unambiguously show that cGAMP mediated protection against viral infections is Fadd-dependent.

3. Relish is cleaved by the caspase Dredd upon STING pathway activation

In order to monitor the processing of Relish during signaling, we used different vectors encoding Relish-110 with either a HA-tag in N-ter (**Figure 12A**) or a V5-tag in C-ter (**Figure 12B**). These vectors were co-transfected in S2 cells with plasmids

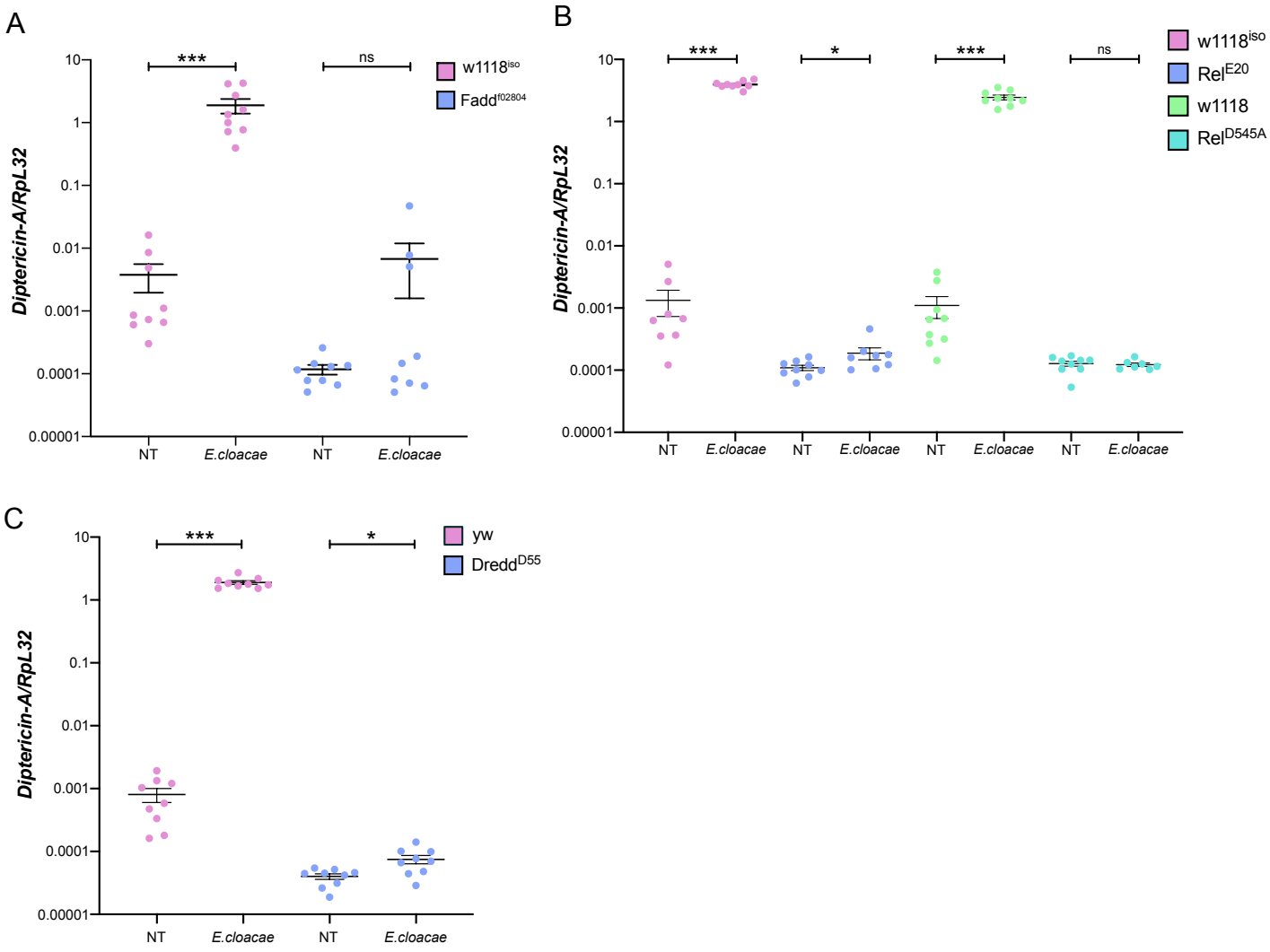

Figure 10: *Fadd*^{f02804}, *Dredd*^{D55}, *Rel*^{E20} and *Rel*^{D545A} mutant flies are deficient for the Imd pathway. Relative gene expression (RT-qPCR) of *Diptericin-A* in **A)** *w1118*^{iso} (WT, pink) and *Fadd*^{f02804} mutant (blue); **B)** *w1118*^{iso} (WT, pink), *Rel*^{E20} (blue), *w1118* (WT, green) and *Rel*^{D545A} (cyan) flies or **C)** *yw* (WT, pink) or *Dredd*^{D55} mutant (blue) flies ; in not treated condition (NT) or 6h after *E.cloacae* pricking. Data show the mean and SEM of N=3 independent experiments, each point representing a pool of six flies. Gene of interest expression is shown relative to the housekeeping gene *RpL32*. Statistics: Multiple Mann-Whitney tests corrected with the Holm-Sidak method: ns $p > 0,05$, *$p \leq 0,05$, **$p \leq 0,01$, ***$p \leq 0,001$.

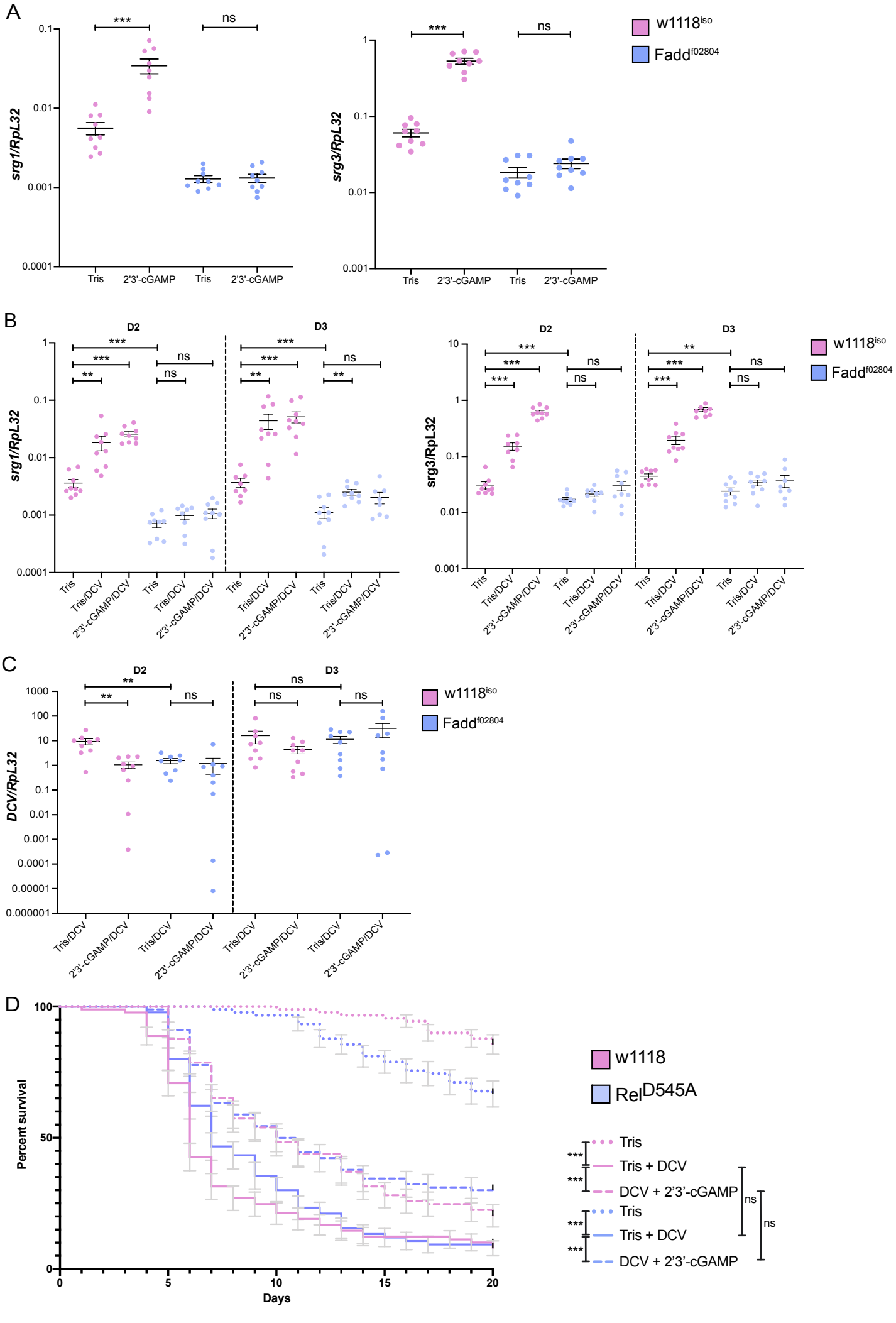
A
srg1/RpL32
srg3/RpL32
Tris
2'3'-cGAMP
w1118iso
Faddf02804
B
D2
D3
Tris/DCV
2'3'-cGAMP/DCV
C
DCV/RpL32
D
Percent survival
Days
w1118
RelD545A
Tris
Tris + DCV
DCV + 2'3'-cGAMP

Figure 11: Fadd is necessary for STING pathway activation. A) Relative gene expression (RT-qPCR) of *srg1* (left) or *srg3* (right) 24h after mock injection (Tris) or 2'3'-cGAMP injection in *w1118*^{iso} (WT, pink) and *Fadd*^{f02804} mutant (blue) flies. **B) and C)** RT-qPCR measuring **B)** relative gene expression of *srg1* (left) and *srg3* (right) or **C)** relative DCV viral load; 48h (D2) or 72h (D3) after Tris+DCV or 2'3'-cGAMP+DCV injection in *w1118*^{iso} (WT, pink) and *Fadd*^{f02804} mutant (blue) flies. **A) to C)** Data show the mean and SEM of N=3 independent experiments,each point representing a pool of six flies. Gene of interest expression is shown relative to the housekeeping gene *RpL32*. Statistics: Multiple Mann-Whitney tests corrected with the Holm-Sidak method: ns $p > 0,05$, *$p \leq 0,05$, **$p \leq 0,01$, ***$p \leq 0,001$. **D)** Survival analysis of *w1118*^{iso} (WT, pink) and *Fadd*^{f02804} mutant (blue) flies, upon mock (Tris, dotted line), Tris+DCV (solid line) or 2'3'-cGAMP+DCV (dashed line) injection. Results from N=3 independent experiments (between 89 and 90 flies per condition) and show standard error for each point (gray). Statistics: Mantel-Cox test: ns $p > 0,05$, *$p \leq 0,05$, **$p \leq 0,01$, ***$p \leq 0,001$.

expressing either PGRP-LC-3xFlag, to activate the Imd pathway, or cGLR1- or cGLR2-3xFlag, to activate the STING pathway. As a negative control, I co-transfected an empty vector (EV). Western blot analysis showed that the activation of the STING pathway by either cGLR1 or cGLR2 overexpression leads to the cleavage of Relish in a similar way to the activation of the IMD pathway (**Figure 12A and B**).

I repeated this experiment, this time using a double tagged pAc-HA-Relish110-V5 construct. Moreover, in addition to S2 cells, the experiment was performed in Dredd-KO cells. Western blot analysis confirmed the cleavage of Relish upon activation of both, the Imd and the STING pathways. Interestingly, no cleavage was detected in *dredd* KO cells, indicating that this caspase, which is required for Relish processing in the Imd pathway, is also involved in the activation of Relish upon activation of the STING pathway (**Figure 12C**).

To confirm these results *in vivo*, we used knock-in mutant flies in which the aspartic acid cleaved by Dredd upon Imd pathway activation (D545) was replaced by an alanine (a kind gift of Professor Neal Silverman). Of note, the Rel^{D545A} mutant flies were isogenized in the *w1118* background and the *w1118* flies used for backcrosses served as controls for the experiments described below. Induction of the Imd pathway upon Gram-negative bacteria infection is abolished in these flies, as previously described in the Rel^{E20} mutants, used as positive controls (**Figure 10B**). Induction of *srg1* was significantly reduced in Rel^{E20} mutant flies compared to controls, as previously described [118,165]. Induction of *srg3*, however, is still observed in Rel^{E20} flies. Strikingly, induction of both SRGs was completely abolished in the Rel^{D545A} mutant flies (**Figure 13A**). Co-injection of the virus with 2'3'-cGAMP resulted in a non-statistically significant reduction of viral RNA in *w1118* flies. This slight antiviral effect of 2'3'-cGAMP was not observed in Rel^{D545A} flies. In addition, we detected an increased viral RNA load in mutant flies compared to control (**Figure 13B**). Rel^{D545A} mutant flies succumbed to DCV infection more rapidly than control flies, confirming that residue D545 plays an important role in the activation of Relish to resist DCV infection *in vivo*. Importantly, the protective effect of the CDN seems reduced when the Dredd cleavage site present in Relish is mutated (**Figure 13C**). Overall, our data indicate that Relish needs to be proteolytically processed at the aspartic acid residue D545 for efficient STING pathway induction and antiviral protection.

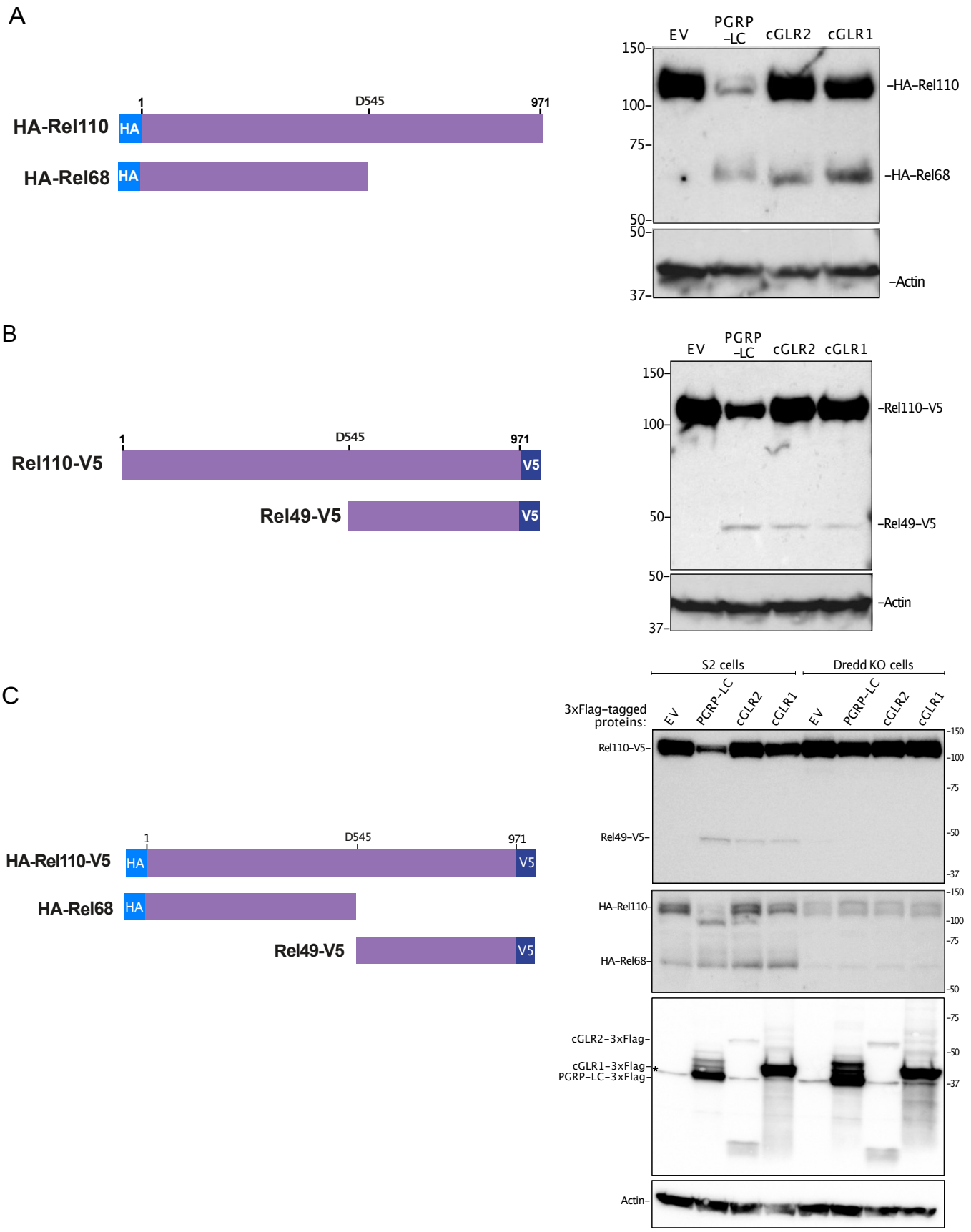

Figure 12: Relish is cleaved by Dredd upon STING pathway activation. Western blot analysis of Relish cleavage status. **A) and B)** S2 cells were transfected with either a pAc-HA-Relish110 construct **(A)** or a pAc-Relish110-V5 construct **(B). C)** S2 cells (left) or *dredd* KO cells (right) were transfected with a pAc-HA-Relish110-V5 construct. **A) B) and C)** In addition to the previously mentioned Relish110 constructs, cells were co-transfected with either the empty pAc-V5-HisA vector (EV), pAc-PGRP-LC-3xFlag, pAc-cGLR2-3xFlag or pAc-cGLR1-3xFlag constructs. After 48h, proteins were extracted and Western blot analysis were performed using anti-V5, anti-HA, anti-Flag and anti-actin antibodies. Star (*) marks aspecific bands. Representative results from **A) and B)** N=1 and **C)** N=3 independent experiments.

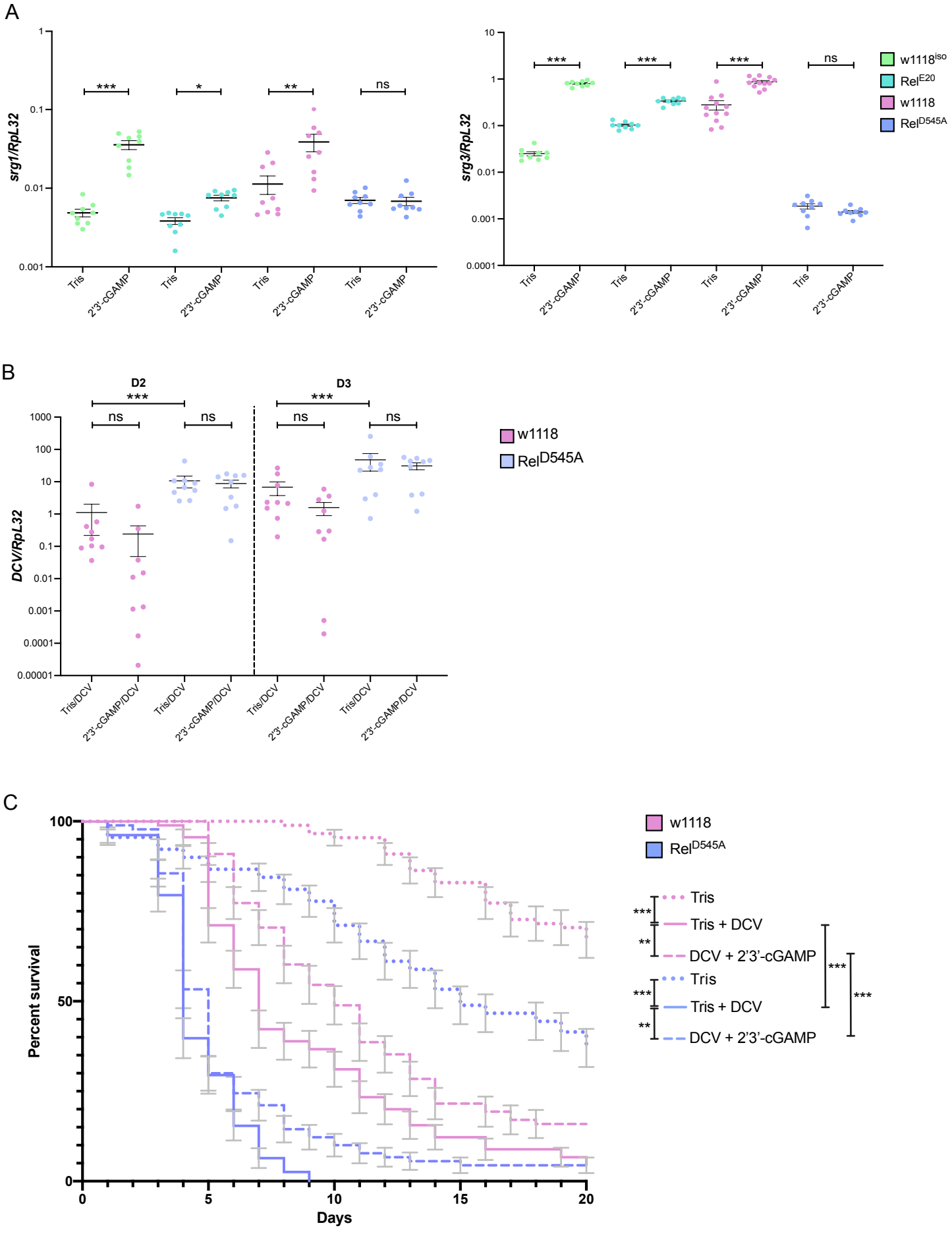
A
srg1/RpL32
srg3/RpL32
***
*
**
ns
Tris
2'3'-cGAMP
w1118iso
RelE20
w1118
RelD545A
B
DCV/RpL32
D2
D3
Tris/DCV
2'3'-cGAMP/DCV
C
Percent survival
Days
Tris
Tris + DCV
DCV + 2'3'-cGAMP

Figure 13: Cleavage of Relish at D545 residue is necessary for STING pathway activation and anti-DCV immunity *in vivo*. A) Relative gene expression (RT-qPCR) of *srg1* (left) or *srg3* (right) 24h after mock injection (Tris) or 2'3'-cGAMP injection in *w1118*^{iso} (WT, green), *Rel*^{E20} (cyan), *w1118* (WT, pink) and *Rel*^{D545A} (blue) flies. B) RT-qPCR measuring relative DCV viral load; 48h (D2) or 72h (D3) after Tris+DCV or 2'3'-cGAMP+DCV co-injection in *w1118* (WT, pink) and *Rel*^{D545A} (blue) flies. A) and B) Data show the mean and SEM of N=3 independent experiments, each point representing a pool of six flies. Gene of interest expression is shown relative to the housekeeping gene *RpL32*. Statistics: Multiple Mann-Whitney tests corrected with the Holm-Sidak method: ns $p > 0,05$, *$p \leq 0,05$, **$p \leq 0,01$, ***$p \leq 0,001$. C) Survival analysis of *w1118* (WT, pink) and *Rel*^{D545A} (blue) flies upon mock (Tris, dotted line), Tris+DCV (solid line) or 2'3'-cGAMP+DCV (dashed line) injection. Results are from N=3 independent experiments (between 78 and 90 flies per condition) and show standard error for each point (gray). Statistics: Mantel-Cox test: ns $p > 0,05$, *$p \leq 0,05$, **$p \leq 0,01$, ***$p \leq 0,001$.

In order to assess the involvement of Dredd in STING signaling *in vivo*, we used loss of function *Dredd*^{D55} mutant flies (kind gift of Professor Bruno Lemaitre). Of note, these flies were not isogenized due to time limitation. As they are in an yellow-white (*yw*) background I used *yw* flies as controls. As expected, induction of the Imd pathway is strongly reduced in these mutants upon infection with Gram-negative bacteria (**Figure 10C**). Induction of *srg1* and *srg3* upon 2'3'-cGAMP injection is prevented in *Dredd*^{D55} mutant flies compared to *yw* controls (**Figure 14A**). Once again, we observed a non-statistically significant reduction of DCV RNA levels in control flies when 2'3'-cGAMP is injected along with DCV. At three-days post-injection we also detected an increased DCV RNA load in *Dredd*^{D55} mutant (**Figure 14B**). Finally, *Dredd*^{D55} mutant flies were more sensitive to DCV infection than controls and were not protected by 2'3'-cGAMP injection (**Figure 14C**). These results confirmed that Dredd is involved in the STING pathway and is necessary for antiviral defenses against DCV.

4. Conclusions and discussion

In conclusion, the data reported in this chapter point to an involvement of two other components of the Imd pathway, besides IKKß and Relish, in STING signaling: the adaptor protein Fadd and the caspase-8 homolog Dredd. We show that Fadd may interact with IKKß and STING using two distinct approaches: (i) unbiased mass-spectrometry analysis of proteins interacting with either IKKß or STING and (ii) co-immunoprecipitations of tagged proteins followed by Western blot analysis. Additionally, we provide genetic evidences that both proteins are necessary for activation of STING-dependent transcriptional response. We also demonstrated that Dredd is important for STING-mediated antiviral response. The caveat of this study resides in the lack of phenotype regarding sensitivity of *Fadd* mutant flies to DCV infection. One possible explanation could be that STING has other antiviral functions which do not depend on Fadd or on the induced transcriptional response. For example, a STING-dependent non-canonical autophagy mechanism may participate in antiviral immunity, as proposed for the control of Zika virus infection in drosophila brain [174]. Alternatively, this discrepancy could result from the dynamic of the response. We can imagine that Fadd is involved in the early response, explaining why we see an impaired induction of *srg1* and *srg3* at early time points (24 to 72 hours) but dispensable for the

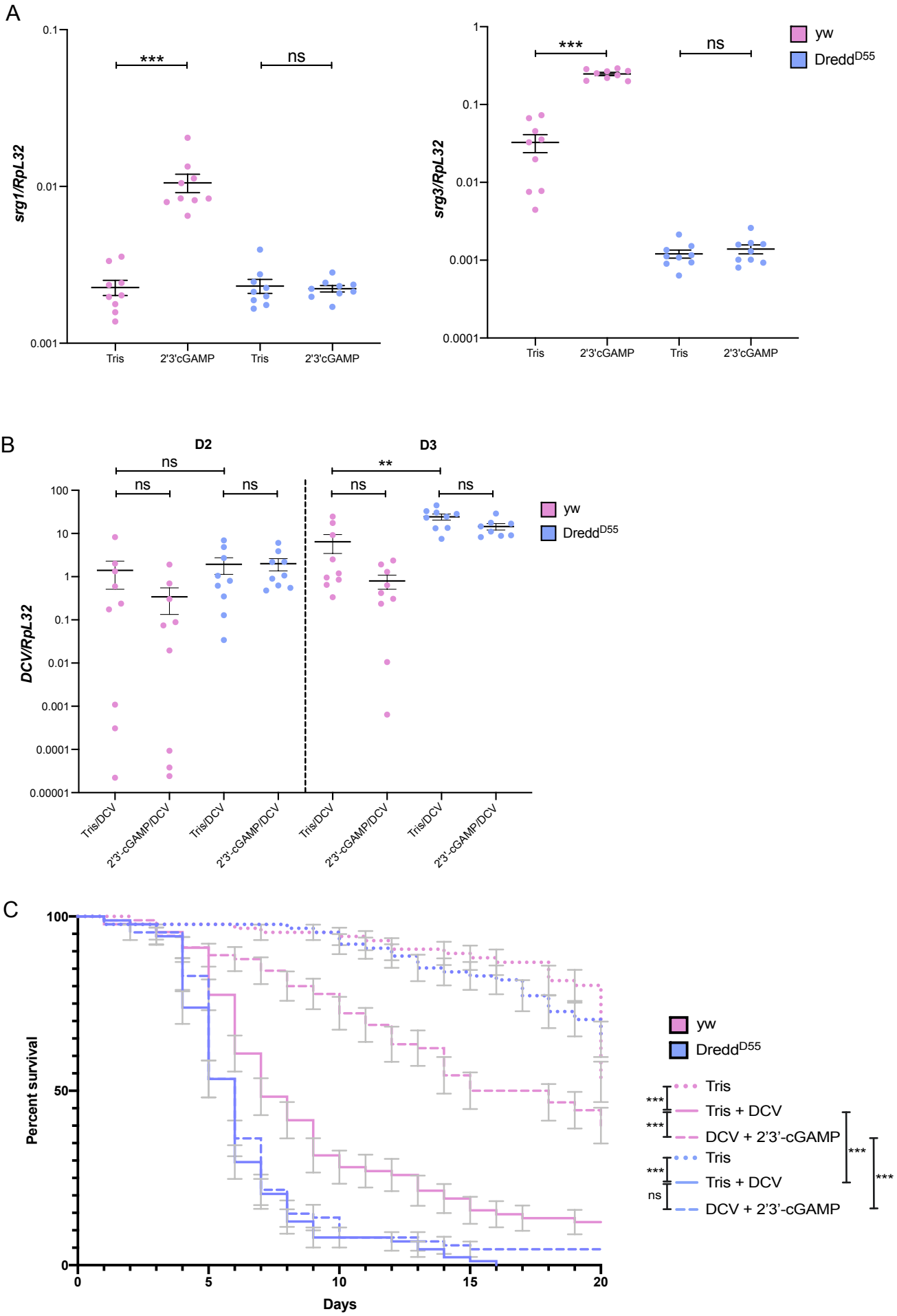
A
srg1/RpL32
0.1
0.01
0.001
***
ns
Tris
2'3'cGAMP
Tris
2'3'cGAMP
srg3/RpL32
1
0.1
0.01
0.001
0.0001
***
ns
Tris
2'3'cGAMP
Tris
2'3'cGAMP
yw
Dredd^D55
B
D2
D3
DCV/RpL32
100
10
1
0.1
0.01
0.001
0.0001
0.00001
ns
ns
ns
ns
**
ns
ns
Tris/DCV
2'3'-cGAMP/DCV
Tris/DCV
2'3'-cGAMP/DCV
Tris/DCV
2'3'-cGAMP/DCV
Tris/DCV
2'3'-cGAMP/DCV
yw
Dredd^D55
C
Percent survival
100
50
0
0
5
10
15
20
Days
yw
Dredd^D55
Tris
Tris + DCV
DCV + 2'3'-cGAMP
Tris
Tris + DCV
DCV + 2'3'-cGAMP
***
***
***
***
ns
***

Figure 14: Dredd is necessary for STING pathway activation and anti-DCV immunity *in vivo*. A) Relative gene expression (RT-qPCR) of *srg1* (left) or *srg3* (right) 24h after mock injection (Tris) or 2'3'-cGAMP injection in *yw* (WT, pink) or *Dredd*^{D55} mutant (blue) flies. **B)** Relative DCV viral load (RT-qPCR) 48h (D2) or 72h (D3) after Tris+DCV or 2'3'-cGAMP+DCV injection in *yw* (WT, pink) or *Dredd*^{D55} mutant (blue) flies. **A) and B)** Data show the mean and SEM of N=3 independent experiments,each point representing a pool of six flies. Gene of interest expression is shown relative to the housekeeping gene *RpL32*. Statistics: Multiple Mann-Whitney tests corrected with the Holm-Sidak method: ns $p > 0,05$, *$p \leq 0,05$, **$p \leq 0,01$, ***$p \leq 0,001$. **C)** Survival analysis of *yw* (WT, pink) or *Dredd*^{D55} mutant (blue) flies, upon mock (Tris, dotted line), Tris+DCV (solid line) or 2'3'-cGAMP+DCV (dashed line) injection. Results are from N=3 independent experiments (between 89 and 90 flies per condition) and show standard error for each point (gray). Statistics: Mantel-Cox test: ns $p > 0,05$, *$p \leq 0,05$, **$p \leq 0,01$, ***$p \leq 0,001$.

long-term response, explaining why we do not see an effect when assessing survival of flies upon DCV infection. In any case, results we obtained concerning Fadd will need to be confirmed using other mutant fly lines or inducing the excision of the transposon present in *Fadd*^{f02804}. This will allow the comparison between flies in which the excision was imprecise *versus* control flies in which the transposon was precisely removed. Experiments in S2 cells KO for *fadd* will also be useful.

The results presented above are contradictory with previously published data from the laboratory, which suggested that Fadd and Dredd were not part of the STING pathway [166]. In their study, Goto and collaborators used dsRNA to knockdown (KD) the expression of *fadd* and *dredd* genes in S2 cells. They then infected these cells with DCV and looked at DCV RNA load as a readout for STING pathway activation. We know that the use of dsRNAs results in residual expression of genes which can be sufficient for normal activity. Additionally, looking at *srg1* and *srg3* induction to assess the involvement of a protein in the STING-pathway seems to be more robust than looking at RNA viral load. In line with results presented in our study, Dredd was already described as essential for antiviral STING-NF-κB pathway activation in another insect, the silkworm *Bombyx mori* [116].

The new data reported in this manuscript raise the question of the involvement of still other proteins of the Imd pathway in STING signaling. Two distinct studies described the involvement of the Imd pathway in defenses against the alphavirus Sindbis virus and the dicistrovirus CrPV, respectively [175,176]. Additionally, a recent study highlighted a role of the tumor suppressor drosophila RASSF (Ras association family) in antiviral response, through the regulation of Imd and JAK/STAT pathways [177]. Goodman and collaborators described the involvement of Imd downstream of STING to activate antibacterial immunity in response to infection with the intracellular bacteria *Listeria monocytogenes* [170]. In order to address this question, our strategy is to use S2 cell lines KO for the different genes involved in Imd signaling. These cell lines are currently developed in the laboratory by another PhD student in the team, Kasper Winther, using CRISPR-Cas9 technology. The *dredd* KO cell line has already been obtained and used to show that Dredd is necessary to activate a STING-luciferase reporter in S2 cells, confirming our *in vivo* results. By contrast, preliminary results using

an *imd* KO cell line in the same assay suggests that Imd is not involved in STING signaling (data not shown).

In mammals, caspase-8 (homolog of Dredd) is known to be a major regulator of cell death programs [178,179]. One of its function is to serve as a scaffold to induce pro-inflammatory responses through NF-κB activation, by forming supramolecular organizing centers with Fadd and receptor-interacting serine/threonine-protein kinase 1 (RIPK1), called FADDosomes. These complexes then induce apoptosis and the production of cytokines downstream of the apoptotic death receptor TRAIL-R [180]. Concerning the role of these proteins in immunity, Barber and collaborators were the first to propose a role for Fadd in innate defenses. They showed that *fadd* null-mutant mammalian cells are more susceptible to viruses and are defective in type I IFN production [181]. This was confirmed by Tschopp and collaborators, who showed that both Fadd and caspase-8 were involved in defenses against RNA viruses. Upon activation of MDA5 or RIG-I receptors, the adaptor protein MAVS (mitochondrial antiviral signaling protein) is recruited and forms a complex with several proteins including TRADD, Fadd and Caspase-8. This complex was called the TRADDosome and regulates cell death and type-I IFN response through NF-κB and IRFs transcription factors (**Figure 15**)[182].

Interestingly, in addition to its role downstream of RIG-I signaling, Ishikawa and Barber proposed that Fadd was also involved in the STING pathway in mammals. Indeed, in the first paper demonstrating a role of STING in innate immunity, these authors showed that mouse embryonic fibroblasts lacking Fadd are not able to activate the type-I IFN response upon STING overexpression [61]. Overall, these observations suggest that Fadd and Dredd have an evolutionarily ancient role in the activation of NF-κB transcription factors in response to viral infection, which is still operating in drosophila and mammalian cells. Whether Fadd and Dredd are part of a higher supramolecular organizing center, such as FADDosome or TRADDosome or not is still an open question. In this case, we can imagine that STING and IKKß are also part of this complex, as they both seem to interact with Fadd (**Figure 15**).

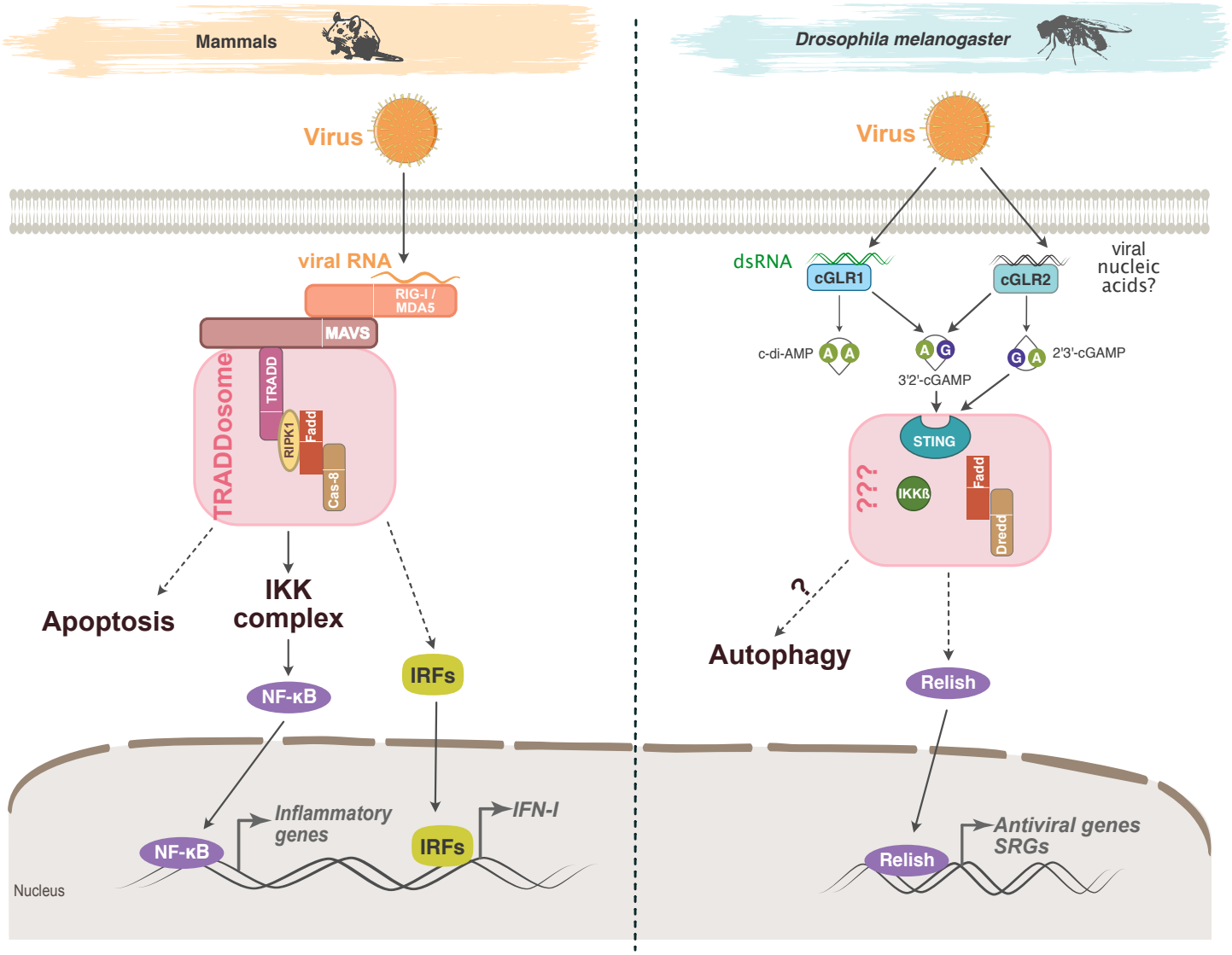

Figure 15: Schematic representation of signaling pathways leading to the TRADDosome formation in mammals and STING pathway in drosophila. Upon activation of RIG-I or MDA5 receptors in mammals (left part) supramolecular organizing centers are formed: the TRADDosome (highlighted in red), allowing an efficient activationof NF-κB. These centers relies on the interaction of several proteins, among those we find Caspase-8 and Fadd. Our study revealed the involvement of the homologue of Caspase-8 in drosophila, Dredd, and the adaptor Fadd in the STING pathway of *Drosophila melanogaster* (right part). Fadd immunoprecipitate with both STING and IKKß. These results suggest that these four proteins are close to each other and work together, maybe in a supramolecular organizing center similar to those find in mammals.

Chapter 3: Other members of NF-κB/IκB families may be involved in STING signaling

1. The IκB protein Charon positively regulates the STING pathway

The discovery that the NF-κB transcription factor Relish and the kinase IKKß, two proteins known for their role in the antibacterial Imd pathway, are involved in antiviral immunity prompted the team to identify IKKß-regulated genes in DCV-infected IKKß mutant flies (*ird5*[1] null mutant) and in S2 cells. This study allowed to identify 10 genes induced following DCV infection in an IKKß-dependent manner in flies and regulated by IKKß in S2 cells [166]. One of these 10 genes is coding for an IκB protein, Charon, presenting seven ankyrin repeats in its C-ter part (Ankyrin rich region, ARR). In addition, RNA-sequencing analysis identified 23 genes induced upon STING overexpression in S2 cells, among which we can also find *charon*. If we cross the different datasets obtained by these transcriptome studies, we notice that *charon* is among the 5 genes IKKß-dependent and induced by STING overexpression *ex vivo* and IKKß-dependent and induced upon DCV infection *in vivo* (**Figure 16A**).

Charon was proposed to participate in Imd pathway regulation. Charon binds to Relish through its ankyrin repeats (**Figure 16B**)[156,157]. However, the two studies describing its role in the Imd pathway present opposing conclusions. One is describing Charon as a negative regulator of the pathway [157] while the other argue that Charon is positively regulating the transcriptional response [156]. These uncertainties concerning the role of Charon coupled to the fact that its expression is induced by DCV infection in flies, by STING overexpression in S2 cells and depends on IKKß, raised the question of a potential role of Charon in the STING pathway.

A

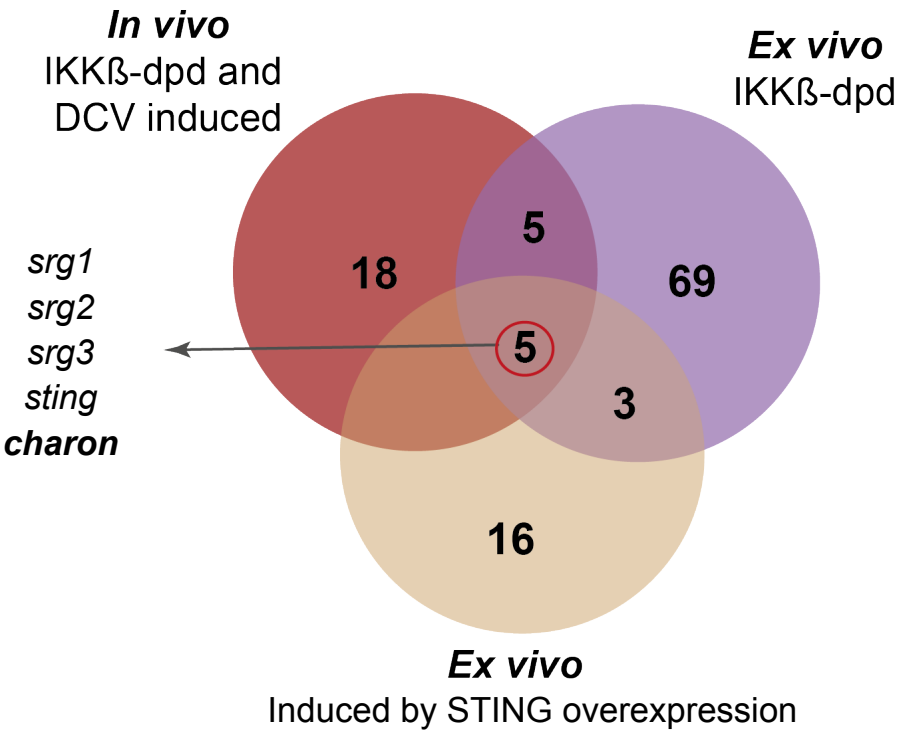

List of genes induced by STING overexpression in S2 cells

Gene	Molecular function
CG43610	Unknown
STING	Mammalian STING homolog
SRG1	Unknown
elA	Unknown
CR44448	lncRNA
Pask	Kinase
Smal	Collagen binding
CG30002	Serine–type endopeptidase activity
CG3515	Chromatin binding
Hsp26	Myosin binding
CG8519	GTPase activity
CG30484	Unknown
Hsp70Aa	ATP dependent activity
Hsp70Ab	ATP dependent activity
Hsp23	Protein binding
CG42268	Unknown
Hsp22	Protein binding
Hsp67Bb	Unknown
SRG2	Hexose transmembrane transporter activity
CG42240	Unknown
Pu	GTP cyclohydrolase activity
CstF–64	mRNA binding
Charon	NF–kB binding
SRG3	Unknown

B

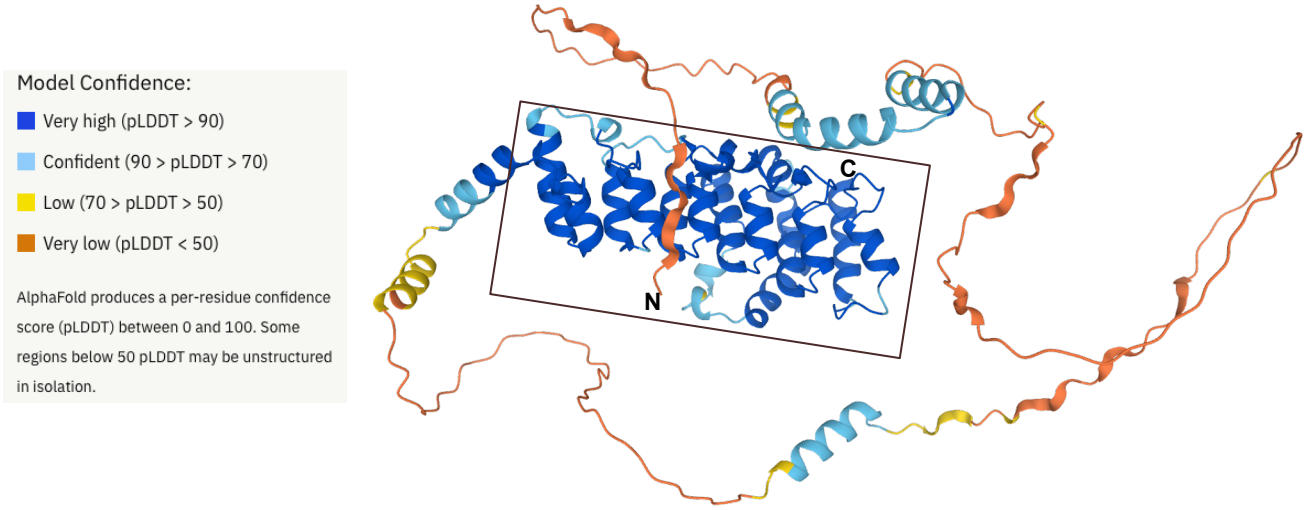

Figure 16: The IκB protein Charon A) Venn diagram representing genes identified by three independent transcriptome analysis. DNA microarray analysis allowed to identify genes regulated by IKKß and induced upon DCV infection in flies (red, 28 genes) and genes whose basal expression depend on IKKß in cells (purple, 82 genes). List of genes contained in red and purple circle can be found in *Goto et al., 2018*. RNA-sequencing of S2 cells identified 24 genes whose expression is induced by STING overexpression (beige, list of genes on the right, *Cai et al., unpublished*). The intercross of these different transcriptome analysis gather 5 genes: *sting*, *CG13641* (*srg1*), *CG42825* (*srg2*), *CG33926* (*srg3*) and *charon*. dpd = dependent **B)** Predicted Charon protein structure obtained with AlphaFold (*Jumper et al., 2021*). Ankyrin repeats are boxed. The structure of this stretch of ankyrin repeats is predicted with a very-high confidence score (dark blue, see legend on the left).

In order to test this hypothesis, I performed assays using a STING-Firefly-luciferase (FLuc) reporter as a readout for STING pathway activity (pSTING-FLuc). I co-transfected S2 cells with this reporter along with a construct encoding the Renilla-luciferase (RLuc) downstream of the Actin5C promoter (pAc5C-RLuc). This second plasmid serves as a transfection efficiency control. The transfection mix also contained a clone coding for STING under the control of the Cupper inducible metallothionein promoter (pMT-STING), allowing the inducible activation of the pathway. Finally, to achieve knock-down of candidate proteins, I also transfected dsRNAs. dsRNAs against *gfp* and *sting* were used as a negative or positive control, respectively. I designed two dsRNAs targeting different regions of *charon* to assess its role in the STING pathway while limiting the risk of off-target effect. The KD efficiency at the RNA level was assessed for each candidate by real-time quantitative polymerase chain reaction (RT-qPCR). KD of *sting* with dsRNAs results in a decrease of approximately 54% of *sting* RNA, KD with dsCharon-1 and dsCharon-2 lead to a decrease of 60% and 58% of the amount of *charon* RNA, respectively (data not shown). Results obtained by luciferase activity measurement show that the KD of *sting* induces an important diminution of the reporter activity compared with dsGFP treated cells. Importantly, KD of *charon* with both dsRNAs also show a severe diminution of STING pathway activity (**Figure 17A**). This result indicates that Charon may be a positive regulator of the STING pathway.

On the other hand, I tested the involvement of Charon in the Imd pathway using a similar assay. In this experiment, I used an Attacin-A (Att-A) reporter (pAttA-FLuc). As a positive control, I used dsRNAs targeting the *ikkß* kinase (decrease of 50% of *ikkß* RNA load, data not shown). The Imd pathway is triggered by addition of heat-killed *E. coli* (HKE) to the cell media. Results show that the KD of *ikkß* leads to a diminution in luciferase activity, as expected. The KD of *charon* by dsCharon-1 does not affect Att-A reporter activity. On the other hand, the KD of *charon* using dsCharon-2 leads to a significative decrease in reporter activity, although this diminution is weaker than in dsIKKß-treated cells (**Figure 17B**). These results suggest a major role of Charon in the STING pathway rather than in the Imd pathway, as first reported [156,157].

I then looked at the impact of *charon* KD on the endogenous STING pathway. To do so, I monitored the expression of *srg1* and *srg3* by RT-qPCR in a stable cell line overexpressing STING upon Cupper treatment. As anticipated knocking down *ikkß*

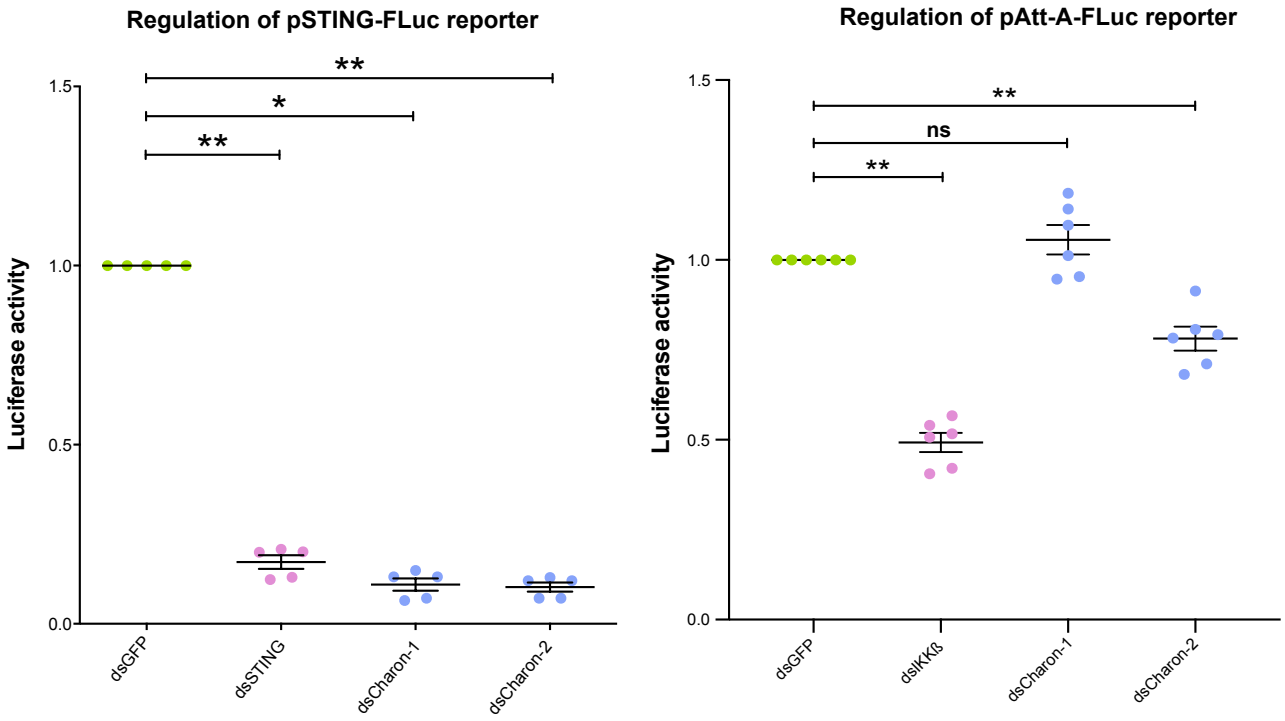

Figure 17: *charon* KD prevents the induction of a STING-luciferase reporter upon STING pathway activation. Dual luciferase assay on S2 cells co-transfected with **A)** pMT-STING, pSTING-FLuc, pAc5C-RLuc and dsRNAs against proteins of interest (see X axis legend) or **B)** pAttA-FLuc, pAc5C-RLuc and dsRNAs against proteins of interest (see X axis legend) and incubated with HKE. **A)** and **B)** Ratio between Firefly-Luciferase and Renilla-Luciferase is calculated for each condition. The ratio of the negative control (dsGFP) is arbitrarily set to 1 and the ratios of the other candidates are normalized by this control. Data show the mean and SEM of N=2 independent experiments. Each independent experiment consists in one transfection of S2 cells, each point representing one measurement of Luciferase. Statistics: Multiple Mann-Whitney tests corrected with the Holm-Sidak method: ns $p > 0,05$, *$p \leq 0,05$, **$p \leq 0,01$, ***$p \leq 0,001$.

leads to a significant decrease of both SRGs induction compared with dsGFP-treated cells. Disappointingly, in *charon* KD conditions, the induction of SRGs upon STING pathway activation resemble that observed in dsGFP treated cells (**Figure 18**). These results are contradictory with the ones previously obtained with the luciferase reporter assay.

In order to clarify the role of Charon in the pathway, we decided to pursue this study in flies. To design a mutant fly line, our collaborators from the gene editing platform at the Sino-French Hoffmann Institute (SFHI, Guangzhou, China) used the CRISPR-Cas9 technology. The fly line obtained present a single nucleotide (nt) deletion (nt 55) at the very beginning of the coding sequence of Charon leading to a frameshift and a premature STOP codon (*Charon*^{S19VfsTer5}, hereafter named *Charon*^{S19fs})(**Figure 19A**). I then looked for a phenotype in the STING pathway, by injecting 2'3'-cGAMP into these flies and monitoring SRGs induction by RT-qPCR. On the other hand, the impact of Charon in the Imd pathway was assessed by pricking flies with the Gram-negative bacteria *Enterobacter cloacae* and looking at *dpt-A* and *att-A* induction by RT-qPCR. Unfortunately, I was not able to detect any difference in gene induction between *Charon*^{S19fs} and control flies neither for SRGs nor for AMPs (data not shown). However, we noticed that *Charon*^{S19fs} flies express similar amount of *charon* RNA than wild-type (WT) flies. This suggests that *charon* mRNAs from *Charon*^{S19fs} flies exists and are not degraded by the non-sense mediated decay pathway (data not shown). Looking carefully at the coding sequence of *charon*, I noticed several possible alternative ATGs which are not disrupted by the mutation (predicted by ATGpr program [183])(**Figure 19A**). The use of an alternative translation initiation site could allow the production of a functional truncated Charon protein, explaining the absence of phenotype in mutant flies.

To solve this issue, our partners at SFHI produced new CRISPR-Cas9 flies with guides RNAs targeting the ARR. Indeed, a mutation in this region should prevent the interaction between Charon and Relish and thus probably block its function in the STING pathway and/or the Imd pathway. These flies, recently arrived at the laboratory, present a deletion of 8 nt (nt 890-897) in the ARR leading to a frameshift (*Charon*^{L297QfsTer351}, hereafter named *Charon*^{L297fs})(**Figure 19A**). In order to assess

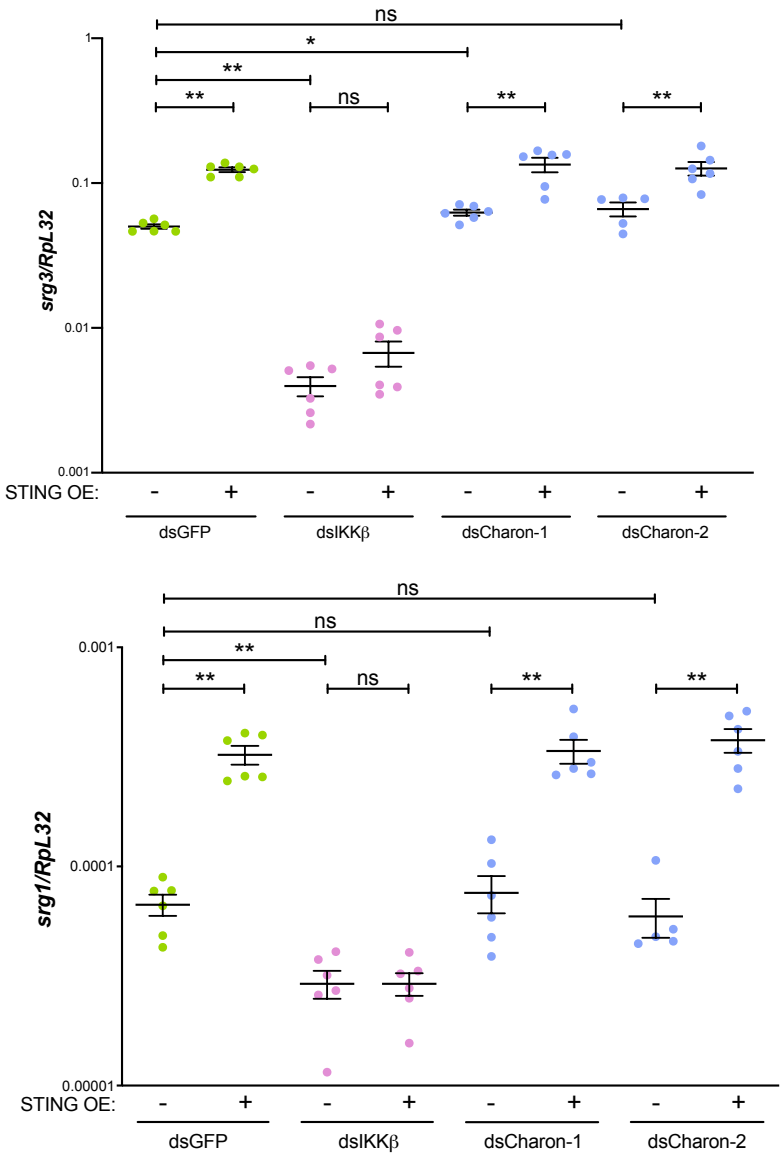

Figure 18: *charon* KD does not impact SRGs induction upon STING pathway activation. Relative gene expression (RT-qPCR) of *srg1* (left) or *srg3* (right) in S2 cells treated with dsRNAs against protein of interest (see X axis legends) in normal condition (-) or in STING overexpression condition (+). Data show the mean and SEM of N=2 independent experiments, each point represents a pool of six flies. Expression is shown relative to the housekeeping gene *RpL32*. Statistics: Multiple Mann-Whitney tests corrected with the Holm-Sidak method: ns $p > 0,05$, *$p \leq 0,05$, **$p \leq 0,01$, ***$p \leq 0,001$.

their phenotype for both the Imd and STING pathways I reproduced the same experiment as for *Charon*^{S19fs} flies.

Concerning the STING pathway, I noticed a diminution of basal levels of *srg1*and *srg3* RNA in *Charon*^{L297fs} flies. Moreover, induction of both SRGs is reduced in these flies upon 2'3'-cGAMP injection (**Figure 19B**). Regarding the Imd pathway, induction of *att-a* and *dpt-A* AMPs does not differ much in mutant flies, except for a slight increase in the induction of *att-A*. Overall, these results suggest that Charon acts as a positive regulator of the STING pathway, but does not have a major effect on the Imd pathway. Further investigation on the function of Charon is clearly necessary, and these results need to be confirmed with isogenized fly lines.

2. The IKKß and Relish interacting protein dorsal-B is a negative regulator of the STING pathway

The study of IKKß interactome mentioned in Chapter 2 allowed the identification of another interesting protein, dorsal (dl)(**Figure 8**). The Toll pathway regulated transcription factor dorsal, is mostly known for its role in embryonic development. It is responsible for the establishment of the dorsoventral axis [184]. Moreover, it was proposed that dl is essential for resistance to oral viral infections [123123]. Intriguingly, two distinct isoforms of dl exist, due to alternative splicing. Retention of the sixth intron of the *dl* gene leads to the formation of dl-B, a larger protein (999 residues for dl-B *versus* 677 residues for dl, http://flybase.org/reports/FBgn0260632). Both isoforms share the N-terminal RHD, which is encoded by the six first exons, but present a completely different sequence afterward (**Figure 20A**)[185]. The dl-B isoform is poorly characterized but was proposed to play a role in antibacterial response [185] and was found associated with neuromuscular junction in larvae [186].

Twelve different peptides belonging to dorsal were detected by the mass-spectrometry analysis of the IKKß interactome. Interestingly, among these peptides, five correspond to the common RHD domain while the other seven match to the specific region of the dl-B isoforms (**Figure 20A**). This result suggests a specific

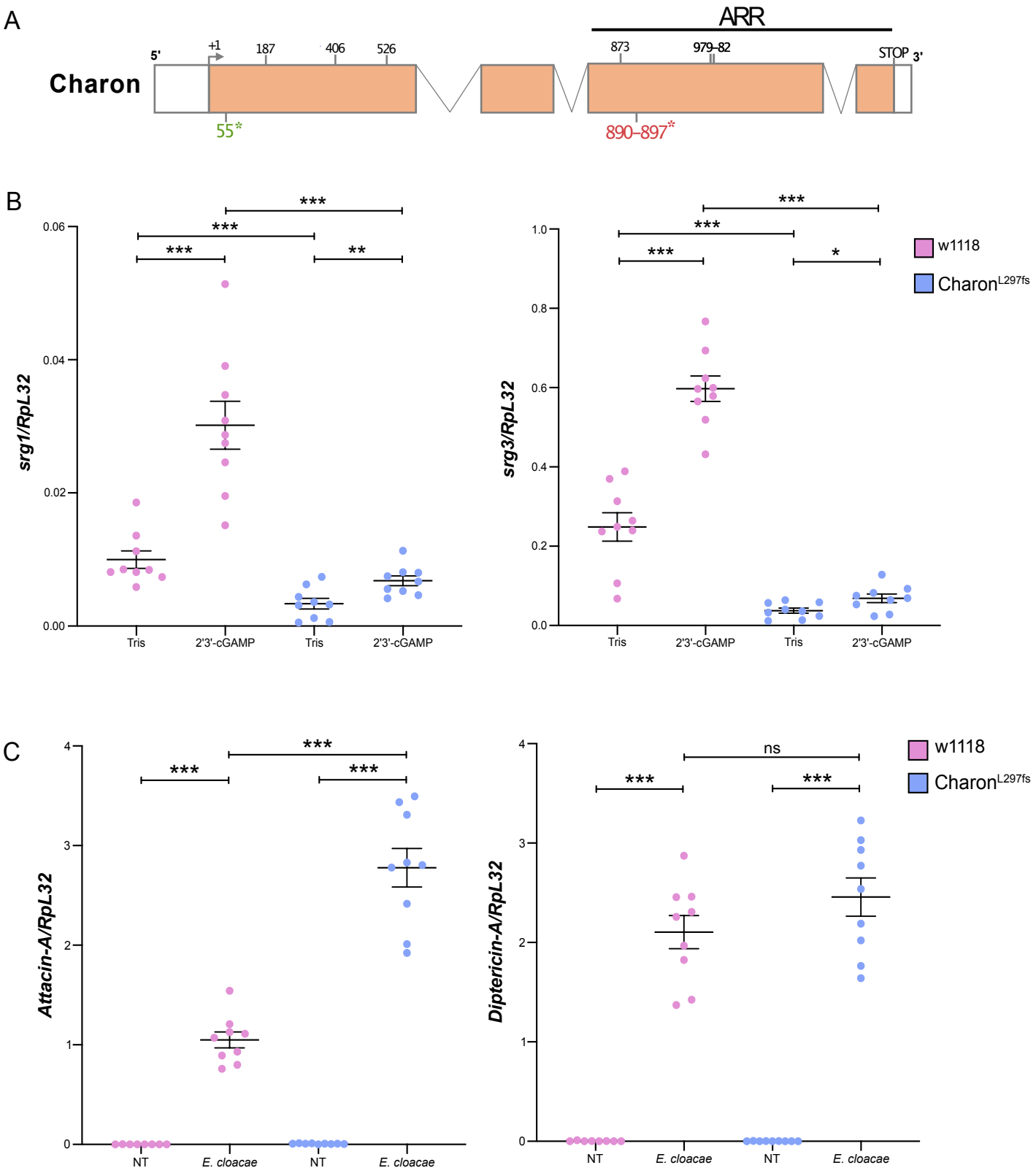

Figure 19: *Charon*^{L297fs} mutant flies have a reduced SRGs induction upon 2'3'-cGAMP injection. A) Schematic representation of Charon RNA. Boxes represents exons (white = untranslated region) and lines introns. Coordinates of first nucleotide of ATG codons that can serve as translation initiation sites are indicated (predicted with a reliability score greater than 0.25 using the ATGpr program (*Nishikawa et al., 2000*)). Deleted nucleotides in *Charon*^{S19fs} (green) and *Charon*^{L297fs} (red) mutants are indicated. **B) and C)** Relative gene expression (RT-qPCR) of **B)** *srg1* (left) or *srg3* (right) 24h after mock injection (Tris) or 2'3'-cGAMP injection and **C)** *Attacin-A* (left) or *Diptericin-A* (right) in not treated condition (NT) or 6h after pricking with *E.cloacae*; in w1118 (WT, pink) and *Charon*^{L297fs} mutant (blue) flies. Data show the mean and SEM of N=3 independent experiments,each point representing a pool of six flies. Gene of interest expression is shown relative to the housekeeping gene *RpL32*. Statistics: Multiple Mann-Whitney tests corrected with the Holm-Sidak method: ns p > 0,05, *p ≤ 0,05, **p ≤ 0,01, ***p ≤ 0,001.

interaction between IKKß and dl-B. In order to confirm this hypothesis, I performed co-IP experiments. I transiently co-transfected S2 cells with plasmids coding either for dl-B-V5 or dl-V5 and HA-IKKß or HA-GST, as a control. I then performed the IP using beads coated with anti-HA antibodies. Results showed that IKKß interacts with dl-B but not with dl, confirming the specific interaction detected by mass-spectrometry. Moreover, I noticed a reproducible increase in the quantity of the total IKKß protein when co-transfected with dl-B, which suggests that this isoform is somehow stabilizing IKKß (**Figure 20B**).

Except for the RHD, there is no described or predicted functional domains in dl-B. In an attempt to better characterize this protein, we wondered which region of it was responsible for the interaction with IKKß. To answer this question, I constructed 5 different plasmids coding for truncated dl-B proteins tagged in C-ter with a V5 tag. One is coding for the RHD domain only (RHD), and is used as a negative control which should not interact with IKKß, as it is common to both isoforms; one is coding for the entire dl-B specific domain (Cter-domain, CTD); and three coding for part of the CTD (CTD-N, CTD-M and CTD-C)(**Figure 20C**). I then performed IP of each of these clones, FLuc-V5, as a negative control, or the full-length dl-B-V5, as a positive control, and checked if HA-IKKß was co-immunoprecipitating. As expected, the interaction between IKKß and dl-B full-length previously mentioned is reproducible. As anticipated, the RHD domain alone and FLuc are not interacting with IKKß. The CTD is interacting with IKKß even if I was not able to detect the protein in the input fraction. This result suggests that the interaction between IKKß and dl-B does not require the full dl-B protein. Interestingly, among the truncated proteins encoding part of the CTD, only the one coding for the central region (CTD-M) interacts with IKKß. However, only the full-length dl-B seems to be able to stabilize IKKß, which suggests a role for the RHD in this stabilization (**Figure 20D**).

NF-κB transcription factors can form homo- or heterodimers and the composition of dimers can lead to different transcriptional responses [157,160,187,188]. Relish is involved in both Imd and STING pathway. However, depending on the activated pathway, it controls different, though overlapping, transcriptional responses (Cai et al., 2020). This is why we wondered if both pathways were regulating different NF-κB dimers. To test the hypothesis of an heterodimerization between Relish and dl-B, I performed co-IP

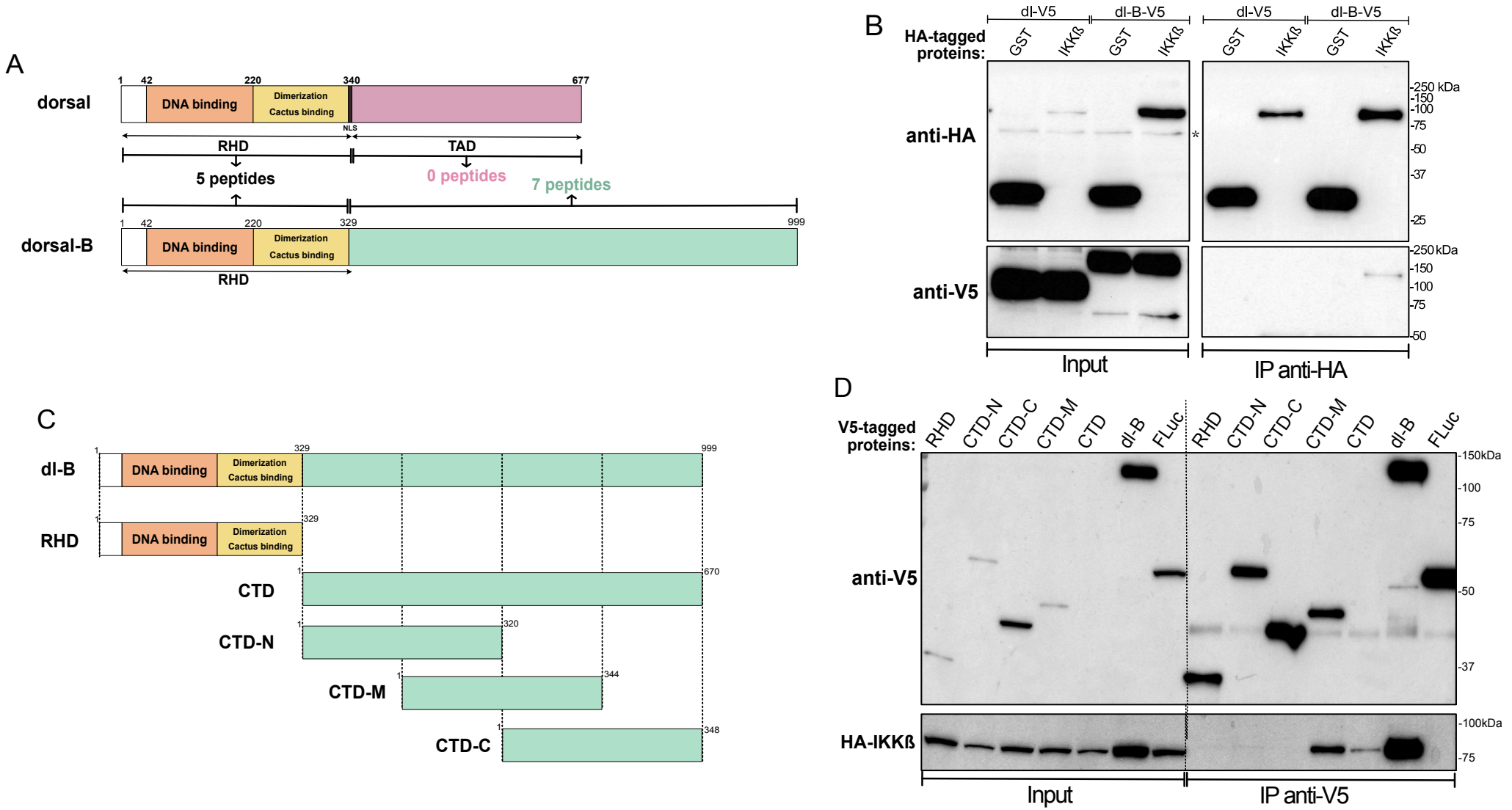

Figure 20: The NF-κB protein dorsal-B interacts with the kinase IKKß. A) Schematic representation of dl and dl-B protein isoforms. Number of peptides identified by mass-spectrometry for each region in the IKKß interactome is indicated between both proteins. **B)** Co-IP studies of dl-V5 or dl-B-V5 and HA-GST or HA-IKKß. S2 cells are transfected with previously mentioned pMT clones, Cupper is added 24h after transfection and proteins extracted at 72h post-transfection. IP is performed with anti-HA agarose beads. 50% of Input (left) and 10% of IP (right) are loaded for Western blot analysis with anti-V5 (top) and anti-HA (bottom) antibodies. Representative result from N=2 independent experiment. **C)** Schematic representation of dl-B protein and the 5 truncated proteins expressed by the constructed plasmids (pMT-V5-HisA backbone) **D)** Co-IP studies of HA-IKKß with dl-B-V5, FLuc-V5 or truncated proteins detailed in **C)**. See **B)** for experimental details. IP is performed with anti-V5 agarose beads. 25% of Input (left) and 25% of IP (right) are loaded for Western blot analysis. Representative result from N=2 independent experiment.

experiments in S2 cells. Cells were transiently transfected with a vector coding for Relish tagged with a Myc-tag in C-ter, and either dl-B-V5, dl-V5 or FLuc-V5, as a negative control. Results show that Relish co-immunoprecipitated only with dl-B and not with dl, suggesting that the formation of a dl-B/Relish heterodimer is possible (**Figure 21A**).

As for the interaction between IKKß and dl-B we then wanted to identify more precisely the region of dl-B responsible for the interaction with Relish. To do so, I repeated the same experiment using dl-B truncated and the clone coding for Relish-Myc . Preliminary results suggest that there is no interaction between Relish and FLuc, nor with the RHD as expected. As previously mentioned, Relish and the full-length dl-B are interacting. The CTD region of dl-B interacts with Relish, such as CTD-M and CTD-C. This could mean that the interacting region is in the common part encoded by both clones. However, interactions of Relish with truncated proteins (CTD, CTD-M and CTD-C) seem to be weaker than the one with full-length dl-B (**Figure 21B**).

In order to study the role of dl-B in the STING and Imd pathways *in vivo*, our collaborators at SFHI (Guangzhou, China) constructed dl-B mutant flies (*dl-B*^{I370TfsTer376}, hereafter named *dl-B*^{I370fs})(**Figure 22A**). I injected these flies or control counterparts with 2'3'-cGAMP or Tris as a control and assessed the RNA levels of *srg1* and *srg3* by RT-qPCR. Results show that the induction of both tested SRGs is increased in *dl-B*^{i370fs} mutant flies compared to WT flies (**Figure 22B**). Concerning the Imd pathway, there is no major differences in AMPs induction upon *E. cloacae* infection in *dl-B*^{i370fs} and WT flies, except for a slight increase for *diptericin-A* induction in mutant flies (**Figure 22C**). These results suggest that dl-B is a negative regulator of the STING pathway, which will have to be confirmed with isogenized fly lines.

3. Conclusions and discussion

In this third chapter, I described results concerning two proteins suspected to be involved in the STING pathway. Concerning the IκB protein Charon, results obtained in two distinct cell assays produced contradictory results. Indeed, Charon positively regulates a STING-FLuc reporter while KD of *charon* in S2 cells did not impact the

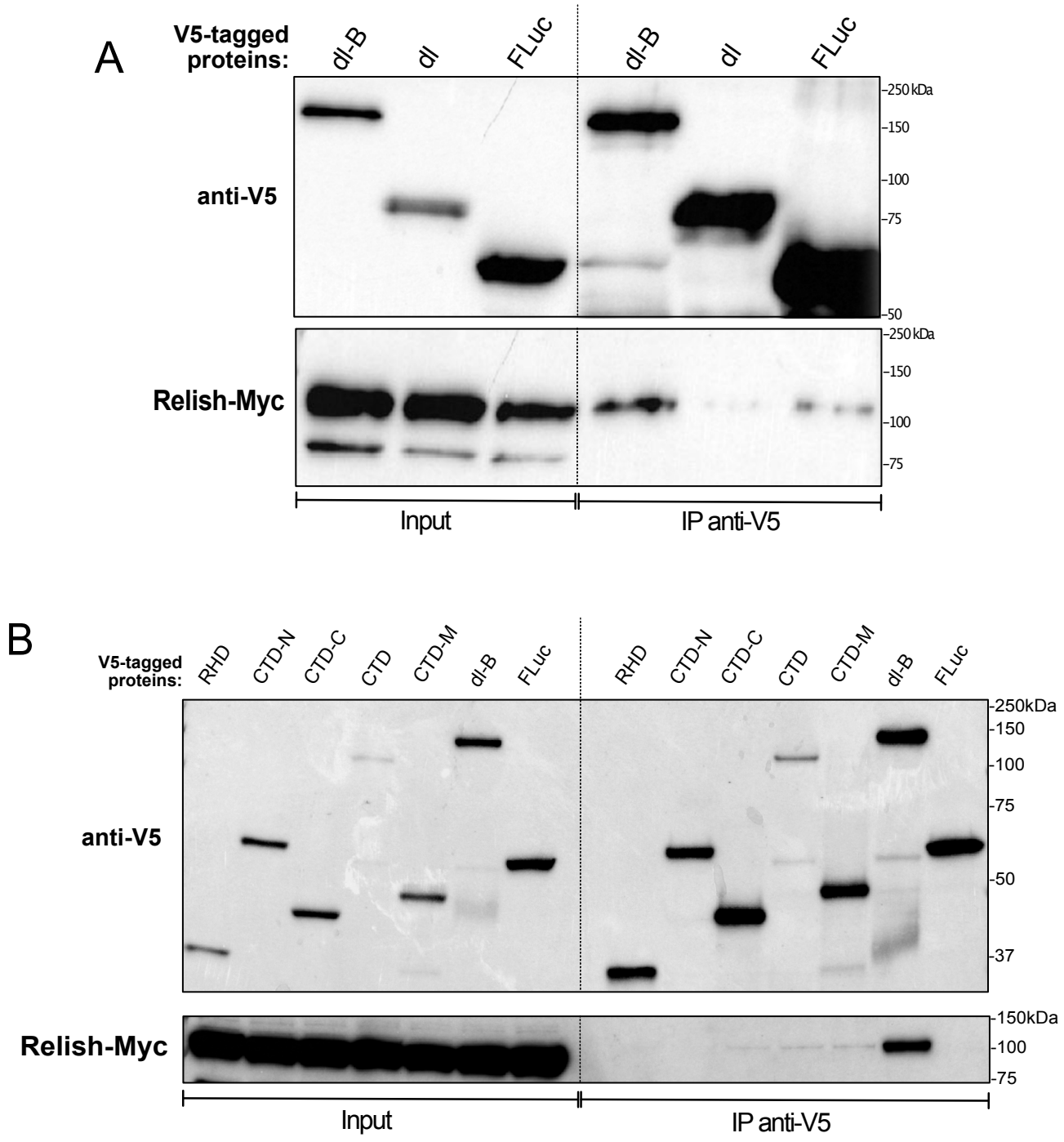

Figure 21: The NF-κB proteins dorsal-B and Relish interacts. A) and B) Co-IP studies of **A)** dl-V5, dl-B-V5 or FLuc-V5 with Relish-Myc or **B)** dl-B-V5, FLuc-V5 or truncated proteins (detailed in Fig. 20C) with HA-IKKß. S2 cells are transfected with previously mentioned pMT clones, Cupper is added 24h after transfection and proteins extracted at 48h post-transfection. IP is performed using anti-V5 agarose beads. 25% of Input (left) and 25% of IP (right) were loaded for Western blot analysis with anti-V5 (top) and anti-Myc (bottom) antibodies. Results from **A)** N=2 and **B)** N=1 experiments.

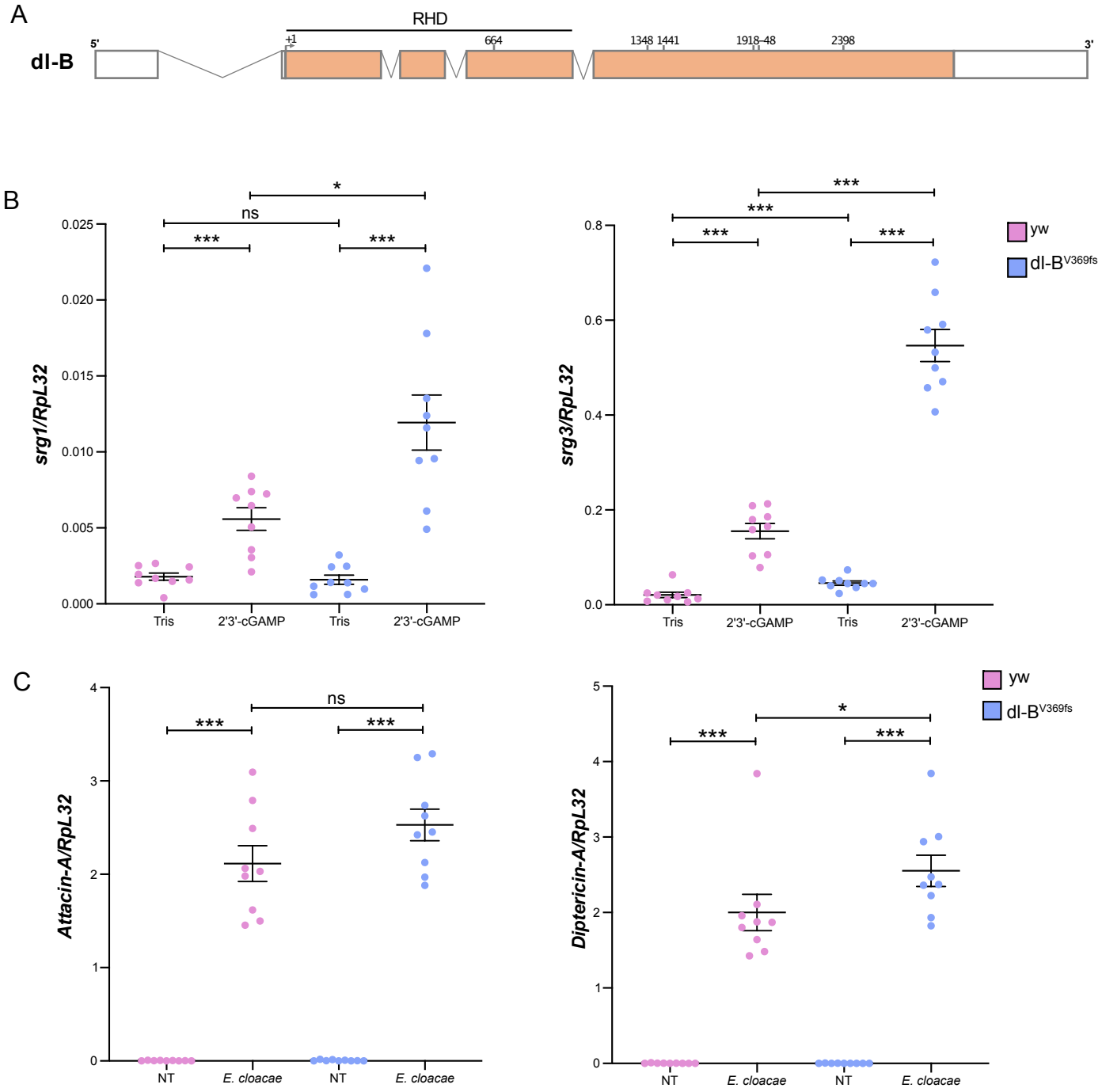

Figure 22: *dl-B*^{V369fs} flies have an increased SRGs induction upon 2'3'-cGAMP injection. A) Schematic representation of dl-B RNA. Boxes represents exons (white ones = untranslated regions) and lines introns. Coordinates of first nucleotide of ATG codons that can serve as translation initiation sites are indicated (predicted with a reliability score greater than 0.25 using the ATGpr program (*Nishikawa et al., 2000*)). **B) and C)** Relative gene expression (RT-qPCR) of **B)** *srg1* (left) or *srg3* (right) 24h after mock injection (Tris) or 2'3'-cGAMP injection and **C)** *Attacin-A* (left) or *Diptericin-A* (right) in not treated condition (NT) or 6h after *E.cloacae* pricking; in *yw* (WT, pink) and *dl-B*^{V369fs} flies (blue). Data show the mean and SEM of N=3 independent experiments, each point represents a pool of six flies. Expression is shown relative to the housekeeping gene *RpL32*. Statistics: Multiple Mann-Whitney tests corrected with the Holm-Sidak method: ns $p > 0,05$, *$p \leq 0,05$, **$p \leq 0,01$, ***$p \leq 0,001$.

endogenous SRGs induction upon STING pathway activation. A possible explanation to this apparent discrepancy could be that the KD of *charon* is not efficient enough to observe an effect on the endogenous STING pathway activation. The amount of Charon protein remaining could be sufficient to perform its normal function. Moreover, in the luciferase reporter assay, cells were transfected with one mix containing dsRNAs, reporter plasmids and pMT-STING for overexpression. The measurement of luciferase activity only takes into account transfected cells among the total cell population, which means cells which received every component of the assay. Opposingly, RT-qPCR experiments were performed in a cell line stably expressing a pMT-STING. In this case, the expression level of genes of interest is assessed in an heterogenous cell population, probably expressing STING at different levels. In addition, these cells were soaked with dsRNAs instead of transfected, which is less efficient and adds a level of variability concerning the quantity of dsRNAs internalized in each individual cell [189].

Results obtained *in vivo* in $Charon^{L297fs}$ mutant flies showed a decreased induction of SRGs upon 2'3'-cGAMP injection. However, characterization of $Charon^{L297fs}$ mutant line still needs complementary experiments. First, we would like to measure *charon* mRNA levels in these mutants to check if there is non-sense mediated decay. In order to confirm that $Charon^{L297fs}$ mutant is indeed a null mutant, we should also verify the absence of Charon protein. This experiment will necessitate the production of anti-Charon antibodies. In addition, $Charon^{L297fs}$ mutant flies need to be isogenized in *w1118* background in order to confirm the results obtained in a controlled genetic background. We would also like to test the sensitivity of these flies to viruses by following their survival and viral RNA load upon infection. Finally, we should construct a rescue line, in which Charon will be reintroduced into $Charon^{L297fs}$ mutant and verify we recovered a WT phenotype. Alternatively, to accurately assess the role of Charon in the STING pathway, we could design a fly line in which the *charon* gene would be completely removed using CRISPR/Cas9 technology.

Intriguingly, results seem to demonstrate a role of positive regulator for the IκB protein Charon, which is unusual for proteins belonging to this family. However, in mammals, the non-classical IκB proteins Bcl-3 and IκBζ are able to positively regulates transcriptional response. By homology, we can imagine that Charon is a co-activator

of Relish guiding this transcription factor towards the selective activation of certain antiviral effectors. This could explain that Relish activates different genes when activated by the STING or by the Imd pathway. Interestingly, phylogenetic analysis of the IκB proteins showed that Charon is in a different clade from Bcl-3 and IκBζ [157]. This indicates that these proteins do not have a common ancestral origin and that some IκB proteins could have evolved to be co-activators independently in vertebrates and invertebrates. Concerning the mechanism involved, Charon could also modify the DNA binding capabilities of Relish, contribute an activator domain, or allow interaction with other transcription factors to direct the response to certain genes.

The second protein studied was the NF-κB transcription factor dl and, more precisely its splicing isoform dl-B. Because of the specific interaction observed between dl-B and IKKß we wondered if this kinase was phosphorylating dl-B. To answer this question, I immunoprecipitated dl-B from S2 cells transiently transfected with a pMT-dl-B-V5 construct. Resulting samples have been given to the proteomic platform at IBMC, Strasbourg, in order to perform a mass spectrometry analysis focusing on post-translational modifications (PTM). This analysis revealed three phosphorylated serines in the dl-B specific region. More precisely, S541 was found phosphorylated in one peptide over eighty, S551 on two over thirty-nine and S827 on all the nine peptides detected (**Figure 23A**). These results are preliminary, as this analysis was performed only one time. In order to confirm these results and check if IKKß is responsible for phosphorylation of dl-B we would like to reproduce this analysis in WT and *ikkß* KO S2 cells.

This study also revealed that dl-B could interact with Relish. This is of particular interest regarding the fact that Relish controls the transcription of different sets of genes depending on whether it is activated by Gram-negative bacteria (Imd pathway) or by viral infection (STING pathway)(Cai et al., 2020). Formation of different NF-κB dimers depending on the activating signal could explain these differences. In order to control this hypothesis, we could compare the transcriptional response induced by STING pathway activation in *dl-B* KO *versus* WT cells. If the transcriptional response generated upon STING pathway activation in these two cell lines is highly divergent, this would confirm that dl-B plays an important role in target genes selection.

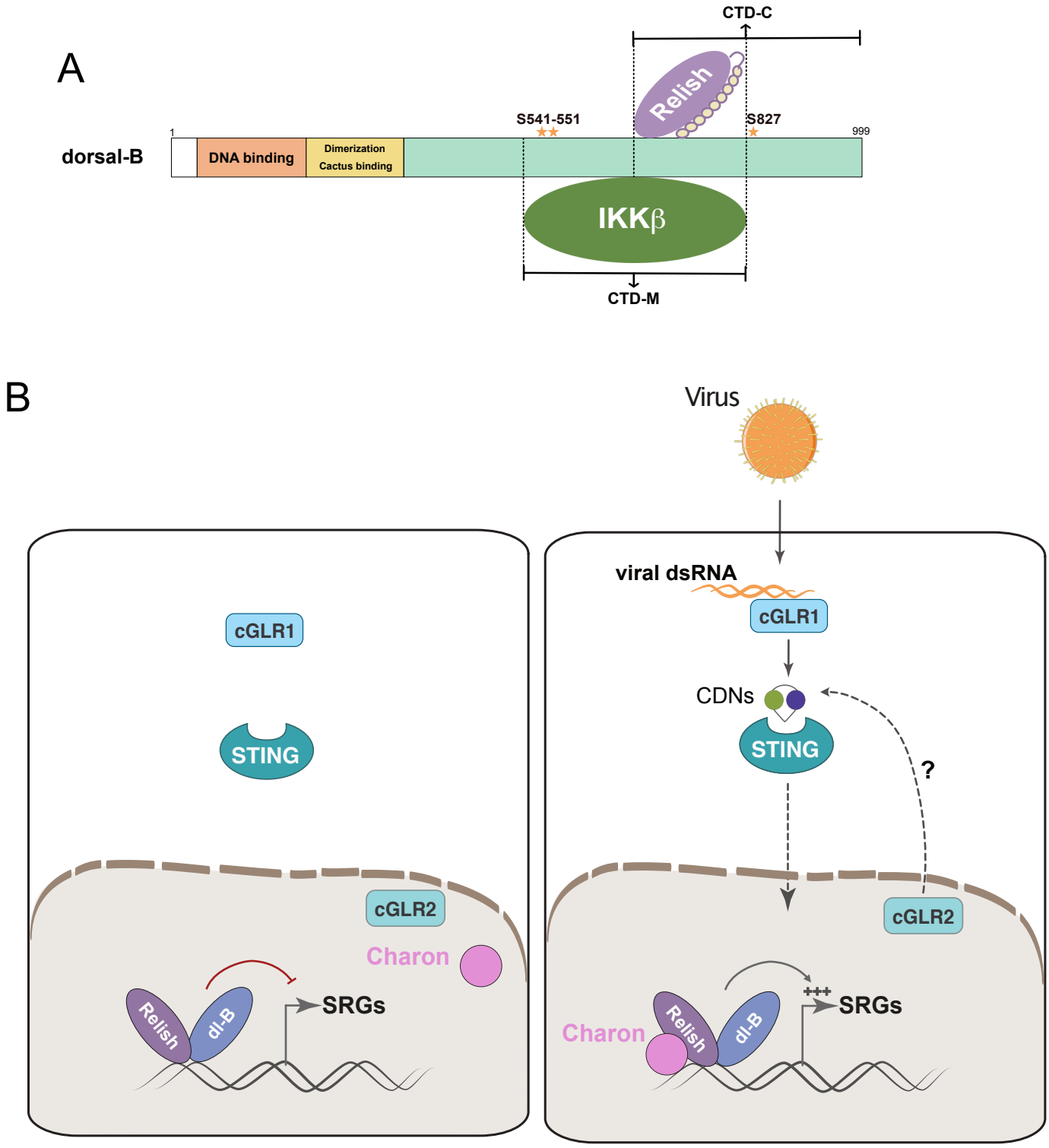

Figure 23: Charon and dl-B may be involved in the STING pathway. A) Schematic representation of the interactions dorsal-B/IKKß and dorsal-B/Relish and phosphorylated serines identified by mass-spectrometry analysis (represented by yellow stars, position indicated above). **B)** Modelization of the hypothetical role of dl-B and Charon in the STING pathway. In resting condition (left) Relish/dl-B dimers occupy the promoters of their target genes but are not able to induce their expression, leading to their repression. When a virus infect the cell (right), the STING pathway is activated and Charon binds to NF-kB dimers, leading to the activation of SRGs expression.

Preliminary results suggest that the third quarter of the dl-B specific region (common between CTD-M and CTD-C) is involved in the interaction with Relish (**Figure 23A**). However, the amount of Relish co-immunoprecipitated with CTD-M and -C truncated proteins is weaker compared to the one retrieved with the full-length dl-B. This suggests that the RHD of dl-B is necessary for a good interaction with Relish, although it is not sufficient. We can then suppose that the dimerization domain contained in the RHD and the interaction domain probably localized in the third quarter of the dl-B specific region need each other to efficiently heterodimerize with Relish. The interaction between IKKß and dl-B, on the other hand, relies on the CTD-M region of dl-B (**Figure 23A**).

Studying the role of dl-B in the STING pathway *in vivo* showed that it acts as a negative regulator of the pathway. This is similar to p50 and p52 homo- or heterodimers in mammals, which repress κB-dependent transcription. Of note, Relish does not present a TAD. An attractive hypothesis would be that dl-B/Relish heterodimers negatively regulates the STING pathway in resting conditions, like p50 and p52 in mammals. On the contrary, when the STING pathway is activated, the atypical IκB protein Charon would bind to these dimers, giving it a positive regulatory role, as suggested for Bcl-3 and IκBζ (**Figure 23B**). Confirming this hypothesis would require several experiments. First, it would be necessary to check if dl-B, Relish and Charon interacts. It would also be interesting to check if dl-B and Relish are able to bind DNA by their own or if they need a cofactor, which could be Charon itself. Importantly, the comparison of dl-B and Relish dependent transcriptional response in WT *versus* *charon* KO cells or flies would be an important tool to understand if they are working together or not. We could also check if the localization of dl-B and Relish changes in *charon* KO cells upon STING pathway activation. If this is the case, it could suggest that Charon is important for NF-κB dimers localization.

Concluding remarks

The global purpose of this PhD work was to progress in the understanding of the antiviral STING pathway in the model organism *Drosophila melanogaster*. More precisely, this project aimed at deciphering the mechanisms of Relish activation downstream of the STING pathway. One hypothesis was that these mechanisms were different from those involved in the Imd pathway, explaining the differences in transcriptional responses regulated by these two pathways.

The results presented in chapter 1 confirmed that there is indeed an independent PRR-dependent pathway regulating Relish activity in the context of viral infection. I participated in the work that showed that the CDN produced by mammals, 2'3'-cGAMP, is the best agonist to activate STING-dependent immunity in flies, compared to bacterial 3'3'-linked CDNs. Of note, the CDN injection assay we established provided an artificial yet powerful way to activate the STING pathway *in vivo.* These gain-of-function experiments revealed a stronger phenotype than expected, as injection of 2'3'-cGAMP in drosophila resulted in an important protection against a set of different viruses (Cai et al., 2020). Altogether, these results confirmed that the STING pathway plays an important role in antiviral immunity in flies. They also provided a simple and robust assay to monitor activation of the pathway *in vivo*, which was useful to document the involvement of other factors in the STING pathway.

The activation of the STING pathway by 2'3'-cGAMP, produced by cGAS in mammals, suggested the existence of a cGAS-like receptor in drosophila. In collaboration with the teams of Philippe Kranzusch (Boston, USA), Rune Hartmann (Aarhus, Denmark) and Hua Cai (Guangzhou, China), the laboratory identified two distinct cGLRs in flies. I participated in the initial characterization of these two receptors. Interestingly, my results suggest that they have different biology. The different subcellular localization of the two receptors is of particular interest and exploiting drosophila genetics to characterize the function of cGLR2 could shed light on the role of cGAS in the nucleus of mammalian cells, which is poorly understood. Additionally, both cGLRs may be differentially regulated as cGLR2 seem to be

regulated by post-translational modifications. Overall, these results confirm the initial hypothesis that a pathway independent of the Imd pathway and triggered by the activation of distinct PRRs operates in drosophila to control viral infections.

The work presented in the second chapter of this manuscript led to the conclusion that the adaptor Fadd and the caspase-8 homolog Dredd are involved in the antiviral STING pathway, besides their described role in the antibacterial Imd pathway. Our results reveal that upon STING pathway activation Dredd is responsible for Relish cleavage at the aspartic acid in position 545, in the same way as for the Imd pathway. Overall, these results suggest that Relish processing relies on similar mechanisms downstream of the two pathways in which it is involved.

However, the efficient activation of Relish-dependent genes upon Imd pathway triggering relies on a second distinct mechanism: the phosphorylation of two serine residues of Relish, S528 and S529, by the IKKß/IKKγ signalosome. Curiously, silencing IKKγ in S2 cells did not impair induction of STING-regulated genes and these results were confirmed *in vivo* using null mutant flies (Goto et al., 2018). The regulatory subunit of the IKK complex, IKKγ/NEMO was described to be important to ensure specificity of IKKß-dependent phosphorylation in mammals [128]. In drosophila, phosphorylation by IKKß has been shown to be important for the recruitment of RNA polymerase II to the promoters of Relish target genes and their subsequent activation [10,58]. By homology with the mammalian system, we can imagine that Relish is differentially phosphorylated depending on the signaling pathway activated and therefore the involvement or not of IKKγ. This could participate in the selectivity of regulated genes. Altogether, the work conducted on this topic during my PhD allowed the identification of two new components of the STING pathway in drosophila, Fadd and Dredd. These results raise perspectives on the role of these proteins in innate antiviral immunity in mammals, beyond their previously proposed role downstream of RIG-I-like receptors.

One possibility explaining the differences in transcriptional response resulting from the activation of these two pathways could be the interaction of Relish with pathway-specific cofactors. During my PhD, I worked on two interesting candidate

partners of Relish in the STING pathway: the IκB protein Charon and the NF-κB transcription factor dl-B. Preliminary results suggest that they act as positive and negative regulators of the STING pathway, respectively. The possible impact of these proteins on the transcriptional response induced by STING pathway activation should be a priority for future studies. The comparison of the transcriptome of WT *versus charon/dorsal-B* mutant flies upon activation of the STING pathway could provide useful information on the contribution of these factors to the selectivity of Relish for gene induction.

On a larger scale, understanding NF-κB activation in the STING pathway in drosophila may provide clues to the mechanisms involved in mammals. Indeed, the way the STING pathway controls the NF-κB transcription factor in mammals is still poorly documented. Recent evidence of the involvement of IRF3-independent functions of the STING pathway in autoimmune diseases such as SAVI, in tumorigenesis but also in the antiviral response demonstrates that this long-neglected branch of the response deserves further research (Luksch et al., 2019; Warner et al., 2017; Wu et al., 2020).

Overall, the work presented in this manuscript allowed us to make a step forward in the understanding of STING pathway functioning in *Drosophila melanogaster.* In particular, the identification of Fadd and Dredd as important components of the pathway. As often in biology, the results I obtained raise many new and fascinating questions.

MATERIALS & METHODS

1. Cell culture

a. Maintenance of S2 cell lines

S2 [191] cells are derived from a primary culture of late-stage drosophila embryos. S2 cells and *dredd* CRISPR/Cas9 KO cells were grown in complete Schneider medium (Biowest) complemented with 10% fetal bovine serum, 2 mM glutamax, 100 U/ml penicillin and 100 µg/ml streptomycin (Life technologies).

b. DNA plasmids transfections

Plasmid transfection was performed using the Effectene kit (Qiagen) following manufacturer's instructions on wells containing 5.10^5 cells (200 ng of DNA transfected) in 24 well plates or 3.10^6 cells (1 µg if DNA transfected, except when otherwise indicated) in 6 well plates. Cells were then harvested for further experiments at indicated time points.

c. Knock-down by dsRNA

Soaking

5.10^5 S2 cells were resuspended in serum free Schneider medium and plated in 24 well plates. 12 µg of dsRNAs were added to each well and incubated for 2 hours at 25°C. Complete Schneider medium was added into wells and cells were incubated for 3 days at 25°C and harvested for further experiments.

Transfection

1 µg of dsRNAs were transfected per well of a 6 well plate containing 3.10^6 S2 cells, using the Effectene kit (Qiagen) following manufacturer's instructions. Cells were incubated for 3 days at 25°C and harvested for further experiments.

d. Heat-Killed Escherichia coli

Escherichia coli (ATCC 23724) cultures were grown in luria broth (LB) medium at 37°C for 15 hours and centrifuged 15 minutes at 2000 relative centrifugal force (rcf). Bacterial pellet was resuspended in phosphate buffered saline (PBS), heated at 60°C for 1 hour, washed three times with PBS and resuspended in 5mL of PBS. The DO_{600nm} was measured and the bacterial concentration calculated. HKE were used at a multiplicity of infection (MOI) of 40 and cells were incubated at 25°C for 2 hours before harvesting for further experiments.

e. Proteasome inhibition by Bortezomib®

Bortezomib® (BTZ, Biosciences) powder was solubilized in dimethylsulfoxyde (DMSO) following manufacturer's instructions. BTZ (or DMSO as a negative control) were diluted in Schneider media at 0,2 µM. Cells to treat were pelleted (centrifugation 10 minutes at 500 rcf) and resuspended in BTZ or DMSO solutions, plated in 24 well plates and incubated at 25°C for 4 hours. Cells were washed with PBS and harvested for further experiments.

1. Fly breeding

a. Stocks used in the study

Fly cultures were grown on standard cornmeal agar medium at 25°C. Strains used were Rel^{E20} (Hedengren et al., 1999), Rel^{D545A} (kind gift of Pr. Neal Silverman), $Fadd^{f02804}$ (from Exelixis collection, Harvard Medical School), $Dredd^{D55}$ (kind gift of Pr. Bruno Lemaitre), $Charon^{L297fs}$ and $dl\text{-}B^{V369fs}$ (gene editing platform at SFHI, Guangzhou, China), w^{1118}, yw. $Fadd^{f02804}$ and Rel^{E20} flies were isogenized into the w^{1118} background at the laboratory. Rel^{D545A} were isogenized in w^{1118} background at Pr. Neal Silverman's lab, we used w^{1118} from the same origin as controls. All the flies used were Wolbachia free.

b. 2'3'-cGAMP injections with or without DCV

2’3’-cGAMP (InvivoGen) was dissolved in 10 mM Tris, pH 7.5 to a concentration of 0,9 mg/ml. 2- to 6-day-old adult flies were injected by intrathoracic injection using a Nanoject II apparatus (Drummond Scientific).

For injections, each fly was injected with 69 nl of 2’3’-cGAMP solution or 10 mM of Tris, pH 7.5 (negative control).

For co-injections with DCV, 30 µl of 2’3’-cGAMP (0,9 mg/ml) or 10 mM Tris, pH 7.5 were mixed with 2 µl of DCV (50 pore-foming unit (pfu)/4,6 nl). Each fly was injected with 69 nl of previously mentioned mixtures (DCV 50 pfu) or 10mM Tris, pH 7.5 (negative control).

For real-time quantitative polymerase chain reaction (RT-qPCR) experiment, injected flies were collected in pools of six individuals (three females + three males) at indicated time points and homogenized for RNA extraction and RT-qPCR.

For survival experiment, thirty individuals (15 females + 15 males) for each condition were injected and conserved at 25°C. Of note, flies which do not wake up from the injection were removed from the analysis. Survival was monitored daily for 20 days.

c. Bacterial infections

Enterobacter cloacae (H. Monteil lab, University Louis Pasteur, Strasbourg) cultures were grown in LB medium at 37°C for 15 hours. Infections were performed on 2- to 6-day-old adult flies by intrathoracic pricking with a needle soaked into *E. cloacae* solution in PBS. Infected and non-treated (NT) flies were kept at 25°C and collected in pools of six individuals (three females + three males) after 6 hours for subsequent RNA extraction and RT-qPCR.

2. Molecular biology techniques

a. Cloning

Cloning of dl-B and truncated versions

Construction of pMT-dl-B-V5 clone was performed using a pGEX-4T-1-dl-B vector, obtained from Pr. Steve Wasserman, as a template. Primers used allowed the

amplification of the sequence of dl-B and the addition of restriction sites for further cloning. A KpnI restriction site was added at the 5' extremity and a NotI restriction site at the 3' extremity. The PCR product obtained was purified by gel extraction using QIAquick Gel Extraction kit (QIAGEN) following manufacturer's instructions. PCR product and pMT-V5-HisA backbone were digested with KpnI and NotIl Anza restriction enzymes (ThermoFisher) following manufacturer's instructions. Ligation was performed with a ratio 1:5 vector:insert using 5 U of T4 DNA polymerase (Thermofisher) overnight at 18°C. Product obtained was used to transform DH5α bacteria by heat shock and grown in LB + 0,1 mg/ml ampicillin media. Plasmidic DNA was extracted from isolated clone using the Plasmid Midi Kit (QIAGEN) and correct insertion of the construct was checked by Sanger sequencing (Eurofins Genomics).

Directed mutagenesis of dl-B was performed by PCR using previously constructed plasmid (pMT-dl-B-V5) to obtain different truncated versions of the protein (RHD, CTD, CTD-N and CTD-C). CTD-M directed mutagenesis was performed by PCR using pMT-RHD-V5 as a template and 4 different primers to remove the C-ter and N-ter regions surrounding the sequence of interest. PCRs products were digested with DpnI (ThermoFisher) to specifically degrade the template pMT-RHD-V5. Transformation and following steps were previously described.

Table 1: List of primers used for cloning of dl-B and truncated versions in 5'-3' orientation:

Clone	Sense	Sequence
pMT-dl-B	Fw	GGTACCATGTTTCCGAACCAGAACAATGG
	Rev	GCGGCCGCggGATGCCATTTGCCGCAGCC
RHD	Fw	CTTCGAGTACGTGCCAATGGACTCAccGCGGCCGCTCGAGTCTAGAGGGC
	Rev	GCCCTCTAGACTCGAGCGGCCGCggTGAGTCCATTGGCACGTACTCGAAG
CTD	Fw	GGGGGATCTAGATCGGGGTACcATGGGTAAACATACATTCTGGAATCTTC
	Rev	GAAGATTCCAGAATGTATGTTTACCCATgGTACCCCGATCTAGATCCCCC
CTD-N	Fw	GATATAATGCCTCCAACTCCGCCCATGccGCGGCCGCTCGAGTCTAGAGGGC
	Rev	GCCCTCTAGACTCGAGCGGCCGCggCATGGGCGGAGTTGGAGGCATTATATC

CTD-M	Fw	GGGGGATCTAGATCGGGGTACCATGGAGGACATGGAGGCGGCGGATGCCC
	Rev	GGGCATCCGCCGCCTCCATGTCCTCCATGGTACCCCGATCTAGATCCCCC
	Fw	CCCGTTCATCTCGAATCCAGCGCCTccGCGGCCGCTCGAGTCTAGAGGGC
	Rev	GCCCTCTAGACTCGAGCGGCCGCggAGGCGCTGGATTCGAGATGAACGGG
CTD-C	Fw	GGGGGATCTAGATCGGGGTACcATGTCGCAATGCGCTCCCGAAGATGCCC
	Rev	GGGCATCTTCGGGAGCGCATTGCGACATgGTACCCCGATCTAGATCCCCC

Red: KpnI restriction site

Green: NotI restriction site

lowercase: nucleotides added to keep the reading frame

Cloning of cGLR2 codon optimized isoforms

cGLR2-PF sequence was codon optimized by two runs in the GenSmart tool (GenScript) excluding NotI and XbaI restriction sites (used for cloning) and resulting sequence was synthesized and cloned in pUC57 backbone by Proteogenix.

Cloning of cGLR2-PF, -PC and -PD pAc-5.1/V5-His B (Invitrogen) and pAc-5.1B-HA (pAc-5.1/V5-His B in which HA-tag was introduced by mutagenesis) backbones were performed as detailed therebefore using pUC57-cGLR2-PF as a template and using NotI (5' end) and XbaI (3' end) restriction sites.

cGLR2-PB and -PE tagged with HA or V5 were produced by directed mutagenesis PCR using either pAc-HA-cGLR2-PF of pAc-cGLR2-PF-V5 as templates, respectively. Method was detailed therebefore.

Table 2: List of primers used for cloning of cGLR2 codon optimized versions, in 5'-3' orientation

Clone	Backbone	Sense	Sequence
cGLR2-PF	pAc-51B-HA	Fw	GAAAAAAGCGGCCGCTGATGAAGGAGTCTCGAAACCTCG
		Rev	GCTCTAGATCACTCCACAATGCCTTCGGAC
	pAc-51B-V5	Fw	GAAAAAAGCGGCCGCCCAACATGAAGGAGTCTCGAAACCTCG
		Rev	GCTCTAGAATCTCCACAATGCCTTCGGAC

cGLR2-PC	pAc-51B-HA	Fw	GAAAAAAGCGGCCGCTGATGTTCGACGATTTGGCTGAAAAC
		Rev	GCTCTAGATCACTCCACAATGCCTTCGGAC
	pAc-51B-V5	Fw	GAAAAAAGCGGCCGCCCAACATGTTCGACGATTTGGCTGAAAAC
		Rev	GCTCTAGAATCTCCACAATGCCTTCGGAC
cGLR2-RD	pAc-51B-HA	Fw	GAAAAAAGCGGCCGCTGATGCTGAAAATCGCAAAGCCG
		Rev	GCTCTAGATCACTCCACAATGCCTTCGGAC
	pAc-51B-V5	Fw	GAAAAAAGCGGCCGCCCAACATGCTGAAAATCGCAAAGCCG
		Rev	GCTCTAGAATCTCCACAATGCCTTCGGAC
cGLR2-PB	pAc-51B-HA	Fw	GCACAGTGGCGGCCGCTGATGAACGCGAAACGTAGCATGCTGACCTTT CAGCGTACCCGCGATAACGATATGGAGCCCGAATCCTATTGGCTGAATC
		Rev	GATTCAGCCAATAGGATTCGGGCTCCATATCGTTATCGCGGGTACGCTGA AAGGTCAGCATGCTACGTTTCGCGTTCATCAGCGGCCGCCACTGTGC
	pAc-51B-V5	Fw	CAGTGGCGGCCGCCCAACATGAACGCGAAACGTAGCATGCTGACCTTT CAGCGTACCCGCGATAACGATATGGAGCCCGAATCCTATTGGCTGAATC
		Rev	GATTCAGCCAATAGGATTCGGGCTCCATATCGTTATCGCGGGTACGCTGA AAGGTCAGCATGCTACGTTTCGCGTTCATGTTGGGCGGCCGCCACTG
cGLR2-PE	pAc-51B-HA	Fw	GCACAGTGGCGGCCGCTGATGAACGCGAAACGTAGCAT GCTGACCTTTCAGCGTACCCGCGATAACGATATGAGCTG
		Rev	GATTCAGCCAATAGGATTCGGGCTCTTTCCACACGCTGCTC AGCAGCAGGCTGGTCCAGCTCATATCGTTATCGCGGGTAC
	pAc-51B-V5	Fw	CAGTGGCGGCCGCCCAACATGAACGCGAAACGTAGCAT GCTGACCTTTCAGCGTACCCGCGATAACGATATGAGCTG
		Rev	GATTCAGCCAATAGGATTCGGGCTCTTTCCACACGCTGCT CAGCAGCAGGCTGGTCCAGCTCATATCGTTATCGCGGGTAC

Red: NotI restriction site

Green: XbaI restriction site

b. Western blot

Cells were homogenized in RIPA lysis buffer (Tris-HCl 20mM pH7,4; NaCl 150mM; EDTA 1mM; SDS 0,1%; Na-deoxycholate 0,1%; Triton 1%) mixed with one dose of protease inhibitor (cOmplete Protease Inhibitor Cocktail, Roche). After 1 hour incubation on ice, cell lysate was centrifuged for 20 minutes at 15000 g at 4°C and the supernatant (SN) was transferred in new tubes.

Proteins were quantified using the Pierce BCA Protein Assay Kit (ThermoFisher) following manufacturer's instructions. Samples were diluted three times in 4x Laemmli

Sample Buffer (BioRad) + 10% ß-Mercaptoethanol and then incubated 3 minutes at 95°C and loaded on 4-15% SDS-PAGE (Biorad) gels.

Semi-dry transfer to nitrocellulose membrane was performed with Biorad TransBlot Turbo machine. Membranes were blocked with 5% non-fat dry milk in Tris-buffered saline (TBS)-Tween 0,05% one hour at room-temperature (RT) and incubated overnight at 4°C with primary antibody in non-fat dry milk 3% TBS-Tween 0,05%. After washing, the secondary anti-Rabbit or anti-Mouse antibodies fused to horseradish peroxidase were added to the membrane in non-fat dry milk 3% TBS-Tween 0,05% for two hours at RT. Membranes were washed and revealed with the Clarity Western ECL substrate (Biorad).

Table 3: Antibodies used for Western blot analysis and dilutions:

Target	**Reference**	**Origin**	**Dilution**
Relish-Cter	DSHB (anti-Relish-C 21F3)	Mouse	1/20 (in 3% BSA)
V5 tag	Life technologies (R96025)	Mouse	1/5000
V5-HRP	ThermoFisher (R96125)	Mouse	1/10000
HA tag	Abcam (ab9110)	Rabbit	1/1000
HA-HRP	Merck (12013819001)	Rat	1/5000
Flag tag	Abcam (ab1162)	Rabbit	1/1000
Actin	Euromedex (GTX80809)	Mouse	1/2000
Ubiquitin-K48	Invitrogen (ARC0811)	Rabbit	1/2000
Mouse-HRP	Amersham (NA931)	Sheep	1/10000
Rabbit-HRP	Amersham (NA934)	Horse	1/10000

c. Co-immunoprecipitations

Co-immunoprecipitation between STING, IKKß and Fadd

2.10^6 S2 cells were seeded per well of 6 well plates and co-transfected with 500 ng of pAc-Fadd-V5 or pAc-RLuc-V5 and 250 ng of pAc-HA-IKKß or 500 ng of pAc-HA-

STING. 2 wells of cells were transfected for each condition (see *DNA plasmids transfection*). When necessary, transfection mix was completed to 1 µg of total DNA using empty vector (pAc-5.1-V5).

Alternatively, transfection mix was composed of either 500 ng of pAc-RLuc-V5, 250 ng of pAc-STING-V5 or 250 ng of pAc-IKKß-V5 along with 1.5 µg of pAc-HA-Fadd. 4 wells of cells were transfected for each condition (see *DNA plasmids transfection*). When necessary, transfection mix was completed to 2 µg of total DNA using empty vector (pAc-5.1-V5).

Cells were harvested 2 days post-transfection, gathering wells transfected with the same mix. After PBS wash, pellets were resuspended in 500 µL of Pierce IP lysis buffer (25 mM Tris-HCl pH 7,4; 150 mM NaCl, 1 mM EDTA, 1% NP40, 5% glycerol and 1X protease inhibitors cocktail). After 30 minutes of incubation on ice, lysate was centrifuged 15 minutes at 20 000 rcf at 4°C. SN was transferred to new tubes, 50 µl of SN of each condition were saved for Input and completed with 50 µl of 2X Protein Sample Buffer (100 mM Tris-HCl pH 6,8; 4% SDS; 20% Glycerol; 0,2 mM DTT; Bromophenol blue 0,05%; Water up to 100mL). 400 µl of Pierce IP lysis buffer was added in tubes with remaining SN (IP tubes).

IP was performed adding 50 µl of of Anti-V5 agarose beads (Merck) previously washed 3 times with Pierce IP lysis buffer (centrifugation at 12000 rcf 1 minute at 4°C) and resuspended in 100 µl of Pierce IP lysis buffer per condition. 100 µl of this solution is added in each IP tube and incubated overnight on an orbital shaker at 4°C. Beads were washed twice using 500 µl of Pierce IP lysis buffer (centrifugation at 2300 rcf 1 minute at 4°C) and last wash was performed with washing buffer (25mM Tris-HCl pH 7,4; 150mM NaCl, 1mM EDTA). 100 µl of 2X Protein Sample Buffer were added to the beads. Samples were boiled at 95°C for 3 minutes, for following steps, refer to *Western blot* protocol. Samples were loaded onto 2 gels probe separately with anti-V5 and -HA antibodies, for precisions on loading volumes see in the legends of corresponding figures.

Co-immunoprecipitation between dl-B, Relish and IKKß

2.10^6 S2 cells were seeded per well of 6 well plates and co-transfected with 500ng of pMT-HA-IKKß or 50 ng of pAHW-GST and 500 ng of pMT-dl-B-V5 or pMT-dl-V5. 2 wells of cells were transfected for each condition (see *DNA plasmids transfection*). When necessary, transfection mix was completed to 1 µg of total DNA using empty

vector (pAc-5.1-V5). After 24 hours $CuSO_4$ (0,5 mM) was added to the cell medium. Cells were harvested 24 hours after $CuSO_4$ addition and IP was realized with anti-HA agarose beads (Merck) following the previously described protocol.

Alternatively, transfection mix was composed of either 500 ng of pMT-dl-B-V5, pMT-dl-V5 or pMT-FLuc-V5 and 500 ng of pMT-Relish-Myc. After 24 hours, $CuSO_4$ (0,5 mM) was added to cell medium. Cells were harvested 24 hours after $CuSO_4$ addition and IP was realized with anti-V5 agarose beads (Merck) following the protocol previously described.

Co-immunoprecipitation between dl-B truncated proteins, Relish and IKKß

2.10^6 S2 cells were seeded per well of 6 well plates and co-transfected with 500 ng of pMT-HA-IKKß and either 10 ng of: pMT-FLuc-V5 or pMT-RHD-V5; 500 ng of: pMT-CTD-V5, pMT-CTD-N-V5, pMT-CTD-C, pMT-CTD-M-V5, pMT-dl-B-V5 or pMT-FLuc-V5. When necessary, transfection mix was completed to 1 µg of total DNA using empty vector (pAc-5.1-V5). After 24 hours $CuSO_4$ (0,5 mM) was added to cell medium. Cells were harvested 24 hours after $CuSO_4$ addition and IP was realized with anti-V5 agarose beads (Merck) following the previously described protocol.

Alternatively, transfection mix was composed of 400ng of pMT-Relish-Myc and either 10 ng of pMT-RHD-V5, 600 ng of pMT-CTD-V5, 500 ng of pMT-CTD-N-V5, 250 ng of pMT-CTD-C-V5, 500 ng of pMT-CTD-M-V5, 200 ng of pMT-dl-B-V5 or 10 ng of pMT-FLuc-V5. When necessary, transfection mix was completed to 1 µg of total DNA using empty vector (pAc-5.1-V5). After 24 hours $CuSO_4$ (0,5 mM) was added to cell medium. Cells were harvested 24 hours after $CuSO_4$ addition and IP was realized with anti-V5 agarose beads (Merck) following the protocol previously described.

d. Immunostaining

Millicell® EZ 8 well Glass slides (Millipore) were treated with Concanavalin A (100µg/ml) for 1 hour and then washed. 2.10^5 transiently transfected S2 cells, expressing the protein of interest tagged with V5, were distributed in each well and incubated for 10 minutes to allow cells to attach. Cells were fixed with a solution of paraformalhehyde 4% in PBS. Cells were blocked with blocking solution (PBS + 0,1% Triton + bovine serum albumin (BSA) 1%) one hour at RT and incubated overnight at

4°C in a humid container with primary antibody diluted in blocking solution. After washing, the secondary anti-Rabbit or anti-Mouse antibodies, fused to fluorescent molecules, diluted in PBS+ BSA 1% + Triton 0,1% were added onto the cells for two hours at RT. After washing, plastic slide chambers were removed and one drop of SlowFade Diamond antifade mountant (Invitrogen) was added to each well. Slides were covered with a coverslip and sealed with nailpolish for further observations.

Table 4: Antibodies used for immunostaining experiments and dilutions:

Target	Reference	Origin	Dilution
Lamin	DSHB (ADL67.10)	Mouse	1/100
V5 tag	Abcam (ab9116)	Rabbit	1/1000
Mouse-Alexa594	Invitrogen (A21203)	Donkey	1/500
Rabbit-Alexa488	Invitrogen (A11008)	Goat	1/500

e. Dual luciferase assay

100 ng of STING-Firefly luciferase (to monitor STING pathway activity) and 10 ng of Actin5C-Renilla luciferase (transfection control) plasmids were transfected into S2 cells in 24 well plate (see DNA plasmid transfection) along with dsRNAs against candidates (see Knock-down by dsRNAs, Transfection). 3 days after transfection, Firefly and Renilla luciferase activities were measured in the cell lysate using Dual Luciferase assay kit (Promega) following manufacturer's instructions.

f. RNA extraction and cDNA synthesis

6 flies were crushed in 400µl of TRIzol (Ambion) using Precellys evolution (Bertin). 80µl of Chloroform-Isoamyl alcohol (Merck) are added and the mix was vortexed thoroughly. After centrifugation, the top aqueous phase was recovered and precipitated with isopropanol. The pellet was washed with 70% ethanol, dried and resuspended in RNAse and DNAse free water (Fisher scientific). RNAs were quantified

and diluted at 125 ng/µl in RNAse and DNAse free water. 500ng of RNAs were used to perform reverse transcription using iScript gDNAclear cDNA synthesis kit (BioRad) following manufacturer's instructions.

g. Real-time quantitative PCR

RT-qPCR was performed using the SYBR Green master mix (BioRad) and 0,5 mM of forward and reverse primers. The RT-qPCR cycle was the following: an initial denaturation of 15 seconds at 98°C, followed by 35 cycles of 2 seconds at 95°C and 30 seconds at 60°C. The threshold cycle (Ct) of each sample is calculated by linear regression. Analysis is made by the ΔCt method using RpL32 as a reference gene: $2^{Ct(RpL32)-Ct(target)}$.

Table 5: List of primers used for qPCR experiments in 5'-3' orientation

Target gene	Orientation	Sequence
DCV	Fw	TCATCGGTATGCACATTGCT
	Rev	CGCATAACCATGCTCTTCTG
SRG1	Fw	GTGTCCATTATCCGCACAAG
	Rev	ACTGGGGTATCTGACGGATG
SRG3	Fw	GCGACCGTCATTGGATTGG
	Rev	TGATGGTCCCGTTGATAGCC
Att-A	Fw	CTGGTCATGGTGCCTCTTT
	Rev	AGACCTTGGCATCCAGATTG
Dpt-A	Fw	GCGCAATCGCTTCTACTTTG
	Rev	CCTGAAGATTGAGTGGGTACTG
RpL32	Fw	GCCGCTTCAAGGGACAGTATCT
	Rev	AAACGCGGTTCTGCATGAG

3. Informatics

a. Analysis of the IKKß interactome

Results obtained after analysis by nano LC MS/MS (FT ICR mass spectrometer) for the three non-infected IKKß expressing cell lines and the two non-infected and two CrPV-infected control cell lines were subjected to a cluster analysis. The three IKKß-expressing cell lines clustered together and separately from the four control cell lines which also clustered together whether they were infected or not.

Results were normalized, Log2 Fold Change (FC) calculated and analyzed using a Welch's test. Results were represented using a Volcano plot and IKKß interactants were selected with a Log2 FC (x axis) >2 and Welch's test (y axis) $p < 0,05$.

b. Confocal microscopy and image analysis

Images were acquired with a Zeiss LSM 700 confocal microscope equipped with a plan-apochromat x63 1.40 NA oil immersion objective. Argon laser 488 nm with collection bandwidth 493-556 nm and DPSS 561 nm laser with collection bandwidth 482-643 nm were used for collecting green and red channels, respectively. Images were analyzed using ImageJ software.

c. Statistics

Statistics were performed using GraphPad Prism9 software. Corrected P-values lower than 0,05 were considered statistically significant (see figure legends for details).

Survival curves were plotted and analyzed two-by-two by log-rank analysis (Mantel-Cox method). P-values were corrected for multiple comparisons using Bonferroni method.

Statistics used for other experiments were non-parametric multiple Mann-Whitney tests. P-values were corrected for multiple comparisons using Holm-Sidak method

BIBLIOGRAPHY

Abe, T., and Barber, G.N. (2014). Cytosolic-DNA-mediated, STING-dependent proinflammatory gene induction necessitates canonical NF-κB activation through TBK1. J. Virol. *88*, 5328–5341. https://doi.org/10.1128/JVI.00037-14.

Abernathy, E., Mateo, R., Majzoub, K., van Buuren, N., Bird, S.W., Carette, J.E., and Kirkegaard, K. (2019). Differential and convergent utilization of autophagy components by positive-strand RNA viruses. PLoS Biol *17*, e2006926. https://doi.org/10.1371/journal.pbio.2006926.

Ablasser, A., and Chen, Z.J. (2019). cGAS in action: Expanding roles in immunity and inflammation. Science *363*. https://doi.org/10.1126/science.aat8657.

Ablasser, A., Goldeck, M., Cavlar, T., Deimling, T., Witte, G., Röhl, I., Hopfner, K.-P., Ludwig, J., and Hornung, V. (2013). cGAS produces a 2'-5'-linked cyclic dinucleotide second messenger that activates STING. Nature *498*, 380–384. https://doi.org/10.1038/nature12306.

Ahn, J., and Barber, G.N. (2019). STING signaling and host defense against microbial infection. Exp Mol Med *51*, 1–10. https://doi.org/10.1038/s12276-019-0333-0.

Almaden, J.V., Tsui, R., Liu, Y.C., Birnbaum, H., Shokhirev, M.N., Ngo, K.A., Davis-Turak, J.C., Otero, D., Basak, S., Rickert, R.C., et al. (2014). A pathway switch directs BAFF signaling to distinct NFκB transcription factors in maturing and proliferating B cells. Cell Rep *9*, 2098–2111. https://doi.org/10.1016/j.celrep.2014.11.024.

Avadhanula, V., Weasner, B.P., Hardy, G.G., Kumar, J.P., and Hardy, R.W. (2009). A novel system for the launch of alphavirus RNA synthesis reveals a role for the Imd pathway in arthropod antiviral response. PLoS Pathog. *5*, e1000582. https://doi.org/10.1371/journal.ppat.1000582.

Balachandran, S., Thomas, E., and Barber, G.N. (2004). A FADD-dependent innate immune mechanism in mammalian cells. Nature *432*, 401–405. https://doi.org/10.1038/nature03124.

Basak, S., Shih, V.F.-S., and Hoffmann, A. (2008). Generation and activation of multiple dimeric transcription factors within the NF-kappaB signaling system. Mol Cell Biol *28*, 3139–3150. https://doi.org/10.1128/MCB.01469-07.

Bischoff, V., Vignal, C., Boneca, I.G., Michel, T., Hoffmann, J.A., and Royet, J. (2004). Function of the drosophila pattern-recognition receptor PGRP-SD in the detection of Gram-positive bacteria. Nat Immunol *5*, 1175–1180. https://doi.org/10.1038/ni1123.

Bours, V., Franzoso, G., Azarenko, V., Park, S., Kanno, T., Brown, K., and Siebenlist, U. (1993). The oncoprotein Bcl-3 directly transactivates through kappa B motifs via association with DNA-binding p50B homodimers. Cell *72*, 729–739. https://doi.org/10.1016/0092-8674(93)90401-b.

Boyer, J.A., Spangler, C.J., Strauss, J.D., Cesmat, A.P., Liu, P., McGinty, R.K., and Zhang, Q. (2020). Structural basis of nucleosome-dependent cGAS inhibition. Science *370*, 450–454. https://doi.org/10.1126/science.abd0609.

Bren, G.D., Solan, N.J., Miyoshi, H., Pennington, K.N., Pobst, L.J., and Paya, C.V. (2001). Transcription of the RelB gene is regulated by NF-kappaB. Oncogene *20*, 7722–7733. https://doi.org/10.1038/sj.onc.1204868.

Bundy, D.L., and McKeithan, T.W. (1997). Diverse effects of BCL3 phosphorylation on its modulation of NF-kappaB p52 homodimer binding to DNA. J Biol Chem *272*, 33132–33139. https://doi.org/10.1074/jbc.272.52.33132.

Burdette, D.L., Monroe, K.M., Sotelo-Troha, K., Iwig, J.S., Eckert, B., Hyodo, M., Hayakawa, Y., and Vance, R.E. (2011). STING is a direct innate immune sensor of cyclic di-GMP. Nature *478*, 515–518. https://doi.org/10.1038/nature10429.

Burroughs, A.M., and Aravind, L. (2020). Identification of Uncharacterized Components of Prokaryotic Immune Systems and Their Diverse Eukaryotic Reformulations. J Bacteriol *202*. https://doi.org/10.1128/JB.00365-20.

Cai, H., Holleufer, A., Simonsen, B., Schneider, J., Lemoine, A., Gad, H.H., Huang, J., Huang, J., Chen, D., Peng, T., et al. (2020). 2'3'-cGAMP triggers a STING- and NF-κB-dependent broad antiviral response in Drosophila. Sci Signal *13*. https://doi.org/10.1126/scisignal.abc4537.

Carmody, R.J., Ruan, Q., Palmer, S., Hilliard, B., and Chen, Y.H. (2007). Negative regulation of toll-like receptor signaling by NF-kappaB p50 ubiquitination blockade. Science *317*, 675–678. https://doi.org/10.1126/science.1142953.

Cerboni, S., Jeremiah, N., Gentili, M., Gehrmann, U., Conrad, C., Stolzenberg, M.-C., Picard, C., Neven, B., Fischer, A., Amigorena, S., et al. (2017). Intrinsic antiproliferative activity of the innate sensor STING in T lymphocytes. J. Exp. Med. *214*, 1769–1785. https://doi.org/10.1084/jem.20161674.

Chen, Q., Sun, L., and Chen, Z.J. (2016). Regulation and function of the cGAS–STING pathway of cytosolic DNA sensing. Nature Immunology *17*, 1142–1149. https://doi.org/10.1038/ni.3558.

Choe, K.-M., Werner, T., Stöven, S., Hultmark, D., and Anderson, K.V. (2002). Requirement for a peptidoglycan recognition protein (PGRP) in Relish activation and antibacterial immune responses in Drosophila. Science *296*, 359–362. https://doi.org/10.1126/science.1070216.

Cohen, D., Melamed, S., Millman, A., Shulman, G., Oppenheimer-Shaanan, Y., Kacen, A., Doron, S., Amitai, G., and Sorek, R. (2019). Cyclic GMP-AMP signalling protects bacteria against viral infection. Nature *574*, 691–695. https://doi.org/10.1038/s41586-019-1605-5.

Costa, A., Jan, E., Sarnow, P., and Schneider, D. (2009). The Imd pathway is involved in antiviral immune responses in Drosophila. PLoS ONE *4*, e7436. https://doi.org/10.1371/journal.pone.0007436.

Cvek, B., and Dvorak, Z. (2011). The ubiquitin-proteasome system (UPS) and the mechanism of action of bortezomib. Curr Pharm Des *17*, 1483–1499. https://doi.org/10.2174/138161211796197124.

De Gregorio, E., Spellman, P.T., Tzou, P., Rubin, G.M., and Lemaitre, B. (2002). The Toll and Imd pathways are the major regulators of the immune response in Drosophila. EMBO J *21*, 2568–2579. https://doi.org/10.1093/emboj/21.11.2568.

Deddouche, S., Matt, N., Budd, A., Mueller, S., Kemp, C., Galiana-Arnoux, D., Dostert, C., Antoniewski, C., Hoffmann, J.A., and Imler, J.-L. (2008). The DExD/H-box helicase Dicer-2 mediates the induction of antiviral activity in drosophila. Nature Immunology *9*, 1425–1432. https://doi.org/10.1038/ni.1664.

Diner, E.J., Burdette, D.L., Wilson, S.C., Monroe, K.M., Kellenberger, C.A., Hyodo, M., Hayakawa, Y., Hammond, M.C., and Vance, R.E. (2013). The innate immune DNA sensor cGAS produces a noncanonical cyclic dinucleotide that activates human STING. Cell Rep *3*, 1355–1361. https://doi.org/10.1016/j.celrep.2013.05.009.

Dostert, C., Jouanguy, E., Irving, P., Troxler, L., Galiana-Arnoux, D., Hetru, C., Hoffmann, J.A., and Imler, J.-L. (2005). The Jak-STAT signaling pathway is required but not sufficient for the antiviral response of drosophila. Nat. Immunol. *6*, 946–953. https://doi.org/10.1038/ni1237.

El Chamy, L., Leclerc, V., Caldelari, I., and Reichhart, J.-M. (2008). Sensing of “danger signals” and pathogen-associated molecular patterns defines binary signaling pathways “upstream” of Toll. Nat. Immunol. *9*, 1165–1170. https://doi.org/10.1038/ni.1643.

Engström, Y., Kadalayil, L., Sun, S.C., Samakovlis, C., Hultmark, D., and Faye, I. (1993). kappa B-like motifs regulate the induction of immune genes in Drosophila. J Mol Biol *232*, 327–333. https://doi.org/10.1006/jmbi.1993.1392.

Ertürk-Hasdemir, D., Broemer, M., Leulier, F., Lane, W.S., Paquette, N., Hwang, D., Kim, C.-H., Stöven, S., Meier, P., and Silverman, N. (2009). Two roles for the Drosophila IKK complex in the activation of Relish and the induction of antimicrobial peptide genes. Proc Natl Acad Sci U S A *106*, 9779–9784. https://doi.org/10.1073/pnas.0812022106.

Fang, R., Wang, C., Jiang, Q., Lv, M., Gao, P., Yu, X., Mu, P., Zhang, R., Bi, S., Feng, J.-M., et al. (2017). NEMO-IKKβ Are Essential for IRF3 and NF-κB Activation in the cGAS-STING Pathway. J Immunol *199*, 3222–3233. https://doi.org/10.4049/jimmunol.1700699.

Ferreira, Á.G., Naylor, H., Esteves, S.S., Pais, I.S., Martins, N.E., and Teixeira, L. (2014). The Toll-dorsal pathway is required for resistance to viral oral infection in Drosophila. PLoS Pathog. *10*, e1004507. https://doi.org/10.1371/journal.ppat.1004507.

Fitzgerald, K.A., McWhirter, S.M., Faia, K.L., Rowe, D.C., Latz, E., Golenbock, D.T., Coyle, A.J., Liao, S.-M., and Maniatis, T. (2003). IKKepsilon and TBK1 are essential components of the IRF3 signaling pathway. Nat Immunol *4*, 491–496. https://doi.org/10.1038/ni921.

Franz, K.M., Neidermyer, W.J., Tan, Y.-J., Whelan, S.P.J., and Kagan, J.C. (2018). STING-dependent translation inhibition restricts RNA virus replication. Proc. Natl. Acad. Sci. U.S.A. *115*, E2058–E2067. https://doi.org/10.1073/pnas.1716937115.

Franzoso, G., Bours, V., Azarenko, V., Park, S., Tomita-Yamaguchi, M., Kanno, T., Brown, K., and Siebenlist, U. (1993). The oncoprotein Bcl-3 can facilitate NF-kappa B-mediated transactivation by removing inhibiting p50 homodimers from select kappa B sites. EMBO J *12*, 3893–3901. https://doi.org/10.1002/j.1460-2075.1993.tb06067.x.

Fritsch, M., Günther, S.D., Schwarzer, R., Albert, M.-C., Schorn, F., Werthenbach, J.P., Schiffmann, L.M., Stair, N., Stocks, H., Seeger, J.M., et al. (2019). Caspase-8 is the molecular switch for apoptosis, necroptosis and pyroptosis. Nature *575*, 683–687. https://doi.org/10.1038/s41586-019-1770-6.

Fujita, T., Nolan, G.P., Liou, H.C., Scott, M.L., and Baltimore, D. (1993). The candidate proto-oncogene bcl-3 encodes a transcriptional coactivator that activates through NF-kappa B p50 homodimers. Genes Dev *7*, 1354–1363. https://doi.org/10.1101/gad.7.7b.1354.

Georgel, P., Naitza, S., Kappler, C., Ferrandon, D., Zachary, D., Swimmer, C., Kopczynski, C., Duyk, G., Reichhart, J.M., and Hoffmann, J.A. (2001). Drosophila immune deficiency (IMD) is a death domain protein that activates antibacterial defense and can promote apoptosis. Dev Cell *1*, 503–514. https://doi.org/10.1016/s1534-5807(01)00059-4.

Ghosh, S., Gifford, A.M., Riviere, L.R., Tempst, P., Nolan, G.P., and Baltimore, D. (1990). Cloning of the p50 DNA binding subunit of NF-kappa B: homology to rel and dorsal. Cell *62*, 1019–1029. https://doi.org/10.1016/0092-8674(90)90276-k.

Gobert, V., Gottar, M., Matskevich, A.A., Rutschmann, S., Royet, J., Belvin, M., Hoffmann, J.A., and Ferrandon, D. (2003). Dual activation of the Drosophila toll pathway by two pattern recognition receptors. Science *302*, 2126–2130. https://doi.org/10.1126/science.1085432.

Goto, A., Okado, K., Martins, N., Cai, H., Barbier, V., Lamiable, O., Troxler, L., Santiago, E., Kuhn, L., Paik, D., et al. (2018). The Kinase IKKβ Regulates a STING- and NF-κB-Dependent Antiviral Response Pathway in Drosophila. Immunity *49*, 225-234.e4. https://doi.org/10.1016/j.immuni.2018.07.013.

Gottar, M., Gobert, V., Michel, T., Belvin, M., Duyk, G., Hoffmann, J.A., Ferrandon, D., and Royet, J. (2002). The Drosophila immune response against Gram-negative bacteria is mediated by a peptidoglycan recognition protein. Nature *416*, 640–644. https://doi.org/10.1038/nature734.

Gottar, M., Gobert, V., Matskevich, A.A., Reichhart, J.-M., Wang, C., Butt, T.M., Belvin, M., Hoffmann, J.A., and Ferrandon, D. (2006). Dual detection of fungal infections in Drosophila via recognition of glucans and sensing of virulence factors. Cell *127*, 1425–1437. https://doi.org/10.1016/j.cell.2006.10.046.

Gray, E.E., Treuting, P.M., Woodward, J.J., and Stetson, D.B. (2015). Cutting Edge: cGAS Is Required for Lethal Autoimmune Disease in the Trex1-Deficient Mouse Model of Aicardi-Goutières Syndrome. J Immunol *195*, 1939–1943. https://doi.org/10.4049/jimmunol.1500969.

Gross, I., Georgel, P., Oertel-Buchheit, P., Schnarr, M., and Reichhart, J.M. (1999). Dorsal-B, a splice variant of the Drosophila factor Dorsal, is a novel Rel/NF-kappaB transcriptional activator. Gene *228*, 233–242. .

Gui, X., Yang, H., Li, T., Tan, X., Shi, P., Li, M., Du, F., and Chen, Z.J. (2019). Autophagy induction via STING trafficking is a primordial function of the cGAS pathway. Nature *567*, 262–266. https://doi.org/10.1038/s41586-019-1006-9.

Haruta, H., Kato, A., and Todokoro, K. (2001). Isolation of a novel interleukin-1-inducible nuclear protein bearing ankyrin-repeat motifs. J Biol Chem *276*, 12485–12488. https://doi.org/10.1074/jbc.C100075200.

Hatada, E.N., Nieters, A., Wulczyn, F.G., Naumann, M., Meyer, R., Nucifora, G., McKeithan, T.W., and Scheidereit, C. (1992). The ankyrin repeat domains of the NF-kappa B precursor p105 and the protooncogene bcl-3 act as specific inhibitors of NF-kappa B DNA binding. Proc Natl Acad Sci U S A *89*, 2489–2493. https://doi.org/10.1073/pnas.89.6.2489.

Hayashi, F., Smith, K.D., Ozinsky, A., Hawn, T.R., Yi, E.C., Goodlett, D.R., Eng, J.K., Akira, S., Underhill, D.M., and Aderem, A. (2001). The innate immune response to bacterial flagellin is mediated by Toll-like receptor 5. Nature *410*, 1099–1103. https://doi.org/10.1038/35074106.

Hedengren, M., Asling, B., Dushay, M.S., Ando, I., Ekengren, S., Wihlborg, M., and Hultmark, D. (1999). Relish, a central factor in the control of humoral but not cellular immunity in Drosophila. Mol Cell *4*, 827–837. https://doi.org/10.1016/s1097-2765(00)80392-5.

Henry, C.M., and Martin, S.J. (2017). Caspase-8 Acts in a Non-enzymatic Role as a Scaffold for Assembly of a Pro-inflammatory "FADDosome" Complex upon TRAIL Stimulation. Mol Cell *65*, 715-729.e5. https://doi.org/10.1016/j.molcel.2017.01.022.

Hoffmann, J.A. (2003). The immune response of Drosophila. Nature *426*, 33–38. https://doi.org/10.1038/nature02021.

Hoffmann, A., Levchenko, A., Scott, M.L., and Baltimore, D. (2002). The IκB-NF-κB Signaling Module: Temporal Control and Selective Gene Activation. Science *298*, 1241–1245. https://doi.org/10.1126/science.1071914.

Hoffmann, A., Natoli, G., and Ghosh, G. (2006). Transcriptional regulation via the NF-kappaB signaling module. Oncogene *25*, 6706–6716. https://doi.org/10.1038/sj.onc.1209933.

Hoffmann, J.A., Kafatos, F.C., Janeway, C.A., and Ezekowitz, R.A. (1999). Phylogenetic perspectives in innate immunity. Science *284*, 1313–1318. .

Holleufer, A., Winther, K.G., Gad, H.H., Ai, X., Chen, Y., Li, L., Wei, Z., Deng, H., Liu, J., Frederiksen, N.A., et al. (2021). Two cGAS-like receptors induce antiviral immunity in Drosophila. Nature *597*, 114–118. https://doi.org/10.1038/s41586-021-03800-z.

Hu, X., Yagi, Y., Tanji, T., Zhou, S., and Ip, Y.T. (2004). Multimerization and interaction of Toll and Spätzle in Drosophila. Proc Natl Acad Sci U S A *101*, 9369–9374. https://doi.org/10.1073/pnas.0307062101.

Hua, X., Li, B., Song, L., Hu, C., Li, X., Wang, D., Xiong, Y., Zhao, P., He, H., Xia, Q., et al. (2018). Stimulator of interferon genes (STING) provides insect antiviral immunity by promoting Dredd caspase-mediated NF-κB activation. J. Biol. Chem. *293*, 11878–11890. https://doi.org/10.1074/jbc.RA117.000194.

Imler, J.-L. (2014). Overview of Drosophila immunity: a historical perspective. Developmental and Comparative Immunology *42*, 3–15. https://doi.org/10.1016/j.dci.2013.08.018.

Imler, J.-L., and Bulet, P. (2005). Antimicrobial peptides in Drosophila: structures, activities and gene regulation. Chem Immunol Allergy *86*, 1–21. https://doi.org/10.1159/000086648.

Ip, Y. (1993). Dif, a dorsal-related gene that mediates an immune response in Drosophila. Cell *75*, 753–763. https://doi.org/10.1016/0092-8674(93)90495-C.

Ishikawa, H., and Barber, G.N. (2008). STING is an endoplasmic reticulum adaptor that facilitates innate immune signalling. Nature *455*, 674–678. https://doi.org/10.1038/nature07317.

Ishikawa, H., Ma, Z., and Barber, G.N. (2009). STING regulates intracellular DNA-mediated, type I interferon-dependent innate immunity. Nature *461*, 788–792. https://doi.org/10.1038/nature08476.

Issa, N., Guillaumot, N., Lauret, E., Matt, N., Schaeffer-Reiss, C., Van Dorsselaer, A., Reichhart, J.-M., and Veillard, F. (2018). The Circulating Protease Persephone Is an Immune Sensor for Microbial Proteolytic Activities Upstream of the Drosophila Toll Pathway. Molecular Cell *69*, 539-550.e6. https://doi.org/10.1016/j.molcel.2018.01.029.

Ji, Y., Thomas, C., Tulin, N., Lodhi, N., Boamah, E., Kolenko, V., and Tulin, A.V. (2016). Charon Mediates Immune Deficiency-Driven PARP-1-Dependent Immune Responses in Drosophila. J. Immunol. *197*, 2382–2389. https://doi.org/10.4049/jimmunol.1600994.

Jumper, J., Evans, R., Pritzel, A., Green, T., Figurnov, M., Ronneberger, O., Tunyasuvunakool, K., Bates, R., Žídek, A., Potapenko, A., et al. (2021). Highly accurate protein structure prediction with AlphaFold. Nature *596*, 583–589. https://doi.org/10.1038/s41586-021-03819-2.

Kappler, C., Meister, M., Lagueux, M., Gateff, E., Hoffmann, J.A., and Reichhart, J.M. (1993). Insect immunity. Two 17 bp repeats nesting a kappa B-related sequence confer inducibility to the diptericin gene and bind a polypeptide in bacteria-challenged Drosophila. EMBO J *12*, 1561–1568. https://doi.org/10.1002/j.1460-2075.1993.tb05800.x.

Kemp, C., Mueller, S., Goto, A., Barbier, V., Paro, S., Bonnay, F., Dostert, C., Troxler, L., Hetru, C., Meignin, C., et al. (2013). Broad RNA interference-mediated antiviral immunity and virus-specific inducible responses in Drosophila. J. Immunol. *190*, 650–658. https://doi.org/10.4049/jimmunol.1102486.

Kieran, M., Blank, V., Logeat, F., Vandekerckhove, J., Lottspeich, F., Le Bail, O., Urban, M.B., Kourilsky, P., Baeuerle, P.A., and Israël, A. (1990). The DNA binding subunit of NF-kappa B is identical to factor

KBF1 and homologous to the rel oncogene product. Cell *62*, 1007–1018. https://doi.org/10.1016/0092-8674(90)90275-j.

Kim, C.-H., Paik, D., Rus, F., and Silverman, N. (2014). The caspase-8 homolog Dredd cleaves Imd and Relish but is not inhibited by p35. J Biol Chem *289*, 20092–20101. https://doi.org/10.1074/jbc.M113.544841.

Kitamura, H., Kanehira, K., Okita, K., Morimatsu, M., and Saito, M. (2000). MAIL, a novel nuclear I kappa B protein that potentiates LPS-induced IL-6 production. FEBS Lett *485*, 53–56. https://doi.org/10.1016/s0014-5793(00)02185-2.

Kleino, A., Valanne, S., Ulvila, J., Kallio, J., Myllymäki, H., Enwald, H., Stöven, S., Poidevin, M., Ueda, R., Hultmark, D., et al. (2005). Inhibitor of apoptosis 2 and TAK1-binding protein are components of the Drosophila Imd pathway. EMBO J *24*, 3423–3434. https://doi.org/10.1038/sj.emboj.7600807.

Kranzusch, P.J. (2019). cGAS and CD-NTase enzymes: structure, mechanism, and evolution. Curr Opin Struct Biol *59*, 178–187. https://doi.org/10.1016/j.sbi.2019.08.003.

Kranzusch, P.J., Wilson, S.C., Lee, A.S.Y., Berger, J.M., Doudna, J.A., and Vance, R.E. (2015). Ancient Origin of cGAS-STING Reveals Mechanism of Universal 2',3' cGAMP Signaling. Mol. Cell *59*, 891–903. https://doi.org/10.1016/j.molcel.2015.07.022.

Kujirai, T., Zierhut, C., Takizawa, Y., Kim, R., Negishi, L., Uruma, N., Hirai, S., Funabiki, H., and Kurumizaka, H. (2020). Structural basis for the inhibition of cGAS by nucleosomes. Science *370*, 455–458. https://doi.org/10.1126/science.abd0237.

Lahaye, X., Gentili, M., Silvin, A., Conrad, C., Picard, L., Jouve, M., Zueva, E., Maurin, M., Nadalin, F., Knott, G.J., et al. (2018). NONO Detects the Nuclear HIV Capsid to Promote cGAS-Mediated Innate Immune Activation. Cell *175*, 488-501.e22. https://doi.org/10.1016/j.cell.2018.08.062.

Lamiable, O., Kellenberger, C., Kemp, C., Troxler, L., Pelte, N., Boutros, M., Marques, J.T., Daeffler, L., Hoffmann, J.A., Roussel, A., et al. (2016). Cytokine Diedel and a viral homologue suppress the IMD pathway in Drosophila. Proc. Natl. Acad. Sci. U.S.A. *113*, 698–703. https://doi.org/10.1073/pnas.1516122113.

Lemaitre, B., and Hoffmann, J. (2007). The host defense of Drosophila melanogaster. Annu. Rev. Immunol. *25*, 697–743. https://doi.org/10.1146/annurev.immunol.25.022106.141615.

Lemaitre, B., Nicolas, E., Michaut, L., Reichhart, J.M., and Hoffmann, J.A. (1996). The dorsoventral regulatory gene cassette spätzle/Toll/cactus controls the potent antifungal response in Drosophila adults. Cell *86*, 973–983. https://doi.org/10.1016/s0092-8674(00)80172-5.

Leulier, F., Rodriguez, A., Khush, R.S., Abrams, J.M., and Lemaitre, B. (2000). The Drosophila caspase Dredd is required to resist gram-negative bacterial infection. EMBO Rep *1*, 353–358. https://doi.org/10.1093/embo-reports/kvd073.

Leulier, F., Vidal, S., Saigo, K., Ueda, R., and Lemaitre, B. (2002). Inducible expression of double-stranded RNA reveals a role for dFADD in the regulation of the antibacterial response in Drosophila adults. Curr Biol *12*, 996–1000. https://doi.org/10.1016/s0960-9822(02)00873-4.

Li, C., and Zamore, P.D. (2019). RNAi in Drosophila S2 Cells by dsRNA Soaking. Cold Spring Harb Protoc *2019*. https://doi.org/10.1101/pdb.prot097477.

Li, J., Mahajan, A., and Tsai, M.-D. (2006). Ankyrin repeat: a unique motif mediating protein-protein interactions. Biochemistry *45*, 15168–15178. https://doi.org/10.1021/bi062188q.

Li, X., Shu, C., Yi, G., Chaton, C.T., Shelton, C.L., Diao, J., Zuo, X., Kao, C.C., Herr, A.B., and Li, P. (2013). Cyclic GMP-AMP Synthase Is Activated by Double-Stranded DNA-Induced Oligomerization. Immunity *39*, 1019–1031. https://doi.org/10.1016/j.immuni.2013.10.019.

Li, Y., Wilson, H.L., and Kiss-Toth, E. (2017). Regulating STING in health and disease. J Inflamm (Lond) *14*, 11. https://doi.org/10.1186/s12950-017-0159-2.

Liang, C., Zhang, M., and Sun, S.-C. (2006). beta-TrCP binding and processing of NF-kappaB2/p100 involve its phosphorylation at serines 866 and 870. Cell Signal *18*, 1309–1317. https://doi.org/10.1016/j.cellsig.2005.10.011.

Liao, G., Zhang, M., Harhaj, E.W., and Sun, S.-C. (2004). Regulation of the NF-kappaB-inducing kinase by tumor necrosis factor receptor-associated factor 3-induced degradation. J Biol Chem *279*, 26243–26250. https://doi.org/10.1074/jbc.M403286200.

Lin, L., and Ghosh, S. (1996). A glycine-rich region in NF-kappaB p105 functions as a processing signal for the generation of the p50 subunit. Mol Cell Biol *16*, 2248–2254. https://doi.org/10.1128/MCB.16.5.2248.

Ling, L., Cao, Z., and Goeddel, D.V. (1998). NF-kappaB-inducing kinase activates IKK-alpha by phosphorylation of Ser-176. Proc Natl Acad Sci U S A *95*, 3792–3797. https://doi.org/10.1073/pnas.95.7.3792.

Liu, F., Xia, Y., Parker, A.S., and Verma, I.M. (2012). IKK biology. Immunol Rev *246*, 239–253. https://doi.org/10.1111/j.1600-065X.2012.01107.x.

Liu, Y., Jesus, A.A., Marrero, B., Yang, D., Ramsey, S.E., Sanchez, G.A.M., Tenbrock, K., Wittkowski, H., Jones, O.Y., Kuehn, H.S., et al. (2014). Activated STING in a vascular and pulmonary syndrome. N Engl J Med *371*, 507–518. https://doi.org/10.1056/NEJMoa1312625.

Liu, Y., Gordesky-Gold, B., Leney-Greene, M., Weinbren, N.L., Tudor, M., and Cherry, S. (2018). Inflammation-Induced, STING-Dependent Autophagy Restricts Zika Virus Infection in the Drosophila Brain. Cell Host Microbe *24*, 57-68.e3. https://doi.org/10.1016/j.chom.2018.05.022.

Lowey, B., Whiteley, A.T., Keszei, A.F.A., Morehouse, B.R., Mathews, I.T., Antine, S.P., Cabrera, V.J., Kashin, D., Niemann, P., Jain, M., et al. (2020). CBASS Immunity Uses CARF-Related Effectors to Sense 3'-5'- and 2'-5'-Linked Cyclic Oligonucleotide Signals and Protect Bacteria from Phage Infection. Cell *182*, 38-49.e17. https://doi.org/10.1016/j.cell.2020.05.019.

Lu, Y., Wu, L.P., and Anderson, K.V. (2001). The antibacterial arm of the *Drosophila* innate immune response requires an IκB kinase. Genes Dev. *15*, 104–110. https://doi.org/10.1101/gad.856901.

Luksch, H., Stinson, W.A., Platt, D.J., Qian, W., Kalugotla, G., Miner, C.A., Bennion, B.G., Gerbaulet, A., Rösen-Wolff, A., and Miner, J.J. (2019). STING-associated lung disease in mice relies on T cells but not type I interferon. Journal of Allergy and Clinical Immunology *144*, 254-266.e8. https://doi.org/10.1016/j.jaci.2019.01.044.

Malek, S., Chen, Y., Huxford, T., and Ghosh, G. (2001). IkappaBbeta, but not IkappaBalpha, functions as a classical cytoplasmic inhibitor of NF-kappaB dimers by masking both NF-kappaB nuclear localization sequences in resting cells. J Biol Chem *276*, 45225–45235. https://doi.org/10.1074/jbc.M105865200.

Margolis, S.R., Wilson, S.C., and Vance, R.E. (2017). Evolutionary Origins of cGAS-STING Signaling. Trends Immunol. *38*, 733–743. https://doi.org/10.1016/j.it.2017.03.004.

Margolis, S.R., Dietzen, P.A., Hayes, B.M., Wilson, S.C., Remick, B.C., Chou, S., and Vance, R.E. (2021). The cyclic dinucleotide 2′3′-cGAMP induces a broad antibacterial and antiviral response in the sea anemone Nematostella vectensis. PNAS *118*. https://doi.org/10.1073/pnas.2109022118.

Martin, M., Hiroyasu, A., Guzman, R.M., Roberts, S.A., and Goodman, A.G. (2018). Analysis of Drosophila STING Reveals an Evolutionarily Conserved Antimicrobial Function. Cell Rep *23*, 3537-3550.e6. https://doi.org/10.1016/j.celrep.2018.05.029.

Martins, N., Imler, J.-L., and Meignin, C. (2016). Discovery of novel targets for antivirals: learning from flies. Curr Opin Virol *20*, 64–70. https://doi.org/10.1016/j.coviro.2016.09.005.

Medzhitov, R., Preston-Hurlburt, P., and Janeway, C.A. (1997). A human homologue of the Drosophila Toll protein signals activation of adaptive immunity. Nature *388*, 394–397. https://doi.org/10.1038/41131.

Medzhitov, R., Preston-Hurlburt, P., Kopp, E., Stadlen, A., Chen, C., Ghosh, S., and Janeway, C.A. (1998). MyD88 Is an Adaptor Protein in the hToll/IL-1 Receptor Family Signaling Pathways. Molecular Cell *2*, 253–258. https://doi.org/10.1016/S1097-2765(00)80136-7.

Meinander, A., Runchel, C., Tenev, T., Chen, L., Kim, C.-H., Ribeiro, P.S., Broemer, M., Leulier, F., Zvelebil, M., Silverman, N., et al. (2012). Ubiquitylation of the initiator caspase DREDD is required for innate immune signalling. EMBO J *31*, 2770–2783. https://doi.org/10.1038/emboj.2012.121.

Meng, X., Khanuja, B.S., and Ip, Y.T. (1999). Toll receptor-mediated Drosophila immune response requires Dif, an NF-kappaB factor. Genes Dev *13*, 792–797. https://doi.org/10.1101/gad.13.7.792.

Michallet, M.-C., Meylan, E., Ermolaeva, M.A., Vazquez, J., Rebsamen, M., Curran, J., Poeck, H., Bscheider, M., Hartmann, G., König, M., et al. (2008). TRADD Protein Is an Essential Component of the RIG-like Helicase Antiviral Pathway. Immunity *28*, 651–661. https://doi.org/10.1016/j.immuni.2008.03.013.

Michalski, S., de Oliveira Mann, C.C., Stafford, C.A., Witte, G., Bartho, J., Lammens, K., Hornung, V., and Hopfner, K.-P. (2020). Structural basis for sequestration and autoinhibition of cGAS by chromatin. Nature *587*, 678–682. https://doi.org/10.1038/s41586-020-2748-0.

Michel, T., Reichhart, J.M., Hoffmann, J.A., and Royet, J. (2001). Drosophila Toll is activated by Gram-positive bacteria through a circulating peptidoglycan recognition protein. Nature *414*, 756–759. https://doi.org/10.1038/414756a.

Minakhina, S., and Steward, R. (2006). Nuclear factor-kappa B pathways in Drosophila. Oncogene *25*, 6749–6757. https://doi.org/10.1038/sj.onc.1209940.

Mishima, Y., Quintin, J., Aimanianda, V., Kellenberger, C., Coste, F., Clavaud, C., Hetru, C., Hoffmann, J.A., Latgé, J.-P., Ferrandon, D., et al. (2009). The N-terminal domain of Drosophila Gram-negative binding protein 3 (GNBP3) defines a novel family of fungal pattern recognition receptors. J. Biol. Chem. *284*, 28687–28697. https://doi.org/10.1074/jbc.M109.034587.

Mitchell, S., Vargas, J., and Hoffmann, A. (2016). Signaling via the NFκB system. WIREs Mechanisms of Disease *8*, 227–241. https://doi.org/10.1002/wsbm.1331.

Morehouse, B.R., Govande, A.A., Millman, A., Keszei, A.F.A., Lowey, B., Ofir, G., Shao, S., Sorek, R., and Kranzusch, P.J. (2020). STING cyclic dinucleotide sensing originated in bacteria. Nature *586*, 429–433. https://doi.org/10.1038/s41586-020-2719-5.

Moretti, J., Roy, S., Bozec, D., Martinez, J., Chapman, J.R., Ueberheide, B., Lamming, D.W., Chen, Z.J., Horng, T., Yeretssian, G., et al. (2017). STING Senses Microbial Viability to Orchestrate Stress-Mediated

Autophagy of the Endoplasmic Reticulum. Cell *171*, 809-823.e13. https://doi.org/10.1016/j.cell.2017.09.034.

Morris, O., Liu, X., Domingues, C., Runchel, C., Chai, A., Basith, S., Tenev, T., Chen, H., Choi, S., Pennetta, G., et al. (2016). Signal Integration by the IκB Protein Pickle Shapes Drosophila Innate Host Defense. Cell Host Microbe *20*, 283–295. https://doi.org/10.1016/j.chom.2016.08.003.

Motoyama, M., Yamazaki, S., Eto-Kimura, A., Takeshige, K., and Muta, T. (2005). Positive and negative regulation of nuclear factor-kappaB-mediated transcription by IkappaB-zeta, an inducible nuclear protein. J Biol Chem *280*, 7444–7451. https://doi.org/10.1074/jbc.M412738200.

Motwani, M., Pesiridis, S., and Fitzgerald, K.A. (2019). DNA sensing by the cGAS-STING pathway in health and disease. Nat Rev Genet *20*, 657–674. https://doi.org/10.1038/s41576-019-0151-1.

Naitza, S., Rossé, C., Kappler, C., Georgel, P., Belvin, M., Gubb, D., Camonis, J., Hoffmann, J.A., and Reichhart, J.M. (2002). The Drosophila immune defense against gram-negative infection requires the death protein dFADD. Immunity *17*, 575–581. https://doi.org/10.1016/s1074-7613(02)00454-5.

Newton, K., Wickliffe, K.E., Maltzman, A., Dugger, D.L., Reja, R., Zhang, Y., Roose-Girma, M., Modrusan, Z., Sagolla, M.S., Webster, J.D., et al. (2019). Activity of caspase-8 determines plasticity between cell death pathways. Nature *575*, 679–682. https://doi.org/10.1038/s41586-019-1752-8.

Nishikawa, T., Ota, T., and Isogai, T. (2000). Prediction whether a human cDNA sequence contains initiation codon by combining statistical information and similarity with protein sequences. Bioinformatics *16*, 960–967. https://doi.org/10.1093/bioinformatics/16.11.960.

Nolan, G.P., Fujita, T., Bhatia, K., Huppi, C., Liou, H.C., Scott, M.L., and Baltimore, D. (1993). The bcl-3 proto-oncogene encodes a nuclear I kappa B-like molecule that preferentially interacts with NF-kappa B p50 and p52 in a phosphorylation-dependent manner. Mol Cell Biol *13*, 3557–3566. https://doi.org/10.1128/mcb.13.6.3557-3566.1993.

Nüsslein-Volhard, C., Lohs-Schardin, M., Sander, K., and Cremer, C. (1980). A dorso-ventral shift of embryonic primordia in a new maternal-effect mutant of Drosophila. Nature *283*, 474–476. https://doi.org/10.1038/283474a0.

Oeckinghaus, A., and Ghosh, S. (2009). The NF- B Family of Transcription Factors and Its Regulation. Cold Spring Harbor Perspectives in Biology *1*, a000034–a000034. https://doi.org/10.1101/cshperspect.a000034.

de Oliveira Mann, C.C., and Hopfner, K.-P. (2021). Nuclear cGAS: guard or prisoner? EMBO J *40*, e108293. https://doi.org/10.15252/embj.2021108293.

de Oliveira Mann, C.C., Orzalli, M.H., King, D.S., Kagan, J.C., Lee, A.S.Y., and Kranzusch, P.J. (2019). Modular Architecture of the STING C-Terminal Tail Allows Interferon and NF-κB Signaling Adaptation. Cell Rep *27*, 1165-1175.e5. https://doi.org/10.1016/j.celrep.2019.03.098.

Orian, A., Schwartz, A.L., Israël, A., Whiteside, S., Kahana, C., and Ciechanover, A. (1999). Structural motifs involved in ubiquitin-mediated processing of the NF-kappaB precursor p105: roles of the glycine-rich region and a downstream ubiquitination domain. Mol Cell Biol *19*, 3664–3673. https://doi.org/10.1128/MCB.19.5.3664.

Orzalli, M.H., Broekema, N.M., Diner, B.A., Hancks, D.C., Elde, N.C., Cristea, I.M., and Knipe, D.M. (2015). cGAS-mediated stabilization of IFI16 promotes innate signaling during herpes simplex virus infection. Proc. Natl. Acad. Sci. U.S.A. *112*. https://doi.org/10.1073/pnas.1424637112.

Paquette, N., Broemer, M., Aggarwal, K., Chen, L., Husson, M., Ertürk-Hasdemir, D., Reichhart, J.-M., Meier, P., and Silverman, N. (2010). Caspase-mediated cleavage, IAP binding, and ubiquitination: linking three mechanisms crucial for Drosophila NF-kappaB signaling. Mol Cell *37*, 172–182. https://doi.org/10.1016/j.molcel.2009.12.036.

Poltorak, A., He, X., Smirnova, I., Liu, M.Y., Van Huffel, C., Du, X., Birdwell, D., Alejos, E., Silva, M., Galanos, C., et al. (1998). Defective LPS signaling in C3H/HeJ and C57BL/10ScCr mice: mutations in Tlr4 gene. Science *282*, 2085–2088. https://doi.org/10.1126/science.282.5396.2085.

Rice, N.R., MacKichan, M.L., and Israël, A. (1992). The precursor of NF-kappa B p50 has I kappa B-like functions. Cell *71*, 243–253. https://doi.org/10.1016/0092-8674(92)90353-e.

Rock, F.L., Hardiman, G., Timans, J.C., Kastelein, R.A., and Bazan, J.F. (1998). A family of human receptors structurally related to Drosophila Toll. Proc Natl Acad Sci U S A *95*, 588–593. https://doi.org/10.1073/pnas.95.2.588.

Rutschmann, S., Jung, A.C., Hetru, C., Reichhart, J.M., Hoffmann, J.A., and Ferrandon, D. (2000a). The Rel protein DIF mediates the antifungal but not the antibacterial host defense in Drosophila. Immunity *12*, 569–580. .

Rutschmann, S., Jung, A.C., Zhou, R., Silverman, N., Hoffmann, J.A., and Ferrandon, D. (2000b). Role of Drosophila IKKγ in a Toll-independent antibacterial immune response. Nat Immunol *1*, 342–347. https://doi.org/10.1038/79801.

Rutschmann, S., Kilinc, A., and Ferrandon, D. (2002). Cutting edge: the toll pathway is required for resistance to gram-positive bacterial infections in Drosophila. J Immunol *168*, 1542–1546. https://doi.org/10.4049/jimmunol.168.4.1542.

Sabatier, L., Jouanguy, E., Dostert, C., Zachary, D., Dimarcq, J.-L., Bulet, P., and Imler, J.-L. (2003). Pherokine-2 and -3. European Journal of Biochemistry / FEBS *270*, 3398–3407. .

Saccani, S., Pantano, S., and Natoli, G. (2003). Modulation of NF-kappaB activity by exchange of dimers. Mol Cell *11*, 1563–1574. https://doi.org/10.1016/s1097-2765(03)00227-2.

Saitoh, T., Fujita, N., Hayashi, T., Takahara, K., Satoh, T., Lee, H., Matsunaga, K., Kageyama, S., Omori, H., Noda, T., et al. (2009). Atg9a controls dsDNA-driven dynamic translocation of STING and the innate immune response. Proc. Natl. Acad. Sci. U.S.A. *106*, 20842–20846. https://doi.org/10.1073/pnas.0911267106.

Schneider, I. (1972). Cell lines derived from late embryonic stages of Drosophila melanogaster. J Embryol Exp Morphol *27*, 353–365. .

Schneider, J., and Imler, J.-L. (2021). Sensing and signalling viral infection in drosophila. Developmental & Comparative Immunology *117*, 103985. https://doi.org/10.1016/j.dci.2020.103985.

Schröfelbauer, B., Polley, S., Behar, M., Ghosh, G., and Hoffmann, A. (2012). NEMO ensures signaling specificity of the pleiotropic IKKβ by directing its kinase activity toward IκBα. Mol Cell *47*, 111–121. https://doi.org/10.1016/j.molcel.2012.04.020.

Senftleben, U., Cao, Y., Xiao, G., Greten, F.R., Krähn, G., Bonizzi, G., Chen, Y., Hu, Y., Fong, A., Sun, S.C., et al. (2001). Activation by IKKalpha of a second, evolutionary conserved, NF-kappa B signaling pathway. Science *293*, 1495–1499. https://doi.org/10.1126/science.1062677.

Severin, G.B., Ramliden, M.S., Hawver, L.A., Wang, K., Pell, M.E., Kieninger, A.-K., Khataokar, A., O'Hara, B.J., Behrmann, L.V., Neiditch, M.B., et al. (2018). Direct activation of a phospholipase by cyclic GMP-AMP in El Tor Vibrio cholerae. Proc Natl Acad Sci U S A *115*, E6048–E6055. https://doi.org/10.1073/pnas.1801233115.

Shen, R., Zheng, K., Zhou, Y., Chi, X., Pan, H., Wu, C., Yang, Y., Zheng, Y., Pan, D., and Liu, B. (2022). A dRASSF-STRIPAK-Imd-JAK/STAT axis controls antiviral immune response in Drosophila. Cell Reports *40*, 111143. https://doi.org/10.1016/j.celrep.2022.111143.

Shi, Y., Evans, J.E., and Rock, K.L. (2003). Molecular identification of a danger signal that alerts the immune system to dying cells. Nature *425*, 516–521. https://doi.org/10.1038/nature01991.

Silverman, N., Zhou, R., Stöven, S., Pandey, N., Hultmark, D., and Maniatis, T. (2000). A *Drosophila* IκB kinase complex required for Relish cleavage and antibacterial immunity. Genes Dev. *14*, 2461–2471. https://doi.org/10.1101/gad.817800.

Slavik, K.M., Morehouse, B.R., Ragucci, A.E., Zhou, W., Ai, X., Chen, Y., Li, L., Wei, Z., Bähre, H., König, M., et al. (2021). cGAS-like receptors sense RNA and control 3'2'-cGAMP signalling in Drosophila. Nature *597*, 109–113. https://doi.org/10.1038/s41586-021-03743-5.

Smale, S.T. (2012). Dimer-specific regulatory mechanisms within the NF-κB family of transcription factors: NF-κB dimer-specific regulatory mechanisms. Immunological Reviews *246*, 193–204. https://doi.org/10.1111/j.1600-065X.2011.01091.x.

Solan, N.J., Miyoshi, H., Carmona, E.M., Bren, G.D., and Paya, C.V. (2002). RelB cellular regulation and transcriptional activity are regulated by p100. J Biol Chem *277*, 1405–1418. https://doi.org/10.1074/jbc.M109619200.

St Johnston, D., and Nüsslein-Volhard, C. (1992). The origin of pattern and polarity in the Drosophila embryo. Cell *68*, 201–219. https://doi.org/10.1016/0092-8674(92)90466-p.

Steward, R. (1987). *Dorsal* , an Embryonic Polarity Gene in *Drosophila* , Is Homologous to the Vertebrate Proto-Oncogene, c- *rel*. Science *238*, 692–694. https://doi.org/10.1126/science.3118464.

Stöven, S., Ando, I., Kadalayil, L., Engström, Y., and Hultmark, D. (2000). Activation of the *Drosophila* NF-κB factor Relish by rapid endoproteolytic cleavage. EMBO Rep *1*, 347–352. https://doi.org/10.1093/embo-reports/kvd072.

Stoven, S., Silverman, N., Junell, A., Hedengren-Olcott, M., D. Erturk, Engstrom, Y., Maniatis, T., and Hultmark, D. (2003). Caspase-mediated processing of the Drosophila NF- B factor Relish. Proceedings of the National Academy of Sciences *100*, 5991–5996. https://doi.org/10.1073/pnas.1035902100.

Sun, S.-C. (2011). Non-canonical NF-κB signaling pathway. Cell Res *21*, 71–85. https://doi.org/10.1038/cr.2010.177.

Sun, S.-C. (2017). The non-canonical NF-κB pathway in immunity and inflammation. Nat Rev Immunol *17*, 545–558. https://doi.org/10.1038/nri.2017.52.

Sun, L., Wu, J., Du, F., Chen, X., and Chen, Z.J. (2013). Cyclic GMP-AMP synthase is a cytosolic DNA sensor that activates the type I interferon pathway. Science *339*, 786–791. https://doi.org/10.1126/science.1232458.

Sun, W., Li, Y., Chen, L., Chen, H., You, F., Zhou, X., Zhou, Y., Zhai, Z., Chen, D., and Jiang, Z. (2009). ERIS, an endoplasmic reticulum IFN stimulator, activates innate immune signaling through dimerization. Proc. Natl. Acad. Sci. U.S.A. *106*, 8653–8658. https://doi.org/10.1073/pnas.0900850106.

Takehana, A., Yano, T., Mita, S., Kotani, A., Oshima, Y., and Kurata, S. (2004). Peptidoglycan recognition protein (PGRP)-LE and PGRP-LC act synergistically in Drosophila immunity. EMBO J *23*, 4690–4700. https://doi.org/10.1038/sj.emboj.7600466.

Tanaka, Y., and Chen, Z.J. (2012). STING specifies IRF3 phosphorylation by TBK1 in the cytosolic DNA signaling pathway. Sci Signal *5*, ra20. https://doi.org/10.1126/scisignal.2002521.

Tanji, T., Hu, X., Weber, A.N.R., and Ip, Y.T. (2007). Toll and IMD pathways synergistically activate an innate immune response in Drosophila melanogaster. Mol Cell Biol *27*, 4578–4588. https://doi.org/10.1128/MCB.01814-06.

Tanji, T., Yun, E.-Y., and Ip, Y.T. (2010). Heterodimers of NF-kappaB transcription factors DIF and Relish regulate antimicrobial peptide genes in Drosophila. Proc. Natl. Acad. Sci. U.S.A. *107*, 14715–14720. https://doi.org/10.1073/pnas.1009473107.

Tauszig-Delamasure, S., Bilak, H., Capovilla, M., Hoffmann, J.A., and Imler, J.-L. (2002). Drosophila MyD88 is required for the response to fungal and Gram-positive bacterial infections. Nature Immunology *3*, 91–97. https://doi.org/10.1038/ni747.

Tsui, R., Kearns, J.D., Lynch, C., Vu, D., Ngo, K.A., Basak, S., Ghosh, G., and Hoffmann, A. (2015). IκBβ enhances the generation of the low-affinity NFκB/RelA homodimer. Nat Commun *6*, 7068. https://doi.org/10.1038/ncomms8068.

Vila, I.K., Chamma, H., Steer, A., Saccas, M., Taffoni, C., Turtoi, E., Reinert, L.S., Hussain, S., Marines, J., Jin, L., et al. (2022). STING orchestrates the crosstalk between polyunsaturated fatty acid metabolism and inflammatory responses. Cell Metabolism *34*, 125-139.e8. https://doi.org/10.1016/j.cmet.2021.12.007.

Warner, J.D., Irizarry-Caro, R.A., Bennion, B.G., Ai, T.L., Smith, A.M., Miner, C.A., Sakai, T., Gonugunta, V.K., Wu, J., Platt, D.J., et al. (2017). STING-associated vasculopathy develops independently of IRF3 in mice. J Exp Med *214*, 3279–3292. https://doi.org/10.1084/jem.20171351.

Watson, R.O., Bell, S.L., MacDuff, D.A., Kimmey, J.M., Diner, E.J., Olivas, J., Vance, R.E., Stallings, C.L., Virgin, H.W., and Cox, J.S. (2015). The Cytosolic Sensor cGAS Detects Mycobacterium tuberculosis DNA to Induce Type I Interferons and Activate Autophagy. Cell Host Microbe *17*, 811–819. https://doi.org/10.1016/j.chom.2015.05.004.

Weber, A.N.R., Tauszig-Delamasure, S., Hoffmann, J.A., Lelièvre, E., Gascan, H., Ray, K.P., Morse, M.A., Imler, J.-L., and Gay, N.J. (2003). Binding of the Drosophila cytokine Spätzle to Toll is direct and establishes signaling. Nature Immunology *4*, 794–800. https://doi.org/10.1038/ni955.

Weber, A.N.R., Moncrieffe, M.C., Gangloff, M., Imler, J.-L., and Gay, N.J. (2005). Ligand-receptor and receptor-receptor interactions act in concert to activate signaling in the Drosophila toll pathway. The Journal of Biological Chemistry *280*, 22793–22799. https://doi.org/10.1074/jbc.M502074200.

Weber, A.N.R., Gangloff, M., Moncrieffe, M.C., Hyvert, Y., Imler, J.-L., and Gay, N.J. (2007). Role of the Spatzle Pro-domain in the generation of an active toll receptor ligand. The Journal of Biological Chemistry *282*, 13522–13531. https://doi.org/10.1074/jbc.M700068200.

Whiteley, A.T., Eaglesham, J.B., de Oliveira Mann, C.C., Morehouse, B.R., Lowey, B., Nieminen, E.A., Danilchanka, O., King, D.S., Lee, A.S.Y., Mekalanos, J.J., et al. (2019). Bacterial cGAS-like enzymes synthesize diverse nucleotide signals. Nature *567*, 194–199. https://doi.org/10.1038/s41586-019-0953-5.

Williams, L.M., and Gilmore, T.D. (2020). Looking Down on NF-κB. Mol Cell Biol *40*, e00104-20. https://doi.org/10.1128/MCB.00104-20.

Woodward, J.J., Iavarone, A.T., and Portnoy, D.A. (2010). c-di-AMP Secreted by Intracellular *Listeria monocytogenes* Activates a Host Type I Interferon Response. Science *328*, 1703–1705. https://doi.org/10.1126/science.1189801.

Wu, J., Chen, Y.-J., Dobbs, N., Sakai, T., Liou, J., Miner, J.J., and Yan, N. (2019). STING-mediated disruption of calcium homeostasis chronically activates ER stress and primes T cell death. J Exp Med *216*, 867–883. https://doi.org/10.1084/jem.20182192.

Wu, J., Dobbs, N., Yang, K., and Yan, N. (2020). Interferon-Independent Activities of Mammalian STING Mediate Antiviral Response and Tumor Immune Evasion. Immunity *53*, 115-126.e5. https://doi.org/10.1016/j.immuni.2020.06.009.

Wu, X., Wu, F.-H., Wang, X., Wang, L., Siedow, J.N., Zhang, W., and Pei, Z.-M. (2014). Molecular evolutionary and structural analysis of the cytosolic DNA sensor cGAS and STING. Nucleic Acids Res. *42*, 8243–8257. https://doi.org/10.1093/nar/gku569.

Xiao, G., Harhaj, E.W., and Sun, S.C. (2001). NF-kappaB-inducing kinase regulates the processing of NF-kappaB2 p100. Mol Cell *7*, 401–409. https://doi.org/10.1016/s1097-2765(01)00187-3.

Yamamoto, M., Yamazaki, S., Uematsu, S., Sato, S., Hemmi, H., Hoshino, K., Kaisho, T., Kuwata, H., Takeuchi, O., Takeshige, K., et al. (2004). Regulation of Toll/IL-1-receptor-mediated gene expression by the inducible nuclear protein IkappaBzeta. Nature *430*, 218–222. https://doi.org/10.1038/nature02738.

Yamashiro, L.H., Wilson, S.C., Morrison, H.M., Karalis, V., Chung, J.-Y.J., Chen, K.J., Bateup, H.S., Szpara, M.L., Lee, A.Y., Cox, J.S., et al. (2020). Interferon-independent STING signaling promotes resistance to HSV-1 in vivo. Nat Commun *11*, 3382. https://doi.org/10.1038/s41467-020-17156-x.

Yamazaki, S., Muta, T., and Takeshige, K. (2001). A novel IkappaB protein, IkappaB-zeta, induced by proinflammatory stimuli, negatively regulates nuclear factor-kappaB in the nuclei. J Biol Chem *276*, 27657–27662. https://doi.org/10.1074/jbc.M103426200.

Yano, T., Mita, S., Ohmori, H., Oshima, Y., Fujimoto, Y., Ueda, R., Takada, H., Goldman, W.E., Fukase, K., Silverman, N., et al. (2008). Autophagic control of listeria through intracellular innate immune recognition in drosophila. Nat Immunol *9*, 908–916. https://doi.org/10.1038/ni.1634.

Yoneyama, M., and Fujita, T. (2010). Recognition of viral nucleic acids in innate immunity: Virus-recognition by PRRs. Rev. Med. Virol. *20*, 4–22. https://doi.org/10.1002/rmv.633.

Yum, S., Li, M., Fang, Y., and Chen, Z.J. (2021). TBK1 recruitment to STING activates both IRF3 and NF-κB that mediate immune defense against tumors and viral infections. Proc Natl Acad Sci U S A *118*. https://doi.org/10.1073/pnas.2100225118.

Zhao, B., Xu, P., Rowlett, C.M., Jing, T., Shinde, O., Lei, Y., West, A.P., Liu, W.R., and Li, P. (2020). The molecular basis of tight nuclear tethering and inactivation of cGAS. Nature *587*, 673–677. https://doi.org/10.1038/s41586-020-2749-z.

Zhong, B., Yang, Y., Li, S., Wang, Y.-Y., Li, Y., Diao, F., Lei, C., He, X., Zhang, L., Tien, P., et al. (2008). The Adaptor Protein MITA Links Virus-Sensing Receptors to IRF3 Transcription Factor Activation. Immunity *29*, 538–550. https://doi.org/10.1016/j.immuni.2008.09.003.

Zhou, B., Lindsay, S.A., and Wasserman, S.A. (2015). Alternative NF-κB Isoforms in the Drosophila Neuromuscular Junction and Brain. PLoS ONE *10*, e0132793. https://doi.org/10.1371/journal.pone.0132793.

ANNEXES

Résumé en français

1. Introduction :

Les infections virales représentent une menace pour tous les organismes vivants. Afin d'y survivre, ils ont développé, au cours de l'évolution, différents mécanismes antiviraux. L'immunité innée est présente chez tous les animaux et est essentielle aux défenses antivirales. Le laboratoire dans lequel j'effectue ma thèse étudie l'immunité innée chez l'organisme modèle *Drosophila melanogaster,* exploitant les nombreux avantages de ce modèle tel que son temps de génération court, les outils génétiques disponibles et l'absence d'immunité adaptative, facilitant l'étude de l'immunité innée.

Chez la drosophile, le mécanisme antiviral le mieux décrit est l'ARN interférence qui confère une protection contre une large diversité de virus. Cependant, des réponses antivirales inductibles ont également été décrites. Parmi ces réponses, l'une implique l'homologue de la protéine antivirale STING (*stimulator of interferon genes)*, connue chez les mammifères pour son rôle antiviral contre les virus à ADN. En effet, la voie STING chez les mammifères est activée par la présence anormale d'ADN double- brin dans le cytosol, détectée par l'enzyme cGAS (*cyclic GMP-AMP synthase*). Après avoir fixé l'ADN double brin, cGAS va produire un messager secondaire, le dinucléotide cyclique 2'3'-cGAMP (*cyclic GMP-AMP*) qui va se lier aux homodimères de STING et les activer. S'en suit une cascade de signalisation menant à l'activation des facteurs de transcription IRF3 (*interferon regulatory factor 3*) et NF-κB (*nuclear factor kappa-B)* induisant la production d'interférons de type I (IFN-I) et la mise en place d'un état antiviral chez l'hôte.

Le laboratoire dans lequel je réalise ma thèse a démontré l'implication de l'homologue de STING chez la drosophile dans l'immunité antivirale (Goto et *al.*, 2018), via l'activation de la kinase IKKß et de Relish, un facteur de transcription de la famille NF-κB. De façon intéressante, ces deux dernières protéines sont connues pour leur rôle dans la voie antibactérienne IMD (*immune deficiency)*, où elles permettent l'induction de l'expression de peptides antimicrobiens afin de lutter contre les infections par des bactéries à Gram négatif. L'activation de Relish (similaire aux facteurs NF-κB p100/p105) dans la voie IMD implique deux mécanismes indépendants mais

complémentaires. D'une part, sa translocation dans le noyau nécessite son clivage endo-protéolytique, permettant la libération de sa partie N-terminale transcriptionnellement active (Rel68) de sa partie C-terminale inhibitrice (Rel49). Ceci est permis par la caspase DREDD (homologue de la caspase-8), aidée de son cofacteur FADD. D'autre part, Relish est phosphorylé par le signalosome IKKß-IKKγ afin de permettre le recrutement de la polymérase II sur les promoteurs des gènes cibles (Ertürk-Hasdemir *et al*, 2009).

Au cours de ma thèse, j'ai eu l'opportunité de participer à l'étude des mécanismes en amont de la voie STING chez la drosophile, particulièrement son activation et l'étude des récepteurs impliqués, qui représentent des questions majeures pour la compréhension de cette voie antivirale. Cependant, l'objectif principal de ma thèse a porté sur l'étude des mécanismes d'activation du facteur de transcription Relish en aval de la voie STING et leur comparaison avec ceux, connus, de la voie IMD. Cet axe d'étude a pour but d'enrichir notre compréhension de la voie de signalisation STING chez la drosophile mais pourrait également aider à élucider le mécanisme d'activation du facteur de transcription NF-κB dans la voie STING chez les mammifères, qui reste mal caractérisé.

2. Résultats

a. Activation de la voie STING chez la drosophile

Au cours de ma thèse j'ai participé à l'étude ayant démontré que, comme chez les mammifères, le messager secondaire 2'3'-cGAMP active efficacement la voie STING chez la drosophile (Cai et *al.*, 2020). Cette découverte suggère la présence d'un récepteur semblable au récepteur cGAS mammifère chez les insectes. Le premier orthologue de cGAS identifié chez la drosophile est CG7194 mais les expériences réalisées suggèrent qu'il ne participe pas à la voie STING. Une analyse informatique réalisée par nos collaborateurs, l'équipe du Professeur Rune Hartmann à Aarhus (Danemark), a permis d'identifier deux autres orthologues de cGAS, appelés cGLR (*cGAS like receptor)* 1 et 2. De façon intéressante, les deux cGLR sont capables d'induire un gène rapporteur STING dans les cellules S2 de drosophile, mais la mutation de leur site actif, prédit informatiquement, supprime cette activité. Des

expériences *in vivo* sur des drosophiles mutantes ont confirmé l'implication des cGLRs dans la voie STING (Holleufer et al, 2021).

Dans ce projet j'ai réalisé des expériences d'immunofluorescence dans le but de localiser les deux cGLR dans des cellules S2 transfectées. J'ai ainsi pu remarquer que, si cGLR1 montre une localisation cytoplasmique diffuse, cGLR2 est localisé dans le noyau. De plus, lorsque le NLS prédit de cGLR2 est muté, il se localise au niveau de la membrane plasmique. Par contre, je n'ai pas observé de changement de localisation des cGLR après infection virale. D'autre part, l'instabilité manifeste de la protéine cGLR2 observée par Western blot nous a également mené à nous demander si celle-ci était dégradée par le protéasome. Afin de le vérifier j'ai réalisé des expériences d'inhibition du protéasome suivies d'analyse par Western blot. Les résultats ont effectivement mis en évidence une stabilisation de cGLR2 lorsque le protéasome est inhibé.

b. Activation du facteur de transcription Relish dans la voie STING

Dans le cadre de la voie antibactérienne IMD, le clivage de Relish par la caspase DREDD est essentiel pour sa translocation nucléaire. Cependant, les résultats initiaux du laboratoire suggèraient que DREDD n'est pas impliquée dans la voie STING, puisque son inhibition n'altérait pas l'efficacité antivirale de la voie (Goto et *al.* 2018). La première question à laquelle je me suis intéressée au cours de ma thèse concernait donc le clivage de Relish après activation de la voie STING. Afin de visualiser ce clivage j'ai réalisé des expériences de Western blot dans des conditions d'activation de la voie IMD ou de la voie STING. J'ai suivi la protéine endogène grâce à des anticorps reconnaissants la partie C-terminale de Relish. Comme attendu, j'ai pu voir l'induction du clivage de Relish lorsque la voie IMD est activée. Au contraire, lors de l'activation de la voie STING je n'ai pas observé de clivage de Relish, suggérant une différence majeure entre ces deux voies.

Afin de confirmer ce résultat *in vivo* j'ai utilisé des drosophiles mutantes présentant une protéine Relish non-clivable par la caspase DREDD, puisque le résidu reconnu par celle-ci est modifié (Rel^{D545A}, Pr. Neal Silverman). Comme attendu, l'expression des peptides antimicrobiens régulés par la voie IMD n'est plus induite après activation de cette voie. Cependant, de façon surprenante, l'induction des gènes régulés par la

voie STING (*STING regulated genes, SRG*) est également abrogée dans ces drosophiles. Ceci démontre que le résidu muté est important pour la signalisation en aval de STING et suggère que DREDD serait malgré tout impliqué dans la voie STING. Afin de vérifier ceci j'ai injecté des drosophiles mutantes pour le gène *Dredd* (*Dredd*^{D55}) avec l'agoniste 2'3'-cGAMP et j'ai suivi l'expression des gènes *SRG* par RT-qPCR. J'ai pu observer une absence totale d'induction des gènes *SRG* dans les drosophiles mutantes, ce qui confirme l'implication de DREDD dans la voie STING. De plus, la même expérience a été réalisée sur des drosophiles mutantes pour FADD, le cofacteur de DREDD, et j'ai pu observer des résultats similaires. Ces résultats vont à l'encontre de ceux obtenus après inhibition de DREDD par ARN interférence dans les cellules S2 (Goto et *al.*, 2018). Une explication probable est que le niveau résiduel de DREDD après inhibition serait suffisant pour l'activation de la voie STING dans les cellules S2.

L'implication de la caspase DREDD démontrée par les expériences *in vivo* remet en question les résultats obtenus quant au clivage de Relish. Afin de vérifier les premiers résultats obtenus sur la protéine Relish endogène, avec un anticorps de mauvaise qualité ciblant la partie C-terminale de la protéine, j'ai construit deux clones différents permettant l'expression de Relish tagué soit en C-terminal avec une étiquette V5 ou en N-terminal avec une étiquette HA, sous le contrôle du promoteur actine. J'ai ensuite transfecté des cellules S2 et réalisé des Western blot pour suivre le clivage de Relish lors de l'activation de la voie IMD ou de la voie STING. Cette expérience m'a permis d'observer le clivage de Relish après induction de la voie IMD mais aussi de la voie STING. Je répète actuellement cette expérience dans des cellules S2 mutantes nulles pour *Dredd* afin de vérifier le rôle de la caspase dans le clivage de Relish après activation de la voie STING.

c. Test de l'implication du facteur de transcription NF-κB dorsal-B et de la protéine IκB Charon dans la voie STING

Avant mon arrivée au laboratoire, une étude de l'interactome de la kinase IKKß, impliquée dans les voies IMD et STING, a été réalisée. Les résultats montrent qu'en plus de Relish, un autre facteur de transcription de type NF-κB, dorsal, interagit avec IKKß. Plus précisément, les résultats de spectrométrie de masse suggèrent une

interaction spécifique d'IKKß avec l'isoforme la moins bien décrite de dorsal, dorsal-B (dl-B), ce qui a été confirmé par des expériences de co-immunoprécipitation. Dans le but de mieux caractériser cette interaction, j'ai construit des plasmides codant pour des formes tronquées de dl-B puis j'ai répété les expériences de co-immunoprécipitation. Ceci a permis de définir que la kinase IKKß interagit avec la partie centrale de dl-B, qui n'est pas présente dans l'isoforme dl-A. Cette interaction spécifique entre IKKß et dl-B questionne sur une possible phosphorylation de dl-B par cette kinase. Afin de tester cette hypothèse j'ai transfecté des cellules S2 avec un clone exprimant dl-B puis, avec l'aide de la plateforme de protéomique de l'IBMC, nous avons réalisé une analyse de spectrométrie de masse centrée sur la recherche de modifications post-traductionnelles. Cette analyse a révélé trois phosphorylations sur des sérines sur dl-B (S541, S551 et S827). Afin de savoir si ces phosphorylations dépendent d'IKKß il faudrait réaliser à nouveau cette analyse dans des cellules S2 mutantes nulles pour IKKß. D'autre part, j'ai souhaité tester l'existence d'un hétérodimère entre Relish et dl-B, ce qui pourrait expliquer les différences dans les réponses transcriptionnelles induites par les voies STING et IMD. Des expériences de co-immunoprécipitation entre ces deux protéines ont montré une interaction spécifique entre dl-B et Relish.

Enfin, des expériences préliminaires sur des drosophiles mutantes pour dl-B semblent indiquer un rôle de régulateur négatif de la voie STING pour ce facteur de transcription. En effet, l'activation des gènes *SRG* après injection de 2'3'-cGAMP est augmentée dans les drosophiles mutantes comparées aux drosophiles sauvages.

D'autre part, avant mon arrivée au laboratoire, une étude des gènes régulés par la kinase IKKß et induits par une infection virale a été réalisé (Goto et *al.,* 2018). Parmi ces gènes, celui codant la protéine IκB Charon a retenu mon attention. Charon présente 7 répétitions Ankyrine dans sa partie C-terminale, lui permettant d'interagir avec Relish. Cependant, les effets observés in vivo sur l'immunité antibactérienne sont faibles et les données publiées sont contradictoires (Morris et *al.*, 2016 et Ji et *al.*, 2016). Je m'interroge donc sur un éventuel rôle de Charon dans la voie STING. J'ai observé que l'inhibition de Charon dans les cellules S2 entraîne une baisse significative de l'activité du gène rapporteur STING. Afin de confirmer ce résultat *in vivo*, j'ai utilisé une lignée drosophiles dans laquelle le domaine de Charon

interagissant avec Relish a été muté. Les résultats préliminaires montrent une diminution de l'activation des gènes *SRG* par injection de 2'3'-cGAMP dans les drosophiles mutantes, ce qui suggère que Charon pourrait en effet jouer un rôle dans la signalisation STING chez la drosophile.

3. Conclusions

Au cours de ma thèse, j'ai participé à l'étude de l'activation de la voie STING par le di-nucléotide cyclique 2'3'-cGAMP qui a donné lieu à une publication en co-auteur. J'ai également pris part au projet visant à caractériser les récepteurs de la voie STING chez la drosophile, cGLR1 et 2. Ce travail a été réalisé dans le cadre d'une collaboration internationale avec les laboratoires du Professeur Rune Hartmann (Aarhus, Danemark) et l'équipe du Dr Hua Cai (Guangzhou, Chine) et je serais co-auteur de l'article décrivant les résultats.

En ce qui concerne l'objectif principal de ma thèse, qui visait à caractériser les mécanismes d'activation du facteur de transcription NF-κB Relish en aval de la voie STING, mes travaux ont permis de démontrer que Relish subissait un clivage, essentiel pour sa fonction dans la voie STING. De plus, j'ai pu identifier deux nouveaux acteurs de la voie STING, la caspase DREDD ainsi que son co-facteur FADD. Ces résultats seront décrits dans un manuscrit que je signerai en premier auteur. Enfin, les résultats préliminaires obtenus sur le facteur de transcription NF-κB dl-B et la protéine IκB Charon suggèrent un rôle de régulateur négatif ou positif, respectivement, de la voie STING qu'il faudra confirmer.

Préambule en français

Tous les organismes vivants sont constamment entourés de micro-organismes potentiellement dangereux. Cette exposition continue a façonné les systèmes de défense de l'hôte tout au long de l'évolution.

Les défenses immunitaires de l'organisme modèle *Drosophila melanogaster* reposent uniquement sur l'immunité innée, car les insectes n'ont pas de système immunitaire adaptatif. Pour se protéger des divers agents pathogènes existants, les drosophiles ont développé différents mécanismes de défense au cours de l'évolution. Ces mécanismes peuvent être soit constitutifs, comme c'est le cas pour l'interférence par acide ribonucléique (ARNi), largement antivirale, soit induits lors d'une infection. Ce dernier cas peut être illustré par deux voies de signalisation bien connues la voie Toll et la voie de l'immunodéficience (Imd), qui confèrent une immunité antibactérienne et antifongique. Toutefois, il est apparu récemment que les réponses inductibles sont également importantes pour défendre les mouches contre les infections virales.

Au cours des 20 dernières années, mon équipe d'accueil s'est particulièrement intéressée à ces défenses antivirales inductibles (Deddouche et al., 2008 ; Dostert et al., 2005 ; Kemp et al., 2013 ; Sabatier et al., 2003). L'équipe a notamment identifié des suppresseurs viraux de la voie Imd dans plusieurs virus à ADN, ce qui suggère que cette voie limite les infections virales (Lamiable et al., 2016). Tout en poursuivant l'exploration d'un rôle possible de la voie Imd dans les défenses antivirales, l'équipe a découvert une nouvelle voie dépendante d'un récepteur de reconnaissance de motifs moléculaire (*Pattern Recognition Receptor,* PRR) qui régule les défenses antivirales chez la drosophile. En effet, peu avant mon arrivée au laboratoire, l'équipe a décrit que deux composants de la voie Imd, le facteur de transcription du facteur nucléaire kappa-B (NF-κB) Relish et la kinase I-kappa-B (IKK)-ß, jouaient un rôle important dans la défense de l'hôte contre le virus C de la drosophile (DCV), un virus de type picorna. Ces protéines sont impliquées dans une voie de signalisation antivirale reposant sur l'homologue drosophile du stimulateur des gènes de l'interféron (STING). Curieusement, les autres composants de la voie canonique Imd ne semblent pas participer à cette voie (Goto et al., 2018). Ces résultats sont intrigants, car Relish doit

être clivé pour transloquer dans le noyau et induire l'expression de ces gènes cibles, et ce clivage est médié par l'homologue de la caspase-8 *Death related ced-3/Nedd2-like caspase* (Dredd) dans la voie Imd (Kim et al., 2014 ; Stoven et al., 2003 ; Stöven et al., 2000). De plus, la sous-unité régulatrice du complexe IKK, IKKγ est également essentielle pour une bonne activation des gènes cibles de Relish (Ertürk-Hasdemir et al., 2009). Le fait qu'aucun de ces composants ne semble être impliqué dans la voie STING a soulevé la question du mécanisme par lequel Relish contrôle la réponse transcriptionnelle lors de l'activation de la voie STING. Une autre question clef lorsque j'ai rejoint le laboratoire était la façon dont la voie STING est activée lors d'une infection virale. L'objectif de mon projet de doctorat était de faire la lumière sur ces questions.

Afin de fournir un contexte au thème général de ma thèse, j'ai structuré l'introduction en trois parties. La première partie fournit une revue des réponses immunitaires chez *Drosophila melanogaster*. La deuxième partie de l'introduction couvre la voie STING et sa conservation au cours de l'évolution. Enfin, la dernière partie de l'introduction est un aperçu des voies NF-κB et de leur régulation chez les animaux.

Introduction en français (première partie)

1. Voies immunitaires chez *Drosophila melanogaster*

Lorsqu'un individu rencontre un agent infectieux, le premier type de défense est mécanique. Elle repose sur la barrière physique qui délimite le "soi" de l'environnement "non soi". La plupart du temps, cette première ligne de défense empêche l'agent pathogène de pénétrer dans l'organisme et de déclencher l'infection. Si cette barrière est franchie ou contournée, d'autres composantes du système immunitaire entrent en jeu pour préserver l'organisme. Dans tous les organismes multicellulaires, on trouve une variété de PRR. Les PRR sont des protéines responsables de la reconnaissance de molécules conservées que l'on trouve fréquemment dans les micro-organismes, appelées motifs moléculaires associés aux micro-organismes (MAMP). Par exemple, la flagelline, la principale protéine composant le flagelle bactérien, est reconnue par le récepteur Toll-like (TLR)-5 chez les animaux (Hayashi et al., 2001). Par ailleurs, les PRR sont capables de détecter des motifs moléculaires associés à des dommages (DAMP) tels que l'acide urique libéré par des cellules endommagées (Shi et al., 2003). La reconnaissance de leur ligand par les PRR permet l'activation de l'immunité innée, ce qui entraîne une réponse rapide et non spécifique à l'infection. Chez les vertébrés, cette branche de la réponse immunitaire permet l'activation d'une immunité adaptative ultérieure, plus lente à se mettre en place mais spécifique et qui donne lieu à une mémoire immunitaire (revue dans Hoffmann et al., 1999).

Mon laboratoire d'accueil étudie l'immunité innée chez la drosophile *Drosophila melanogaster* qui appartient à l'ordre des diptères. Elle présente de nombreux avantages, parmi lesquels sa petite taille, son temps de génération court et sa facilité de manipulation. De plus, la variété des outils génétiques qu'elle offre et l'absence d'immunité adaptative en font un modèle très attractif pour étudier la réponse immunitaire innée. Il est important de noter que les insectes représentent près de 70 % de la faune terrestre et qu'ils sont sensibles à des agents pathogènes similaires à

ceux qui infectent l'homme. L'étude de leurs mécanismes immunitaires peut donc révéler des stratégies qui peuvent être conservées ou transposées à l'homme (revue dans Martins et al., 2016). Un exemple notable est l'identification de voies de signalisation inductibles médiant l'expression des peptides antimicrobiens (AMP) chez la drosophile (revue dans Imler, 2014). Les AMP sont de petites protéines cationiques produites par le corps gras (équivalent fonctionnel du foie des mammifères) et sécrétées dans l'hémolymphe (liquide analogue au sang des vertébrés). Elles présentent diverses activités contre les bactéries et les champignons (voir Imler et Bulet, 2005). L'expression des gènes AMP est régulée par deux voies de signalisation distinctes, les voies Toll et Imd (revue dans Hoffmann, 2003 ; Lemaitre et Hoffmann, 2007).

a. Défenses antibactériennes et antifongiques

Voie Toll

Il est intéressant de noter que des sites de liaison pour les facteurs de transcription NF-κB/Rel ont été identifiés dans les promoteurs des gènes AMP. La mutation de ces sites abolit l'induction des AMP lors des infection (Engström et al., 1993 ; Kappler et al., 1993). Ceci suggère une implication des membres de la famille NF-κB dans les voies immunitaires chez la drosophile. À l'époque, un seul membre de la famille NF-κB avait été identifié chez la drosophile, dorsal (dl). dl participe à la structuration dorso-ventrale de l'embryon précoce (Nüsslein-Volhard et al., 1980). L'activation de ce facteur de transcription s'est avérée similaire à l'induction de NF-κB lors de la réponse inflammatoire chez les mammifères. En effet, elle dépend de sa dissociation de la protéine Cactus (une protéine inhibitrice homologue à l'inhibiteur de NF-κB (IκB)). Cet événement est déclenché par la liaison de la protéine de type cytokine appelée Spätzle au récepteur transmembranaire Toll, ce qui entraîne l'activation de la signalisation (Weber et al., 2003 ; revue dans St Johnston et Nüsslein-Volhard, 1992). Il a ensuite été démontré que le récepteur Toll de la drosophile jouait un rôle important dans la lutte contre les infections fongiques et les infections à Gram positif (Lemaitre et al., 1996 ; Rutschmann et al., 2002). Il est important de noter que le facteur de transcription NF-κB responsable de la régulation de l'expression des AMP

n'est pas dorsal, mais le facteur étroitement apparenté Dif (*dorsal-related immunity factor*) (Ip, 1993 ; Meng et al., 1999 ; Rutschmann et al., 2000a).

Cette découverte chez la drosophile a suscité la recherche et l'identification ultérieure d'une famille de TLR chez les mammifères. Alors que Toll agit comme un récepteur de la cytokine Spätzle chez la drosophile, les TLR des mammifères sont des PRR qui détectent directement les infections en reconnaissant une variété de MAMP (Medzhitov et al., 1997 ; Poltorak et al., 1998 ; Rock et al., 1998). Chez la mouche, la détection de l'infection se produit en amont de Toll. Les peptidoglycanes (PGN) de type LYS présents dans la membrane externe des bactéries à Gram-positif sont détectés par les récepteur PGRP (*peptidoglycan-recognition protein*)-SA ou GNBP (*gram-negative binding protein*)-1 (Gobert et al., 2003 ; Michel et al., 2001). Les ß-glucanes composant la paroi cellulaire des champignons sont reconnus par le récepteur GNBP-3 (Gottar et al., 2006 ; Mishima et al., 2009). Par ailleurs, les protéases sécrétées par les champignons entomopathogènes, mais aussi par les bactéries à Gram positif et négatif, induisent la maturation du zymogène Perséphone en une protéase active (El Chamy et al., 2008 ; Gottar et al., 2006 ; Issa et al., 2018). Finalement, ces systèmes de détection convergent et conduisent à la maturation protéolytique extracellulaire de Spätzle (DeLotto et DeLotto, 1998 ; Mizuguchi et al., 1998). Un dimère de Spätzle actif se lie au domaine extracytoplasmique d'un dimère de récepteurs transmembranaires Toll. Cela induit la liaison croisée des deux ectodomaines Toll et des changements de conformation ultérieurs conduisant à la signalisation (Hu et al., 2004 ; Weber et al., 2003, 2005, 2007). Lors de l'activation, l'adaptateur cytoplasmique *myeloid differentiation primary-response gene 88* (MyD88) est recruté par l'interaction de son domaine *Toll/interleukine-1 receptor* (TIR) avec le domaine TIR de la queue intracytoplasmique du récepteur Toll. Par l'intermédiaire de son domaine de mort (DD), MyD88 recrute l'adaptateur Tube, qui possède un DD bivalent et qui, à son tour, recrutera la sérine-thréonine kinase Pelle contenant un DD (Tauszig-Delamasure et al., 2002). Finalement, l'homologue de IκB chez les mammifères, Cactus, est phosphorylé, ce qui entraîne son ubiquitination et sa dégradation. Ceci permet la libération du facteur de transcription NF-κB like dorsal (chez l'embryon) ou Dif (chez l'adulte), suivie de sa translocation nucléaire et de l'activation de gènes cibles, parmi lesquels des AMP comme la Drosomycine (Figure 1A). La voie Toll de la drosophile est homologue à la cascade de signalisation des

mammifères en aval du récepteur de l'interleukine-1 et des TLR, ce qui indique une ascendance commune de ces différents mécanismes immunitaires (Medzhitov et al., 1998 ; revu dans Hoffmann, 2003 ; Hoffmann et al., 1999).

La voie Imd

La voie Imd a été nommée d'après une mutation appelée immunodéficience qui altère l'expression de certains AMP, mais pas de la drosomycine qui est régulée par la voie Toll. Les mouches imd présentent une grande sensibilité aux bactéries Gram négatives mais sont résistantes aux champignons et aux bactéries Gram positives. Il est important de noter que la surexpression d'imd entraîne une augmentation de l'expression des AMPs dans des conditions non infectées, ce qui démontre son rôle central dans la réponse immunitaire systémique de la drosophile (Georgel et al., 2001). La protéine codée par imd contient un DD qui présente des similitudes de séquence avec le DD de la protéine RIP (*receptor-interacting protein*) des mammifères (Georgel et al., 2001).

Les PGN de type acide diaminopimélique contenus dans l'enveloppe cellulaire des bactéries Gram négatives sont reconnus par le récepteur transmembranaire PGRP-LC ou par des isoformes cytoplasmiques ou sécrétées du récepteur PGRP-LE. La forme cytoplasmique de PGRP-LE est impliquée dans l'activation de l'autophagie lors de l'infection par des bactéries intracellulaires, indépendamment de la voie Imd (Yano et al., 2008). En revanche, l'activation des deux PGRP par la liaison d'un ligand entraîne l'activation de la voie Imd par le recrutement de l'adaptateur proximal Imd. Cette protéine fonctionne comme une plaque tournante de signalisation initiant deux processus distincts, finalement responsables de l'activation du facteur de transcription de type NF-κB Relish (Choe et al., 2002 ; Gottar et al., 2002 ; Hedengren et al., 1999 ; Takehana et al., 2004).

Le premier processus commence par le recrutement de la protéine adaptatrice *Fas-associated protein with death domain* (Fadd) par Imd grâce à l'interaction DD-DD. Ensuite, Fadd recrute la caspase Dredd par l'interaction de leur domaine effecteur de mort (DED) respectif (Leulier et al., 2000, 2002 ; Naitza et al., 2002). Dredd est ensuite ubiquitiné (Meinander et al., 2012), ce qui le rend actif et lui permet de cliver Relish au

niveau d'un résidu spécifique (acide aspartique en position 545, D545). Cette transformation libère la partie active amino-terminale (N-ter) (Rel68) présentant le domaine d'homologie Rel (RHD) de la partie inhibitrice carboxy-terminale (C-ter) (Rel49) contenant des répétitions d'ankyrine et une séquence PEST (Kim et al., 2014 ; Stoven et al., 2003 ; Stöven et al., 2000). Ce processus permet la translocation nucléaire de Rel68, tandis que Rel49 reste dans le cytoplasme (Figure 1A et B).

De plus, pour activer efficacement la transcription de ses gènes cibles, tels que le gène codant pour l'AMP (Dpt), Relish doit être phosphorylé. Ce second processus repose sur le clivage dépendant de Dredd d'un fragment N-ter d'Imd, permettant son ubiquitination K63 (Meinander et al., 2012 ; Paquette et al., 2010). Imd est alors capable de recruter et d'activer le complexe Tab2/Tak1. Ce complexe est responsable de l'activation du complexe IKKß-IKKγ par phosphorylation (Kleino et al., 2005 ; Lu et al., 2001 ; Rutschmann et al., 2000b ; Silverman et al., 2000). Finalement, le complexe IKK phosphoryle deux résidus sérine de Relish (S528 et S529), nécessaires au recrutement efficace de l'ARN polymérase II sur les promoteurs des gènes cibles de Relish (Figure 1A et B) (Ertürk-Hasdemir et al., 2009 ; Silverman et al., 2000). Cette voie est homologue à la voie dépendante du récepteur du facteur de nécrose tumorale (TNFR) chez les mammifères (revue dans Hoffmann, 2003).

b. Immunité antivirale

Notre connaissance de la réponse immunitaire antivirale chez la drosophile a longtemps été limitée à l'ARNi. Cependant, bien que cette réponse soit essentielle pour défendre l'organisme contre tous les types de virus, on sait maintenant que des réponses antivirales inductibles existent et sont également importantes pour la survie des mouches aux infections virales.

Les connaissances acquises et les avancées récentes sur l'immunité antivirale de la drosophile ont fait l'objet d'une revue publiée en 2021 dans la revue *Developmental and Comparative Immunology* (Schneider et Imler, 2021)

Université de Strasbourg

Juliette SCHNEIDER

École Doctorale des Sciences de la Vie et de la Santé STRASBOURG

Caractérisation de la voie STING chez *Drosophila melanogaster :* signalisation et activation du facteur NF-κB

Résumé

Les virus sont une menace pour tous les organismes vivants qui ont développé divers mécanismes pour leur résister. En travaillant sur l'organisme modèle *Drosophila melanogaster*, mon laboratoire d'accueil a découvert une nouvelle voie antivirale impliquant l'orthologue de la protéine mammifère STING et deux composants de la voie antibactérienne Imd, la kinase IKKß et le facteur de transcription NF-κB Relish. Au cours de ma thèse, j'ai travaillé sur deux questions concernant cette voie : (i) comment est-elle déclenchée chez la drosophile ? et (ii) comment STING active-t-il IKKß et Relish ?

D'une part, j'ai participé aux travaux montrant que STING est activé par des dinucléotides cycliques chez la drosophile, en particulier le produit de l'enzyme cGAS mammifère : 2'3'-cGAMP. Par la suite, deux orthologues de cGAS ont été identifiés chez la drosophile et j'ai commencé leur caractérisation fonctionnelle.

J'ai également exploité les interactomes de STING et IKKß et identifié deux nouvelles protéines, l'adaptateur Fadd et la caspase Dredd, comme des composants importants de la voie STING chez la drosophile. Enfin, j'ai travaillé sur deux protéines NF-κB et IκB mal caractérisées qui pourraient participer à la voie STING chez la drosophile.

Mots clés : STING – NF-κB – voie antivirale- dinucléotides cycliques – othologues de cGAS - *Drosophila melanogaster*

Résumé en anglais

Viruses are a threat to all living organisms who developed diverse mechanisms to resist them. Working on the model organism *Drosophila melanogaster*, my host laboratory discovered a new antiviral pathway involving the ortholog of the mammalian antiviral protein STING and two components of the antibacterial immune deficiency pathway, the kinase IKKß and the NF-κB transcription factor Relish. During my thesis I attempted to answer two questions about this pathway: (i) how is it triggered in drosophila? and (ii) how does STING activate IKKß and Relish?

To do so, I participated in the work demonstrating that drosophila STING is activated by cyclic-dinucleotides, in particular the product of the mammalian enzyme cGAS: 2'3'-cGAMP. Subsequently, two cGAS-like receptors were identified in drosophila and I started their functional characterization.

I also exploited the interactomes of STING and IKKß and identified two new proteins, the adaptor Fadd and the caspase-8 homolog Dredd, as important components of the STING pathway in drosophila. Finally, I worked on two poorly characterized drosophila NF-κB and IκB proteins which may participate in STING signaling.

Keywords: STING – NF-κB – antiviral pathway - cyclic dinucleotides - cGAS-like receptors - *Drosophila melanogaster*